# INFORMATION TO USERS

This manuscript has been reproduced from the microfilm master. UMI films the text directly from the original or copy submitted. Thus, some thesis and dissertation copies are in typewriter face, while others may be from any type of computer printer.

**The quality of this reproduction is dependent upon the quality of the copy submitted.** Broken or indistinct print, colored or poor quality illustrations and photographs, print bleedthrough, substandard margins, and improper alignment can adversely affect reproduction.

In the unlikely event that the author did not send UMI a complete manuscript and there are missing pages, these will be noted. Also, if unauthorized copyright material had to be removed, a note will indicate the deletion.

Oversize materials (e.g., maps, drawings, charts) are reproduced by sectioning the original, beginning at the upper left-hand corner and continuing from left to right in equal sections with small overlaps.

Photographs included in the original manuscript have been reproduced xerographically in this copy. Higher quality 6" x 9" black and white photographic prints are available for any photographs or illustrations appearing in this copy for an additional charge. Contact UMI directly to order.

ProQuest Information and Learning
300 North Zeeb Road, Ann Arbor, MI 48106-1346 USA
800-521-0600

# Spatial distribution of ventilation and perfusion in the lateral decubitus posture

Hung Chang

A dissertation submitted in partial fulfillment
Of the requirements for the degree of

Doctor of Philosophy

University of Washington

2001

Program Authorized

To Offer Degree Department of Physiology and Biophysics

UMI Number: 3022816

UMI Microform 3022816



Bell & Howell Information and Learning Company
300 North Zeeb Road
P.O. Box 1346
Ann Arbor, MI 48106-1346

In presenting this dissertation in partial fulfillment of the requirements for the Doctoral Degree at the University of Washington, I agree that the Library shall make its copies freely available for inspection. I further agree that extensive copying of this dissertation is allowable only for scholarly purposes, consistent with "fair use" as prescribed in the U.S. Copyright Law. Requests for copying or reproduction of this dissertation may be Referred to University Microfilms, 1490Eisenhower Place, P.O. Box 975, Ann Arbor, MI 48106, to whom the author has granted "the right to reproduce and sell (a) copies of the manuscript in microform and/or (b) printed copies of the manuscript made from microform."

Signature Hung Chang

Date August 15, 2001

University of Washington
Graduate School

This is to certify that I have examined this copy of a doctoral dissertation by
Hung Chang

And have found that it is complete and satisfactory in all respects,
And that any and all revisions required by the final
examining committee have been made

Chair of Supervisory Committee:

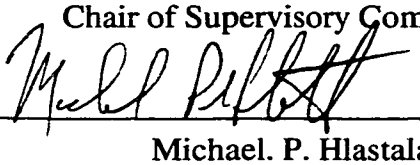

Michael. P. Hlastala

Reading committee:

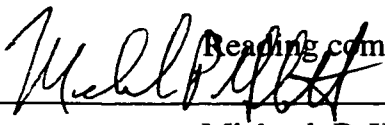

Michael. P. Hlastala

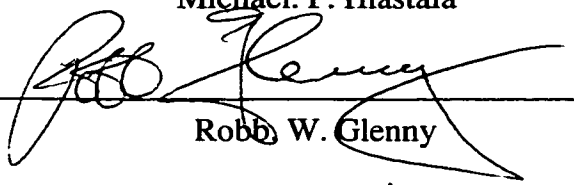

Robb. W. Glenny

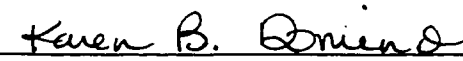

Karen. B. Domino

Date: August 8, 2001

University of Washington

Abstract

Spatial distribution of ventilation and perfusion in the lateral decubitus posture

By Hung Chang

Chairperson of the Supervisor Committee: Professor Michael, P. Hlastala

Department of Physiology and Biophysics

Pulmonary blood flow distribution is affected by many factors, including gravity, hypoxic pulmonary vasoconstriction (HPV), lung volume and positive end-expiratory pressure (PEEP). In the lateral posture, the effects of posture, bilateral PEEP, differential ventilation with unilateral PEEP and left lung atelectasis on regional ventilation ($\dot{V}_A$) and perfusion ($\dot{Q}$) in the lateral decubitus posture were studied. $\dot{Q}$ and $\dot{V}_A$ were measured using 15-μm i.v. injected and 1-μm aerosolized fluorescent microspheres and analyzed in ~1.7 $cm^3$ lung volume pieces. Multiple linear regression analysis was used to evaluate 3-dimensional spatial gradients of $\dot{Q}$, $\dot{V}_A$, $\dot{V}_A/\dot{Q}$ and regional $PO_2$ ($P_RO_2$).

In the left lateral decubitus (LLD) posture, a gravity-dependent vertical gradient in $\dot{Q}$ was observed in conjunction with a reduced blood flow and $P_RO_2$ to the dependent left lung. This observation was consistent with HPV occurring in the dependent left lung. Either a change from the LLD to the RLD posture or 10 cm $H_2O$ PEEP increased local $\dot{V}_A/\dot{Q}$ and $P_RO_2$ in the left lung and minimized any role of hypoxia. Lung distortion caused by the mediastinum was a major factor that determines regional blood flow and ventilation. In this respect, the smaller left lung was the most susceptible to impaired gas exchange in the LLD posture.

With 100% $O_2$ ventilation, the A-a$DO_2$ observed with conventional ventilation doubled with differential ventilation, with no change in blood flow. Unilateral PEEP increased dependent left lung FRC with no change in either blood flow or A-a$DO_2$. Bilateral PEEP produced no change in A-a$DO_2$ with an increased dependent blood flow. Lower dependent blood flow and A-a$DO_2$ in the LLD posture during differential

ventilation with unilateral dependent PEEP was not due primarily to airway closure, lung volume distortion or $\dot{V}_A/\dot{Q}$ inequality.

HPV in the atelectatic lung shifted flow to the ventilated lung. The increased flow in the ventilated lung ensured adequate gas exchange, compensating for the shunt contributed by the atelectatic lung. A-a$DO_2$ increased with left lung atelectasis and was exacerbated in the LLD posture by 10 cm $H_2O$ PEEP, a result of increased $\dot{Q}$ to the atelectatic lung. This PEEP-induced $O_2$ deficit was eliminated with inversion to the RLD posture.

TABLE OF CONTENT

TABLE OF CONTENTS
(continued)

Page

LIST OF FIGURES

LIST OF FIGURES
(continued)

## LIST OF TABLES

LIST OF TABLES
(continues)

## ACKNOWLEDGMENTS

This work would not have been possible without the help and persistent support of my family, church friends and coworkers. I am greatly indebted to my thesis advisor, Michael P. Hlastala, for his teaching, guidance, consistent encouragement, extraordinary patience and providing an exciting and stimulating laboratory allowed me to pursuit my research career. I also like to thank the members of my supervisory committee, Robb B. Glenny and Karen B. Domino for their constructive comments on this thesis and providing scientific support. I always feel lucky that I can work with these gifted and inspiring scientists, they are all my research idols. I hope that some day I can learn their ability to logically target and solve scientific questions.

I am also grateful to Wayne Lamm and Ian Starr for their valuable suggestions, excellent technical assistance and friendship. They welcomed me warmly everyday and taught me how to balance life between family and school, they were my stress-outlet for a long time. I thank Carmel Schimmel, Dowon An, Shen-shen Wang, Erin Shade and Jenny Souders in collecting and processing the data. The computer technical expertise of Dave Frazer has been greatly appreciated. I particularly thank him for solving the multiple tough computer problems. I also like to thank Dr Melisa Kruger for her suggestions about how to formulate my thesis. I would also like to thank the past and present fellow of Hlastala's and Glenny's lab, especially Dr Alteimier for his valuable suggestions and discussions.

I thank my parents, Chao Chun, Chang and Pi O, Lee for their valuable lessons taught to me since my childhood. They have encouraged me to pursuit what I am most interested in and never ever give up. This really helped me to sustain and overcome this most difficult time in my life.

I gratefully acknowledge the support I have received from the government, Taiwan, R.O.C and the thesis project has been supported by NIH grants.

**ACKNOWLEDGMENTS**
**(continued)**

I can not use word to express how my gratitude to my wife, Mei-Ling, Pao, and our son, Stanley, and our daughter Audrey for their endless love and support and understanding of how time demanding graduate school is. It was always heart breaking not be able to spend the quality time with my family that my son and little daughter deserved. I am greatly indebted to my wife for her hard work and assuming my responsibility to take care of the whole family. She honored me with love while I was away. If not for the constant love and joy from my lovely family, I would not have succeeded in this tough PhD program.

## DEDICATION

I would especially like to thank Dr. Jacob Hildebrandt for his countless hours and unselfish teaching. I always remember the weekend independent study on select topic in respiratory physiology. He always challenged me with the very simple question and made me feel how innocent I am. Despite being well prepared and confident before class, Dr Jacob Hildebrandt always asked accurate and reasonable questions which frustrated me every time. His remarkable energy, unselfish donation of time, gradual and logical approach to solve questions and stubborn statue will root in my mind forever. Whenever there is a need for a suggestion or editing for publishing or experimental questions, Jack is always there. You can not ask for any better professor for consulting and commitment to teach throughout your process of graduate study.

To Dr. Stephen J. Lai-fook whom I owe some of the most valuable lessons of my career. I thank him for his helping to develop the data correction while he spent sabbatical time in our lab. He is also unselfish in every aspect and was willing to spend time with me. I thank his guidance, support, friendship and by his example reminding me how hard scientist work to solve questions day in and day out and insist on the truth. He made coming to the lab to work a pleasure in the later tough stage of this thesis work. I consider myself very lucky to have such a privilege to work with Steve and gain extra stimulation and inspiration. I cherished Steve's discussion in terms of science, life philosophy and importance of family. In addition, Steve made me feel the great time spent in Seattle was even better in this big commitment of my whole life.

# CHAPTER 1
# INTRODUCTION TO THE HISTORY AND PHYSIOLOGY OF LATERAL DECUBITUS POSTURE

## Background review and significance

Pulmonary gas exchange and tissue oxygenation depend upon matching of regional ventilation and perfusion (158). Ventilation-perfusion inequality in the lung has been scrutinized for more than four decades. Oxygen exchange inefficiency has been attributed to regional variations in ventilation and perfusion throughout the lung. Body position impacts gas exchange by changing spatial distribution of ventilation and perfusion, and altering the matching of ventilation and perfusion (17; 86; 113). The lateral decubitus position is commonly used during thoracic surgery, especially in conjunction with one-lung ventilation. One-lung ventilation allows surgeons optimal management of the surgical field, easy access to hilar structures and the performance of complex tracheobronchial and esophageal surgery. In addition, one-lung ventilation can prevent infected material from spilling from a diseased lung to the healthy dependent lung. However, severe hypoxia may occur in some patients with unilateral lung ventilation and the mechanism is unclear (128). Moreover, the lateral decubitus position also can affect gas exchange in patients with unilateral lung disease. Studies (28; 63) have shown that oxygenation improves when the healthy lung is dependent and the diseased lung is non-dependent. Improved gas exchange has resulted from better matching of ventilation and perfusion and reduced shunt. However, a study by Choe et al (28) has demonstrated that unilateral ventilation of the healthy lung positioned dependent with unilateral lung disease did not always improve gas exchange. In addition, patients with congestive heart failure and ventricular hypertrophy prefer to lie down in the right lateral decubitus posture (161). Therefore, the factors affecting gas exchange in the lateral decubitus position are still unclear. Furthermore, the lateral position is a common

position for humans during sleep. Thus, the efficiency of gas exchange in this body position is of general interest from both a medical and physiologic perspective.

The introduction chapter reviews the factors that determine regional blood flow and ventilation distribution. A review of physiology of the lateral decubitus position and its effect on gas exchange are presented and provide a background for the further discussion. Different modes of mechanical ventilation help to improve gas exchange in the lateral decubitus posture are summarized. The effect of hyperoxia and lung hyperinflation caused by mediastinal content shifts during unilateral lung ventilation (left lung atelectasis) on regional perfusion and ventilation and gas exchange is addressed. The focus is on three experimental studies designed to assess the effect of the lateral decubitus posture on regional distribution of perfusion, ventilation and gas exchange.

## Factors determining the regional distribution of blood flow

### Gravity

In order to describe the effect of pulmonary arterial, venous and alveolar pressures on the distribution of pulmonary blood flow, many prior investigators have divided the lung into three zones regarding the relationship among the pulmonary arterial (Pa), alveolar (PA) and venous (Pv) pressures (159). In zone 1, part of the lung alveolar pressure exceeds arterial pressure. Thus, no perfusion occurs in the compressed capillary bed of those alveoli (Fig 1). In general, zone 1 condition does not exist in normal lung, because the heart is located close to the top of the lung. The pulmonary arterial pressure is almost always sufficient to perfuse the top part of the lung unless in pathological conditions, such as in shock and congestive heart failure that cause reduced cardiac output or with positive end-expiratory pressure (PEEP) that increases alveolar pressure above pulmonary arterial pressure. However, study (92) has demonstrated a small blood flow that passes through the extra-alveolar vessels and engages in gas exchange in zone 1 regions.

In zone 2, pulmonary arterial pressure exceeds alveolar pressure and alveolar pressure is greater than venous pressure (Pa > PA > Pv). The collapsible capillary

surrounding by numerous alveoli with higher alveolar pressure in zone 2 has been compared to a starling resistor. Thus, the driving pressure in zone 2 depends on the difference between pulmonary arterial pressure and alveolar pressure. This behavior has been described as the waterfall effect. The flow is determined by flow gradient above the fall instead of the height below the fall. Since the alveolar pressure is constant, pulmonary arterial pressure increases down the lung. Blood flow continuously increases going down the lung in the zone 2 area.

In zone 3, pulmonary venous pressure exceeds the alveolar pressure. Regional blood flow depends on the driving pressure, the difference between Pa and Pv. Descending toward the bottom of the lung, both Pa and Pv increase equally and Pa-Pv remains constant. However, the increase in capillary pressure down the lung increases capillary diameter and decreases vascular resistance, while the increase in Pv is associated with capillary recruitment. Thus, blood flow continuously increases down the lung in zone 3. .

At the bottom of the lung, there exists a region where blood flow decreases. This Zone 4 region was attributed to intravascular hydrostatic pressure induced interstitial edema that compresses extra-alveolar vessels.

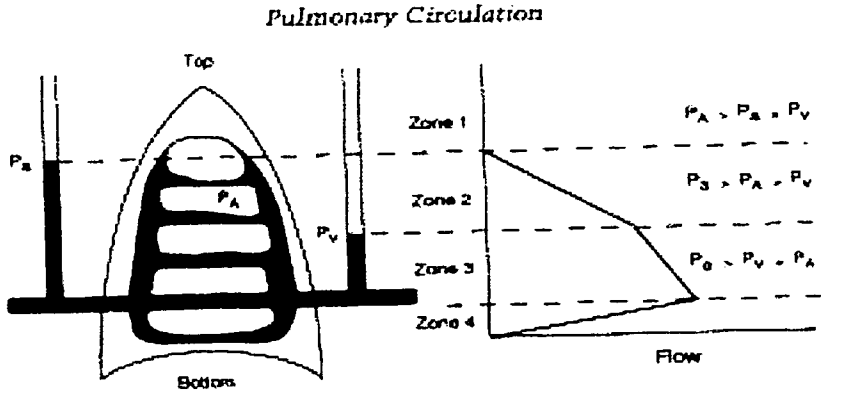


Fig 1. Four-zone model of pulmonary circulation.
(Adapted from Michael P. Hlastala, Physiology of Respiration, 1996)

In humans studied in the lateral decubitus position, the results have been explained by the classical gravitational model, with regional blood flow ($\dot{Q}$) increasing down the lung in the direction of gravity (8; 23; 78; 82; 93; 119; 134; 157). The above conclusion has been drawn from different methodology, anesthesia, ventilation condition, position, species. Using Xenon133 intravenous injection at FRC and scintillation counter count at TLC, Kaneko et al (82) found that $\dot{Q}_{alv}$ increased down the lung in supine, prone, RLD and LLD in awake human study. Amis et al (7) using very short life radioactive $^{81}Kr^{M}$ infusion during spontaneous ventilation and periods breath hold with scintillation counter counting demonstrated that $\dot{Q}/V$ increases 6% of vertical axis in the upper lung but evenly distributed in the lower lung in the lateral decubitus posture in awake human. Landmark et al (93) using intravenous $Xe^{133}$ injection during awake human with breath hold at TLC or anesthetized with thiopental and succinylcholine with lung inflated to 25-40 cm $H_2O$ showed that $\dot{Q}_{alv}$ increased down the lung in supine, sitting, RLD postures. No significant change of $\dot{Q}_{alv}$ between awake and anesthetized-paralyzed subjects was noted. Orphanidou et al (119) using injected $^{81m}Kr$ with SPECT during quiet breathing in FRC status and examining $\dot{Q}$ at 1.9 $cm^3$ lung region in awake human also observed that $\dot{Q}$ increased in the direction of gravity in supine, prone, LLD and RLD postures. Reed and Wood (127) studied regional blood flow distribution by using intravenous injected radioactive microspheres in pentothal anesthetized and mechanical ventilated dogs with 10 cm $H_2O$ PEEP found that $\dot{Q}$ increased down the lung be decrease in zone 4 in supine, prone, LLD, RLD, head up and head down postures.

In summary, the gravitational model predicts that pulmonary perfusion increases from non-dependent to dependent lung region. Blood flow at a given isogravitational plane depends upon interaction among alveolar, arterial blood, and venous blood pressures. Pulmonary blood flow will be altered as vertical height is changed. Pulmonary blood flow reduced in the most dependent lung region was ascribed to gravity effect of increasing interstitial pressure (78). However, the conclusions of gravitational model were drawn from data obtained using low-resolution methods to quantify blood

flow to large lung regions. The four-zone model of pulmonary blood flow distribution also fails to predict any organized variation in blood flow within isogravitational planes in the lung.

**Non-gravational factors**

**Lung Volume and pulmonary vascular resistance**

Lung volume also has a critical influence on blood flow distribution. Hughes et al (78) demonstrated gravity had less effect on $\dot{Q}$ as blood flow increased down the lung in upright human at total lung capacity (TLC). At residual volume, blood flow difference was less between apical and basal lung regions. At functional residual capacity (FRC), blood flow increased in dependent the lung up to 2/3 below the apex, then blood flow decreased toward the bottom. Lung volume had various effects on blood flow distribution in different zonal conditions. Beck and Lai-Fook (15) studied the relationship between pulmonary blood flow vs. gas volume at various perfusion pressures in isolated rabbit lungs and demonstrated that blood flow increased to the bottom in zone 3 regardless of changes in lung volume. However, in zone 2 conditions, blood flow decreased at lower lung volume and total lung capacity, but increased when lung volume was close to FRC. Overall, pulmonary vascular resistance was composed of cumulative extra-alveolar and alveolar resistance. At higher lung volumes, alveolar vessels between alveolar septa were compressed, while the corner vessels (extra-alveolar) between alveolar were pulled open. By contrast, at lower lung volumes, extra-alveolar vessels were compressed, but alveolar vessels were open. Thus, lung volume affects regional blood flow distribution in a complex way depending on zonal conditions and type of vessels.

The four-zone gravitational model (78; 159) was postulated based on low-resolution techniques that measuring blood flow within large region. However, with higher resolution techniques, blood flow measured in smaller regions produced a more complex picture. In addition to the vertical gradient of $\dot{Q}$, cranial-caudal and central-

peripheral gradients were observed in many studies (7; 60). These cranial-caudal and central-peripheral gradients were unexplained by the four-zone gravitational model. Greenleaf et al (56) studied spatial distribution of pulmonary blood flow in dogs in the LLD posture using injected radioactive microspheres obtained the blood flow distribution in 1-cm-thick lung slices. They found that regional blood flow in an individual lobe was greater in the periphery than in the interior. Hakim et al (61) using single-photon emission computed tomography in supine humans and dogs reported that blood flow was 10 fold greater in the central than in the peripheral lung regions. This gravity-independent blood flow inequality was independent of changes in cardiac output. When cardiac output doubled, blood flow increased uniformly in every part of the lung, maintaining the central-peripheral gradient (62). This unique finding was attributed to the resistive property of the pulmonary vascular tree. The central-peripheral gradient of $\dot{Q}$ was supported by studies in supine dogs (51; 153), prone sheep (152) and upright baboons (48) by even a higher resolution technique (~ 2 $cm^3$) using fluorescent microspheres. By contrast, Nicolaysen et al. (116) studied blood flow distribution in prone dogs with labeled albumin macroaggregates and 1-cm lung slices were imaged with a gamma camera. They found no central-peripheral gradient of $\dot{Q}$, but some gravity-unrelated inhomogeneity in blood flow distribution was observed at FRC. These contradictory findings may result from errors in reconstruction of 3-D images and filtering effect of the single-photon emission computed tomography technique.

Beck et al. (16) studied the vascular resistance with radioactive microsphere measuring blood flow at four different levels of Ppa-PA in dogs breathing 95% oxygen. They demonstrated that dorso-caudal regions had higher vascular conductance than ventro-cranial region in supine, head-up and LLD posture, independent of lung volume and vertical height. This study emphasized that intrinsic vascular conductance was an important factor affecting regional blood flow distribution besides gravity, lung inflation, hypoxic pulmonary vasoconstriction.

**Isogravitational perfusion heterogeneity**

Recent studies have shown that heterogeneity of pulmonary blood flow distribution was dependent on the spatial resolution (53; 55). As the piece size of lung became smaller and spatial resolution improved, the measured perfusion heterogeneity increased (49). Perfusion heterogeneity (SD/Mean) was about 55% when the pulmonary blood flow distribution was examined with lung piece size of ~2 $cm^3$ (50). As spatial resolution becomes higher near to the actual gas exchange area, perfusion heterogeneity might be greater (50). Although pulmonary blood flow distribution was heterogeneous, regional perfusion was spatially correlated, ie, neighboring regions of the lung often had similar flow magnitudes (52). The spatial correlation of pulmonary perfusion was attributed to the asymmetrical pulmonary vascular branching characteristics (50; 52). Recent studies (48; 50; 70; 71; 113; 114; 151; 152) using methods with high spatial resolution have demonstrated that isogravitational perfusion heterogeneity exists and that this variability was not random. This finding implies that the distribution of pulmonary blood flow is not dependent solely on gravity. This agrees with older studies in the dog that found that regional perfusion within isogravitational planes was not uniform (56; 116; 127). The spatial distribution of blood flow in anesthetized dogs at resting lung volume was only slightly related to gravity (50). Glenny et al. (50) also demonstrated that regional pulmonary blood flow was markedly heterogeneous within any isogravitational plane and independent of gravity in anesthetized dogs ventilated without PEEP. The effect of gravity explained only 4% of the variance of blood flow distribution in dogs when blood flow was measured in the prone and supine positions. The high degree of correlation between simultaneously aerosolized and intravenously injected microsphere distribution has been demonstrated by Robertson et al. (132). The results also showed that isogravitational ventilation heterogeneity exists.

**Non-gravitational distribution of flow**

Perfusion is predominated in dorsal regions regardless of body posture (16; 50; 120). These observations suggest that the anatomic structure of the pulmonary vascular tree is an important factor in determining pulmonary blood flow distribution (16). In the standing, awake horse, with a 50 cm vertical distance from the top to the bottom of the lung, blood flow increased was greater in the dorsal than in the ventral lung regions, opposite to the predictions of the gravitational model (70).

Pulmonary blood flow tends to have a radial distribution with greater perfusion of the central (hilar) regions of lung (60). Although isogravitational perfusion heterogeneity has been found in many species, this observation has not yet been confirmed in humans. Hughes speculated that isogravitational perfusion heterogeneity may result from differences in lung volume between quadrapeds and bipeds (77). Baboons have pulmonary vascular structure and a hypoxic response similar to those in humans and spend most of their time in the upright position. Results in baboons (48) suggest that gravity has more influence on the pulmonary blood flow distribution in upright primates compared to quadrapeds. However, gravity is still a secondary factor affecting the pulmonary blood flow distribution.

The findings of the high-resolution methods have questioned the belief that gravity plays the dominant role in determining the distribution of pulmonary perfusion. In addition, the presence of isogravitational perfusion heterogeneity in prone animals and gravity-independent central to peripheral flow gradients (152) imply that other factors in addition to gravity play a significant role in determining the distribution of pulmonary blood flow. Mure et al (114), using fluorescent microspheres found that the fraction of the blood flow to the left lung did not change between the LLD and supine posture. Moreover, the distribution of blood flow of each lung piece was highly correlated between supine and LLD posture and no gravitational gradient of blood flow was found in the LLD posture in dogs. This finding seriously questioned the role of gravity on the blood flow distribution in the lateral decubitus posture. In order to separate the contribution of gravity and vascular structure to reginal perfusion, Glenny et al (51) flew

the pigs on aircraft with a series of parabolas during weightlessness and 1.8-G conditions and regional blood flow was marked by injected fluorescent microspheres. They found that both gravity and pulmonary vascular branching structure affected regional pulmonary blood flow. Moreover, the structure of the pulmonary vascular tree was the primary determinant of regional perfusion.

**Atelectasis (mechanical factor)**

Local factors might affect pulmonary vascular resistance (PVR) and pulmonary blood flow distribution. For example, pulmonary vascular resistance is affected by lung volume. Alveolar corner vessels of intra-alveolar region and septal vessel respond in two different ways under the influence of lung volume expansion (87). Pulmonary vascular resistance is lowest when the lung volume equals FRC. Whether the lung volume is decreased or increased from FRC, the pulmonary vascular resistance is increased (25; 144). The increase in pulmonary vascular resistance when lung volume increases from FRC is attributed to compression of alveolar septal vessels. The increase in pulmonary vascular resistance when lung volume is reduced below FRC is attributed to an increased resistance of large extra-alveolar corner vessel. Old studies suggest that the increased pulmonary vascular resistance in the atelectatic lung is due to mechanical kinking or tortuosity of pulmonary blood vessels (25). However, recent studies provided evidence that the increased pulmonary vascular resistance in the atelectatic lung is mainly due to hypoxic pulmonary vasoconstriction rather than passive mechanical factor (18; 45; 121).

**Hypoxic pulmonary vasoconstriction**

Hypoxic pulmonary vasoconstriction (HPV) is a critical factor in regulating the regional pulmonary blood flow distribution. Unlike other systemic circulations such as the cerebral, coronary and renal circulations where blood vessel dilates in response to hypoxia, pulmonary arterioles constrict with hypoxia. HPV can divert pulmonary blood flow away from hypoxic regions toward normal regions of the lung (103) and achieve improved $\dot{V}_A/\dot{Q}$ matching and maintain efficient arterial oxygenation. The primary

stimulus for HPV is alveolar oxygen tension. However, HPV response is also influenced by the oxygen tension in the mixed venous blood especially in the presence of atelectasis (34). Other factors such as hypercapnia or abnormal pH also can contribute to HPV response. The blood flow diversion occurred within seconds in response to hypoxia, reaching a maximum at about 20 minutes in dogs (30) and in humans (26). Glasser et al. (45) showed that the maximal HPV response was reached at 30 minutes after atelectasis, longer than after exposure to hypoxic gas. Recent studies (35; 147) indicated that a relatively slow HPV response helped to improved ventilation and perfusion matching after 2 hours of exposure to hypoxic gas.

Marshall derived an equation describing the dose-hypoxic response relationship for HPV in canine lung (101). The pulmonary vascular resistance depends on the stimulus of oxygen tension. The oxygen tension ($PsO_2$) stimulus is determined by the alveolar oxygen tension and oxygen tension in the mixed venous blood. The HPV stimulus-response curve has a sigmoid shape, and pulmonary vascular resistance attained a 50% response at 55 mmHg $P_AO_2$ reaching a maximal response when $PsO_2$ equal 10 mm Hg. The increased pulmonary vascular resistance at $PsO_2$ of 10 mm Hg is about three times that with 100% $O_2$ ventilation (101). The stimulus- hypoxic response curve relating blood flow to pulmonary venous $PO_2$ showed that slope of the curve became steeper when $PO_2$ falls below 60 torr. The mean blood flow decrease by 11.8% for every 20 torr in $PO_2$ in dogs (13). HPV decreases blood flow to the hypoxic lung and increases the pulmonary perfusion pressure depending upon the size of the hypoxic segment. Small hypoxic segments of lung will predominantly have flow diversion where blood flow is diverted away from hypoxic lung towards normoxic lung. In contract, whole lung expose to hypoxia, such as exposure at high altitude, will only increase pulmonary arterial pressure as flow diversion to the normoxic lung is not possible (103). In contrast to the sigmoid shape stimulus-response curve in the dogs, a biphasic response of pulmonary vascular resistance with hypoxia was demonstrated by Sylvester et al (142) in the pig.

The strength of HPV differs across animal species. The HPV effect is most prominent in pigs with less collateral ventilation. Dogs possess extensive collateral ventilation and less intense HPV, although consistent HPV responses are demonstrated (90). HPV is critical to maintain ventilation and perfusion matching and reduced shunt in pathological conditions (100), while its function in the normal lung is unclear (104).

HPV alters the distribution of flow in the hypoxic lung. Pulmonary arterioles (30-50μm) were the major site responsible for vascular constriction during acute hypoxia. Pulmonary veins and capillary constricted minimally in response to acute hypoxia (29; 57). Both alveolar and extra-alveolar vessels demonstrated HPV response during hypoxia in pigs (143). Large pulmonary arterioles (> 500 μm) did not constrict in response to acute hypoxia (98). In contrast to in vivo findings, in vitro the HPV response occurred in pulmonary vessels of all sizes (105).

The vascular endothelium was not required to trigger the HPV response (106). Thus the sensor for hypoxia was most likely located in pulmonary vascular smooth muscle since vascular smooth muscle cell alone can cause vascular contraction during hypoxia (115). HPV might result from hypoxia induced vasoconstriction by opening calcium or closing potassium channels (146). Farrukh et al (38) showed that the effect of HPV was attenuated with lower extracellular calcium level. Recent studies using specific Ca+ and ATP-gated K+ channel antagonist (156) demonstrated that hypoxia acting via voltage-gated Ca + channel induced Ca++ influx and inhibited K+ currents in pulmonary arterial smooth muscle. Moreover, ATP-sensitive K+ channel induced HPV through depletion of sub-sarcolemmal ATP and attenuated K+ channel phosphorylation (163). Nitric oxide is an important pulmonary endothelium produced mediator and can cause pulmonary vasodilatation and modulate the potency of the HPV response (41). Another endothelial-derived factor, prostacyclin, might diminish the flow diversion from the hypoxic alveoli and reduce gas exchange efficiency (138).

Mechanical factors may also influence the effect of HPV. Positive end-expiratory pressure (PEEP) to well ventilated lung regions might reduce the effect of HPV in the underventilated lung regions due to pneumonia or in atelectatic lung regions (33; 96).

Therefore, PEEP might force blood flow through the atelectatic or flooded alveoli and causing an increased shunt and decrease in $PaO_2$. Increased pulmonary arterial and venous pressures can attenuate the potency of HPV (19). An increase in left atrial pressure to 25 mmHg, abolished the HPV response (95). Since $P\bar{v}O_2$ changes with cardiac output, both $P\bar{v}O_2$ and cardiac output can affect the HPV response. Acid-base status also modified the HPV response (21). In general, metabolic alkalosis inhibited HPV and metabolic acidosis augmented HPV. During metabolic alkalosis and respiratory alkalosis, HPV was significantly reduced and resulted in poor $\dot{V}_A/\dot{Q}$ matching and oxygenation in normal lung and under pathological conditions (32; 141).

In studies of unilateral hypoxia in prone and supine dogs using fluorescent microsphere, Mann et al (99) found in the hyperoxic lung that 90-95% of the blood flow heterogeneity and 70-80% of the variance in blood flow was nonspatially determined and atttributed this heterogeneity to the vascular structure. Compared to normoxia, the hilar-to-peripheral gradient in blood flow decreased with hypoxia but was unaffected by hyperoxia. The authors concluded that HPV exerts its effect on the regional distribution of flow in the hypoxic lung not the hyperoxic lung (99). This finding was consistent with measurements of $\dot{V}_A/\dot{Q}$ distribution using MIGET in studies where the left lower lobe was ventilated with hypoxic gas (31). $\dot{V}_A/\dot{Q}$ heterogeneity was increased in the hypoxic lobe compared to the lobe ventilated with 100% oxygen. The HPV-induced blood flow diversion measured using fluorescent microspheres was greater in the supine than prone posture (153). The mechanism might result from a less heterogeneous and a reduced gravity-dependent blood flow distribution in the prone posture. The conclusion of these studies was limited by the lack of regional ventilation data.

**Factors determining regional distribution of ventilation**

**Pleural pressure vertical gradient**

Ventilation is not distributed uniformly throughout the lung. A nonuniform spatial ventilation distribution has been found in many human and experimental animal studies (8; 24; 74; 82; 110). This regional difference in ventilation was thought to be due

primary to the vertical gradient in transpulmonary pressure (Ptp) and in regional lung volume. Many studies (11; 12; 75; 79; 89; 110; 140) have demonstrated a significant vertical Ptp gradient, particularly in the upright and supine body positions. A study by Milic-Emili et al. (110) using radioactive xenon in the intact thorax of human showed that upper alveoli were more expanded than the lower alveoli. This finding was attributed to the vertical Ptp. A Ptp gradient was mainly observed in the vertical direction (influence by the gravity), whereas Ptp was generally uniform along the horizontal direction. The vertical Ptp gradient was attributed to the lung weight (89; 160). The lung fits into the thoracic cavity and has been characterized with fluid-like property (89). The lung distortion was heavily influenced by the chest wall compliance and orientation. The lung was supported mainly by the hilar structure or peripheral structure in order to accordance with the chest wall change, the lower part of lung was sustained more pressure than the top lung. This leads to the topographical distribution of the pleural pressure. Compared to the bottom part of alveoli, the top alveoli were expanded by the weight of the lower alveoli. This finding was verified by the morphological measurements of alveolar size (46) and of lung density (74) from frozen dogs. In addition, factors such as lung inflation, body size and body position may influence magnitude of the Ptp gradient. For example, the vertical Ptp gradient decreased in the supine and lateral posture compared to the upright position (82) and diminished after applying PEEP (2) or during lung inflation (110). Studies by West and Matthews (160) using finite element analysis demonstrated that gravity acting on the upright lung confined within a rigid thorax generates a vertical Ptp gradient of 0.2 cm $H_2O.cm^{-1}$. This value for the gradient was less than values measured by a variety of experimental techniques, such as liquid-filled catheters, rib capsules and counter pressure device. In addition to the lung weight, the weight of the heart increased the vertical Ptp gradient due to lung weight (79; 97). Ganesan et al (43) considered the contribution of the abdominal weight and compliant diaphragm to the vertical Ptp gradient. Using finite element analysis, the vertical Ptp gradient was 0.2 cm $H_2O.cm^{-1}$ with the lung within a stiff chest wall. The vertical Ptp gradient increased to 0.5 cm $H_2O.cm^{-1}$ after stepwise inclusion of

the heart, compliant diaphragm, and abdomen. This implied that the weight of heart and abdomen and compliant diaphragm also play a role in determining the regional distribution of ventilation.

According to the vertical Ptp gradient and uniform intrinsic elastic properties of the lung, Milic-Emili (110) proposed a simple mechanical model to elucidate the static behavior of the lung in situ. At TLC, the top and bottom parts of the lung are uniformly expanded. With expiration from TLC, both top and bottom parts of the lung are located on the low compliant part of the static pressure-volume curve (Fig 2). Although the vertical Ptp gradient exists, differences in regional lung expansion should be very small.

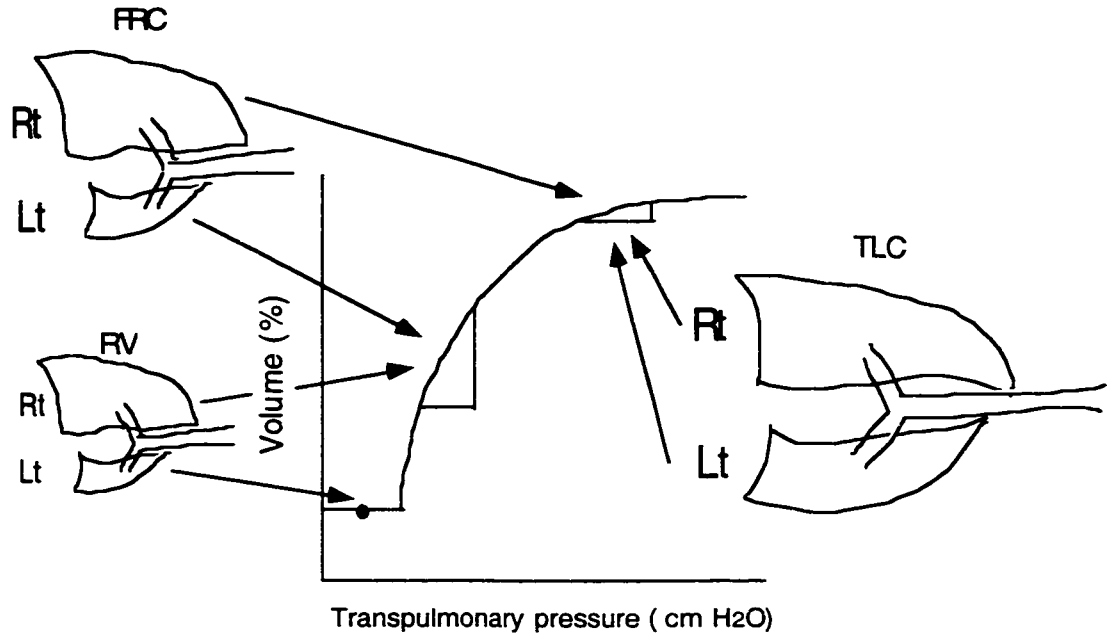


Fig 2. Schematic illustration demonstrating the nonuniformity of ventilation Distribution during awake breathing from FRC; functional residual capacity, RV: residual volume and TLC: total llung capacity. Rt: right lung, Lt: left lung

Therefore, regional ventilation will be uniform throughout the lung during full inspiration (TLC). When the lung volume decreases from TLC to FRC, the upper part of the lung remains on the low compliant part of the P-V curve, while the lower part of the lung remains at high compliant part of the P-V curve. During inspiration from FRC during awake breathing, transpulmonary pressure increases uniformly, and regional ventilation favors the dependent lung with it greater compliance. With exhalation from

FRC to RV, the Ptp of the lower part of the lung decreases, reaching its closing volume and trapping gas. In elderly humans and in disease lungs, this behavior occurs during part of the normal ventilation cycle with no ventilation in the dependent lung where closing volume is greater than FRC. When inflation from RV, unless the transpulmonary pressure exceeds the opening airway pressure in the dependent lung, ventilation goes preferentially to the nondependent lung.

Human studies (8; 82; 119; 129; 130) in the lateral decubitus position show that with spontaneous breathing, ventilation goes preferentially to the dependent part of the lung while with anesthesia and paralysis, ventilation goes preferentially to the non-dependent part of the lung. Despite the general conclusion can be drawn from the above human study, the methodology, position, anesthesia and ventilation conditions of the human studies was varied. Kaneko et al (82) using injected $Xe^{133}$ during FRC and counted at TLC in awake human found that pulmonary ventilation was greater in the dependent than the nondependent lung in all postures. Amis et al (8) using radioactive $^{85}Kr^{M}$ inhalation with scintillation counter in awake human during spontaneous ventilation with periods of breath holding, demonstrated that higher ventilation per unit volume in the lower lung than in the upper lung in the lateral postures. Rehder et al (129) using inhaled $Xe^{133}$ with $O_2$ in awake and anesthetized-paralyzed human subjects with thiopental, succinylcholine and meperidine showed that ventilation preferrential went to dependent part lung in spontaneous breathing while ventilation went to nondependent lung regions in anesthetized-paralyzed condition in right lateral posture. Orphanidou et al (119) using inhaled $^{81m}Kr$ with SPECT and studying the $\dot{V}_A$ at 1.9 $cm^3$ size lung in awake human during quiet breathing in FRC status found that $\dot{V}_A$ increased in the direction of gravity in supine, RLD and LLD postures but not when in the prone posture.

**The effect of mediastinal content shift and the shape of diaphragm**

The regional ventilation distribution is different between spontaneous awake breathing and paralyzed mechanically ventilated conditions. Froese et al (40) observed that in paralyzed and mechanically ventilated subjects, the motion of the diaphragm was

greater in the nondependent part than in the dependent part. In contrast, during awake spontaneous breathing, the motion of the diaphragm was greater in the dependent part. This behavior was confirmed by Roussos et al (135) who measured the distribution of regional lung volume with the radioactive gas. Roussos et al. (135) attributed this behavior to the transmission of the hydrostatic pressure gradient of the abdominal contents across the flaccid paralyzed diaphragm to the lung during mechanical ventilation, reducing the dependent lung volume and increasing ventilation to the dependent lung. By contrast, an actively contracting diaphragm during awake breathing can resist the hydrostatic gradient of the abdomen resulting in a different distribution of regional lung volume and ventilation (88; 155). Hoffman et al (73) using dynamic spatial reconstructor studied the regional air content in the dog and sloth and found that distribution of air content is more uniform in the prone than the supine posture. They pointed out that the weight of mediastinal contents, especially heart, was an important determinant on the distribution of air content in the intact thorax. Olson (117) studied the effect of posture on lung volume and pulmonary mechanics in unilateral pneumonectomized (left) rabbits and observed that the remaining lung volume (right) after pneumonectomy did not change between the supine and prone postures. However, the remaining lung volume increased in the left lateral decubitus posture more than in the right lateral decubitus posture. This finding suggested that the effect of mediastinal and abdominal contents on the remaining lung volume was more important in the lateral posture than in the prone and supine postures. Wiener et al observed that left lower lobe ventilation was impeded in the supine patient with cardiomegaly (161), while the ventilation improved in the prone posture. Albert et al (3) using computed tomography studied the regional lung volume compressed by the heart in human subjects and demonstrated that a large portion of the compressed lung volume was under the heart in the supine posture. In the prone position, lung compression is less because the weight of the heart is supported by the sternum. The above evidence indicates that the weight of heart can affect regional lung volume, and thus affect regional ventilation, perfusion and matching of ventilation and perfusion.

**PEEP-lung volume**

Positive end-expiratory pressure (PEEP) can improve arterial oxygenation by recruiting atelectatic or collapsed alveoli. The improvement of pulmonary gas exchange by PEEP is attributed to decreased intrapulmonary shunt and perfusion of low $\dot{V}_A/\dot{Q}$ regions by increasing $\dot{V}_A$ of these regions (36). A side effect of PEEP is increased lung stiffness. Thus PEEP reduces the compression of the dependent lung by the weight of the mediastinum and abdomen and increases closing volume above FRC, resulting in better ventilation to the dependent lung. Measurements of blood flow by fluorescent microspheres in anesthetized supine dogs (81) showed that PEEP increased the dorsal-to-ventral gradient of pulmonary blood flow, shifting blood flow to the dependent from nondependent lung regions. This behavior was consistent with predictions from the zone model. However, PEEP accounted for a small fraction of the total variance of the blood flow distribution. A large proportion of the total variance was attributed to structural factors (81).

In the lateral posture with anesthesia, FRC of the nondependent lung is markedly increased while that of the dependent lung is decreased (66; 67; 130). When PEEP is applied with mechanical ventilation, a greater fraction of the tidal volume goes to the nondependent lung (130). This might be attributed to compression of the dependent lung by increased compression of the dependent lung by the abdomen acting across a passive diaphragm, resulting in airway closure. This effect will cause the compliance of nondependent lung to be greater than that of the dependent lung.

In summary, in the lateral decubitus posture with anesthesia, the nondependent lung is well ventilated but poorly perfused, while the dependent lung is well perfused but poorly ventilated. PEEP restores FRC of the dependent lung back to that occurring in the awake state, locating the dependent lung to the more compliant part of the pressure-volume curve while forcing the nondependent lung to the less compliant part of the pressure-volume curve. Ultimately, the ventilation and perfusion matching and gas exchange were improved.

**The effect of lateral decubitus position on $\dot{V}_A$, $\dot{Q}$ and $\dot{V}_A/\dot{Q}$ matching**

**A) Atelectasis**

Airway closure often occurs in the dependent region of the lung in the lateral decubitus position (86). If the closing volume is less than the FRC, no airway will close during tidal breathing and these respiratory units are normally ventilated. When the closing capacity is larger than FRC, the respiratory unit with closed airways is in effect atelectatic with no ventilation. This respiratory unit with low $\dot{V}_A/\dot{Q}$ develops hypoxemia, resulting in hypoxic vasoconstriction and diverting blood flow to well ventilated regions.

**B) Distribution of ventilation & perfusion with anesthesia in closed chest animals**

With the induction of general anesthesia, lung volume of both nondependent and dependent lungs decreases. This effect moves the non-dependent lung to the less compliant part of the pressure-volume curve to the more compliant part of the curve and moves the dependent lung from the more compliant part to less compliant part of the PV curve. Thus the compliance of the non-dependent lung increases while the compliance of the dependent lung decreases after general anesthesia (94). In contrast to the awake state, in the lateral posture with anesthesia ventilation preferentially goes to the non-dependent lung instead of dependent lung. In addition, the mediastinum compresses the dependent lung and hinders dependent lung expansion. If the diaphragm is paralyzed, the abdominal contents impede the expansion of the dependent lung (129). When rabbits were inverted from the LLD to the RLD posture, lung volume at FRC was significantly reduced and the heart moved to a more dependent and dorsal position (118). This behavior suggests that the effects of the heart weight are different between the LLD and RLD postures.

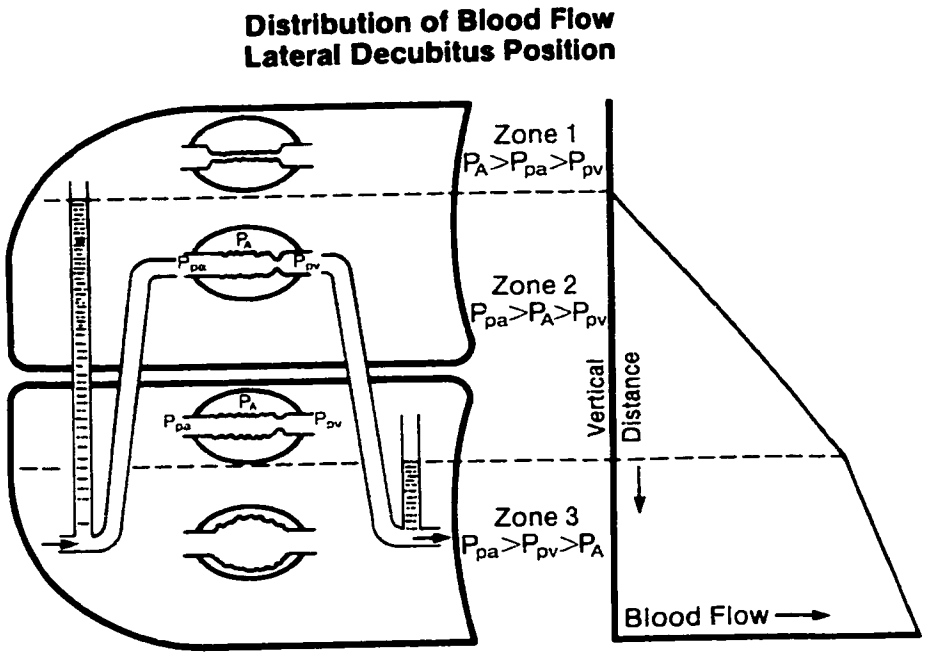


Fig 3 Effects of gravity on the pulmonary blood flow distribution in the lateral decubitus position. (Adapted from Benumof JL: Anesthesia for Thoracic Surgery, Chapter 4, P126)

In the lateral decubitus position, the vertical gradient of blood flow is smaller in the dependent lung than in the nondependent lung because of the reduced dependent lung volume (7). Based on the gravitational model, blood flow is greater in the dependent than in the nondependent lung because of the shift from zone 2 to zone 3 conditions with distance down the lung (Fig 3). Early studies using a method with low spatial resolution provided evidence that blood flow was decreased in the non-dependent lung in the lateral position (7; 82; 93; 119). One study most comparable to ours is that of Reed and Wood (127) who measured blood flow distribution in the anesthetized and left lateral positioned dog by using microspheres with flow normalized at TLC. A gravitational gradient in blood flow was observed and was more prominent in the non-dependent lung. This result was obtained under halothane anesthesia that probably reduced lung volume and produced dependent lung atelectasis (22). By contrast, blood flow measured using fluorescent microspheres in dogs showed no gravitational gradient in blood flow and no

change in the mean blood flow with a change in body position from the supine to LLD posture (114).

**B) Distribution of pulmonary blood flow and ventilation with anesthesia in open chest animals**

When the chest is open, the nondependent lung is no longer restricted by the chest wall. The increased ventilation observed in the dependent lung in the awake closed chest condition is diverted to non-dependent lung on opening the chest. However, with the chest open, perfusion is greater in the dependent lung than in the nondependent lung. This results in further mismatching of ventilation and perfusion. Bilateral ventilation in the open chest condition increases the alveolar-arterial oxygen partial pressure difference, and causes less optimal oxygenation (19). The reasons for these effects are not apparent. It may relate to the absence of pleural pressure alveolar gradient.

The lateral decubitus position is used in several surgical procedures, especially thoracic surgery. However, its effects on the pulmonary blood flow and ventilation distribution or $\dot{V}_A/\dot{Q}$ matching are not well understood. The lateral decubitus position is often used for the care of patients with unilateral lung disease, especially in the intensive critical care unit. Although there is some evidence describing the position effects on $PaO_2$ in patient with unilateral lung disease, there are limited data available for describing the effects of either right or left lateral position on gas exchange or pulmonary blood flow distribution. One study on the effect of the lateral position dependency on $PaO_2$ in 100 patients with unilateral lung diseases concluded that placing the healthy lung dependent did not always yield maximal $PaO_2$ (28). Therefore, it is important to understand the basic mechanisms of the gas exchange and $\dot{V}_A/\dot{Q}$ matching in the lateral decubitus position.

**Ventilation heterogeneity**

In the past, the regional distribution of ventilation studied by bronchospirometry was limited to a comparison of ventilation between the right and left lungs. With the

introduction of radioactive gases, more precise measurement of topographical differences in regional ventilation became possible. Hubmayr et al. (76), using metallic bead tetrahedra to mark lung parenchymal movement in spontaneous breathing dogs, inferred that regional ventilation was heterogeneous and stated that their results were inconsistent with the classic model of regional ventilation. Moreover, the variability of parenchymal expansion was also found by Rodarte et al (133) by using computed tomography with higher resolution. As technology continuously evolved, the distribution of regional ventilation could be measured by aerosolized fluorescent microspheres in the 2 $cm^3$ lung pieces. Recent high-resolution studies using 1-μm aerosolized fluorescent microspheres (5; 44; 132) or 0.005-μm 99mTc-labeled carbon particles (108; 109) revealed that regional ventilation was heterogeneous and both regional ventilation and perfusion was highly correlated. Regional ventilation heterogeneity was also found in human using nitrogen washout technique during microgravity condition in the shuttle fight study (124). These findings implied that regional ventilation was not solely determined by the gravity and challenged the framework that regional ventilation was gravity-mediated (110). Altemeier et al (4) demonstrated that regional ventilation distribution is similar to regional perfusion distribution, both having a fractal nature. Robertson et al (131) hypothesized that to achieve efficient gas exchange, both regional ventilation and perfusion must be highly correlated despite the heterogeneous ventilation and perfusion distributions. Regional ventilation may not be as heterogeneous as regional perfusion as the resolution increases because gas mixing and diffusion homogenize differences in regional ventilation.

**Ventilation-Perfusion Matching**

Because $\dot{V}_A$ and $\dot{Q}$ are unevenly distributed in the upright human lung, gas exchange efficiency is mainly determined by inequality of ventilation-perfusion ratios within the lung (157; 158). Ventilation-perfusion mismatch will reduce the potency of uptake and elimination of all gases. In general, the vertical distribution of $\dot{V}_A/\dot{Q}$

decreases from upper to the lower lung in the lateral decubitus position (7; 82; 93; 119). In the awake state, the distribution of $\dot{V}_A$ or $\dot{Q}$ relative to $\dot{V}_A/\dot{Q}$ showed no significant different between the supine and right lateral decubitus positions. However, in anesthetized-paralyzed subjects, the $\dot{V}_A/\dot{Q}$ mismatching increased (129). Kaneko et al (82) using injected $Xe^{133}$ in awake human during FRC status and counting at TLC with scintillation counter found that $\dot{V}_A/\dot{Q}$ was lowest at 20 cm from dependent lung in lateral position. $\dot{V}_A/\dot{Q}$ was decreased below this point but increased above this point. Amis et al (7) using intravenous infused radioactive $^{81}Kr^M$ with scintillation counter recording radioactivity during spontaneous ventilation and periods breath holding in awake human demonstrated that vertical distribution of $\dot{V}_A/\dot{Q}$ decreased from upper to lower lung in all postures but increased in the dependent lung in lateral and supine postures. Landmark et al (93) using injected $Xe^{133}$ with scintillation detector in both awake human with inspiration to TLC with a breath hold and anaesthetized subjected with a vasalva maneuver to an airway pressure around 25 to 40 cm $H_2O$ found that $\dot{V}_A/\dot{Q}$ was greater in the nondependent lung in supine, sitting and RLD postures. The distribution of $\dot{V}_A/\dot{Q}$ became less uniform in the RLD in anesthetized and paralyzed subjects. Orphanidou et al (119) using $^{81m}Kr$ with SPECT to examine the $\dot{V}_A/\dot{Q}$ distribution showed that $\dot{V}_A/\dot{Q}$ was decreased from top to the bottom in prone, RLD and LLD postures.

Previous studies (82; 93) using injected or inhaled radioactive gas to examine the distribution of $\dot{V}_A/\dot{Q}$ had some drawbacks. First, subjects often were asked to breath hold at total lung capacity during injection or inhalation of radioactive gas. Thus, the distribution of $\dot{V}_A/\dot{Q}$ did not represent that of quiet breathing from FRC. Second, both $\dot{V}_A$ and $\dot{Q}$ were not measured in the same time.

The multiple inert gas elimination technique developed by Wagner et al (150) is a standard method used to assess the distribution of $\dot{V}_A/\dot{Q}$. With injection of six gases covering a range of solubility, the retention and excretion of the different solubility gas are fitted to 50 compartment $\dot{V}_A/\dot{Q}$ distributions including shunt and dead space.

However, the MIGET cannot provide spatial information within the distribution of $\dot{V}_A/\dot{Q}$.

Melsom et al (109) studied regional ventilation and blood flow distribution in 1.5 $cm^3$ lung pieces simultaneously in awake goats using radioactive microspheres markers for blood flow distribution and 99m Tc-aerosols as a ventilation tracer. They found no systemic gradient of $\dot{V}_A/\dot{Q}$ ratio down the lung. In addition, the distribution of $\dot{V}_A/\dot{Q}$ was narrower than either the distribution of $\dot{V}_A$ or $\dot{Q}$. Prisk et al (123; 125) studied distribution of $\dot{V}_A/\dot{Q}$ in normal human subjects in both gravity and microgravity condition and stated that gravity was not the major factor determining the $\dot{V}_A/\dot{Q}$ distribution. Based on the highly correlated $\dot{V}_A$ and $\dot{Q}$ distributions and efficient gas exchange in normal lung, Altemeier et al (4) pointed out the three possible explanations for $\dot{V}_A/\dot{Q}$ matching: changes in $\dot{Q}$ adjust to changes in $\dot{V}_A$, changes in $\dot{V}_A$ adjust to changes in $\dot{Q}$ or $\dot{V}_A$ and $\dot{Q}$ passively matched through innate pulmonary structure. Regional ventilation matching to $\dot{Q}$ was ruled out because minimal ventilation redistribution occurred during microembolism in pigs (6).

The effect of hypoxic pulmonary vasoconstriction in normal lung has not been well studied. Although hypoxic pulmonary vasoconstriction is an appealing mechanism to ensure the matching of regional ventilation and perfusion, vasomotor tone has been shown did not account for the ventilation and perfusion coupling and blood flow heterogeneity in baboon with infusion of a vasodilator (54). Altemeier el al (4) proposed that repetitive branching bronchus and vascular structure would better explain the high correlation between $\dot{V}_A$ and $\dot{Q}$ and achieve efficient gas exchange. They reasoned that the repetitive fractal branching structure was the most effective way to fill the three-dimensional structure and reduced energy consumption for matching $\dot{V}_A$ and $\dot{Q}$.

There is no general agreement about the vertical (gravitational) distribution of $\dot{V}_A/\dot{Q}$. Wilson and Beck (162) derived a model to describe the relationship among the ventilation heterogeneity, blood flow heterogeneity and ventilation-perfusion heterogeneity. The variance of the $\dot{V}_A/\dot{Q}$ distributions equaled the sum of the variance

of $\dot{V}_A$ and $\dot{Q}$ distributions and minus product term of correlation coefficient between $\dot{V}_A$ and $\dot{Q}$ and standard deviation of $\dot{V}_A$ and $\dot{Q}$. Since the gas exchange was efficient and with prominent $\dot{V}_A$ and $\dot{Q}$ heterogeneity in the normal lung, one can speculate that coefficient of correlation between $\dot{V}_A$ and $\dot{Q}$ was very high based on the Wilson and Beck's model (131; 162). The strong correlation between $\dot{V}_A$ and $\dot{Q}$ remained high across different sample size by using high-resolution fluorescent technique and fractal analysis supported the above speculation (131). In summary, the complexity of regional ventilation and perfusion matching may not be simply attributable to the overall effect of gravity on the pulmonary vasculature and parenchyma.

Body position may affect both ventilation and pulmonary blood flow distribution. Oxygenation and pulmonary gas exchange improvement in the prone position in the anesthetized pig was attributed to a decreased heterogeneity of the ventilation distribution and increased correlation of the ventilation and pulmonary blood flow distribution (17; 113). Most studies have shown that the decreased perfusion heterogeneity in the prone posture when compared to the supine posture, with resultant decreased heterogeneity of the $\dot{V}_A/\dot{Q}$ distribution (as measured by MIGET ) in the prone position is due to improved correlation of $\dot{V}_A$ and $\dot{Q}$(17; 113). The following scatter plots of ventilation vs. blood flow for the same lung piece in either prone and supine position show that ventilation and perfusion are better correlated in the prone posture compared to supine (Fig 4).

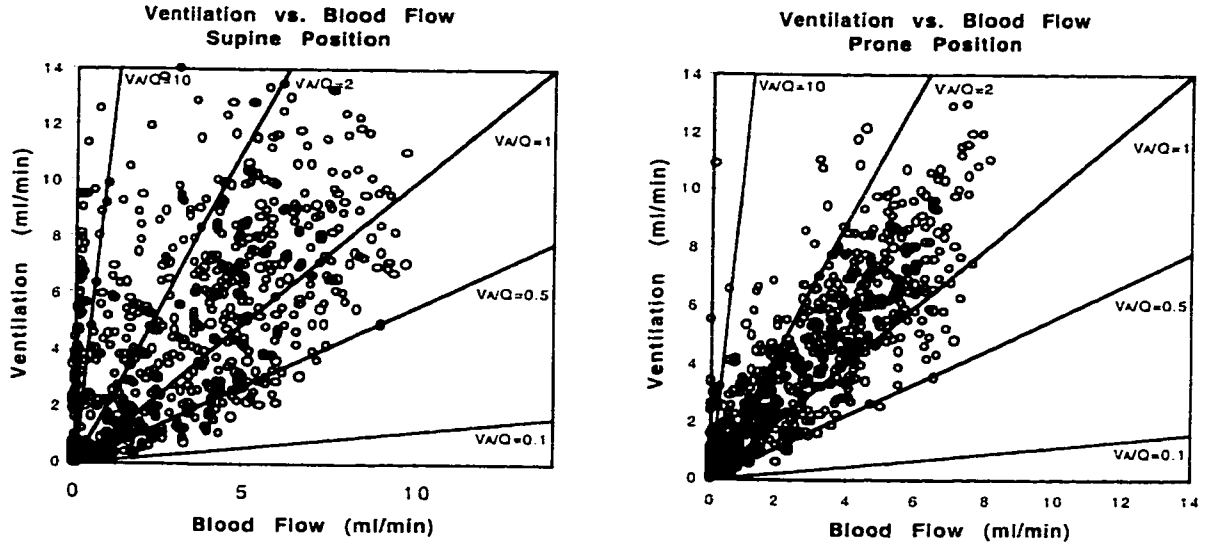


Fig 4. Position effect on ventilation and perfusion matching for each lung pieces (adapted from Mure et al. *J Appl Physiol* 88: 1076-1083, 2000.)

## Modes of mechanical ventilation

### Differential ventilation with unilateral PEEP *vs.* conventional mechanical ventilation

The volume of the nondependent and dependent lung is reduced during general anaesthesia and mechanical ventilation whe the diaphragm was paralyzed. Because the combined effect of the weight of mediastinal contents (3; 73; 117; 118) and weight of abdominal contents induced the cranial shift of the relaxed diaphragm (88), the dependent lung has a greater reduction in lung volume than nondependent lung. Thus, the transpulmonary pressure of the dependent lung is reduced (1; 2). This enhanced small airway closure and reduced ventilation of the dependent lung (63). Ventilation preferentially goes to the nondependent lung due to poorer lung compliance (110; 129; 130) and increased airway resistance of the dependent lung.

The above hypotheses were verified by computerized tomography studies (86; 145). Dense lung areas appeared immediately in the dependent region after induction of anesthesia in the supine human. Both human (22) and animal (65) studies suggested that the dependent lung density was represented atelectasic regions and probably resulted

from a reduction in the lung elastic recoil. Based on the gravitational model, perfusion increased to the dependent lung due to the force of gravity. The inequality of regional ventilation and perfusion in the dependent lung produces $\dot{V}_A/\dot{Q}$ mismatching and results in an increased alveolar and arterial $O_2$ tension difference (20).

Application of positive end-expiratory pressure (PEEP) reduces the decrease of lung volume of the dependent lung. However, bilateral PEEP does not evenly distribute ventilation between the nondependent and dependent lungs. Instead, the nondependent lung becomes more expanded than the dependent lung because of its greater compliance (64; 130). Moreover, by increasing alveolar pressure, positive end-expiratory pressure reduces pulmonary blood flow uniformly in the lung, especially in the non-dependent lung (66; 67). Furthermore, bilateral PEEP decreases cardiac output by interfering with venous return and thereby increases blood flow to dependent lung.

In order to match ventilation and perfusion in the lateral decubitus posture during general anesthesia, differential ventilation with unilateral PEEP to the dependent lung has been proposed as a mode of ventilation which is better than conventional ventilation with bilateral PEEP (63). Maintaining regional ventilation in proportion to regional perfusion can be achieved by separately ventilated individual lung with double-lumen endobronchial tube in the lateral posture. In addition, PEEP applied solely to the dependent lung can diminish its effect on reducing the venous return. Instead of allowing gas distribution to freely distribute between nondependent and dependent lung during conventional ventilation with single-lumen tube, differential ventilation with equal ventilation to both lungs and dependent PEEP improved $PaO_2$ and reduced A-a$DO_2$ in anesthetized humans (9). In addition, this ventilation technique also worked in intensive care patients with bilateral lung disease and respiratory failure (10; 63). A human CT scan study (86) showed that the atelectatic region, in the dependent lung was improved by differential ventilation with unilateral dependent PEEP in the lateral decubitus posture. Moreover, the shunt and perfusion of region with low $\dot{V}_A/\dot{Q}$ ratios measured with multiple inert gas elimination technique (MIGET) was reduced. However, MIGET provided overall $\dot{V}_A/\dot{Q}$ matching, shunt and deadspace information with no spatial

information. Thus, it is still not clear that improved $\dot{V}_A/\dot{Q}$ matching and increased $PaO_2$ in the lateral position with differential ventilation and unilateral dependent PEEP is mainly due to changes in perfusion, ventilation or both.

**Hyperoxia and one lung ventilation (left lung atelectasis) modified the effect of lateral posture and PEEP on $\dot{Q}$, $\dot{V}_A$ and $\dot{V}_A/\dot{Q}$ distribution**

Thoracic surgery is usually performed with the patient in the lateral decubitus posture. The operative field is the non-dependent hemi-thorax. Initially, bilateral lung ventilation is used during chest wall incision. In order to enhance surgical exposure, unilateral ventilation with the collapse of the non-dependent lung is employed during pleural incision. Basically, the nondependent unventilated lung is a shunt region during unilateral lung ventilation. Therefore, compared to bilateral ventilation, unilateral ventilation creates greater alveolar-to-arterial oxygen difference and reduced arterial oxygen tension (18; 45; 58; 59). However, passive mechanical factors and hypoxic pulmonary vasoconstriction in the non-dependent atelectatic lung helped to reduce the shunt during unilateral lung ventilation. The dependent lung may suffer from a reduced lung volume and ventilation due to mediastinal and abdominal compression. The dependent lung with lower ventilation and perfusion ratios is often supplied with high-inspired oxygen, which may result in absorption atelectasis.

Studies using dogs (80) and (117) rabbits after pneumonectomy demonstrated that the remaining lung after unilateral pneumonectomy will fill the thoracic cavity. However, the effect of the mediastinal shift on the hyperinflated remaining lung (such as unilateral lung atelectasis with PEEP in the other lung) has not yet been studied.

Although many studies have addressed the blood flow redistribution between lungs, there have not been any pervious studies on the spatial distribution of perfusion and ventilation during unilateral ventilation. Hypoxia may occur during unilateral lung ventilation (128). In addition to shunt, the spatial inequality of ventilation and perfusion in the ventilated lung may also contribute to hypoxia.

Prefaut et al. (122) suggested that hypoxic pulmonary vasoconstriction occurred when closing volume exceeded FRC in the dependent lung region in supine human, modifing the gravity dependent blood flow distribution. In other words, the vertical distribution of perfusion will be reversed by the hypoxic pulmonary vasoconstriction. When the subjects breathed oxygen-enriched gas, hypoxic pulmonary vasoconstriction was abolished and blood flow increased to the dependent lung. In the lateral decubitus posture with unilateral lung ventilation, HPV may occur in the dependent lung with air breathing. Therefore, with 100% $O_2$ breathing, the passive mechanical factors affecting the distribution of perfusion will be further examined by the high-resolution technique fluorescent microsphere technique.

**Specific Aims**

Although extensive work has been done to address the regional distribution of blood flow, ventilation and $\dot{V}_A/\dot{Q}$ in the past studies with high-resolution methods stressed the complexity of lung structure and function and offered a different perspective on regional distribution of blood flow, ventilation and gas exchange. In addition, very few studies have addressed the lateral posture effect on $\dot{Q}$, $\dot{V}_A$ and $\dot{V}_A/\dot{Q}$ distribution. The experimental findings with low-resolution techniques in the past studies were confined to whole lung, individual left and right lung or individual lobe. Other important non-gravitational factors, such as mediastinal shift and abdominal content induced individual lung volume changes in the lateral decubitus posture and their effect on regional perfusion and ventilation has not been addressed in any detail.

With the advantage of the high-resolution fluorescent microsphere technique, the proposed studies will examine the mechanisms involved and fill the gap in our understanding about the regional distribution of perfusion, ventilation and gas exchange in the lateral decubitus posture. Potential factors such as gravity, regional pulmonary vascular resistance, intrinsic pulmonary vascular and bronchus branching structure, and asymmetrical effect of the heart and regional lung expansion will be examined.

The experiments were designed to assess the effect of lateral posture and lung volume change on the distributions of $\dot{Q}$, $\dot{V}_A$ and $\dot{V}_A/\dot{Q}$. Three major questions are studied in this thesis. First, how do left and right lateral postures affect individual lung volumes, $\dot{Q}$, $\dot{V}_A$ and regional gas exchange? Second, how do unilateral and bilateral PEEP affect relative volumes, $\dot{Q}$, $\dot{V}_A$ and regional gas exchange in the lateral decubitus posture? Third, how does unilateral atelectasis modify lateral postural and PEEP-induced effects on lung volume, $\dot{Q}$, $\dot{V}_A$ and gas exchange? In order to answer these questions, three experimental protocols were designed to evaluate the regional distribution of $\dot{Q}$, $\dot{V}_A$ and $\dot{V}_A/\dot{Q}$ in the lateral decubitus posture.

Chapter 2 describes the experimental techniques used to measure individual lung volume, overall shunt, deadspace and $\dot{V}_A/\dot{Q}$ heterogeneity and regional distribution of $\dot{Q}$, $\dot{V}_A$ and $\dot{V}_A/\dot{Q}$, as well as predicted regional $PaO_2$, $PaCO_2$ and $A\text{-}aDO_2$ in the anesthetized dog.

Chapter 3 addresses the first question by examining the effect of changing from the right to left lateral decubitus on the spatial distributions of perfusion and ventilation. In addition, the effect of 10 cm $H_2O$ PEEP is studied.

Chapter 4 describes how different modes of mechanical ventilation (differential ventilation) with unilateral dependent or bilateral PEEP compared with conventional mechanical ventilation (addressed in first chapter) affect lung volume, spatial distribution of ventilation and perfusion and regional gas exchange in left lateral decubitus posture in the anesthetized dogs.

Chapter 5 deals with the effects of left lung atelectasis in conjunction with PEEP and body positions on the ventilated lung. During unilateral ventilation, I examine how the left lung atelectasis affects the spatial distribution of $\dot{Q}$, $\dot{V}_A$, $\dot{V}_A/\dot{Q}$ and $P_RO_2$ in the ventilated lung in both left and right lateral decubitus posture and with PEEP. These studies attempt to provide more detailed mechanistic explanation of lateral posture effect on regional distribution of $\dot{Q}$, $\dot{V}_A$ and $\dot{V}_A/\dot{Q}$ in normal and atelectasic lung.

# CHAPTER 2

# GENERAL METHODS

## Animal preparation

Healthy mongrel dogs of either sex were used in these studies. Animals were anesthetized with pentobarbital sodium (~4-8mg·kg$^{-1}$) intravenously and maintained with a pentobarbital infusion sufficient to achieve a surgical plane of anesthesia and eliminate spontaneous ventilation (~10-17 mg· kg$^{-1}$· h$^{-1}$). The trachea was orally intubated with a single-lumen endotracheal tube by the direct viewing of the vocal cords with a larygoscope. Catheters were placed in one femoral artery and both femoral veins by cutdown procedure to hemodynamics. A pulmonary artery catheter was introduced into the right external jugular vein and used for measuring cardiac output $\dot{Q}_T$ (thermal dilution) and core temperature Tc. Systemic arterial (Pa), pulmonary arterial (Ppa), pulmonary arterial wedge pressure (Ppcw) and airway pressure (Paw) and airway pressure were recorded continuously on a data management system (Western Graphic Mach 12 DMS 1000). Tracheostomy was performed and oral entotracheal tube was removed and inserted directly via the subcricoid tracheostomy and securely fixed with tape. The tip of trachea tube was carefully placed before the carina of trachea to prevent one-lung ventilation.

Dogs were mechanically ventilated with Harvard single piston ventilator (Harvard instruments, south natick, MA) with tidal volume 15 ml· kg$^{-1}$ and the respiratory rate was adjusted to maintain $PaCO_2$ between 35 and 40 mmHg. The tidal volume was maintained constant throughout the study. The lungs were hyperinflated every 15-30 min to prevent microatelectasis. PEEP was generated by immersion of the distal expiratory tube in the water. Minute ventilation was measured with a spirometer. End-tidal $PCO_2$ and $PO_2$ were measured with a mass spectrometer (Perkin Elmer, Medical Gas Analyzer Instrumentation Laboratories 1302). Anatomic dead space $V_D$ was determined

from exhaled end-tidal $P_{ET}CO_2$ and expiratory air flow were digitally sampled with an infrared $CO_2$ detector (Perkin Elmer, Plumsteadville, PA) and a pneumotachograph, respectively. Arterial and mixed venous blood gases were measured with an automated blood gas analyzer (ABL 300, Radiometer, Copenhagen, Denmark) and corrected for temperature. Body temperature was maintained using heat lamps and pads.

**Separated lung preparation**

A double-lumen endotracheal tube (broncho-Cath, left; Mallinckrodt Medical, Inc.) was inserted via a subcricoid tracheostomy. The complete isolation of left lung from the right lung was confirmed by hyperventilating one lung and checking for changes in volume in the other lung as indicated by an absence of air bubbling from an extension tube immersed in water and no significant airway pressure elevation. In addition, no cross contamination was detected when each lung was ventilated with helium. Both lungs were ventilated synchronously with a dual-piston ventilator (Harvard Instruments, South Natick, MA). Both tracheal and bronchial tube of double-lumen endotracheal tube were connected to separate ventilator. Thus, gas was able to distribute freely to both right and left lungs. After left and right tidal volumes were determined in turn by in-line pneumotachographs (Korr Medical Inc, Utah, USA), both lungs were connected to a Harvard dual-piston ventilator via separate gas circuits. When the separated lung preparation was used, the right lung was ventilated with room air or 100% $O_2$, and after the left lung was made atelectatsis, the right lung was ventilated with different levels of PEEP.

**Functional residual capacity measurement**

The Helium (He) gas dilution technique (69) was used to measure FRC. The anesthetized dog was connected to a large syringe containing He gas. The helium concentration in the lung and syringe was equilibrated by ventilating to TLC several times. The amount of helium gas before equilibrium equaled the amount of helium gas after equilibrium. The initial and final helium concentration was measured usnig the mass spectrometer. FRC of total lung can be calculated from the mass balance equation. [ $C_1$

x $V_1 = C_2$ x ($V_1 + V_2$), where $C_1$ is the initial He concentration in the syringe volume, $C_2$ is final He concentration, $V_1$ is initial syringe volume, and $V_2$ is the functional residual capacity (FRC) of the dog.] FRC of right and left lung in right lateral decubitus, left lateral decubitus, supine and prone position and in 0 cm or 10 cm PEEP were measured using a single lumen tracheal tube. For the separated lung experiment, a Kottmeier double-lumen endotracheal tube was used to measure FRC in each lung.

**Multiple inert gas elimination technique measurement of ventilation-perfusion distribution**

Theory

Analysis of the exchange property of a trace amount of inert gases infused into the venous circulation and excreted by the lung can provide information of shunt, dead space and distribution of $\dot{V}_A/\dot{Q}$ (150). According to Henry's law, the blood concentration of inert gas is proportional to its partial pressure. Under the assumption of steady state gas exchange, in the absence of diffusion limitation between alveolar gas and end-capillary blood, and non-pulsatile ventilation and perfusion (150), the relationship between alveolar, arterial and mixed venous partial pressures of inert gases for a single compartment lung model can be derived from mass balance principle (68).

$$\frac{Pa}{P\bar{v}} = \frac{P_A}{P\bar{v}} = \frac{\lambda}{\lambda + \frac{\dot{V}_A}{\dot{Q}}}$$

The ratio of Pa (arterial) to $P\bar{v}$ (mixed venous) partial pressure is defined as inert gas retention (R) and the ratio of PA to $P\bar{v}$ is defined as inert gas excretion (E). Thus, the retention or excretion of inert gas depends on the blood-gas partition coefficient ($\lambda$), the alveolar ventilation $\dot{V}_A$ and alveolar perfusion ($\dot{Q}$). When an inert gas with $\lambda$ = 1 pass is eliminated through the homogeneous lung with $\dot{V}_A/\dot{Q}$ = 1, the retention of this inert gas = 0.5. Half of this inert gas will be retained in the blood and the other half will be excreted by the alveolar (Fig 5). In terms of $\lambda$, more inert gas will be retained if the higher $\lambda$ gas is eliminated through the same $\dot{V}_A/\dot{Q}$ regions, while less will be remained with low $\lambda$

gas flow through this regions. In terms of $\dot{V}_A/\dot{Q}$, with same $\lambda$ inert gas, low $\dot{V}_A/\dot{Q}$ region will retain more inert gas than high $\dot{V}_A/\dot{Q}$ regions.

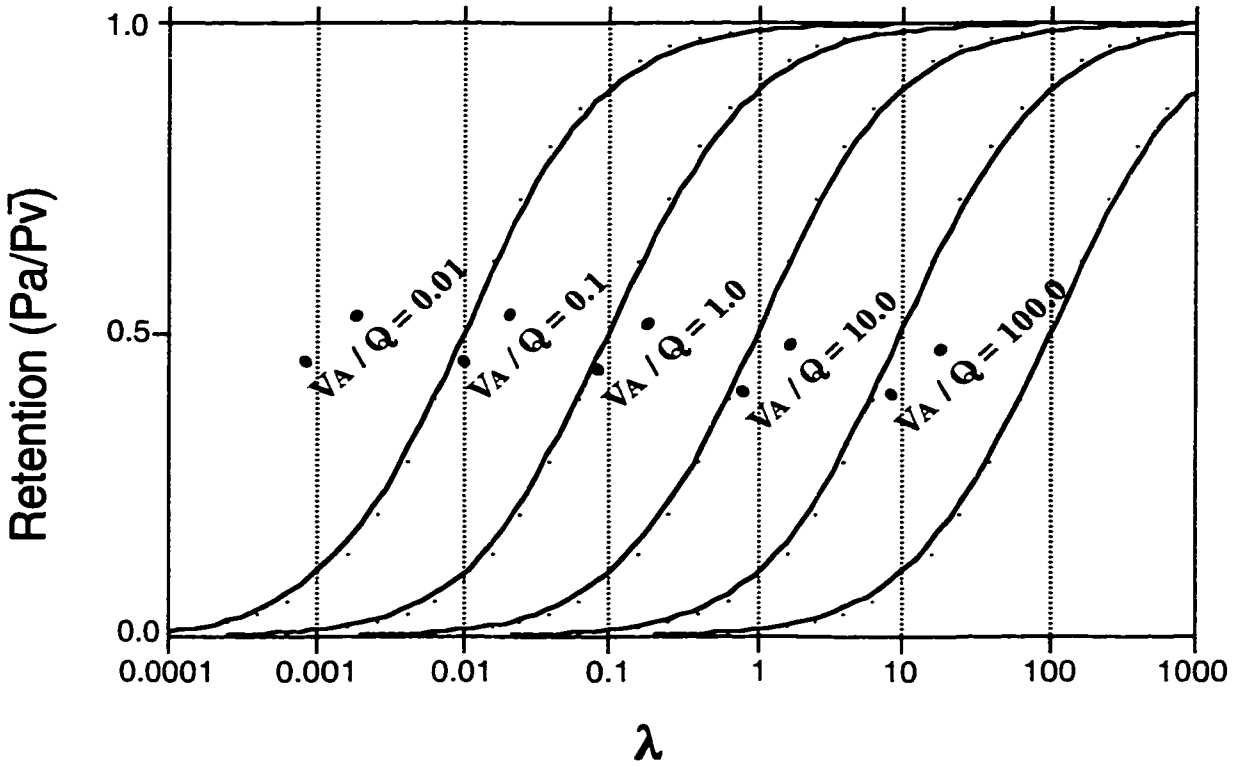


Fig 5. Retention of inert gas plot against blood-gas partition coefficient ($\lambda$) with respect to different $\dot{V}_A/\dot{Q}$

However, the lung is made up of millions of alveoli with a wide range of $\dot{V}_A/\dot{Q}$ distributions, including shunt and deadspace regions. The simple lung model described above can not really capture the complexity of different gas exchange regions. Wagner et al (150) developed a method to estimate the continuous distributions of $\dot{V}_A/\dot{Q}$ ratios. The lung was modeled as 50 compartments including shunt and dead space. The fraction of total blood flow and ventilation was assigned and distributed to different $\dot{V}_A/\dot{Q}$ regions and created the 48 $\dot{V}_A/\dot{Q}$ compartments. The overall retention and excretion in the modeled lung can be calculated from the sum of the R & E from individual compartments,

$$R_i = \frac{\sum_{j=1}^{n}\left(\frac{\dot{Q}_j * \lambda_i}{\lambda_i + \dot{V}_j/\dot{Q}_j}\right)}{\sum_{j=1}^{n}\dot{Q}_j} \qquad E_i = \frac{\sum_{j=1}^{n}\left(\frac{\dot{V}_j * \lambda_i}{\lambda_i + \dot{V}_j/\dot{Q}_j}\right)}{\sum_{j=1}^{n}\dot{V}_j}$$

where i represents each gas and j indicates the one of the 48 compartments. With an iterative process, the distribution of $\dot{V}_A$ and $\dot{Q}$ among different compartment was adjusted and compared to measured R and E to minimize the sum of squares between calculated and measured R. Although the recovered distributions of calculated blood flow was compatible with original theoretical distribution of blood flow in both unimodel and bimodel distributions with narrow or wide functions, there is no unique solution for the $\dot{V}_A/\dot{Q}$ distribution of 50 compartments (37). It is unlikely that only six inert gases can exactly produce the distributions of $\dot{V}_A/\dot{Q}$ to 50 compartments.

Hlastala et al. (72) offered an alternative approach to analyze the MIGET data. They took the raw data of both R and E of these six inert gases plotted against $\lambda$ and used the 50-compartment analysis. The ideal homogeneous R and E curve can be generated with measured $\dot{V}_A$, $\dot{Q}$ and known $\lambda$ of six inert gases. The measured raw data of R and E of the six inert gases is compared with the computer predicted curve. In the ideal homogenous lung (single compartment), the R and E curve will superimpose, but will separate in the multiple compartments of a heterogeneous lung. With shunt and deadspace, the E curve will be positioned below and the R curve will be positioned above the ideal curve (fig 6). By definition, there is no interaction between ventilation and perfusion in regions of deadspace where there is no perfusion. Addition of deadspace reduces the excretion of inert gas and depressed the excretion curve, while the retention curve was not affected. Thus, all E values were reduced by a fraction ($V_D/V_T$) with respect to the homogeneous excretion curve. For example, higher $\lambda$ inert gases can totally excrete passing through alveoli, but the E of high $\lambda$ inert gas can only be eliminated (1- $V_D/V_T$) with the existence of dead space.

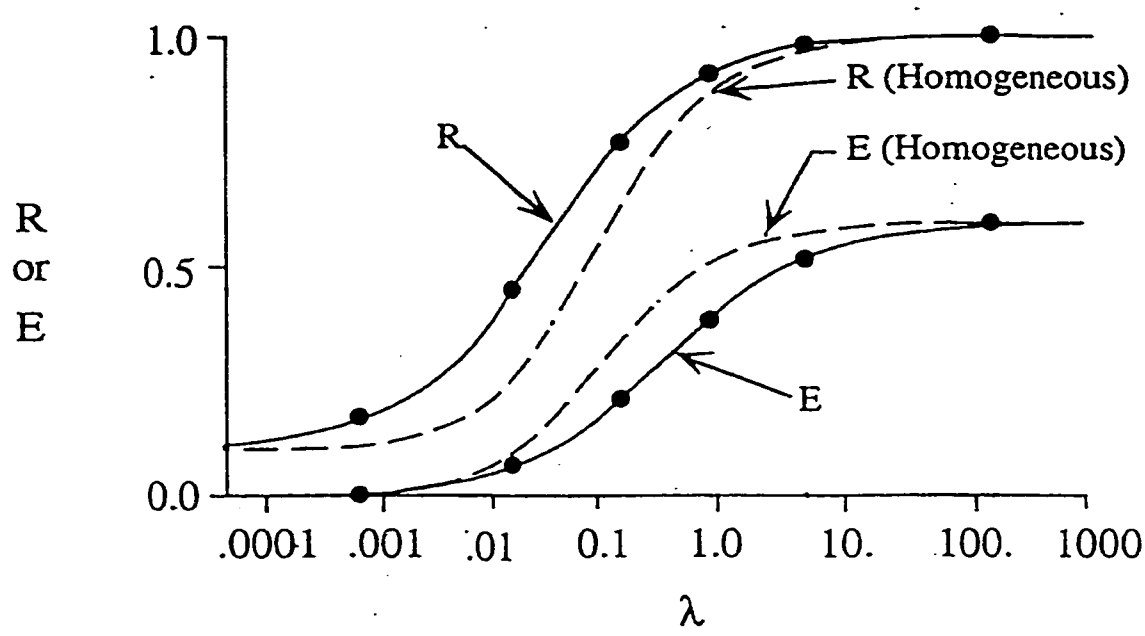


Fig 6. Retention and excretion of inert gas versus blood-gas partition. Coefficient ($\lambda$) in both ideal (dotted lines) and heterogeneous lung (solid lines) with shunt ($\dot{Q}s/\dot{Q}t$) and deadspace ($V_D/V_T$). The total area, (a-A)D area, between homogeneous and heterogeneous R and E curves represented $\dot{V}_A/\dot{Q}$ heterogeneity (68).

Shunt is a region with blood flow in an atelectatic region with no ventilation (right to left shunt). The effect of shunt is to increase retention of all inert gas with respect to the fraction of total blood flow with no effect on the excretion. This resulted in every R value increasing by an amount equaled to $\dot{Q}s/\dot{Q}t$ times 1-R (72). The lowest $\lambda$ gas will have R value equal to shunt ($\dot{Q}s/\dot{Q}t$) and the highest $\lambda$ gas will totally remained in blood with R = 1. The shunt and dead space can be determined from the extrapolation limit of the retention and excretion curve. The accuracy of the shunt and dead space depended on the precision of measured R value of lower $\lambda$ gas and the E value of higher $\lambda$ inert gas.

With increasing $\dot{V}_A/\dot{Q}$ heterogeneity in this 50-compartment homogeneous lung model, the R and E curves separate from the ideal $R_{homo}$ and $E_{homo}$ curves. Because the perfusion comes more from alveoli with lower $\dot{V}_A/\dot{Q}$ than from alveoli with mean

$\dot{V}_A/\dot{Q}$, the heterogeneous retention curve lies above the homogeneous retention curve. In addition, the ventilation comes more from alveoli with $\dot{V}_A/\dot{Q}$ greater than the mean. Thus, the heterogeneous excretion curve lies below the homogeneous excretion curve. Total $\dot{V}_A/\dot{Q}$ heterogeneity is the sum of the areas between R and $R_{homo}$ curves indicating blood flow heterogeneity whereas the ventilation heterogeneous is the sum of the areas between E and $E_{homo.}$ curves (68; 72). The arterial and alveolar difference (a-A)D of MIGET was used quantify the $\dot{V}_A/\dot{Q}$ heterogeneity. The amount of (a-A)D resulting from $\dot{V}_A/\dot{Q}$ heterogeneity equals the sum of areas between R and $R_{homo}$ and E and $E_{homo}$ curves. The major portion of (a-A)D comes from the $\dot{V}_A/\dot{Q}$ regions with intermediate $\lambda$ inert gas and approached zero in the $\dot{V}_A/\dot{Q}$ regions with higher and lower solubility gas.

**Experimental method**

Six inert gases (sulfur hexafluoride, ethane, cyclopropane, halothane, diethyl ether, and acetone), covering a wide range of blood-gas partition coefficients diluted in 5% dextrose solution, were infused in the jugular vein (149). After one hour to achieve a steady state, expiratory gas was collected after flowing through Plexiglas mixing chamber. The arterial and mixed venous blood were drawn simultaneously and mixed expired gas was sampled after a time delay calculated from the ratio of the volume of the mixing tube to $\dot{V}_E$. The inert gas concentration of every gas sample was measured by gas chromatography using a flame ionization or electron capture detector. To avoid water vapor condensation and loss of highly soluble gases, gas samples were kept warmer than body temperature. Gas concentration in blood sample was measured after equilibrating in an air-filled syringe placed in a continuously shaking water bath for 45 min. The equilibrated gases were drawn into gas tight syringe and injected in the gas chromatograph for analysis. The initial blood concentration was calculated from the gas extraction method as described by the Wagner et al (149).

Each retention ratio ($R=P_a/P_V$) and excretion ratio ($E=P_E/P_V$) of the six inert gases resulted in information about the distribution of blood flow to regions of no perfusion (shunt), ventilation to regions with no blood flow (dead space), and three modes of ventilation and perfusion in the middle zone. We took actual retention and excretion ratio of each inert gas and plotted the curve, and calculated dead space, shunt, and arterial-alveolar difference (a-A)D. $\dot{V}_A/\dot{Q}$ heterogeneity was quantified from the area under the curve of (a-A)D vs. blood-gas partition coefficient ($\lambda$) on a log scale (72). Other $\dot{V}_A/\dot{Q}$ heterogeneity indices were relative parameters of dispersion as root mean square difference between measured retention's and excretions ($DISP_{R-E}$) , and root mean square difference between measured retention adjusted for shunt and those of the homogeneous lung ($DISP_{R*}$), and root mean square difference between measured excretion (adjusted for dead space; $V_{DIG}$) and those of the homogenous lung ($DISP_{E*}$) (31; 42). All dispersion indices have their own feature. Since these lungs have relatively normal distribution of $\dot{V}_A/\dot{Q}$, we focus on the dispersion indices and $\log\sigma\dot{Q}$ and $\log\sigma\dot{V}_A$ as the key indicators.

**Fluorescent Microsphere Technique**

**Injected fluorescent microsphere - blood flow distribution**

Intravenous injected fluorescent 15-μm-diameter microspheres (FluoSperes, Molecular Probes, Eugene, OR) of eight different colors (blue, blue-green, green, red, crimson, scarlet and dark red) were used to measure regional pulmonary blood flow. To ensure that clumping was avoided, microspheres were sonicated and vortexed prior to administration. Regional blood flow was proportional to the number of microspheres trapped in the region of interest with suitable sized microspheres (14). $2x10^6$ microspheres with densities of 1.04 $g\cdot ml^{-1}$ of one color were injected to make sure enough number of microspheres were delivered with suitable density. Two sets of stacked breaths were given before each microspheres injection followed by a 10 ml saline flush after microspheres injection. The fluorescent microsphere technique was developed and validated by Glenny et al (47) in this laboratory and is an accepted method to

measure the regional blood flow distribution. Compared to radioactive and colored microsphere, fluorescent microsphere technique is less expansive, and has less health-related concerns (47).

**Aerosolized fluorescent microsphere – ventilation distribution**

Sterile, 1-μm diameter fluorescent microspheres (FluoSpheres, Molecular Probes, Eugene, OR) are used as markers to measure the distributions of ventilation (132). Four different colors labeled fluorescent microspheres (yellow, yellow-green, orange and orange-red) were administered in distilled water with 0.01% thimerosal and 0.02% Tween 80. Before delivery, the aerosolized fluorescent microspheres are vortexed and sonicated to facilatate mixing and prevent settling. A constant-output atomizer (TSI model 3076, Thermo Systems, St, Paul, MN) was used to draw the fluorescent microsphere suspension from the aerosol reservoir and maintain the aerosolized microspheres with a fixed concentration. Then the aerosols was passed through a silica gel diffusion drier (TSI 3062) to reduce the water content and a krypton-85 source-charge neutralizer (TSI 3012) to lessen settlement of charged aerosol on the wall of the delivery system. Additional gas was added to the reservoir bag mixed with the aerosol to provide the required minute ventilation. A laser particle counter (LPC, TSI model 7400) was used to monitor the aerosol concentration and size. A Piston-pump ventilator was used to administer gas-aerosol mixture to the anesthetized dogs. Regional ventilation and perfusion were measured by simultaneous administration of aerosolized and intravenous injection of fluorescent microspheres. Microsphere colors were randomly selected within each group for administration in a given condition and color assignment varied across experiments. Aerosolized 1-μm microspheres were delivered over a 5-min period as described by Robertson et al. (132) to achieve a sufficient deposition level. Simultaneously, 15-μm microspheres were intravenously administered in multiple, uniform doses throughout the aerosol delivery period. The fluorescent microsphere technique was allowed multiple and repeated measures of regional ventilation and perfusion in small volume lung pieces in the same animal. The schematic

diagram (Fig 7) of differential ventilation with selective unilateral dependent PEEP insertion and aerosolized fluorescent microspheres delivery was showed as follows:

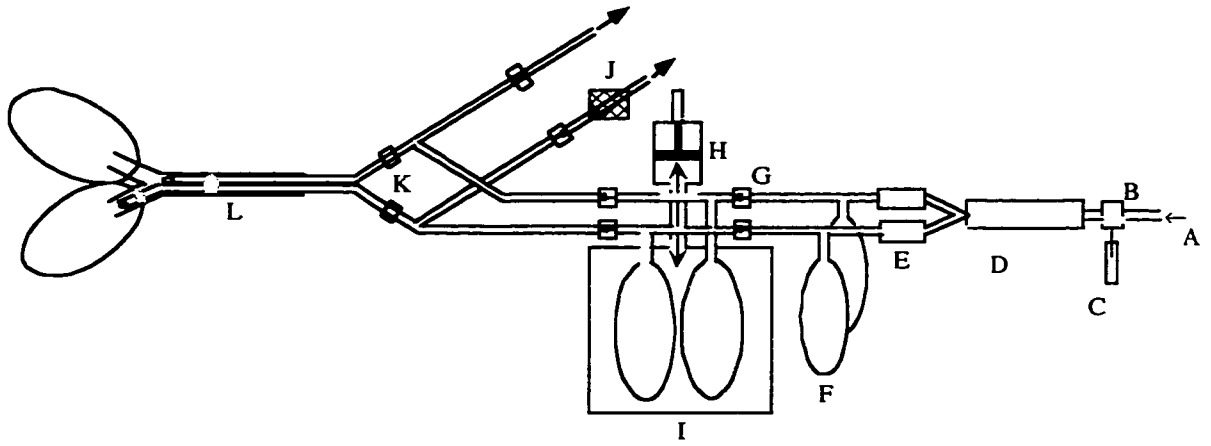


Fig 7. Diagram of dual aerosol administration system. A, filtered gas supplies (21% $O_2$); B, constant-output atomizers; C, aerosol mixtures; D, silica gels diffusion driers; E, charge neutralizers; F, reservoir bags; G, one-way valves; H, piston pump ventilator; I, bags-in-box ventilation system; J, unilateral Dependent PEEP; K, pneumotachs (tidal volume); L, bifurcated endotracheal Tube.

**Lung preparation and sample measurement**

After final delivery of intravenous and aerosolized fluorescent microspheres, the animal was deeply anesthetized with sodium thiopental (150 mg/kg i.v.) and saline was rapidly infused. Heparin (20,000 units) and papaverine ( 2 mg/kg) were given to dilate the pulmonary vasculature and to aid in flushing. The animal was exsanguinated via the arterial cannula. A median sternotomy was performed, and the left atrium and pulmonary artery were cannulated with large-bore catheters, the aorta tied off and the lungs perfused with 2% dextran solution until the left atrium effluent was clear. En bloc resection of the lungs was performed, the trachea was connected to a pressure source (approximately 25-30 cm $H_20$), the lungs inflated to total lung capacity and dried. The pleura was pierced in several locations with a long 18-gauge needle to facilitate rapid drying. To maintain a more normal anatomic configuration, the apical and most ventro-caudal rims of the left and right lungs were glued together with cyanoacrylate glue (Duro Superglue, Loctite, Cleveland, OH).

The lungs were dried for 7 days and then coated with polyurethane foam (Kwik Foam, DAP, Dayton, OH). The foam coated lungs were carefully put in a plastic-lined square box and maintained the caudal-cranial axis of the lung parallel to the wall of box. The box was filled with a rapidly setting foam (Polyol and isocynate, International Sales, Seattle, WA). The rectangular shape foaming block was sliced into 1.2-cm-thick slices with a band saw. Using a miter box, the lung slices were diced into cubes ~ 1.7 $cm^3$ in volume. Samples that weighed less than 0.008 g were excluded. Each lung cubic piece was weighed and assigned unique $X_0$, $Y_0$, and $Z_0$ coordinates (Fig 8), that represented the left to right, dorsal to ventral and caudal to cranial directions, respectively, from the left, dorsal and caudal lung edges. Fluorescent dye was extracted by soaking each piece in 1.5 ml 2-ethoxy ethyl acetate (Cellosolve, Aldrich Chemical, Milwaukee, WI) for 48 h. Dye concentrations were measured with a luminescence spectrophotometer equipped with an automated sampler (Perkin-Elmer, Model LS-50B, Norwalk, CT) at the dye-specific excitation and emission wavelength. After fluorescent intensities are corrected for background, a matrix inversion method (136; 137) was used to correct the fluorescent signal spillover from adjacent colors.

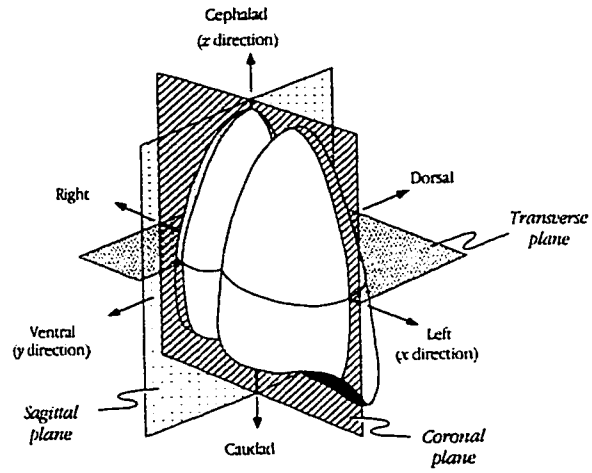


Fig.8 Orthogonal coordinate system used to designate spatial coordinates of lung pieces and directional perfusion gradients. (Adapted from Glenny R. W (48) )

**Using $\dot{V}_A/\dot{Q}$ of each lung piece to predict the regional $PO_2$ and $PCO_2$**

The $\dot{V}_A/\dot{Q}$ ratio was used to calculate end-capillary $PO_2$. We used the method described by Altemeier et al. (5) to calculate arterial $PO_2$, $PCO_2$, alveolar-arterial $O_2$ differences and end-capillary $PO_2$ from the measured $\dot{V}_A$ and $\dot{Q}$ fluorescent intensities, Hb concentration, body temperature and mixed venous blood gases. With the measured $\dot{V}_A/\dot{Q}$ for each piece, the mass balance equations for $O_2$, $CO_2$, $N_2$, end-capillary $O_2$, and $CO_2$ contents were solved to obtain regional alveolar $PO_2$ and $PCO_2$ for each piece. Regional alveolar gas tensions of each piece were ventilation-weighted and end-capillary gas contents were perfusion weighted and summed to yield mixed alveolar gas tension and mixed arterial gas content. The oxygen- and carbon dioxide-Hb dissociation curves for the dog were used to convert arterial $O_2$ and $CO_2$ content to gas tensions.

**Data correction**

**Correcting cube dimensions from TLC back to in situ FRC conditions**

To accurately estimate spatial gradients in blood flow and ventilation from lung cubes cut at TLC, the dimensions of each cube were adjusted to represent in vivo values using previous measurements from anesthetized dogs (56; 127). In the LLD posture, the ratios of the maximum lung lengths at FRC to those at TLC measured radiographically were 0.68 (0.85 in RLD posture), 0.76 and 0.84 in the left-right (X), dorsal-ventral (Y) and caudal-cranial (Z) axis, respectively. Corrected vertical heights at FRC averaged 11.1 ± 0.9 cm and 14.0 ± 1.2 cm in the LLD and RLD posture, respectively, without PEEP; and 16.4 ± 1.5 cm for both postures with PEEP. The corrected dorsal-ventral and caudal-cranial lengths averaged 13.1 ± 1.1 cm and 23.9 ± 2.3 cm, respectively.

A second correction was made for the nonuniform deformation caused by the vertical gradient in transpulmonary pressure (Ptp). At the corrected lung height Xi measured from the bottom of the lung, (Ptp)i is given by:

$$(Ptp)i = GXi \qquad (1)$$

G is the vertical Ptp gradient (0.5 cm $H_2O \cdot cm^{-1}$ height) measured in the lateral posture in the dog (1). (Ptp)min is 0 cm $H_2O$ at the bottom of the lung at Xmin = 0 (1) and increases linearly to (Ptp)max at the top of the lung at Xmax. Typically, Xmax at FRC was 13 cm and (Ptp)max was 6.5 cm $H_2O$. We used the Ptp-lung volume (PV) curve of an isolated dog lung (91). to determine the changes in length corresponding to different values of Ptp along the height of the lung (Xi). Lung volume (Vi) at each Xi is given by:

$$Vi = Vmin + (Vmax - Vmin)\,(\Delta Ptp)i/(\Delta Ptp)max \qquad (2)$$

$(\Delta Ptp)i$ is the Ptp change from the value at Vmin and $(\Delta Ptp)max$ is the maximum change in Ptp from Vmin to Vmax. We assumed that the PV curve is linear in this Ptp range. Vmin (20% TLC) is the lung volume at Ptpmin at the bottom of the lung Xmin. Vmax (65%TLC) is the lung volume at (Ptp)max. The cube at mid lung height (Xmid), equal to (Xmax+Xmin)/2, is assumed to remain undistorted with a cube length equal to the value after the reduction from TLC to FRC ($\Delta Xu$). The deformed length ($\Delta Xi$) for the ith cube at Xi is assumed to vary as $V^{1/3}$, given by the PV curve, at each (Ptp)i:

$$\Delta Xi/\Delta Xu = (Vi/Vmid)^{1/3} \qquad (3)$$

Vmid equals (Vmax +Vmin)/2. The cube lengths were reduced below and expanded above the undeformed mid-lung height. The X-positions of the deformed cubes were obtained by summing the deformed cube lengths starting from the bottom. The Y-and Z-dimensions of all cubes at each Xi were adjusted by multiplying the values obtained after correction from TLC to FRC by $\Delta Xi/\Delta Xu$ (Eq. 3).

We assumed no vertical Ptp gradient in the lateral position with PEEP (2). In addition, lung volume at 10 cm $H_2O$ PEEP was ~ 85%TLC, thus cube length (proportional to $V^{1/3}$) was 0.95 times the cube length at TLC. Accordingly no correction was made to the dried lung lengths at 10 cm $H_2O$ PEEP.

**Correcting cube dimensions from TLC back to regional lung volume with 5 cm $H_2O$ unilateral PEEP to the dependent left lung.**

The lung pieces were sorted to separate the right from the left lung. Since 5cm $H_2O$ PEEP to the dependent lung increased its lung volume, the cubic length correction in the dependent left lung was based on lung volume measured using the hilum dilution method. First, the ratio between measured $V5s_{PEEP}$ (FRC with 5 cm $H_2O$ unilateral PEEP) and $V_{FRC}$ (0 cm $H_2O$ PEEP) in the dependent lung in the LLD posture was calculated. As described in the above section, we used the deflation limb of the PV curve of dog lung (91) to correct each cube length and assumed the curve is linear between 20% TLC (Vmin at bottom of the lung) to 65% TLC (Vmax at top of the lung). The average regional lung volume (Vmid) at mid lung height is equal to (Vmax +Vmin)/2 for the whole lung.

With 0 cm $H_2O$ PEEP, the mid regional lung volume was (60%TLC + 20% TLC)/2 or 42.5% TLC for the whole lung in the lateral posture, and was the Vmax for the dependent lung. Thus, the mid regional lung volume of the dependent lung equals (Vmin + Vmax)/2 = (20+42.4)/2 or 31.2%TLC. We assumed that end-expiratory volume (FRC) of the dependent left lung with 5 cm $H_2O$ PEEP was larger than that at 0 cm $H_2O$ PEEP in proportion to the measured values (Table 1, Chapter 4). FRC at 0 cm $H_2O$ PEEP averaged 183 ml and at 5 cm $H_2O$ PEEP averaged 283 ml. The ratio of left lung FRC with 5 cm $H_2O$ PEEP (V5peep) to the FRC value without PEEP (V0peep) was 283/182 or 1.54. Thus $V5s_{PEEP}$ at mid lung height was 31.2% TLC X 1.54 or 48% TLC. Based on a uniform expansion, the left dependent lung cube length with 5 cm $H_2O$ PEEP($L5s_{PEEP}$) corrected from TLC to FRC was:

$$L5s_{PEEP}/L_{TLC} = (V5s_{PEEP}/TLC)^{1/3} \qquad (4)$$

$L5s_{PEEP}/L_{TLC}$, the ratio of the lung length at FRC to that at TLC was $(48/100)^{1/3}$, that is, 0.78. The 3 spatial dimensions of the lung cubes dried at TLC was multiplied by 0.78 to obtain values at FRC.

A further correction was made for the nonuniform deformation imposed by the vertical Ptp gradient. At the corrected lung height Xi measured from the bottom of the lung, (Ptp)i equaled the product of the corrected lung cube height at FRC and the vertical Ptp gradient. We assume that the vertical Ptp gradient during 5cm $H_2O$ PEEP was 0.25 cm $H_2O \cdot cm^{-1}$ in the lateral decubitus posture. This gradient was half the Ptp gradient of 0.5 cm $H_2O \cdot cm^{-1}$ measured with 0 cm $H_2O$ PEEP and the gradient of 0 cm $H_2O \cdot cm^{-1}$ measured with 10 cm $H_2O$ PEEP, in the lateral posture in the dog (1). A typical value for Xmax at 5 cm $H_2O$ PEEP in left dependent lung was 6.5 cm. Thus Ptpmax was 1.6 cm $H_2O$. As described above, we used the Ptp-lung volume (PV) curve in isolated dog lung (91) to define the change in cube length with the different values of Ptp along the height of the lung. Again, we assumed that the PV curve was linear in the range of Ptp considered and the slope did not change with the 5cm $H_2O$ PEEP. Based on the compliance of the PV curve, (65-20)/6.5 = 6.9% TLC/cm $H_2O$, and the change in Ptp of 1.6 cm $H_2O$ over the height of the lung (6.5 cm), the change in regional volume was 11 % TLC.

With the 5 cm $H_2O$ PEEP, Vmin was 48%TLC-5.5%TLC or 42.5%TLC at the base of the lung and Vmax was 48%TLC + 5.5%TLC or 53.5% TLC at the top of the lung. Again, we assumed that the mid lung piece in the dependent left lung was undistorted with a cube length equal to the value after reduction from the TLC cube length to a cube length with 5cm $H_2O$ PEEP ($\Delta Xu$). As described in equation 2, the distorted length ($\Delta Xi$) for the ith cube piece at Xi was proportional to $V^{1/3}$ at specific ($\Delta Ptp$)i. Similarly, the Y- and Z- dimensions of all cubes at each Xi were corrected by multiplying the values obtained after correction from TLC to 5 cm $H_2O$ PEEP by $\Delta Xi/\Delta Xu$.

To correct the nondependent right lung with 5 cm $H_2O$ PEEP applied to the dependent left lung, we applied the corrections used previously for the whole lung in the LLD posture, then eliminated the left lung pieces to produce only the right lung. To reassemble the whole lung, we maintained the vertical spacing between the base of nondependent lung and top of the dependent lung identical to that existing before the correction for the

vertical Ptp gradient. The X-coordinate of each lung piece was calculated by summing the deformed cube lengths starting from the base (X = 0 cm) of the dependent lung with 5 cm $H_2O$ PEEP to the top of the nondependent lung without PEEP.

**Correcting cube dimensions from TLC back to FRC with 10 cm $H_2O$ unilateral PEEP to the dependent left lung.**

From the measured FRC values, the ratio of $V10s_{PEEP}/V0_{PEEP}$ was ~2.1. The middle regional lung volume of the whole lung without PEEP was 42.5% TLC. Lung volume of the left dependent lung with 10 cm $H_2O$ PEEP was ~90% TLC, producing a cube length of 0.96 times the dry cube length at TLC. Thus no correction was made for the TLC cube length with 10 cm $H_2O$ PEEP to the left lung. To correct the nondependent right lung with 10 cm $H_2O$ PEEP to the dependent left lung, we followed the procedure used for 5 cm $H_2O$ PEEP to the left lung.

**Correcting cube dimensions from TLC back to in situ FRC conditions after left lung atelectasis.**

The lung pieces were sorted to separate the right from the left lung. We assumed that the atelactatic left lung was isotropically expanded and reduced each spatial dimension equally from that at TLC. The atelactatic lung volume consisted of the volume of the wet tissue mass and blood. The wet tissue mass was the product of the total dry weight and the wet-to-dry weight ratio (4.7) (139). We used the density of tissue (1 $g \cdot ml^{-1}$) to obtain tissue volume. Tissue volume averaged ~7% TLC. Blood volume is given by:

$$\text{Blood volume} = \dot{Q} \times \text{lung vascular transit time} \qquad (5)$$

We used a lung transit time of 5 seconds measured previously in the dog (14). Blood flow to the atelactatic lung was the product of the cardiac output and fluorescent microsphere intensity as a fraction of the total (left and right lung intensity). The blood volume of the atelectatic left lung averaged 42.7 ± 24.3 ml or 6.7 ± 3.7%TLC in the LLD posture and it varied with body inversion to the RLD posture (30.1 ± 14.3 ml or 4.9 ±

2.3%TLC) and PEEP in the right lung. The corrected lung cubic length ($L_{ATEL}$) of each left lung piece after left lung atelectasis was given by:

$$L_{ATEL}/L_{TLC} = (V_{ATEL}/V_{TLC})^{1/3} \quad (6)$$

Here $V_{ATEL}$ (%TLC) is the sum of blood volume and tissue volume. $L_{ATEL}/L_{TLC}$ averaged ~0.5. Thus, the X-, Y-, and Z- dimensions of each left lung cubic piece after atelectasis were reduced by half the dry lung cube length.

Second, the dimensions of the right lung with the left lung atelactatic were calculated as follows. First, a correction from TLC to FRC was calculated based on a uniform contraction. TLC was based on the wet weight (4.7 x dry weight) equal to 7%TLC. Total lung volume at FRC ($V_{FRC}$) was equal to the sum of air volume at FRC, volume of the wet tissue mass and the blood volume. The cube dimension at FRC ($L_{FRC}$) was related to $V_{FRC}$ as follows:

$$L_{FRC}/L_{TLC} = (V_{FRC}/TLC)^{1/3} \quad (7)$$

The cube dimension at TLC ($L_{TLC}$) was 1.2 cm. FRC (gas volume) of the right lung was obtained by the helium dilution method (Table 1, chapter 5).

With left lung atelectasis, the right lung at FRC expanded by 25.5 ± 27.3%, producing a regional volume of 67.4 ± 22.5%TLC and a cube dimension of 88 ± 4% times the value at TLC. The right lung dimension in each coordinate was reduced by the latter fraction to obtain the dimension at FRC. No correction was made for the vertical Ptp gradient because of the small changes in regional lung volume with Ptp in the expanded lung in conjunction with a reduced vertical Ptp gradient with lung inflation (2).

**Volume normalization of blood flow**

Fluorescent intensity of each color microsphere representing blood flow ($\dot{Q}$) or ventilation ($\dot{V}_A$) to each piece (cube) was converted to units of blood flow (ml/min) by dividing the fluorescence intensity of each piece by the sum of the fluorescent intensities of all pieces and then multiplying by cardiac output (ml·min$^{-1}$). $\dot{Q}$ and $\dot{V}_A$ of each piece was then converted to units of ml/min per unit regional lung volume at FRC by dividing

by its volume (ΔVi). ΔVi at Xi was calculated from its dry weight ΔWi, mean lung density (ρ), and the deformed cube length (Eq. 8):

$$\Delta Vi = 4.7\ \Delta Wi\ (\Delta Xi/\Delta Xu)^3 / \rho \qquad (8)$$

The term $(\Delta Xi/\Delta Xu)^3$ corrects the mean density for changes due to the Ptp gradient. The product of ΔWi and 4.7, lung wet-to-dry-weight ratio (139), is the wet weight. Mean lung density at FRC was equal to total lung wet weight (total dry weight x 4.7) divided by total lung volume at FRC (air volume, FRC + volume of tissue mass). Tissue density was 1 $g \cdot ml^{-1}$. The measured FRC values are summarized in Table 1 of chapter 5. Lung dry weight averaged 10.1 ± 0.7 gm and 13.6 ± 0.95 gm for the left and right lung, respectively. Left lung weight was 24 % smaller than right lung weight. Mean lung density averaged 0.14 ± 0.02 and 0.08 ± 0.01 $g \cdot ml^{-1}$ at FRC and 10 cm $H_2O$ PEEP, respectively.

By an independent calculation in one lung, we determined whether the latter correction for regional volume was equivalent to a piece-by-piece correction of all the pieces. The incomplete or partial cube pieces amounted to 60% of the total number of pieces. The total number of pieces were sorted into two groups, one group of 60% of the pieces with the lowest dry weights and the other group of the remaining pieces. The latter group was considered complete cube pieces. A separate count determined that 10% overlap occurred between the two groups. The flow of the complete cubes was divided by the cube volume at TLC corrected to FRC and for the vertical gradient in transpulmonary pressure, as described above. The flow of each partial cube piece was corrected by dividing the flow by its dry weight and then multiplying by the average dry weight of the complete cubes. A comparison of the piece-by-piece flows per unit regional volume between the two methods showed an $R^2$ value of 0.98. Accordingly, we used the simpler method with the mean lung density for the analysis.

The anatomic deadspace was estimated using Fowler's method (39) using plots of exhaled $CO_2$ concentration vs. exhaled tidal volume. Anatomic dead space was the

average result from 3 measurements. Total minute ventilation was calculated by multiplying ventilation frequency by tidal volume less anatomic deadspace. Pieces were excluded if the fluorescent intensity was outside the range of mean ± 4SD. For the multiple linear regression analysis of $\dot{V}_A/\dot{Q}$ and end-capillary $P_RO_2$, we excluded pieces outside the range of mean ± 3SD of ln ($\dot{V}_A/\dot{Q}$). This procedure excluded pieces of very high $\dot{V}_A/\dot{Q}$(deadspace) and very low $\dot{V}_A/\dot{Q}$ (shunt). The spatial variation in $\dot{V}_A/\dot{Q}$ and end-capillary $PO_2$ ($P_RO_2$), the correlation between perfusion and ventilation, and the degree of heterogeneity expressed as SD/mean were not affected by the volume normalization. $\dot{V}_A$- and $\dot{Q}$- weighted $\dot{V}_A/\dot{Q}$ distribution derived from microsphere data were compared with MIGET results and gas exchange prediction using ventilation and perfusion data in units of ml·min$^{-1}$.

**Statistical analysis.**

Volume-normalized flows (flow per unit regional lung volume) were used for all analyses. Values were presented as means ± SD. ANOVA repeat measurement was used to evaluate differences among more than two groups. The coefficient of variation (CV = 100 x SD/mean) was used to characterize perfusion and ventilation heterogeneity. Paired t-test was used to compare $\dot{Q}$ and $\dot{V}_A$ heterogeneity between postures and between 0 and 10 cm $H_2O$ PEEP in the same posture. Heterogeneity was also analyzed with a multiple linear regression model entailing three rectangular coordinate axes, as described below. $R^2$ from the multiple linear regression model represented the degree of flow variability that was caused by the flow variation with respect to the three coordinate axes. ($1-R^2$) represented intraregional variation and indicated the portion of flow variance not accounted for by spatial factors.

**Multiple linear regression model $\dot{Q}$, $\dot{V}_A$, and $\dot{V}_A/\dot{Q}$ distribution**

A multiple linear regression model was used to characterize the magnitude of flow (and other variables $\dot{V}_A$, $\dot{V}_A/\dot{Q}$ and $PO_2$) as a linear function of the rectangular coordinates, X (vertical height in the lateral posture, left-right direction), Y (dorsal-ventral direction) and Z (caudal-cranial direction):

$$\dot{Q} = I + aX + bY + cZ + dXY + eYZ + fZX + gXYZ \qquad (9)$$

The corrected FRC total length in X was 11.1±0.9 cm and 14.0±1.2 cm for LLD and RLD, respectively. The corrected length of left-right direction with PEEP was 16.4±1.5 cm for both LLD and RLD. The corrected length of dorsal-ventral direction and caudal-cranial direction was 13.1±1.1cm and 23.9±2.3 cm, respectively. We subtracted the distances of the center of mass in the X, Y and Z directions from the original coordinate system used for locating each lung cube to describe the flow in relation to the center of mass (X = Y = Z = 0). The intercept (I) represents the mean flow at the center of mass. The coefficients (a-g) in the linear equation (4) obtained from the regression analysis describe the mean flow at an arbitrary position (X, Y, Z) within the lung. The coefficients a, b and c define the flow gradients with respect to the X, Y, Z coordinate axes, respectively, at the center of mass. The coefficients d, e and f are coefficients that describe the variation of the flow gradient in one coordinate axis with regard to another axis. For example, the partial derivative of $\dot{Q}$ with respect to X results in the following equation describing the flow gradient in the X-direction:

$$\partial\dot{Q}/\partial X = a + dY + fZ + gYZ \qquad (10)$$

At Y = Z = 0 and for all X, the vertical flow gradient is equal to the coefficient a. At Y = 0, the vertical gradient is equal to a + fZ, that is, it varies linearly with Z and the coefficient f is the slope of the vertical flow gradient in the Z direction. Thus the flow gradient in any coordinate axis can be calculated for any arbitrary position within the lung.

Multiple linear regression was used to describe the spatial distribution of flow and other variables in both LLD and RLD postures, with and without PEEP. Multilinear

regression analysis was carried out on the data from the whole lung and after separating the data into the left and right lung. The regression analysis provides a P value, a measure of the reliability, for each constant in the best-fit linear equation. Only constants with $P < 0.05$ were considered significant. The intercepts, coefficients and $R^2$ values from the six animals studied were pooled and their mean values and SD calculated. Significance difference of these coefficients from zero were determined using a single group one-tailed t test. We took as meaningful coefficients only if the group data proved to be significant. In many instances, coefficients that were significant in a single animal proved to be not significant among the 6 animals. ANOVA was used to determine the difference in the gradients between LLD and RLD postures and between 0 cm $H_2O$ and 10 cm $H_2O$ PEEP in the same posture. Volume-normalized flow plotted against vertical distance (left-right axis, X) was used to characterize the effect of gravity on flow. The coefficient of linear correlation (*r*) was used to quantify the strength of the relationship between two states (LLD vs. RLD) and between ventilation and perfusion.

Changes in mean blood flow resulting from the application of 10 cm $H_2O$ PEEP were compared between the nondependent and dependent lung using a paired *t*-test in LLD and RLD postures. Paired t tests were used to evaluate differences in mean $P_RO_2$ between 0 cm $H_2O$ and 10 cm $H_2O$ PEEP and differences in the coefficient of linear correlation (*r)* of ventilation vs. perfusion between LLD and RLD postures and between 0 and 10 cm $H_2O$ PEEP.

### $\dot{V}_A/\dot{Q}$ heterogeneity analyzed based on Wilson and Beck's model

We evaluated the heterogeneity of $\dot{V}_A$, $\dot{Q}$ and $\dot{V}_A/\dot{Q}$ distributions using the coefficient of variation ($\sigma$), the standard deviation of regional $\dot{V}_A$ and $\dot{Q}$ values divided by mean values. Variance ($\sigma^2$) of $\dot{V}_A/\dot{Q}$ was computed from the variances of $\dot{V}_A$ and $\dot{Q}$ with Pearson's correlation coefficient ($\rho_c$) between $\dot{V}_A$ and $\dot{Q}$ (162):

$$\sigma^2 \dot{V}_A/\dot{Q} = \sigma^2 \dot{V}_A + \sigma^2 \dot{Q} - 2\rho\sigma \dot{V}_A \cdot \sigma \dot{Q} \qquad (11)$$

Heterogeneity in $\dot{V}_A/\dot{Q}$ measured by the log normal standard deviations ($\log\sigma \dot{V}_A$ and $\log\sigma \dot{Q}$) of $\dot{V}_A$- and $\dot{Q}$-$\dot{V}_A/\dot{Q}$ distribution curves were obtained from MIGET and the fluorescent microspheres (FMS) data.

To separate the heterogeneity in $\dot{V}_A$, $\dot{Q}$ and $\dot{V}_A/\dot{Q}$ due to spatial variations from that due to other factors (residual), the variance of the mean summed square of the residuals, (measured - predicted values)/mean value (17), was obtained from the multiple linear regression analysis. This analysis was repeated using a fourth-order regression equation (31 terms) with terms up to third order in each coordinate and up to fourth order in each term ($X^pY^q$, $p + q = 4$). Preliminary analysis indicated no further decrease in the non-spatial variance (or increase in $R^2$) with a higher order regression equation. The residual variance/total variance equals 1- $R^2$, where $R^2$ is the adjusted coefficient of determination from the regression analysis

# CHAPTER 3
# SPATIAL DISTRIBUTION OF VENTILATION AND PERFUSION IN THE LATERAL POSTURE IN DOGS

## INTRODUCTION

Studies (17; 113) have shown that regional blood flow and ventilation are more uniform in the prone compared to supine posture. This has been attributed to greater regional perfusion and ventilation to the dorsal lung regions, offsetting the effects of gravity. Also, the reduction in the dependent lung volume by the weight of the heart might contribute to differences in regional perfusion and ventilation (3). In the lateral decubitus posture, the compression of the dependent lung by the heart might be greater than that in either supine or prone posture. Furthermore, the dependent lung has a smaller lung volume in the left lateral decubitus posture (LLD) than in the right lateral decubitus posture (RLD) (118), consistent with differing effects of the heart between the two postures.

Regional blood flow increases from the nondependent to dependent lung in the lateral decubitus posture in the human (7; 82; 93) and the dog (56; 127). In addition, the intrapulmonary ventilation distribution is altered in the lateral posture after anesthesia and mechanical ventilation (129; 130). Impaired gas exchange after anesthesia and mechanical ventilation has been attributed to a mismatch between ventilation and perfusion. The relative matching of pulmonary blood flow and ventilation distribution in the lateral decubitus posture remains uncertain.

Positive end-expiratory pressure (PEEP) is often applied to improve arterial oxygenation during anesthesia with mechanical ventilation (93; 129; 130). In the lateral posture, PEEP reduced the difference in ventilation between the two lungs (130). In these studies (93; 129; 130), ventilation was measured in relatively large regions, such as a single lobe or lung. Accordingly, direct evidence using a high spatial resolution

measure of the $\dot{V}_A$ distribution in the lateral decubitus posture after induction of anesthesia with PEEP is lacking.

We hypothesize that the distributions of $\dot{V}_A$ and $\dot{Q}$ are different between the LLD and RLD posture due to differences in lung distortion from the weight of the heart and abdomen. PEEP reduces lung distortion due to heart weight, affecting the smaller left dependent lung to a greater degree, and producing a larger decrease in pulmonary vascular resistance in the LLD posture. PEEP increases both $\dot{V}_A$ and $\dot{Q}$ to dependent lung regions, particularly to the dependent left lung in the LLD posture.

This study examines the effect of posture and PEEP on regional blood flow, ventilation and gas exchange in the lateral decubitus posture in anesthetized, mechanically ventilated dogs using both aerosolized and intravenously injected fluorescent microspheres.

## METHODS

### Animal Preparation and Physiologic Measurements

General methodology was mentioned in the chapter 2. Briefly, this study was approved by the University of Washington Animal Care Committee. Six healthy mongrel dogs of either sex [22.8 ± 2.8 (SD, n = 6) kg] were anesthetized with pentobarbital sodium (~4-8mg·kg$^{-1}$) intravenously and maintained with a pentobarbital infusion sufficient to achieve a surgical plane of anesthesia and eliminate spontaneous ventilation (~10-17 mg· kg$^{-1}$· h$^{-1}$). Dogs were mechanically ventilated with air via tracheostomy (tidal volume 15 ml·kg$^{-1}$). The respiratory rate was adjusted to maintain $PaCO_2$ between 35 and 40 mmHg. Minute ventilation was measured with a spirometer. Catheters were placed in one femoral artery and both femoral veins. A pulmonary artery catheter was introduced into the right external jugular vein and used for measuring cardiac output $\dot{Q}_T$ (thermal dilution) and core temperature Tc. Systemic arterial (Pa), pulmonary arterial (Ppa), pulmonary arterial wedge pressure (Ppcw) and airway pressure (Paw) were recorded continuously on a data management system (Western Graphic Mach 12 DMS 1000). For determination of anatomic dead space $V_D$, exhaled end-tidal $P_{ET}CO_2$

and expiratory airflow flow $\dot{V}$ were digitally sampled with an infrared $CO_2$ detector (Perkin Elmer, Plumsteadville, PA) and a pneumotachograph, respectively. Arterial and mixed venous blood gases were measured with an automated blood gas analyzer (ABL 300, Radiometer, Copenhagen, Denmark) and corrected for temperature. Body temperature was maintained using heat lamps and pads.

**Study protocol**

Animals were studied in the right and left lateral decubitus postures in random order and 0 or 10 cm $H_20$ PEEP were administered. The lungs were hyperinflated (30-40 cm $H_20$) 5 min before each experimental measurement to remove atelectasis. In each trial, we measured Pa, Ppa, Ppcw, $\dot{Q}_T$, Tc, $V_T$ and arterial and venous blood gas composition and arterial, venous and mixed expired MIGET sample immediately before fluorescent microsphere administration. Regional perfusion was measured with intravenously injected microspheres and regional ventilation was measured with fluorescent aerosols. Functional residual capacity (FRC) was measured by He dilution during each experimental condition.

**RESULTS**

**Physiological Data**

Table 1 and 2 summarizes the physiological data. Body position and PEEP had no effect on cardiac output, heart rate, temperature, respiration rate, $pH$, $P\bar{v}O_2$ and hemoglobin. PEEP decreased Psa and increased Ppa, Ppcw and peak Paw in both LLD and RLD postures. $Pa_{O_2}$ was greater in the LLD than RLD posture, while alveolar-arterial $O_2$ difference ($A\text{-}aD_{O_2}$) was less in the LLD than RLD posture. The addition of PEEP increased $Pa_{CO_2}$ by ~2 mm Hg in both postures. PEEP increased FRC by 65% and 76% in the LLD and RLD posture, respectively.

Inert gas shunt ($\dot{Q}_S/\dot{Q}_T$) and deadspace ($V_D/V_T$) showed no change between the LLD (0.15±0.3 and 43.5±4.8) and RLD (0.18±0.24 and 43.6±4.6) postures. PEEP increased $V_D/V_T$ in both the LLD (49.1±8.5) and RLD (48.9±6.7) postures and decreased $\dot{Q}_S/\dot{Q}_T$

in the LLD (0.03±0.05) but not the RLD (0.15±0.24) posture. Inert gas shunt was similar to that measured by the FMS data. Inert gas deadspace was greater than that measured by Fowler's method (Table 1).

Table 1. The Effect of Position and PEEP on Physiological Variables

| | ZEEP | | PEEP | |
|---|---|---|---|---|
| | LLD | RLD | LLD | RLD |
| Psa (mmHg) | 89.8±9.6 | 81.8±11.1 | 87.9±10.4 | 75±15.5 |
| Ppa ($cmH_2O$) | 19.5±5.5 | 16.2±4.7 | 26.4±5.4§ | 25.1±3.2§ |
| Ppcw ($cmH_2O$) | 8.6±2.8 | 6.0±3.9 | 13.0±4.2* | 11.6±2.7† |
| Paw ($cmH_2O$) | 9.7±1.2 | 11.3.±1.2§ | 20.2±1.7‡ | 20.8±1.3‡ |
| $\dot{Q}_T$ $L \cdot min^{-1}$ | 3.7±1.2 | 3.7±0.7 | 3.7±0.7 | 3.5±0.8 |
| $R_T$, $cmH_2O \cdot L^{-1} \cdot min^{-1}$ | 3.0±1.2 | 2.6±1.4 | 3.8±1.1 | 4.4±1.5* |
| $R_L$, $cmH_2O \cdot L^{-1} \cdot min^{-1}$ | 8.3±4.0 | 7.3±4.0 | 8.3±2.5 | 13.1±3.5* |
| $R_R$, $cmH_2O \cdot L^{-1} \cdot min^{-1}$ | 4.8±1.8 | 4.0±2.3 | 7.2±2.6 | 6.6±2.6* |
| HR ($beats \cdot min^{-1}$) | 129±19 | 128±35 | 125±13 | 127±23 |
| $V_T$ (ml) | 345±58 | 344±58 | 341±68 | 339±62 |
| $V_D/V_T$ (%) | 32.5±3.4 | 29.2±5.6 | 33.1±1.6 | 33.2±4.6 |
| $V_E$ ($L \cdot min^{-1}$) | 5.9±1.1 | 5.7±1.1 | 5.9±0.8 | 5.7±0.5 |
| RR ($breaths \cdot min^{-1}$) | 18±5 | 17±4 | 16±5 | 17±4 |
| FRC (ml) | 625±212 | 599±215 | 1009±271‡ | 1053±317‡ |

Values are means ± SD (n = 6). ZEEP, zero end-expiratory pressure; PEEP, 10 $cmH_2O$ end-expiratory pressure; Psa, systemic arterial pressure; Ppa, main pulmonary artery pressure; Ppcw, pulmonary capillary wedge pressure; Paw, peak airwary pressure; $\dot{Q}_T$, cardiac output; R: Pulmonary vascular resistance = $(Ppa-Ppcw)/\dot{Q}$, T: total lung; L: left lung; R: right lung; HR, heart rate; $V_D/V_T$, Foweler's dead space; $V_T$, tidal volume; $V_E$, minute ventilation; RR, respiratory rate; FRC, functional residual capacity. *$P < 0.05$ †$P < 0.01$, ‡$P < 0.001$ compared with ZEEP in the same posture. § $P < 0.05$, compared with LLD in the same PEEP condition.

Table 2. Measured and fluorescent microsphere predicted arterial partial pressure of $O_2$ , $CO_2$ , A-a$DO_2$ and measured mixed venous $O_2$, pH and Hb

| | ZEEP | | PEEP | |
|---|---|---|---|---|
| | LLD | RLD | LLD | RLD |
| $Pa_{O_2}$ mmHg | 111±8 | 103±9§ | 108±6 | 114±19 |
| $Pa_{CO_2}$ mmHg | 36±4 | 36±2 | 39±3* | 38±3‡ |
| A-a$DO_2$ mmHg | 4±5 | 12±9§ | 4±4 | 5±5 |
| $Pa_{O_2}$, mmHg, FMS | 103±11 | 104±11 | 106±9 | 106±8 |
| $Pa_{CO_2}$ mmHg, FMS | 35±4 | 35±3 | 37±3 | 37±3 |
| A-a$DO_2$ mmHg, FMS | 9±7 | 7±4 | 5±3 | 5±2 |
| pH | 7.39±0.05 | 7.33±0.02 | 7.37±0.03 | 7.34±0.02 |
| $P_{\bar{v}O_2}$ mmHg | 48.0±6.9 | 48.0±5.5 | 47.3±5.4 | 47.0±5.5 |
| Hb, g·dl$^{-1}$ | 10.6±0.8 | 11.2±0.6 | 9.9±0.7 | 10.8±2.2 |

Values are means ± SD (n = 6). ZEEP, zero end-expiratory pressure; PEEP, 10 cm $H_2O$ end-expiratory pressure; $Pa_{O_2}$, arterial $O_2$ tension; $Pa_{CO_2}$, arterial $CO_2$; FMS, microsphere predicted; $P_{\bar{v}O_2}$, mixed venous $O_2$ tension; Hb, blood hemoglobin; *P < 0.05 †P < 0.01, ‡P < 0.001 compared with ZEEP in the same posture. § P < 0.05, compared with LLD in the same PEEP condition.

*Microsphere Data.* A total of 1378 - 1654 lung pieces per animal were processed for regional blood flow and ventilation. We discarded lung pieces (135 ± 49) with >25% pulmonary airways and with fluorescent intensity (11±10) outside the range of ± 4 SD of any of the mean values. Analysis of blood flow and ventilation was carried out on 90.4 ± 5% of the total lung pieces. For the analysis of $\dot{V}_A/\dot{Q}$ and $P_{RO_2}$, data were accepted with the range of mean ± 3SD of ln ($\dot{V}_A/\dot{Q}$). This eliminated the pieces associated with deadspace (very large $\dot{V}_A/\dot{Q}$) and with shunt (very low $\dot{V}_A/\dot{Q}$). The number of pieces eliminated averaged 3 ± 4 % of the total.

Table 2 summarizes the X, Y, Z coordinate distances (cm) of the center of mass of left, right and whole lung, relatively to the original coordinate axes (Xo, Yo, Zo) oriented at the edges of the lung. As lung volume increased with PEEP, the coordinate distances

between the center of mass and original coordinate axes increased. The increase in distance was greatest (~50%) in the LLD posture and least (~10%) in the RLD posture.

TABLE 3. x, y, z coordinate distances (cm) between center of mass and original coordinate system at caudal edge ($z_0$=0), left edge ($x_0$=0), dorsal edge ($y_0$=0) of the lung

| | | LLD | | ΔL (%) | RLD | | ΔL (%) |
|---|---|---|---|---|---|---|---|
| PEEP, cm $H_2O$ | | 0 | 10 | | 0 | 10 | |
| | X | 6.1±0.7 | 9.6±0.9 | 50 | 7.9±0.2 | 9.5±0.5 | 20 |
| Whole lung | Y | 6.5±0.4 | 8.6±0.5 | 30 | 6.5±0.4 | 8.6±0.5 | 30 |
| | Z | 11.5±0.9 | 13.6±1.0 | 20 | 11.5±0.8 | 13.6±1.0 | 20 |
| | X | 8.3±0.9 | 12.7±1.3 | 50 | 5.1±0.3 | 6.3±0.5 | 20 |
| Right lung | Y | 7.3±0.4 | 9.0±0.6 | 20 | 6.6±0.5 | 9.0±0.6 | 30 |
| | Z | 12.2±0.9 | 13.7±1.0 | 12 | 10.9±0.8 | 13.7±1.0 | 20 |
| | X | 3.2±0.4 | 5.3±0.6 | 65 | 11.6±0.6 | 13.7±0.9 | 20 |
| Left lung | Y | 5.5±0.3 | 8.0±0.6 | 45 | 6.5±0.4 | 8.0±0.6 | 20 |
| | Z | 10.5±0.9 | 13.5±1.0 | 30 | 12.2±0.9 | 13.5±1.0 | 10 |

$\Delta L = (L_{PEEP10} - L_{PEEP0}) / L_{PEEP0}$ for X, Y, Z respectively.

**Spatial gradients in $\dot{Q}$, $\dot{V}_A$, $\dot{V}_A/\dot{Q}$ and $P_{RO2}$**

Multiple regression analyses revealed systematic variations of blood flow in the 3 coordinates. Because the blood flow distribution described by the multiple linear regression equation (Eq. 9) for each animal showed that most (6 of 7) coefficients were significant, we used the equation to describe $\dot{Q}$, $\dot{V}_A$, $\dot{V}_A/\dot{Q}$ and $P_{RO2}$ for all conditions. The use of the equation was further justified because $R^2$ for the best-fit regression was lower when only terms of 1 or 2 coordinates were included. The coefficients of the 6 animals were pooled for each condition and the significance tested to determine its validity in describing the blood flow distribution. In many instances, coefficients that were significant in a single animal proved to be not significant among the 6 animals. Coefficients were considered meaningful only if the coefficients of the 6 animals were significant. The present study showed values of $R^2$ of ~0.40, indicating that ~40% of the variability in the data were attributed to spatial variations.

Significant vertical, dorsal-ventral and caudal-cranial spatial gradients of $\dot{Q}$, $\dot{V}_A$, $\dot{V}_A/\dot{Q}$ and $P_{RO2}$ are summarized in Table 3, 4, 5, and 6. Fig. 9 shows $\dot{Q}$ plotted versus

TABLE 4. Coefficients and $R^2$ of multiple linear regression equation† fit to $\dot{Q}$ data for whole, left and right lung,

| lung | Position | PEEP | Intercept | a | b | c | d | e | f | g | $R^2$ |
|---|---|---|---|---|---|---|---|---|---|---|---|
| | LLD | 0 | 5.0 | **-0.27** | 0.078 | **-0.079** | -0.037 | **-0.024** | **0.046** | **0.006** | 0.44 |
| Whole | | | ±2.1 | **±0.11*** | ±0.090 | **±0.032*** | ±0.038 | **±0.004*** | **±0.024*** | **±0.005*** | ±0.12 |
| | LLD | 10 | 2.8 | **-0.12** | **-0.024** | **-0.021** | -0.007 | **-0.006** | **0.005** | **0.002** | 0.42 |
| | | | ±0.7 | **±0.08*** | **±0.017*** | **±0.016*** | ±0.009 | **±0.005*** | **±0.005*** | **±0.001*** | ±0.13 |
| | RLD | 0 | 5.2 | **-0.42** | 0.010 | **-0.074** | **0.035** | **-0.035** | 0.011 | 0.001 | 0.23 |
| | | | ±1.5 | **±0.39*** | ±0.015 | **±0.49*** | **±0.028*** | **±0.022*** | ±0.014 | ±0.005 | ±0.13 |
| | RLD | 10 | 2.5 | **-0.14** | -0.0001 | -0.021 | 0.0001 | -0.004 | -0.001 | -0.0002 | 0.56 |
| | | | ±0.8 | **±0.07*** | ±0.04 | ±0.027 | ±0.002 | ±0.006 | ±0.006 | ±0.001 | ±0.15 |
| | LLD | 0 | 5.8 | **-0.60** | **0.26** | **-0.18** | 0.11 | **-0.074** | 0.041 | **0.020** | 0.52 |
| Left | | | ±2.2 | **±0.40*** | **±0.24*** | **±0.11*** | ±0.14 | **±0.03*** | ±0.046 | **±0.016*** | ±0.14 |
| | LLD | 10 | 4.0 | **-0.15** | 0.09 | -0.012 | **0.02** | **-0.019** | -0.003 | **0.003** | 0.37 |
| | | | ±1.1 | **±0.12*** | ±0.05 | ±0.02 | **±0.015*** | **±0.008*** | ±0.006 | **±0.002*** | ±0.09 |
| | RLD | 0 | 3.9 | -0.04 | **0.18** | -0.04 | -0.037 | **-0.033** | 0.007 | -0.0002 | 0.39 |
| | | | ±1.4 | ±0.19 | **±0.15*** | ±0.06 | ±0.02* | **±0.021*** | ±0.008 | ±0.0030 | ±0.11 |
| | RLD | 10 | 1.9 | **-0.06** | 0.006 | **-0.024** | -0.024 | **-0.007** | 0.004 | -0.00007 | 0.27 |
| | | | ±0.8 | **±0.04*** | ±0.045 | **±0.019*** | ±0.019 | **±0.005*** | ±0.05 | ±0.002 | ±0.11 |
| | LLD | 0 | 4.6 | **-0.37** | -0.06 | 0.006 | -0.001 | -0.014 | **0.015** | **0.005** | 0.39 |
| Right | | | ±2.2 | **±0.22*** | ±0.09 | ±0.03 | ±0.02 | ±0.014 | **±0.012*** | **±0.004*** | ±0.06 |
| | LLD | 10 | 2.4 | **-0.12** | **-0.07** | -0.008 | **-0.005** | -0.002 | **0.007** | 0.001 | 0.37 |
| | | | ±0.7 | **±0.05*** | **±0.043*** | ±0.02 | **±0.002*** | ±0.004 | **±0.005*** | ±0.001 | ±0.10 |
| | RLD | 0 | 5.8 | -0.56 | -0.006 | -0.065 | 0.03 | -0.046 | 0.064 | 0.10 | 0.47 |
| | | | ±3.8 | ±0.68 | ±0.2 | ±0.11 | ±0.053 | ±0.057 | ±0.061 | ±0.24 | ±0.17 |
| | RLD | 10 | 3.4 | **-0.14** | -0.015 | -0.016 | 0.001 | -0.006 | 0.004 | 0.001 | 0.37 |
| | | | ±1.2 | **±0.11*** | ±0.042 | ±0.046 | ±0.07 | ±0.009 | ±0.015 | ±0.002 | ±0.18 |

Values are presented as mean ± SD (n=6), * $P < 0.05$ Compared with zero by 1-tailed unpaired t test.

† Equation: variable = I + ax + by + cz + dxy + eyz + fzx + gxyz All intercepts are significant.

TABLE 5. Coefficients and $R^2$ of multiple linear regression equation† fit to $\dot{V}_A$ data for whole, left and right lung

| lung | Position | PEEP | Intercept | a | b | c | d | e | f | g | $R^2$ |
|---|---|---|---|---|---|---|---|---|---|---|---|
| | LLD | 0 | 5.1 | -0.068 | 0.27 | -0.03 | **-0.053** | **-0.043** | **0.04** | **0.009** | 0.39 |
| Whole | | | ±1.4 | ±0.27 | ±0.25* | ±0.10 | **±0.04*** | **±0.026*** | **±0.02*** | **±0.009*** | ±0.11 |
| | LLD | 10 | 2.9 | **-0.072** | -0.003 | 0.013 | **-0.021** | **-0.011** | **0.006** | **0.002** | 0.28 |
| | | | ±0.7 | **±0.06*** | ±0.023 | ±0.024 | **±0.015*** | **±0.009*** | **±0.005*** | **±0.001*** | ±0.10 |
| | RLD | 0 | 5.5 | **-0.58** | 0.31 | -0.055 | 0.024 | **-0.049** | 0.006 | 0.005 | 0.47 |
| | | | ±1.4 | **±0.34*** | ±0.25* | ±0.14 | ±0.04 | **±0.02*** | ±0.019 | ±0.005 | ±0.17 |
| | RLD | 10 | 2.8 | -0.079 | 0.016 | -0.001 | -0.004 | -0.006 | -0.003 | -0.0004 | 0.32 |
| | | | ±0.6 | ±0.089 | ±0.067 | ±0.028 | ±0.009 | ±0.009 | ±0.007 | ±0.001 | ±0.15 |
| | LLD | 0 | 4.6 | -0.45 | **0.41** | -0.07 | 0.083 | **-0.088** | **0.049** | 0.015 | 0.50 |
| Left | | | ±1.8 | ±0.49 | **±0.22*** | ±0.13 | ±0.12 | **±0.076*** | **±0.046*** | ±0.022 | ±0.14 |
| | LLD | 10 | 3.1 | -0.03 | **0.13** | -0.002 | 0.014 | **-0.025** | 0.001 | 0.001 | 0.43 |
| | | | ±1.0 | ±0.1 | **±0.097*** | ±0.009 | ±0.023 | **±0.017*** | ±0.013 | ±0.001 | ±0.17 |
| | RLD | 0 | 3.2 | **-0.20** | **0.27** | -0.038 | -0.003 | -0.023 | -0.005 | **0.007** | 0.55 |
| | | | ±0.9 | **±0.16*** | **±0.20*** | ±0.11 | ±0.03 | ±0.021 | ±0.025 | **±0.006*** | ±0.12 |
| | RLD | 10 | 2.5 | **-0.08** | -0.017 | -0.016 | -0.003 | -0.009 | **0.01** | 0.002 | 0.27 |
| | | | ±0.7 | **±0.04*** | ±0.067 | ±0.012 | ±0.02 | ±0.009 | **±0.003*** | ±0.004 | ±0.08 |
| Right | LLD | 0 | 5.5 | **-0.50** | 0.09 | 0.021 | 0.032 | **-0.027** | 0.004 | **0.012** | 0.42 |
| | | | ±1.7 | **±0.21*** | ±0.20 | ±0.092 | ±0.073 | **±0.020*** | ±0.025 | **±0.008*** | ±0.15 |
| | LLD | 10 | 2.8 | **-0.22** | -0.11 | 0.018 | -0.011 | -0.007 | **0.007** | **0.001** | 0.43 |
| | | | ±0.7 | **±0.04*** | ±0.05* | ±0.034 | ±0.013 | ±0.007 | **±0.006*** | **±0.001*** | ±0.14 |
| | RLD | 0 | 6.9 | **-0.64** | 0.27 | -0.03 | 0.038 | **-0.084** | **0.099** | 0.001 | 0.38 |
| | | | ±2.3 | **±0.58*** | ±0.35 | ±0.16 | ±0.050 | **±0.05*** | **±0.092*** | ±0.013 | ±0.14 |
| | RLD | 10 | 3.3 | -0.09 | 0.016 | 0.018 | -0.007 | -0.01 | 0.009 | -0.001 | 0.23 |
| | | | ±1.7 | ±0.11 | ±0.072 | ±0.049 | ±0.019 | ±0.012 | ±0.013 | ±0.002 | ±0.1 |

Values are presented as mean ± SD (n=6), * $P < 0.05$ Compared with zero by 1-tailed unpaired t test.
† Equation: variable = I + ax + by + cz + dxy + eyz + fzx + gxyz All intercepts are significant.

TABLE 6. Coefficients and $R^2$ of multiple linear regression equation† fit to $\dot{V}_A / \dot{Q}$ data for whole, left and right lung, respectively

| lung | Position | PEEP | Intercept | a | b | c | d | e | f | g | $R^2$ |
|---|---|---|---|---|---|---|---|---|---|---|---|
| | LLD | 0 | 1.21 | 0.047 | 0.042 | 0.019 | -0.001 | -0.005 | -0.002 | 0.001 | 0.43 |
| | | | ±0.50 | ±0.05 | ±0.037 | ±0.023 | ±0.007 | ±0.005 | ±0.003 | ±0.002 | ±0.10 |
| Whole | LLD | 10 | 1.10 | 0.018 | 0.015 | 0.011 | -0.003 | **-0.002** | 0.0000 | 0.000004 | 0.30 |
| | | | ±0.24 | ±0.032 | ±0.032 | ±0.014 | ±0.005 | **±0.002*** | ±0.002 | ±0.001 | ±0.19 |
| | RLD | 0 | 1.08 | -0.008 | **0.035** | 0.015 | **0.004** | -0.004 | **-0.001** | 0.00005 | 0.50 |
| | | | ±0.43 | ±0.056 | **±0.02*** | ±0.027 | **±0.003*** | ±0.004 | **±0.001*** | ±0.002 | ±0.37 |
| | RLD | 10 | 1.25 | **0.035** | 0.003 | 0.014 | -0.002 | -0.001 | 0.0000 | 0.0001 | 0.26 |
| | | | ±0.32 | **±0.027*** | ±0.012 | ±0.017 | ±0.004 | ±0.003 | ±0.002 | ±0.001 | ±0.10 |
| | LLD | 0 | 0.92 | -0.004 | **0.053** | 0.038 | 0.013 | -0.01 | 0.002 | -0.0002 | 0.48 |
| Left | | | ±0.38 | ±0.04 | **±0.03*** | ±0.037 | ±0.02 | ±0.017 | ±0.005 | ±0.003 | ±0.10 |
| | LLD | 10 | 0.99 | **0.03** | **0.03** | 0.014 | -0.0002 | -0.003 | 0.002 | **-0.001** | 0.46 |
| | | | ±0.27 | **±0.01*** | **±0.02*** | ±0.013 | ±0.005 | ±0.003 | ±0.003 | **±0.001*** | ±0.19 |
| | RLD | 0 | 1.02 | -0.15 | 0.042 | 0.009 | 0.013 | -0.001 | -0.003 | **0.002** | 0.54 |
| | | | ±0.53 | ±0.06 | ±0.036 | ±0.026 | ±0.015 | ±0.009 | ±0.004 | **±0.001*** | ±0.20 |
| | RLD | 10 | 1.42 | -0.001 | -0.011 | 0.013 | 0.004 | -0.001 | 0.002 | 0.001 | 0.21 |
| | | | ±0.45 | ±0.046 | ±0.032 | ±0.018 | ±0.006 | ±0.003 | ±0.006 | ±0.002 | ±0.11 |
| | LLD | 0 | 1.40 | -0.022 | 0.032 | 0.01 | 0.011 | -0.004 | **-0.004** | 0.001 | 0.31 |
| Right | | | ±0.60 | ±0.035 | ±0.045 | ±0.032 | ±0.020 | ±0.006 | **±0.004*** | ±0.002 | ±0.05 |
| | LLD | 10 | 1.22 | -0.03 | -0.015 | **0.014** | -0.002 | -0.001 | 0.0002 | 0.0003 | 0.27 |
| | | | ±0.24 | ±0.045 | ±0.022 | **±0.006*** | ±0.005 | ±0.002 | ±0.003 | ±0.0010 | ±0.15 |
| | RLD | 0 | 1.09 | 0.014 | **0.035** | 0.023 | 0.006 | -0.006 | 0.005 | -0.0002 | 0.48 |
| | | | ±0.39 | ±0.022 | **±0.022*** | ±0.025 | ±0.011 | ±0.006 | ±0.008 | ±0.001 | ±0.09 |
| | RLD | 10 | 1.13 | **0.04** | 0.012 | 0.017 | -0.003 | -0.002 | **0.003** | -0.00034 | 0.35 |
| | | | ±0.24 | **±0.02*** | ±0.012 | ±0.02 | ±0.007 | ±0.003 | **±0.003*** | ±0.001 | ±0.06 |

Values are presented as mean ± SD (n=6), * $P < 0.05$ Compared with zero by 1-tailed t test.

† Equation: Variable = I + ax + by + cz + dxy + eyz + fzx + gxyz. All intercepts are significant.

TABLE 7. Coefficients and $R^2$ of multiple linear regression equation† fit to $P_RO_2$ data for whole, left and right lung, respectively

| lung | Position | PEEP | Intercept | a | b | c | d | e | f | g | $R^2$ |
|---|---|---|---|---|---|---|---|---|---|---|---|
| | LLD | 0 | 113.4 | **1.30** | **1.15** | **0.50** | -0.14 | **-0.16** | -0.060 | 0.03 | 0.51 |
| Whole | | | ±6.7 | **±1.20*** | **±0.89*** | **±0.26*** | ±0.19 | **±0.15*** | ±0.051 | ±0.04 | ±0.15 |
| | LLD | 10 | 113.8 | 0.43 | 0.45 | **0.33** | -0.08 | **-0.074** | -0.004 | 0.006 | 0.30 |
| | | | ±4.2 | ±0.82 | ±0.80 | **±0.23*** | ±0.14 | **±0.054*** | ±0.048 | ±0.017 | ±0.17 |
| | RLD | 0 | 111.3 | -0.59 | **1.43** | 0.59 | 0.20 | -0.21 | -0.013 | 0.003 | 0.57 |
| | | | ±8.7 | ±1.10 | **±0.73*** | ±0.70 | ±0.23 | ±-0.13 | ±0.028 | ±0.029 | ±0.09 |
| | RLD | 10 | 113.8 | **0.65** | 0.06 | 0.31 | -0.05 | -0.017 | -0.018 | 0.004 | 0.30 |
| | | | ±5.2 | **±0.45*** | ±0.24 | ±0.33 | ±0.07 | ±0.057 | ±0.035 | ±0.013 | ±0.14 |
| | LLD | 0 | 104.9 | 0.21 | **2.80** | **0.85** | 0.50 | -0.42 | 0.08 | -0.04 | 0.52 |
| Left | | | ±12.0 | ±2.40 | **±2.60*** | **±0.67*** | ±0.57 | ±0.50 | ±0.32 | ±0.15 | ±0.16 |
| | LLD | 10 | 112.3 | **0.83** | **1.07** | **0.40** | 0.05 | **-0.15** | 0.02 | **-0.02** | 0.47 |
| | | | ±6.8 | **±0.77*** | **±0.85*** | **±0.30*** | ±0.13 | **±0.13*** | ±0.07 | **±0.02*** | ±0.22 |
| | RLD | 0 | 109.2 | -0.61 | **1.98** | 0.45 | 0.13 | -0.20 | -0.04 | 0.036 | 0.60 |
| | | | ±12.0 | ±1.00 | **±1.70*** | ±0.87 | ±0.20 | ±0.21 | ±0.13 | ±0.037 | ±0.21 |
| | RLD | 10 | 117.2 | -0.25 | -0.23 | 0.19 | 0.02 | -0.025 | 0.06 | 0.018 | 0.24 |
| | | | ±5.9 | ±0.84 | ±0.66 | ±0.37 | ±0.09 | ±0.056 | ±0.09 | ±0.031 | ±0.12 |
| Right | LLD | 0 | 118.6 | -0.25 | 0.55 | 0.2 | 0.17 | -0.087 | -0.07 | 0.013 | 0.35 |
| | | | ±4.3 | ±0.36 | ±0.57 | ±0.30 | ±0.23 | ±0.110 | ±0.08 | ±0.028 | ±0.14 |
| | LLD | 10 | 117.9 | -0.75 | -0.4 | **0.34** | -0.05 | -0.013 | 0.04 | 0.002 | 0.30 |
| | | | ±3.2 | ±0.76 | ±0.47 | **±0.16*** | ±0.10 | ±0.045 | ±0.07 | ±0.008 | ±0.15 |
| | RLD | 0 | 112.6 | -0.03 | 0.88 | 0.67 | 0.19 | -0.26 | 0.22 | -0.011 | 0.50 |
| | | | ±7.3 | ±0.40 | ±0.64 | ±0.55 | ±0.16 | ±0.16 | ±0.26 | ±0.025 | ±0.08 |
| | RLD | 10 | 111.6 | **0.90** | 0.23 | 0.44 | -0.08 | -0.054 | 0.06 | -0.007 | 0.38 |
| | | | ±4.7 | **±0.34*** | ±0.34 | ±0.49 | ±0.17 | ±0.074 | ±0.07 | ±0.019 | ±0.06 |

Values are presented as mean ± SD (n=6), * $P < 0.05$ Compared with zero by 1-tailed t test.

† Equation: Variable = I + ax + by + cz + dxy + eyz + fzx + gxyz. All intercepts are significant.

vertical height (X-coordinate) up the lung in the LLD and RLD postures with and without PEEP for a representative animal. The lines represent $\dot{Q}$ vs. height (X) at the center of mass (Y = Z = 0), determined from the regression analysis. Fig. 9, 11 and 12 are equivalent data for $\dot{V}_A$, $\dot{V}_A/\dot{Q}$ and $P_{RO_2}$.

**Effect of posture without PEEP**

***Regional distribution of*** $\dot{Q}$**.** As indicated by the X-coefficent (a) for the whole lung, there was a significant negative (gravity dependent) vertical gradient (Table 2, -0.27 and -0.42 $\dot{Q}\cdot ml^{-1}\cdot cm^{-1}$) in $\dot{Q}$ that was greater in the RLD posture (-0.42) than in the LLD posture (-0.27) implying that blood flow in the dependent lung was less in the LLD than in the RLD posture.

A smaller blood flow in the dependent lung in the LLD than RLD posture was verified by the fact that total blood flow (% total) was less in the dependent left lung (37%) than in the nondependent lung (63%) in the LLD posture but was greater in the dependent right lung (64%) than in the nondependent lung (36%) in the RLD posture (Table 3). Given the same cardiac output in both postures (Table 1), the fraction of the cardiac output corrected for tissue mass to either lung did not change with body position.

Table 8. Percent cardiac output and ventilation to left and right lung from microsphere data

| | | LLD | | RLD | |
|---|---|---|---|---|---|
| | PEEP, cm $H_2O$ | 0 | 10 | 0 | 10 |
| $\dot{Q}$ (%) | Left lung | 37±6 | 49±8* | 36±4 | 32±5† |
| $\dot{Q}$ (%) | Right lung | 63±6‡ | 51±8* | 64±4‡ | 68±5†‡ |
| $\dot{V}_A$ (%) | Left lung | 28±6 | 43±6* | 34±9 | 37±7 |
| $\dot{V}_A$ (%) | Right lung | 72±6‡ | 57±6*‡ | 66±9‡ | 63±7‡ |

Values are means ± SD (n = 6). * $P < 0.05$, significant change with PEEP; † $P < 0.05$ Significant difference with change in posture. ‡ $P < 0.05$, significant difference between left lung and right lung

In both left and right lung, the vertical gradients (-0.60 and -0.37) observed in the LLD posture were eliminated with body inversion to the RLD posture. These gradients

represented a 70-150% change in the mean blood flow over the height of the lung (~15 cm) or 5-10% $cm^{-1}$.

In the left lung, there was a positive dorsal-ventral gradient (0.26 and 0.18) in the LLD and RLD posture with the ventral regions having the greater blood flow. The dorsal-ventral gradient in the left lung was accompanied with a negative caudal-cranial gradient in the LLD posture (-0.18), with blood flow greatest in the caudal regions.

Regional variation in the spatial gradients

The coefficients d-f of the independent variable XY, YZ and ZX in the linear equation (Eq. 9) are measures of the variation of the spatial gradients in any one coordinate along an orthogonal coordinate (Table 4). For the whole lung without PEEP in the LLD posture, the vertical gradient ($\partial\dot{Q}/\partial X$) in blood flow increased linearly with Z (coefficient f, 0.046):

$$\partial\dot{Q}/\partial X = -0.27 + 0.046Z \qquad (12)$$

At Y = 0, the vertical blood flow gradient increase from a value of –0.59 $\dot{Q}\cdot ml^{-1}\cdot cm^{-1}$ in the caudal region at Z = -7 cm to a value of 0.05 in the cranial regions at Z = 7 cm. Thus the vertical gradient was maximal in the caudal regions and vanished in the cranial regions. The application of PEEP reduced this Z-variation of the vertical gradient to 9% (coefficient f, 0.005).

Similarly in the left dependent lung in the LLD posture, the significant coefficient e (-0.074, Table 4) implies that the dorsal-ventral gradient in $\dot{Q}$ also varied linearly with Z (X = 0):

$$\partial\dot{Q}/\partial Y = 0.26 - 0.074\,Z \qquad (13)$$

Thus the dorsal-ventral gradient increased to 0.78 in the cranial regions (Z = 7 cm) and became negative (-0.26) in the caudal regions (Z = -7 cm). Similar variations in other spatial gradients were present for both $\dot{Q}$ and $\dot{V}_A$. Variations in the gradients in $\dot{V}_A$ were substantial only in the LLD posture without PEEP.

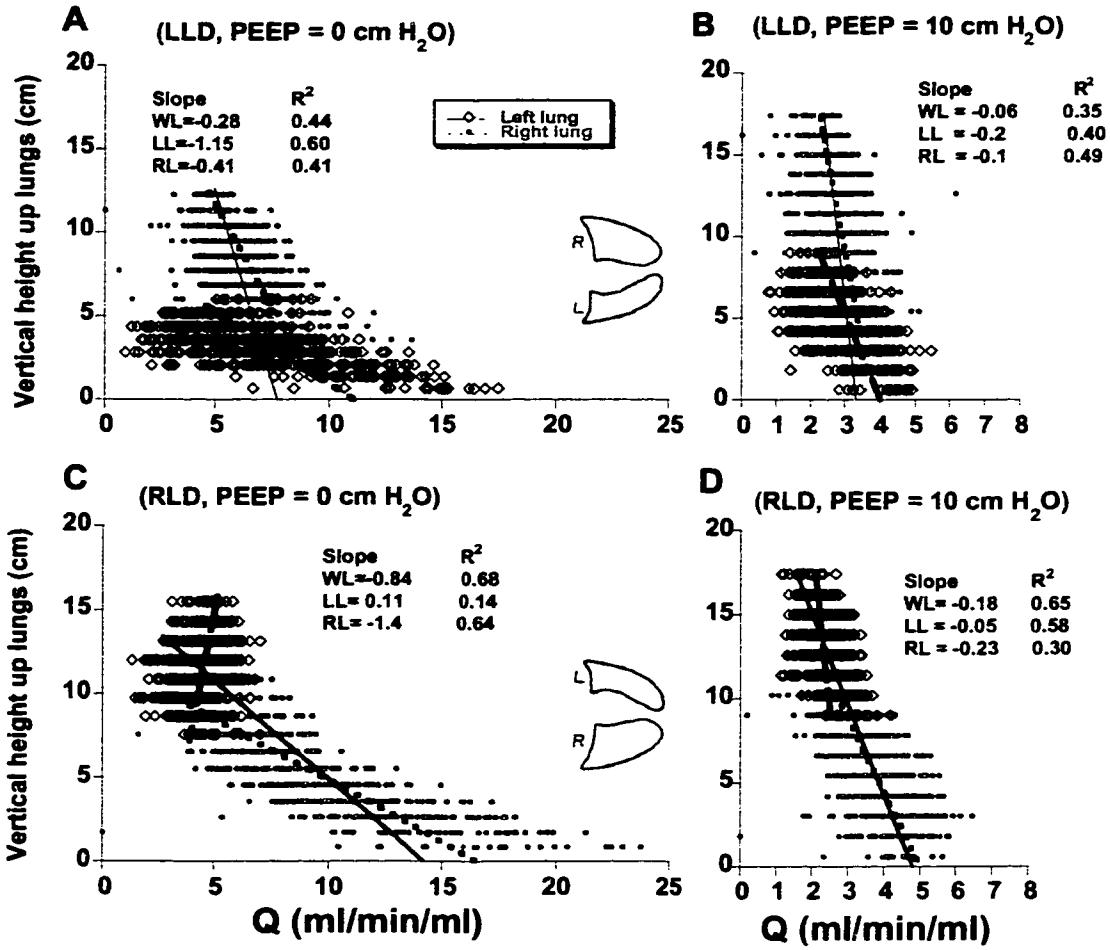


Fig 9. Blood flow per unit regional lung volume (ml· $min^{-1}$· $ml^{-1}$) vs. lung height for a representative dog, in the LLD (posture) without PEEP (A), LLD with 10 cm $H_20$ PEEP (B), RLD posture without PEEP (C) and RLD with 10 cm $H_2O$ PEEP (D). R represents right lung (open circle), L the left lung (open diamond) and The lines represent best-fit values from multiple linear regression analysis. $R^2$ indicated that ~40% of the variability in blood flow was spatially determined. WL: whole lung; RL: right lung; LL: left lung. Independent and dependent axes have been interchanged for presentation.

***Regional distribution of*** $\dot{V}_A$. For the whole lung, the largest vertical gradient in $\dot{V}_A$ was observed in the RLD posture (Fig 10 and Table 5, -0.58) and occurred in conjunction with a positive dorsal-ventral gradient (0.31) that was eliminated with inversion to the LLD posture. In the LLD posture, the only substantial gradient occurred in the dorsal-ventral direction (0.27).

Similar to the behavior in cardiac output, total ventilation was smaller in the dependent lung than in the nondependent lung in the LLD posture but larger in the dependent lung in the RLD posture (Table 5). For constant ventilation in both postures, body position had no effect on ventilation in either lung. In the left lung in the RLD posture, significant vertical (-0.20) and dorsal-ventral (0.27) gradients were observed.

***Relationship between regional*** $\dot{Q}$ ***and*** $\dot{V}_A$***, and total*** $\dot{Q}$ ***and*** $\dot{V}_A$ ***for each lung.*** The vertical gradients in regional $\dot{Q}$ and $\dot{V}_A$ (Table 4 and 5) measured in this study might appear at first sight to be at odds with the total $\dot{Q}$ and $\dot{V}_A$ values measured for each lung (Table 8). For the whole lung the vertical gradient in regional $\dot{Q}$ in the LLD posture would suggest a greater blood flow in the dependent lung than in the nondependent lung (Table 4). On the other hand the total $\dot{Q}$ to the dependent left lung in the LLD posture was clearly lower than that to the nondependent lung. This apparent discrepancy is due to the fact that the total $\dot{Q}$ to the lung is the product of the mean regional $\dot{Q}$ and the total lung volume. This relationship allowed the estimate of FRC to each lung. The smallest FRC was predicted to occur in the left lung in the LLD posture. In the LLD posture, mean regional $\dot{Q}$ (Table 4) averaged 5.8 and 4.6 ml$\cdot$ min$^{-1}\cdot$ ml$^{-1}$ in the left and right lung pieces, respectively. Cardiac output (3.6 L$\cdot$min$^{-1}$) was distributed 1.3 L$\cdot$min$^{-1}$ (37%) to the left lung and 2.3 L$\cdot$min$^{-1}$ (67%) to the right lung (Table 8). Thus, the estimated FRC was 220 ml in the left lung and 500 ml in the right lung, resulting in a total FRC of 720 ml. This value was close to the measured value (758 ml) equal to the air volume (645 ml, Table 1)) and wet tissue volume (113 ml) based on lung wet weight (4.7 x 24 g dry weight).

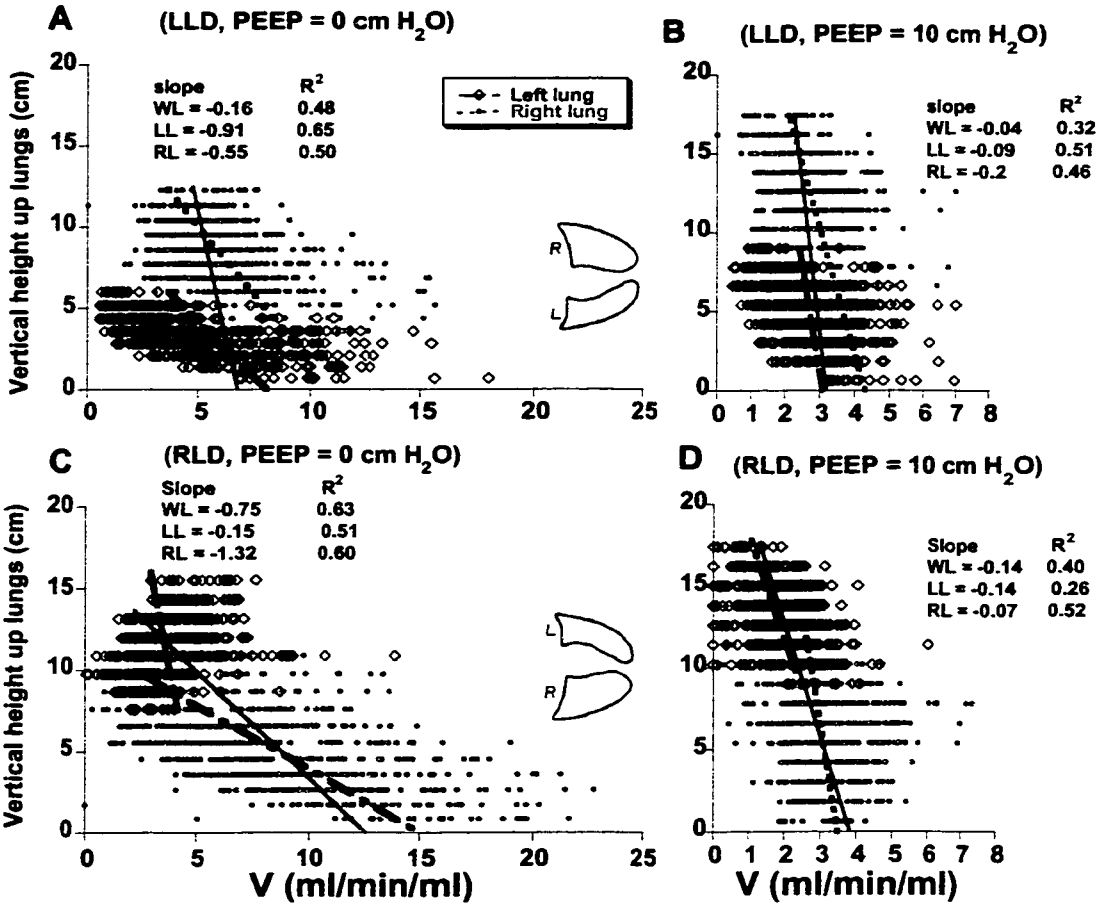


Fig 10. Ventilation per unit regional lung volume (ml· $min^{-1}$· $ml^{-1}$) vs. lung height for the representative animal in LLD without PEEP (A), LLD with 10 cm $H_2O$ PEEP (B), RLD without PEEP (C), and RLD with 10 cm $H_2O$ PEEP. The lines represent the best-fit values from multiple linear regression analysis.

The predicted left lung FRC was 31% total FRC. The expected FRC of a uniformly inflated left lung based on tissue mass was 43% total FRC. This value was reduced by ~25% via the vertical Ptp gradient, resulting in a left lung FRC of 32%, near the predicted value of 31%. Accordingly, the reduced blood flow to the dependent left lung in the LLD posture was consistent with a reduced FRC caused by the vertical Ptp gradient. Evidently vertical gradients in regional blood flow require knowing regional lung volume to accurately predict relative blood flow to each lung. A similar argument applies to $\dot{V}_A$ measurements.

***Regional distribution of*** $P_{RO_2}$ ***and*** $\dot{V}_A/\dot{Q}$. The largest gradient in $P_{RO_2}$ (1.3, Table 7) was observed in the vertical direction for the whole lung in the LLD posture and was positive, indicating that $P_{RO_2}$ on the average, was smaller in the dependent (left) lung than in the nondependent (right) lung (intercepts, Table 7). This vertical gradient was abolished with inversion to the RLD posture and was accompanied with positive dorsal-ventral and caudal-cranial gradients.

To determine whether $P_{RO_2}$ observed in the dependent lung in the LLD posture was low enough to trigger a hypoxic vasoconstriction response, the minimum $P_{RO_2}$ value was obtained from regression analysis for the six animals studied. The linear equation with mean intercept and coefficients for the whole lung was as follows (Table 7):

$$P_RO_2 = 113 + 1.3X + 1.15Y + 0.5Z - 0.14XY - 0.16YZ - 0.06ZX + 0.03XYZ \quad (14)$$

The minimum value of $P_{RO_2}$ ($81 \pm 21$ mmHg) occurred in the dependent ($X = -4$ cm), dorsal ($Y = -5$ cm) and caudal ($Z = -8$ cm) regions of the lung (Fig. 12). The maximum value of $P_{RO_2}$ ($124 \pm 5$ mmHg) was located in the nondependent ($X = +4$ cm), ventral ($Y = +5$ cm) and cranial ($Z = +8$ cm) region of the lung. In the RLD posture, minimum and maximum $P_{RO_2}$ values evaluated at similar (X, Y, Z) values used for the LLD posture were $96 \pm 10$ and $117 \pm 8$ mmHg, respectively (Fig. 11). Note that $P_{RO_2}$ was reduced below 100 mmHg only in the dependent lung in the LLD posture.

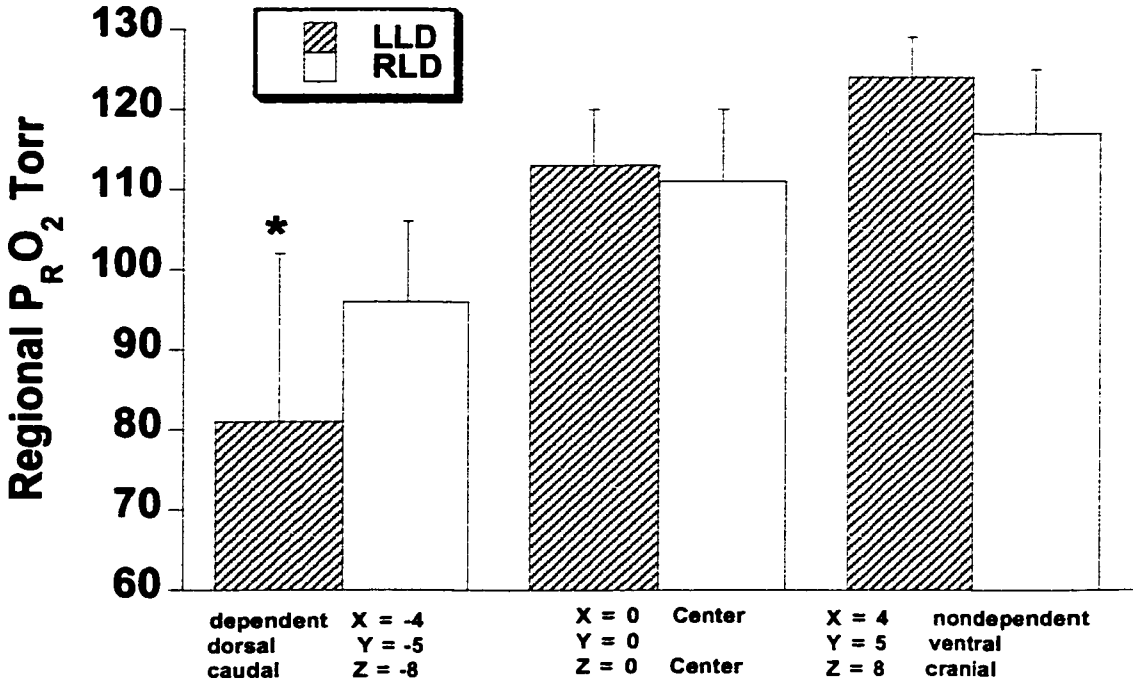


Fig 11. Minimum and maximum $P_{RO_2}$ values from best-fit multiple linear regression equation in the LLD and RLD postures. * $P < 0.05$, LLD vs RLD posture. The minimum $P_{RO_2}$ values in the LLD posture are consistent with a hypoxic vasoconstriction response that would account for the reduced blood flow measured in the dependent left lung (Table 4).

The low $P_{RO_2}$ originating from the dependent caudal-dorsal regions of the dependent left lung in the LLD posture without PEEP was increased by inversion to the RLD posture (Fig 13). That body inversion from the LLD to the RLD posture increased $P_{RO_2}$ in the caudal regions was consistent with the reduction or elimination of significant positive vertical, dorsal-ventral and caudal-cranial $P_{RO_2}$ gradients for the whole lung (Table 7).

In the left and right lung, small but significant gradients in $P_{RO_2}$ and $\dot{V}_A/\dot{Q}$ were observed in all 3 coordinates (Fig 12, Table 6 and 7). However, the detection of a significant $\dot{V}_A/\dot{Q}$ ($P_{RO_2}$) gradient was associated with a significant $P_{RO_2}$ ($\dot{V}_A/\dot{Q}$)

gradient only in the left dependent lung in the LLD posture. In the left (dependent) lung in the LLD posture, a dorsal-ventral $\dot{V}_A/\dot{Q}$ gradient (0.053) were associated with significant $P_{RO2}$ gradients (2.8).

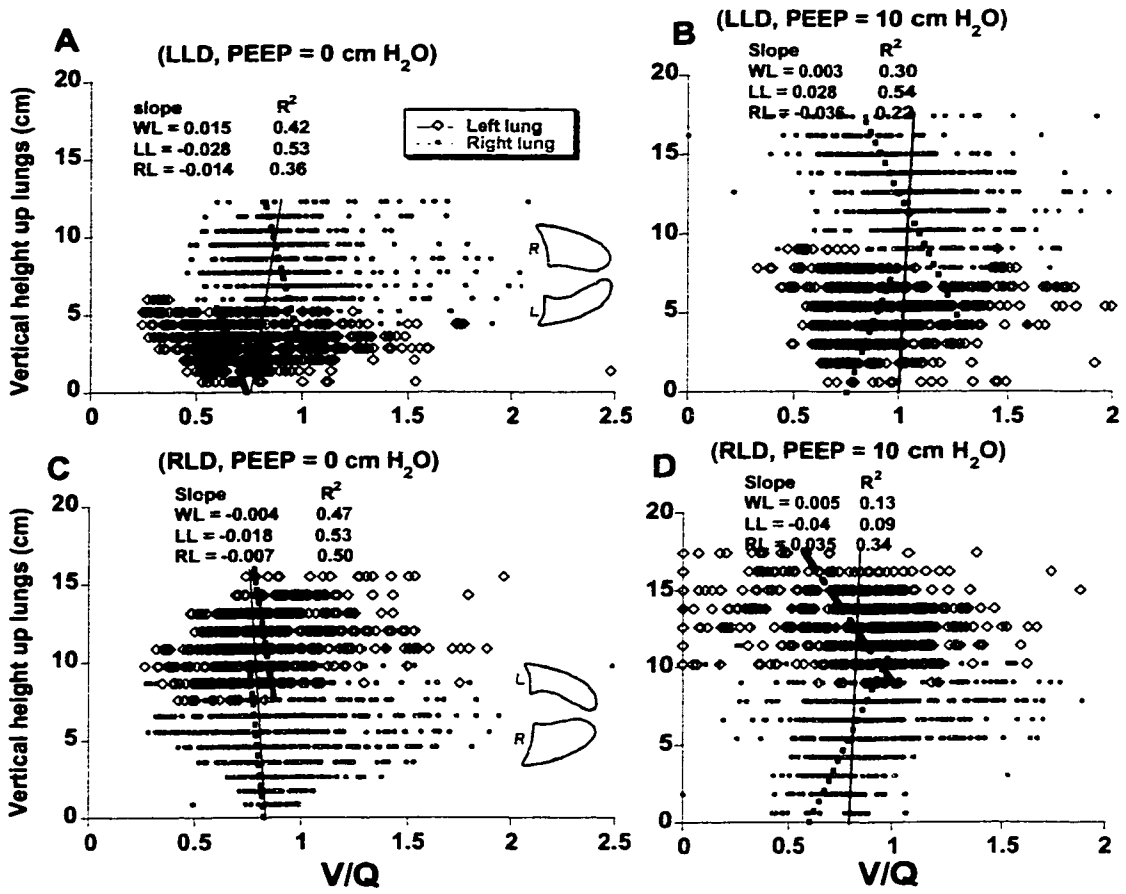


Fig 12. $\dot{V}A/\dot{Q}$ vs. lung height for the representative animal in LLD without PEEP (*A*), LLD with 10 cm $H_2O$ cm PEEP (*B*), RLD without PEEP (*C*) and RLD with 10 cm $H_2O$ PEEP (*D*). The lines represent the best-fit values from multiple linear regression analysis.

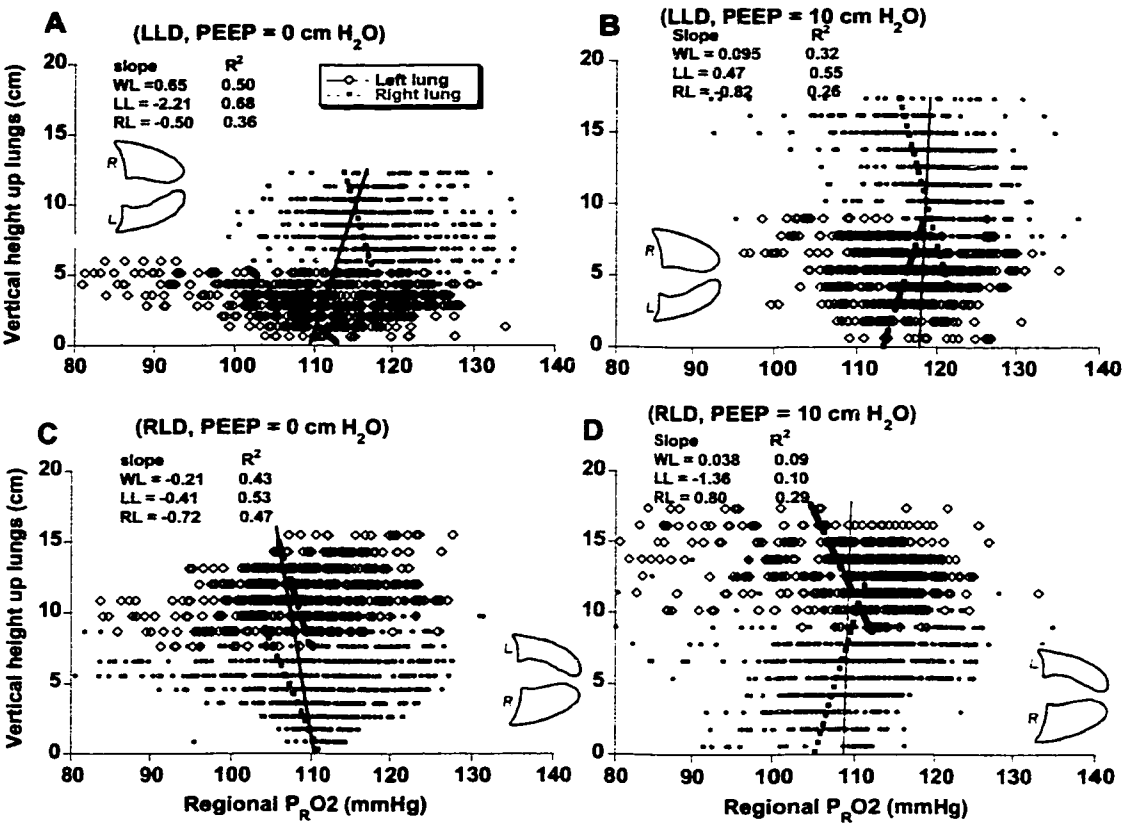


Fig 13. Regional $PO_2$ ($P_RO_2$) vs. lung height for the representative animal in LLD without PEEP (*A*), LLD with 10 cm $H_2O$ cm PEEP (*B*), RLD without PEEP (*C*), and RLD with 10 cm $H_2O$ PEEP (*D*). The lines represent the best-fit values from multiple linear regression analysis. Note that the low $P_RO_2$ values in the dependent lung in the LLD posture (A) was eliminated with the addition of PEEP (B).

## Comparison between predicted and measured gas exchange

Predicted $PaO_2$ and $PaCO_2$ calculated from regional $\dot{V}_A/\dot{Q}$ data did not differ from measured $PaO_2$ and $PaCO_2$ in both the LLD and RLD posture (Table 2) and the measured A-a$DO_2$ was well predicted from the microsphere data in the LLD posture. However, the predicted values of A-a$DO_2$ were significantly ($P < 0.05$) less in the LLD than in the RLD posture (Table 2).

**Mean $\dot{V}_A/\dot{Q}$ and $P_RO_2$ changes of nondependent and dependent lung**

In the LLD posture (intercepts, Table 6), $\dot{V}_A/\dot{Q}$ was greater in the nondependent right lung (1.42 ± 0.45) than in the dependent lung (0.93 ± 0.37). In the right lung, $P_RO_2$ increased with body inversion from the RLD (113 ± 7 mmHg) to the LLD (119 ± 4 mmHg) posture. This was associated with an increase in $\dot{V}_A/\dot{Q}$ from 1.09 ± 0.39 in the RLD posture to 1.40 ± 0.60 in the LLD posture. This behavior was accompanied with a dorsal-ventral $\dot{V}_A/\dot{Q}$ gradient that was significant (0.035) only in the RLD posture.

**Effect of PEEP**

***Regional distribution of*** $\dot{Q}$. In general PEEP either reduced or eliminated the spatial gradients in $\dot{Q}$ and $\dot{V}_A$ that occurred without PEEP (Table 4 and 5). The decrease in the vertical gradient with PEEP was associated with a decrease (30-50%) in the mean blood flow (intercepts, Table 4). With PEEP, the dependent right lung in the RLD posture had the greater blood flow, similar to the behavior without PEEP (Table 8). By contrast, in the LLD posture PEEP eliminated the left-right lung difference in blood flow measured without PEEP.

PEEP increased the low $P_RO_2$ originating from the dependent caudal-dorsal regions of the dependent left lung in the LLD posture (intercepts, Table 7). The latter effect of PEEP was consistent with the PEEP-induced reduction of the caudal-cranial $\dot{V}_A/\dot{Q}$ gradient (from 0.053 to 0.03, Table A3) and 50% reduction of the caudal-cranial $P_RO_2$ gradient (from 0.85 to 0.40) in the left lung.

Similar to the data without PEEP, with PEEP $PaO_2$ and $PaCO_2$ calculated from regional $\dot{V}_A/\dot{Q}$ data did not differ from measured $PaO_2$ and $PaCO_2$ in both the LLD and RLD posture and the measured A-a$DO_2$ was well predicted from the microsphere data (Table 2). PEEP reduced the relatively high $\dot{V}_A/\dot{Q}$ of the nondependent right lung to a value closer to 1 (Table A3, 1.22 ± 0.24). In the right lung with PEEP, $\dot{V}_A/\dot{Q}$ increased

with body inversion from the RLD posture (1.13 ± 0.24) to the LLD posture (1.22 ± 0.24).

In the left lung in the LLD posture, PEEP increased $P_{R}O_2$ from 105 ± 12 to 112 ± 7 mmHg (Table 7). This behavior was associated with a PEEP-induced vertical $P_RO_2$ gradient (0.83) in conjunction with reduced dorsal-ventral and caudal-cranial $P_RO_2$ gradients.

**Regional perfusion correlation between postures with and without PEEP**

Fig. 14 shows regional blood flow to each lung piece in the LLD posture plotted against blood flow of the same piece in the RLD posture of one representative animal without PEEP (A) and with PEEP (B). Except for the left lung without PEEP (R = 0.66), blood flow to each piece was poorly correlated (R = 0.044-0.22) between LLD and RLD posture. In other words, lung pieces with high (or low) blood flow in the LLD posture received low (or high) blood flow in the RLD posture. This behavior was consistent with the gravity-dependent vertical gradients observed for both right and left lungs and for the whole lung in both postures, opposite to that found between the supine and prone position (50).

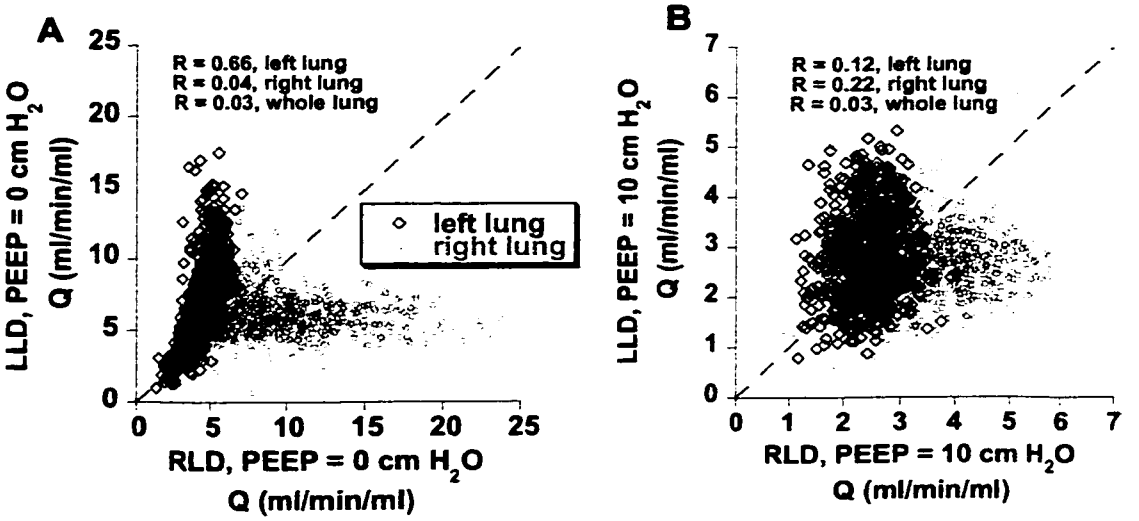


Fig 14. Correlation between pulmonary blood flow in the LLD and RLD measured in one representative animal without PEEP (A) and with PEEP (B). The dotted line is line of identity. Note that lung pieces with high (low) blood flow in the LLD posture received low (high) blood flow in the RLD posture, consistent with a gravity-dependent vertical gradient measured by multiple linear regression analysis (Fig. 1B)

Table 9. Effect of position & PEEP on heterogeneity of ventilation ($\dot{V}_A$), and perfusion ($\dot{Q}$) distribution: FMS and MIGET

| Method | $\sigma^2$, lnSD or $\rho_c$ | LLD ZEEP | RLD ZEEP | LLD PEEP | RLD PEEP |
|---|---|---|---|---|---|
| FMS (total) | $\sigma^2 \dot{V}_A$ | 0.42±0.10 | 0.58±0.40 | 0.24±0.06* | 0.25±0.07 |
| FMS (total) | $\sigma^2 \dot{Q}$ | 0.26±0.16 | 0.28±0.12 | 0.16±0.07 | 0.19±0.05 |
| FMS (total) | $\rho_c(\dot{V}_A : \dot{Q})$ | 0.60±0.15 | 0.73±0.10 | 0.65±0.09 | 0.61±0.09† |
| FMS (total) | $\sigma^2 \dot{V}_A/\dot{Q}$ | 0.27±0.13 | 0.26±0.15 | 0.14±0.04 | 0.15±0.06 |
| residual | $\sigma^2 \dot{V}_A$ | 0.14±0.04 | 0.21±0.07 | 0.14±0.04 | 0.12±0.05† |
| residual | $\sigma^2 \dot{Q}$ | 0.09±0.02 | 0.12±0.04 | 0.09±0.04 | 0.10±0.06 |
| residual | $\sigma^2 \dot{V}_A/\dot{Q}$ | 0.08±0.04 | 0.09±0.06 | 0.07±0.02 | 0.08±0.03 |
| residual | $\rho_c(\dot{V}_A : \dot{Q})$ | 0.65±0.12 | 0.75±0.12 | 0.71±0.10 | 0.61±0.12 |
| residual/total (%) | $\sigma^2 \dot{V}_A$ | 34±6.0 | 44±18 | 63±11 | 57±41 |
| residual/total (%) | $\sigma^2 \dot{Q}$ | 41±15 | 56±36 | 55±18 | 52±30 |
| residual/total (%) | $\sigma^2 \dot{V}_A/\dot{Q}$ | 35±16 | 44±13 | 54±15 | 60±26 |
| residual (4th order) | $\sigma^2 \dot{V}_A$ | 0.08±0.03 | 0.09±0.06 | 0.07±0.04 | 0.08±0.05 |
| residual (4th order) | $\sigma^2 \dot{Q}$ | 0.14±0.04 | 0.18±0.12 | 0.11±0.04 | 0.10±0.04 |
| residual (4th order) | $\sigma^2 \dot{V}_A/\dot{Q}$ | 0.09±0.04 | 0.09±0.05 | 0.07±0.02 | 0.09±0.05 |
| residual (4th order) | $\rho_c(\dot{V}_A : \dot{Q})$ | 0.59±0.16 | 0.71±0.06 | 0.64±0.12 | 0.50±0.18† |
| residual /total (%), 4th order | $\sigma^2 \dot{V}_A$ | 34±13 | 37±18 | 48±16 | 47±35 |
| residual /total (%),4th order | $\sigma^2 \dot{Q}$ | 35±13 | 32±8 | 47±17 | 45±31 |
| residual /total (%),4th order | $\sigma^2 \dot{V}_A/\dot{Q}$ | 36±13 | 37±15 | 48±13 | 45±31 |
| FMS | $\mathrm{lnSD}\,\dot{V}_A$ | 0.40±0.07 | 0.36±0.07 | 0.30±0.04 | 0.36±0.07 |
| FMS | $\mathrm{lnSD}\,\dot{Q}$ | 0.45±0.16^ | 0.48±0.18 | 0.35±0.07 | 0.36±0.08 |
| MIGET | $\mathrm{lnSD}\,\dot{V}_A$ | 1.07±0.60 | 1.04±0.59 | 1.00±0.57 | 1.24±0.54 |
| MIGET | $\mathrm{lnSD}\,\dot{Q}$ | 0.71±0.24 | 0.60±0.14 | 0.68±0.40 | 0.52±0.17 |

Data are presented as mean ± SD (n = 6). LLD, left lateral position; RLD right lateral position. ZEEP, 0 cm $H_2O$ end expiratory pressure; PEEP, 10 cm $H_2O$ end expiratory pressure; $\sigma^2$,variance; $\rho_c$, correlation coefficient between $\dot{V}_A$ and $\dot{Q}$; $\mathrm{lnSD}\,\dot{V}_A$ and $\mathrm{lnSD}\,\dot{Q}$, log normal standard deviation of $\dot{V}_A$- and $\dot{Q}$- $\dot{V}_A/\dot{Q}$ distributions;

*P < 0.05 compared with ZEEP in LLD.

†P < 0.05 compared with ZEEP in RLD.

^P < 0.02 compared with MIGET .

*$\dot{Q}$ and $\dot{V}_A$ heterogeneity*

The mean CV of $\dot{Q}$ and $\dot{V}_A$ (30-60%) was similar to reported values (50; 70; 99; 113; 132). Table 9 summarizes the heterogeneity in $\dot{V}_A$ and $\dot{Q}$ evaluated by 3 methods: (total) variances of $\dot{V}_A$, $\dot{Q}$ and $\dot{V}_A/\dot{Q}$; widths (lnSD $\dot{V}_A$ and lnSD $\dot{Q}$) of the $\dot{V}_A$-$\dot{V}_A/\dot{Q}$ and $\dot{Q}$-$\dot{V}_A/\dot{Q}$ distribution curves measured by FMS and MIGET.

The variance of the data based on regional values was similar to that based on uncorrected data. The coefficients of correlation ($\rho_c$) between $\dot{V}_A$, and $\dot{Q}$ (Pearson's method) were similar to those computed using $\sigma\dot{V}_A$, $\sigma\dot{Q}$ and $\sigma^2\dot{V}_A/\dot{Q}$ in Eq. 5 (113). The total variance data showed that in the LLD posture PEEP reduced the variance in $\dot{V}_A$ and $\dot{V}_A/\dot{Q}$ but not in $\dot{Q}$, consistent with a more uniformly inflated lung at the higher lung volume. This PEEP-induced change in variance was undetected by the other two methods. Neither body position nor PEEP affected the total variance in $\dot{Q}$. Neither PEEP nor body position changed the correlation between $\dot{V}_A$ and $\dot{Q}$. There was a tendency for heterogeneity measured by lnSD $\dot{V}_A$ and lnSD $\dot{Q}$ to be greater with MIGET than with FMS but the difference was only significant for $\dot{Q}$ in the LLD posture without PEEP. The broader distribution measured with MIGET than with topographical data has been noted in previous studies (44; 148). The difference has been attributed to the coarse scale of the $\dot{V}_A/\dot{Q}$ distribution inherent in MIGET (148).

Heterogeneity in $\dot{V}_A$, $\dot{Q}$ and $\dot{V}_A/\dot{Q}$ that was attributed to residual (non-spatial) variation as measured by the residuals of the regression analysis was reduced from 65 ± 16 % of the total variance in the linear regression analysis to 41 ± 6 % of the total variance in the fourth-order regression analysis (Table 9). These values are in line with the coefficients of determination ($R^2$) of ~40 and 60% that implicated ~60 and 40 % of the variability to residual variation. Similar to the total variance, PEEP reduced the non-spatial variance of $\dot{V}_A$ in the RLD posture. Neither body position nor PEEP affected the non-spatial variance in $\dot{Q}$. There was a tendency for PEEP to increase the non-spatial-to-total variance fraction in $\dot{V}_A$ and $\dot{V}_A/\dot{Q}$ but this was only significant in the LLD posture.

The coefficient of correlation ($\rho_c$) between $\dot{V}_A$ and $\dot{Q}$ calculated using the non-spatial variances (0.59-0.75, Table 9) in Eq. 5 was similar to the correlation coefficient between $\dot{V}_A$ and $\dot{Q}$ (0.57-0.71).

## DISCUSSION

### Methodological Issues

*The fluorescent microsphere technique.* The microsphere technique as implemented in this study has been validated in previous studies (50; 132). Regional deposition of aerosolized and injected microspheres allowed simultaneous measurements of ventilation and perfusion distribution that predicted regional gas exchange with high spatial resolution.

*Volume Adjustment to FRC and vertical Ptp gradient.* Injected and aerosolized fluorescent microspheres were delivered *in vivo* near FRC, whereas the fluorescent signals were measured *in vitro* in the dried lung inflated to total lung capacity (TLC). Accordingly, we made several corrections to the weight of each piece to extrapolate to piece volume *in vivo* and to determine $\dot{Q}$ and $\dot{V}_A$ per unit regional lung volume at FRC.

First, the lung volume of each piece was adjusted from TLC to FRC by reducing the cube lengths in the 3 dimensions. This correction resulted in an anisotropically inflated lung (56) and a homogeneous (constant) deformation along each axis. Second, we imposed a distortion to the vertical dimension (X) of each lung piece to produce a vertical Ptp gradient as previously measured (1). This distortion in the X dimension at each height was based on the pressure-volume (PV) curve of an isolated lung (91), and was applied to all Y- and Z- dimensions at the same height. This preserved the homogeneous deformation in the Y and Z coordinates and the anisotropy in regional volume at FRC, in effect producing changes in regional volume identical to those given by the PV curve (Eq. 2). These corrections for the vertical Ptp gradient increased the (maximum) dependent-to-nondependent ratio (D/N) for $\dot{Q}$ by a factor of ~3, the N/D in regional lung volume and D/N in regional lung density (46). Implicit in this correction for lung density

is the scaling of tissue mass to capillary density. Accordingly, regional lung density changes caused by the vertical Ptp gradient were the dominant contributor to the vertical gradient in regional $\dot{Q}$ and $\dot{V}_A$.

The correction for the vertical changes in regional lung density produced vertical gradients in regional $\dot{Q}$ that were substantially greater than those estimated in previous studies in which the vertical Ptp gradient was ignored (48; 50; 70; 71; 113; 114). These studies need further evaluation, particularly in the supine and upright body positions under both normal and increased acceleration loads with relatively large Ptp gradients (1; 2).

We made no correction for Ptp gradients in the other two axes (Y and Z), in the absence of reported data. Blood volume was ignored in the calculation of lung density and regional lung volume because the dry weight used in the calculation of mean lung density was blood-free.

**Distribution of regional perfusion**

*Effect of gravity.* The effects of gravity on the vertical gradient in blood flow in the lung has been described in terms of the relation among the pulmonary arterial (Ppa), pulmonary venous (Ppv) and alveolar (Palv) pressures (157; 159). This theory predicts a decreasing blood flow up the height of the lung (in our nomenclature, a negative vertical gradient). Most of the vertical gradients measured in the present study are explainable, at least qualitatively, with the gravitational model. The vertical gradients in blood flow measured in the LLD and RLD posture with and without PEEP were expected and confirmed previous findings (7; 56; 82; 93; 119; 127).

*Effect of lung volume and vascular resistance.* The fact that the gravity-dependent vertical gradients in $\dot{Q}$ decreased with a change from RLD to LLD posture and with PEEP indicates that factors other than gravity contributed to the blood flow distribution. A major factor was the lung volume-induced vascular resistance that changed with body position and PEEP. Pulmonary vascular resistance depends on lung volume (78); its changes with lung volume are different for zone 2 (Ppa > Palv > Ppv) and zone 3 (Ppa >

Ppv > Palv) conditions (15). By this theory (78), regional blood flow is proportional to Ppa – Palv in zone 2 and Ppa – Ppv in zone 3. The increased flow down the lung is due to Ppa increasing down the lung in zone 2 and Ppv-induced capillary recruitment or vascular distention in zone 3.

In the latter study (15), pulmonary blood flow and vascular resistance were measured versus lung volume (%TLC) at constant values of Ppa-Palv and Ppv-Palv under both zone 2 and zone 3 conditions in isolated rabbit lungs. In zone 3, for Ppa-Palv of 18 mmHg, blood flow increased linearly with a decrease in lung volume from TLC to RV. In zone 2, blood flow increased as lung volume decreased from TLC to 50%TLC but decreased from 60%TLC to RV, a behavior consistent with the U-shape curve describing the relationship between vascular resistance and lung volume (144). Whatever the lung volume-induced differences in blood flow, blood flow was greater in zone 3 than in zone 2.

In the present study, without PEEP, Ppv averaged 8.4 cm $H_2O$ in the LLD posture and 6.1 cm $H_2O$ in the RLD posture (Table 1, Ppcw) relative to mid heart level. With a mean Paw of 5 cm $H_2O$ (Table 1), the dependent lung was in zone 3 in both postures whereas the nondependent lung was predominantly in zone 2, more so in the RLD than in the LLD posture. PEEP increased Ppv to 10 cm $H_2O$ and mean Paw to 15 cm $H_2O$ in both postures, placing the nondependent lung and half of the dependent lung in zone 2. Pulmonary vascular resistance, (Ppa - Ppcw)/blood flow, was greater in the dependent than nondependent lung in both postures and increased with PEEP (Table 1).

The gravity dependent vertical gradients in blood flow measured in both postures for the whole lung without PEEP (Table 4, Fig. 8A and 8C) were consistent with the shift from zone 2 to zone 3 conditions down the lung but these gradients were accentuated by the 3 fold increase in lung density down the lung. The removal of the density gradient with PEEP reduced the gradients to 44 and 33% in the LLD and RLD posture, respectively (Table 4, Fig. 8B and 8D). Thus the 2-3 fold increase in the gradient with the removal of PEEP was attributed almost entirely to the lung density gradient. A

similar behavior was observed for both left and right lungs in the LLD posture (Fig. 8A and 8B).

Blood flow was lower in the dependent left lung than in the nondependent lung (Table 3), consistent with the results of a previous study (114). This behavior was opposite to that predicted by gravity, indicating that factors other than gravity contributed to blood flow distribution in the LLD posture. One factor has been associated with the vascular structure (48; 114). The reduced blood flow to the dependent left lung was not caused by a heart weight induced lower lung volume per se because a reduced lung volume is associated with a lower vascular resistance in zone 3 (15). It is possible that a nonuniform lung distortion due to heart and abdominal weight might conceivably cause an increased vascular resistance. Another mechanism such as hypoxic vasoconstriction remains an alternative explanation in vivo, particularly in view of the positive gradient in $P_RO_2$ measured (see below).

*Nongravitational gradients in* $\dot{Q}$. An important finding of this study relates to other nongravitational gradients in $\dot{Q}$. Specifically, in the isogravitational (Y-Z) plane (X = 0), a positive dorsal-ventral gradient in $\dot{Q}$ occurred in the left dependent lung in the LLD posture, with blood flow maximal in the ventral regions (Table 4, 0.26). The smaller blood flow in the dorsal regions was opposite to that observed in the supine dog (16) in which the dorsal lung regions had the larger blood flow. Thus the present measurements would not support an intrinsic greater vascular conductance postulated for the dorsal lung regions (16). Thus extrinsic factors such as hypoxic vasoconstriction and lung distortion caused by the weight of the heart and abdomen might be crucial.

The positive dorsal-ventral gradient in $\dot{Q}$ observed in the left lung in the LLD posture occurred in conjunction with a negative caudal-cranial gradient in $\dot{Q}$ with $\dot{Q}$ increasing in the caudal region, in the absence of any gradient in the right lung. Both these gradients were abolished with PEEP, indicating a lung volume-induced relative shift of blood flow from the ventral-caudal to the dorsal-cranial regions.

The decrease in blood flow in the caudal-cranial direction for the whole lung in the LLD posture is consistent with the results of Greenleaf (56) in the mechanically ventilated anesthetized dog. This contrasts to the absence of a caudal-cranial gradient in spontaneously breathing humans in the lateral decubitus posture (7).

**Distribution of ventilation**

*Effect of posture without PEEP.* In contrast to the absence of a vertical $\dot{V}_A$ gradient in the LLD posture (Table 5), total ventilation was greater in the nondependent than dependent lung in the LLD posture (Table 8). This difference was similar to the behavior in blood flow and was most likely due to a smaller FRC in the dependent left lung. Body inversion from LLD to RLD posture produced a substantial negative gradient in $\dot{V}_A$ (-0.58) that was consistent with the greater total ventilation measured in the right dependent lung than in the nondependent lung. This behavior in the anesthetized dog is consistent with results from the anesthetized human in the lateral decubitus posture (129; 130). These results with anesthesia differed substantially from those in awake humans showing greater ventilation in the dependent than nondependent lung in both the LLD and RLD posture (8; 82; 110). The latter behavior was explained by the vertical Ptp gradient causing a lower lung volume and greater lung compliance in the dependent lung regions. The absence of a caudal-cranial gradient in $\dot{V}_A$ in the lateral decubitus posture in the anesthetized dog was consistent with the results in awake humans measured using radioactive gas inhalation and external scintillation counters (8; 82). This behavior was attributed to a uniform Ptp in the horizontal direction.

The differences in ventilation measured between the anesthetized and awake state might be related to the anesthesia-induced reduction in FRC observed in both lungs (129; 130). The following factors might be involved. First, the nondependent lung would move from the upper low-compliant part of its PV curve during awake breathing to the lower high-compliant part after anesthesia, resulting in better ventilation. Second, the closing volume of the dependent lung might be greater than its FRC (122), consistent with the absence of ventilation to part of the dependent lung and with reduced ventilation.

Third, atelectasis and small airway closure in the dependent lung with its lower Ptp and higher closing volume would serve to shunt ventilation to the nondependent lung. Fourth, in addition to the anesthesia-induced reduction in FRC, the weight of the heart and abdomen would compress the dependent lung and expand the nondependent lung. This effect of gravity would be greater in the smaller dependent left lung in the LLD posture than the relatively larger dependent right lung in the RLD posture, accounting for the difference between the two postures

Except for the left lung in the LLD posture, significant negative vertical $\dot{V}_A$ gradients were observed in the left lung in the RLD posture and in the right lung in both postures. These gradients were accentuated by the imposed vertical gradient in regional volume. In addition, a positive dorsal-ventral gradient in $\dot{V}_A$ was observed in the left lung in both postures. The reason for this gradient was not apparent.

*Effects of PEEP.* Like the blood flow distribution, PEEP reduced the difference in $\dot{V}_A$ between the dependent and nondependent lung in the LLD posture (Figs. 9A and 9B, Table 5), similar to the behavior found in the anesthetized human (130) and dog (122). The PEEP-induced change in the vertical gradient in $\dot{V}_A$ in the LLD posture occurred in conjunction with the elimination of the positive dorsal-ventral gradient in $\dot{V}_A$ (Table 5). PEEP eliminated or reduced the negative gradient in $\dot{V}_A$ observed for the whole lung and left lung in the RLD posture, and in the right lung in both postures. A similar effect was observed for dorsal-ventral gradients for the whole lung and for the left lung in both postures. Accordingly, in general the effect of PEEP was to reduce the spatial variations in ventilation by increasing regional lung volume to a less compliant part of the PV curve where tidal-volume induced changes in airway resistance are minimal.

**Distribution of regional $\dot{V}_A/\dot{Q}$**

The $\dot{V}_A/\dot{Q}$ ratio was greater in the nondependent lung than in the dependent lung in the LLD posture (Table 6). There was a tendency (not significant) for this behavior to be reversed in the RLD posture with the dependent lung having the greater $\dot{V}_A/\dot{Q}$,

consistent with the results in the anesthetized human subjected to positive airway pressure (93). The latter result is supported by the PEEP-induced increase in the vertical $\dot{V}_A/\dot{Q}$ gradient in the RLD posture (Table 6). Furthermore, PEEP produced a positive vertical gradient in $\dot{V}_A/\dot{Q}$ in the dependent lung in both postures. By contrast, in keeping with the PEEP-induced reduction in the spatial variation in $\dot{V}_A$, PEEP eliminated or reduced the dorsal-ventral gradient in $\dot{V}_A/\dot{Q}$ observed for the whole lung in the RLD posture and in the dependent lung in both postures. These nongravitational gradients measured in the anesthetized dog with PEEP were not observed in the awake human (7).

**Distribution of $P_RO_2$**

A major advantage of the fluorescent microsphere technique over other techniques is the ability to estimate regional values and spatial gradients in $P_RO_2$. Regional $P_RO_2$ values predicted using microsphere data of $\dot{Q}$ and $\dot{V}_A$ were consistent with measured values in the anesthetized dog in the present study, confirming the results measured in the pig (5). However in the present study, microsphere data underestimated A-a$DO_2$. This might be attributed to more heterogeneous perfusion and ventilation with the greater spatial resolution (5).

Based on multiple linear regression analysis of the regional $P_RO_2$ data and the calculated spatial gradients, $P_RO_2$ in the LLD posture was greater in the nondependent, ventral and cranial lung regions than in the dependent, dorsal and caudal lung regions, respectively. These differences were either eliminated or reduced with PEEP.

In the left lung in the LLD posture, PEEP increased $P_RO_2$ from a mean value of 106 ± 11 to 112 ± 7 mmHg (Table 7). This was accompanied with a PEEP-induced reduction of significant dorsal-ventral and caudal-cranial $P_RO_2$ gradients (Table 7). Accordingly, the dependent lung in the LLD posture without PEEP had the lowest $\dot{V}_A/\dot{Q}$ (Table 7) and the lowest $P_RO_2$. Inversion of the dependent lung to the nondependent position and PEEP both served to increase $\dot{V}_A/\dot{Q}$ and $P_RO_2$.

In general, the $P_RO_2$ distribution was less uniform in the left lung than in the right lung especially in the dependent LLD posture and PEEP produced a more uniform $P_RO_2$ distribution in the dependent left lung. Compared to the dependent right lung in RLD position, the greater lung distortion caused by the weight of the heart and abdomen acting on the smaller dependent left lung in the LLD posture might contribute to a less uniform $P_RO_2$ distribution.

**Hypoxic pulmonary vasoconstriction and zone 4**

Many studies (50; 56; 78; 83; 122) have demonstrated that blood flow decreased in the most dependent lung regions (zone 4), opposite to the behavior predicted from the effects of gravity in zone 3 (159). This behavior has been attributed to increased vascular resistance caused by hypoxic pulmonary vasoconstriction (50; 56; 83; 122) or reduced vascular diameter in the most dependent lung regions (50; 56; 83; 122). The latter effect was attributed either to a low lung volume or perivascular cuff formation due to increased transvascular fluid flux (78).

Hypoxic pulmonary vasoconstriction might regulate regional perfusion to match regional ventilation to achieve efficient gas exchange (102). Our estimates of regional $\dot{V}_A/\dot{Q}$ and $P_RO_2$ provided evidence that this mechanism might be at work in the left dependent lung in the LLD posture. In the present study, some lung pieces of the dependent lung in the LLD posture showed relatively low $P_RO_2$ values (Fig 12A and 12C) that were consistent with values ($P_RO_2 < 100$ mmHg) associated with hypoxic pulmonary vasoconstriction (13; 34; 102). Estimates of $P_RO_2$ from the data analysis (Fig. 10) provided evidence that in the LLD posture hypoxic vasoconstriction occurred in the dependent lung where total blood flow was reduced relative to the nondependent lung (Table 4). PEEP increased both $\dot{V}_A/\dot{Q}$ and $P_RO_2$ in the dependent left lung (Figs. 6 and 7) and eliminated the hypoxic vasoconstriction, resulting in a gravity dependent greater blood flow in the dependent lung than in the nondependent lung.

**The effect of heart and abdominal weight on blood flow distribution**

Some studies (3; 73; 118; 129; 135) have suggested that lung volume and blood flow of the dependent lung are reduced in the lateral decubitus posture because of a mediastinal shift due to heart and abdominal weight. In the dog, the weight of the heart compressed the dependent lung regions to a greater extent in the supine than in the prone position (73). The heart weight-induced change in lung volume was greater with body inversion from LLD to RLD posture than from the prone to supine posture (118).

Mean regional blood flow calculated by the regression analysis indicated that the PEEP-induced reduction in regional perfusion at the center of mass near the heart was greater in the nondependent than in the dependent lung (Table 4, intercepts). This effect was greater in the left than in the right lung. Thus the effect of PEEP on the blood flow distribution was greater in the left lung in the LLD posture than in the right lung in the RLD posture. The difference in the pre-inspiratory lung volume between the left and right lung may be involved, in view of studies in anesthetized humans (129) showing that FRC of the right lung in the RLD posture was larger than FRC of left lung in the LLD posture, while FRC of the nondependent right lung was similar to the dependent right lung in the RLD posture. Thus the PEEP-induced lung expansion might be greater in the right dependent lung than in the left dependent lung that was closer to its closing volume. The reduced effect of PEEP in the left dependent lung in the LLD posture might be exacerbated during anesthesia, which might reduce diaphragmatic tone and reduce the diaphragmatic support of abdominal weight (40; 135). Thus the nonuniform ventilation distribution observed in the LLD posture can be alleviated by inversion to the RLD or with PEEP.

**$\dot{Q}$ and $\dot{V}_A$ Heterogeneity**

The regional perfusion and ventilation heterogeneity in this study as measured by CV of $\dot{Q}$ and $\dot{V}_A$ (30-60%) is consistent with previous studies using fluorescent microspheres (48; 50; 70; 99; 113; 114; 132). However, based on a one-dimensional linear regression analysis, the latter studies concluded that >90% of the heterogeneity in $\dot{Q}$ was due to

factors other than spatial variation. In contrast, the multiple linear regression analysis in the present study showed values of $R^2$ of ~0.40, suggesting that ~60% of the variability in the data were attributed to residual variation. The multiple linear regression analysis also indicated that 50% of the total variance in the $\dot{Q}$ and $\dot{V}_A$ distribution was attributed to residual variation (Table 9). This result for the $\dot{Q}$ distribution was similar to that measured in the supine dog (17).

The factors that contributed to the residual variance include heterogeneity on a scale that was smaller than ~ 1 cm, the dimension of the lung cube in which $\dot{Q}$ and $V_A$ were measured (162). The variances of $\dot{V}_A$, $\dot{Q}$ and $\dot{V}_A/\dot{Q}$ attributed to residual variation produced a correlation between $\dot{V}_A$ and $\dot{Q}$ similar to that produced by the total variability (~0.65). This might be in part due to a small-scale spatial variation associated with terms of second order and higher in the coordinates of the regression equation. The latter can only reduce the predicted residual variability. The similar correlation between $\dot{V}_A$ and $\dot{Q}$ observed for the spatial and non-spatial inhomogeneities suggests that matching of $\dot{V}_A$ and $\dot{Q}$ is not predominantly associated with small-scale variability. The relative contribution of small-scale variability using multiple linear regression analysis in previous studies (48; 50; 70; 71; 99; 113; 114; 132) needs further evaluation.

In conclusion, blood flow to the dependent left lung in the LLD posture was lower than that expected due to gravity. The reduced blood flow resulted from hypoxic vasoconstriction that occurred because of a reduced ventilation to the dependent lung compressed by the mediastinal contents. These effects were abolished with 10 cm $H_2O$ PEEP and inversion to the RLD posture.

# CHAPTER 4:

## Spatial Distribution of Ventilation and Perfusion during Differential Ventilation with Unilateral and Bilateral PEEP in the Lateral Posture in Dogs

### Introduction

In the LLD posture, the dependent left lung is particularly prone to poor ventilation and impaired gas exchange, presumably because its relatively small size makes it susceptible to distortion by the mediastinal contents (73; 118) and abdomen (40; 135). In the clinical setting, this effect is exacerbated by anesthesia that increases atelectasis (shunt) in the dependent lung and the use of positive end-expiratory pressure (PEEP) with mechanical ventilation has been shown to improve gas exchange efficiency (9; 86). The effect of PEEP is to increase lung volume and lung stiffness, reducing small airway closure and lung distortion. However, PEEP is accompanied with deleterious effects of lung barotrauma and reduced cardiac output (63).

In Chapter 3, the relatively low blood flow to the dependent left lung in the LLD posture of anesthetized dogs was increased with 10 cm $H_2O$ PEEP. In Chapter 5, the blood flow to the dependent left lung was greater with 100% $O_2$ ventilation than with air ventilation (chapter 3), indicative of hypoxic pulmonary vasoconstriction occurring with air ventilation.

The use of controlled ventilation to each lung (differential ventilation) with unilateral PEEP to the dependent lung in the LLD posture has been proposed as a mode of ventilation that is superior to conventional ventilation with bilateral PEEP (63). In anesthetized humans, equal ventilation to both lungs with differential ventilation produced higher $PaO_2$ and a lower A-a$DO_2$ than a single ventilator supplying a free distribution of ventilation between lungs either with or without 9 cm $H_2O$ PEEP. Similar studies in anesthetized humans showed a 30% reduction in A-a$DO_2$ with equal ventilation to both lungs and a further 13% reduction in A-a$DO_2$ with unilateral PEEP to the dependent lung (9). This behavior was attributed to the increased compliance, reduced

airway resistance, and a more even ventilation distribution in the dependent lung as a result of the differential ventilation without and with unilateral PEEP (85).

The aim of this study was to investigate the spatial distribution of blood flow and ventilation during differential ventilation to determine the factors responsible for the improvement of gas exchange in the LLD posture. I studied in the anesthetized dog the effects of 5 and 10 cm $H_2O$ unilateral PEEP to the dependent left lung and 10 cm $H_2O$ bilateral PEEP with a distribution of ventilation between lungs similar to that occurring with conventional ventilation without PEEP. Cardiac output was maintained constant by saline infusion. Regional distribution of blood flow and ventilation was measured using injected and aerosolized fluorescent microspheres. Blood flow to the dependent lung did not change with either unilateral or bilateral PEEP, while FRC increased 50-100%. PEEP had no effect on A-a$DO_2$. $\dot{V}_A/\dot{Q}$ inequalities measured by spatial gradients in $\dot{V}_A/\dot{Q}$ were absent with differential ventilation.

## METHODS

### Animal Preparation

The animal and split lung preparation was made as described in chapter 2. Both right and left lungs were ventilated with room air throughout the study. Tidal volume of the left and right lung was measured in the LLD posture without PEEP by a spirometer and maintained constant. Intravenous fluid (100-200 $ml \cdot h^{-1}$ of 0.9% normal saline) was administered to maintain constant cardiac output during 10 cm $H_2O$ PEEP. PEEP (5 and 10 cm $H_2O$) was generated by immersing the exhalation tube of the ventilator beneath 5 and 10 cm of water.

Study protocol

Dogs were studied in the left lateral decubitus (LLD) posture. After obtaining the tidal volume of right and left lung at FRC, the dependent left lung received 0, 5, or 10 cm $H_2O$ PEEP and both lungs 10 cm $H_2O$ cm PEEP, in random order. After 20 minutes stabilization and hyperinflation the lung, for each condition the tidal volume of each lung,

arterial and mixed blood gases, exhaled $CO_2$ for calculating Fowler's dead space, hemodynamic measurements, functional residual capacity was obtained. Then different-colored aerosolized microspheres were delivered to both lungs and simultaneously intravenous microspheres were injected, over 5 min.

## RESULTS

### Physiological measures.

Cardiac output, Psa, Ppa, heart rate, body temperature, hemoglobin, respiratory rate, and tidal volume to right and left lung, respectively, were constant throughout the study (Table 10).

***Lung volumes.*** LLD posture decreased FRC in dependent lung compared to supine posture (Fig 15). The left and right lung volume ratio decreased from 1/2 to 1/3. Compared to 0 cm $H_2O$ PEEP, FRC of the left lung increased 55 and 110% with 5 and 10 cm $H_2O$ (unilateral) PEEP to the left lung, respectively, and 83% with 10 cm $H_2O$ (bilateral) PEEP to both lungs. Left lung FRC was larger with 10 cm $H_2O$ unilateral PEEP than with 10 cm $H_2O$ bilateral PEEP. FRC of the right lung was unaffected with unilateral PEEP, but more than doubled with 10 cm $H_2O$ bilateral PEEP. Bilateral PEEP increased the L/R disparity during LLD.

Table 10. Cardiopulmonary variables during unilateral dependent and bilateral PEEP in left lateral decubitus posture

| PEEP ($cmH_2O$) | | o | 5 | 10 | 10 |
|---|---|---|---|---|---|
| lung | | both | dependent | dependent | both |
| BT ($^0C$) | | 37.3±0.4 | 37.5±0.4 | 37.2±0.4 | 37.3±0.5 |
| Psa (mmHg) | | 114±14 | 102±12 | 107±9 | 103±19 |
| HR ($beats \cdot min^{-1}$) | | 110±18 | 111±12 | 115±16 | 116±15 |
| Ppa ($cmH_2O$) | | 24±7 | 24±8 | 26±6 | 29±4 |
| Ppaop ($cmH_2O$) | | 7±4 | 9±6 | 9±6 | 13±4* |
| $\dot{Q}_T$ ($l \cdot min^{-1}$) | | 2.8±0.3 | 2.7±0.2 | 2.6±0.3 | 2.7±0.4 |
| $R_T$, $cmH_2o \cdot L^{-1} \cdot min^{-1}$ | | 6.2±1.4 | 5.7±1.3 | 6.4±1.5 | 5.9±2.6 |
| $R_L$, $cmH_2o \cdot L^{-1} \cdot min^{-1}$ | | 15.3±3.9 | 15.1±9.7 | 18.4±7.3 | 11.8±6.4‡ |
| $R_R$, $cmH_2o \cdot L^{-1} \cdot min^{-1}$ | | 10.4±5.6 | 9.3±7.4 | 10.0±7.5 | 12.2±5.2 |
| RR($breaths \cdot min^{-1}$), | | 18±2 | 17±2 | 18±2 | 18±2 |
| $V_T$ (ml), | left | 119±31 | 119±33 | 120±32 | 119±33 |
| | right | 217±39 | 214±39 | 215±39 | 215±37 |
| MV ($l \cdot min^{-1}$), | left | 2.1±0.7 | 2.0±0.7 | 2.1±0.8 | 2.1±0.8 |
| | right | 3.7±0.4 | 3.6±0.4 | 3.7±0.4 | 3.6±0.4 |
| $V_D/V_T$ (%) | left | 40±5 | 45±3 | 48±4 | 45±6 |
| $V_D/V_T$ (%) | right | 29±6 | 31±4 | 29±4 | 36±6 |
| Paw ($cmH_2O$), | left | 11±2 | 17±3* | 20±2*† | 20±2* |
| | right | 11±2 | 10±2 | 11±1 | 23±3*†‡ |
| $PaO_2$ (mmHg) | | 98±18 | 99±12 | 107±26 | 93±19 |
| $PaCO_2$ (mmHg) | | 31±3 | 31±3 | 31±3 | 34±3 |
| A-$aDO_2$ (mmHg) | | 26±17 | 24±11 | 23±13 | 28±19 |
| pH | | 7.38±0.03 | 7.39±0.62 | 7.36±0.03 | 7.34±0.02 |
| $P\bar{v}O_2$ (mmHg) | | 44±6 | 43±6 | 45±6 | 43±4 |
| $P\bar{v}CO_2$ (mmHg) | | 36±4 | 36±5 | 37±3 | 39±3 |
| FRC (ml) | left | 183±48 | 283±74* | 386±65*† | 335±66*†‡ |
| | right | 402±80 | 392±95 | 354±79 | 879±104*†‡ |
| Hb ($g \cdot dl^{-1}$) | | 13±2 | 13±1 | 13±1 | 13±1 |

Values are mean ± SD (n = 6). BT, body temperature; Psa, mean systemic arterial pressure; HR, heart rate; Ppa, mean pulmonary artery pressure; Ppaop, pulmonary artery occlusion pressure; $\dot{Q}_T$, cardiac output; RR, respiratory rate; $V_T$, tidal volume; R: resistance; MV, minute ventilation; Paw, peak airway pressure;$PaO_2$, arterial $O_2$ tension; $PaCO_2$, arterial carbon dioxide tension; A-$aDO_2$, alveolar and arterial $O_2$ tension difference; pH, arterial blood pH; $P\bar{v}O_2$, mixed venous oxygen tension; $P\bar{v}CO_2$, mixed venous carbon dioxide tension; FRC, functional residual capacity; Hb: arterial hemoglobin. * $P < 0.05$, compared with no PEEP. † $P < 0.05$, compared with 5 cm $H_2O$ selective PEEP. ‡ $P < 0.05$, compared with 10 cm $H_2O$ selective PEEP.

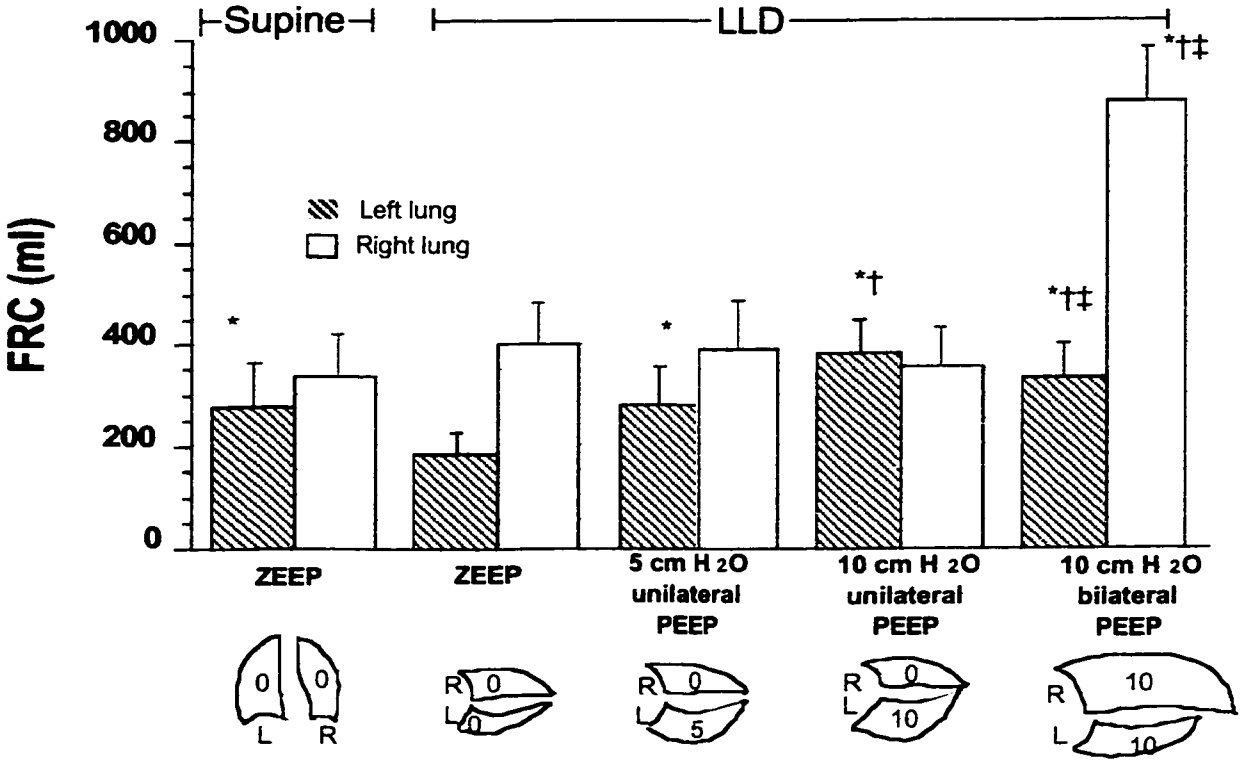


Fig 15. Left and right lung volume changes with unilateral and bilateral PEEP in LLD posture. Values are mean ± SD (n = 6). *P < 0.05 comparison of same lung with no PEEP. † P < 0.05, significantly different from 5 cm $H_2O$ unilateral dependent PEEP in the same lung. ‡ P < 0.05, significantly different from 10 cm $H_2O$ unilateral dependent PEEP in the same lung.

*Pulmonary vascular resistance and redistribution of blood flow between lungs*

Pulmonary vascular resistance (PVR), defined as cardiac output/(Ppa - Pcwp), of the whole lung and right lung did not change with unilateral PEEP (5 or 10 cm $H_2O$) or with 10 cm bilateral PEEP. PVR of the left lung was greater with 10 cm $H_2O$ unilateral PEEP than with 10 cm $H_2O$ bilateral PEEP. PVR was 50-80% greater in the left lung than in the right lung with 0 cm $H_2O$ PEEP and unilateral PEEP (5 and 10 cm$H_2O$), but equal with 10 cm $H_2O$ bilateral PEEP. This is consistent with the increased blood flow to the left lung only with 10 cm $H_2O$ bilateral PEEP (Fig 16).

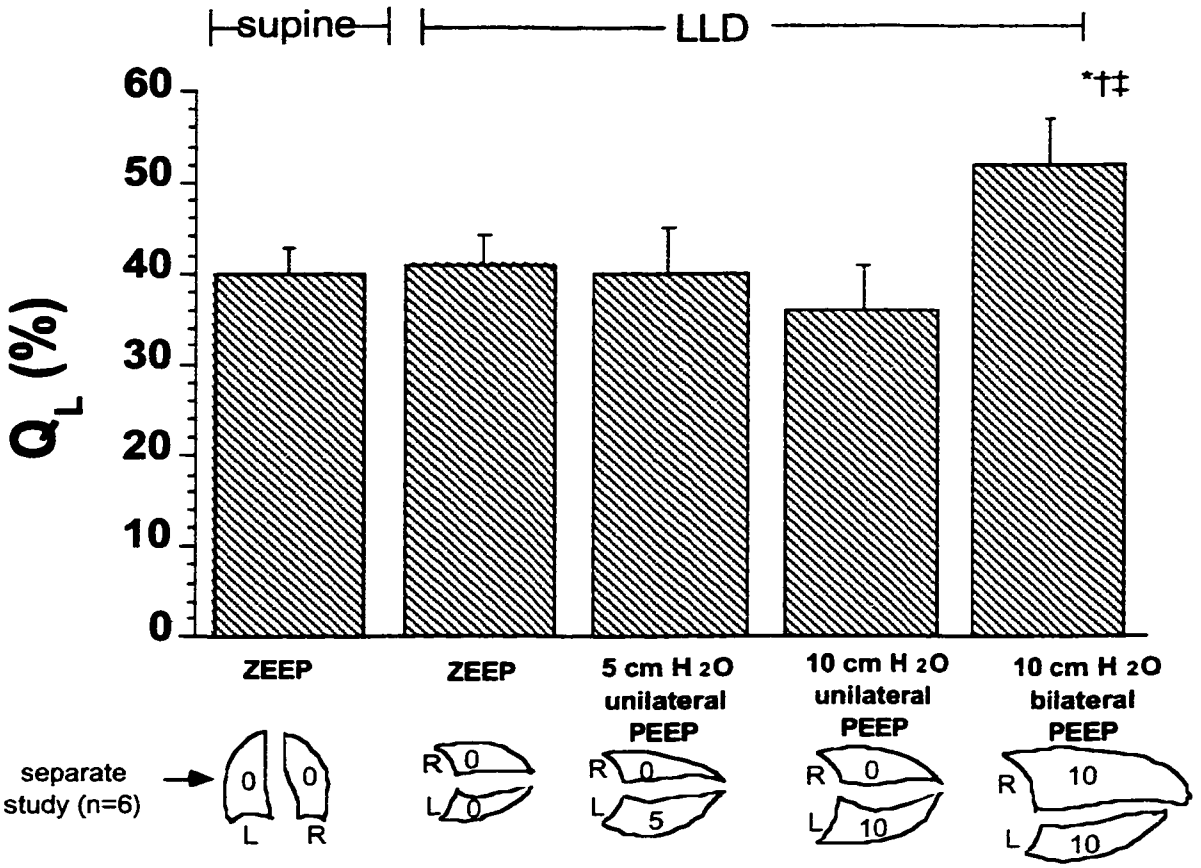


Fig 16. Percentage of blood flow and ventilation to left lung in the left lateral decubitus posture without PEEP, with 5 or 10 cm $H_2O$ unilateral dependent PEEP and 10 cm $H_2O$ bilateral PEEP. * $P < 0.05$, significantly different from no PEEP. † $P < 0.05$, significantly different from 5 cm $H_2O$ unilateral dependent PEEP. ‡ $P < 0.05$, significantly different from 10 cm $H_2O$ selective PEEP.

*Gas exchange.* Compared to 0 cm $H_2O$ PEEP, $PaO_2$ and $PaCO_2$ did not change with unilateral PEEP to the left lung or with 10 cm $H_2O$ bilateral PEEP. A-a$DO_2$, calculated using the alveolar gas equation (68) and a respiratory quotient of 0.8, with unaffected by PEEP.

**Distribution of $\dot{Q}$ and $\dot{V}_A$ between lungs: effect of PEEP.**

For all conditions with and without PEEP, tidal volume to the dependent left lung (119 ml) was ~55% that of the right lung, the tidal volumes measured without PEEP using ventilation through a single lumen tracheal tube. This relatively low tidal volume

in the left lung in conjunction with a constant ventilation frequency indicated lower ventilation in the left lung compared to the right lung. Ventilation to the left lung was lower than that based on lung size, since the left lung weighed ~25% less than the right lung. Ventilation calculated by the product of frequency and tidal volume corrected for dead space was maintained constant to each lung for each PEEP condition.

The total blood flow measured by fluorescent microspheres was distributed 41% to the dependent left lung and 59 % to the nondependent lung with 0 cm $H_2O$ PEEP (Fig 16 and Table 11).

Table 11. Percentage of fluorescent microsphere signal represents cardiac output and minute ventilation to left and right lung, respectively during differential ventilation with selective dependent lung and both lungs PEEP in left lateral decubitus posture

| | | LLD | | | |
|---|---|---|---|---|---|
| | PEEP (cm $H_2O$) | 0 | 5 dependent | 10 dependent | 10 bilateral |
| $\dot{Q}$ (%) | Left lung | 41±3 | 40±5 | 36±5 | 52±5*†‡ |
| $\dot{Q}$ (%) | Right lung | 59±3 | 60±5 | 64±5 | 48±5 |
| $V_A$(%) | Left lung | 29±10 | 26±9 | 22±6*† | 33±10†‡ |
| $V_A$(%) | Right lung | 71±10 | 74±9 | 78±6 | 67±10 |

Values are mean ± SD (n = 6). LLD: left lateral decubitus posture. 5 dependent: 5 cm H2O selective dependent PEEP. 10 dependent: 10 cm H2O selective dependent PEEP. 10 bilateral: 10 cm H2O PEEP to both right and left lung. * $P < 0.05$, compared with no PEEP. † $P < 0.05$, compared with 5 cm H2O selective PEEP. ‡ $P < 0.05$, compared with 10 cm H2O selective PEEP.

LLD posture did not alter blood flow to dependent lung compared to supine posture (Fig 16). In addition, unilateral PEEP (5 or 10 cm $H_2O$) did not change blood flow to the left lung or the blood flow distribution between lungs. This behavior in conjunction with the constant or reduced ventilation indicated that unilateral PEEP per se had no beneficial effect on gas exchange to the left lung. By contrast, 10 cm $H_2O$ bilateral PEEP increased the fraction of cardiac output to the left lung by 11-16% compared to 0 cm $H_2O$ PEEP or unilateral PEEP (5 and 10 cm $H_2O$). This blood flow increase in the left lung with 10 cm $H_2O$ bilateral PEEP was produced by the reduced PVR due to increased Pcwp and the

imposed zone 3 conditions, and not by an increase in $PaO_2$. The PEEP-induced increase in $PO_2$ to the lung in Chapter 3 was caused by a relative increase in ventilation to the left lung. This increase in left lung ventilation was absent in the present study, since ventilation to the left lung was kept equal to that measured without PEEP.

**Microsphere data**

Analysis of regional perfusion and ventilation was carried out on 1058-1337 lung pieces (93.3 ± 2.6%) per animal. Lung pieces (82 ± 40) with > 25% pulmonary airways and with fluorescent microsphere intensity (11 ± 7) beyond the range of ± 4SD of the mean values were discarded. For the analysis of $\dot{V}_A/\dot{Q}$ and regional $P_RO_2$, data were rejected (19 ± 7 lung pieces or 1.6%) outside the range of mean ± 3SD of ln ($\dot{V}_A/\dot{Q}$) to eliminate lung pieces predominantly with deadspace (large $\dot{V}_A/\dot{Q}$) and shunt (low $\dot{V}_A/\dot{Q}$).

The X, Y, Z coordinate distances of the center of mass of left, right and whole lung, relatively to the original coordinate axes ($X_0$, $Y_0$, $Z_0$) oriented at the edges of the lung are shown in Table 12. The coordinate distances between the center of mass and original coordinate axes increased when the lung volume increased with PEEP. The vertical distance increase was greatest (~56%) with 10 cm $H_2O$ bilateral PEEP and least (~23%) with 5 cm $H_2O$ unilateral PEEP to the dependent left lung.

Table 12. x, y, z coordinate distances between center of mass and original coordinate system at caudal edge ($z_0 = 0$), left edge ($x_0 = 0$), dorsal edge ($y_0 = 0$) of the lung

| PEEP,cm $H_2O$ | | 0 | 5s | ΔL (%) | 10s | ΔL (%) | 10G | ΔL (%) |
|---|---|---|---|---|---|---|---|---|
| | X | 6.2±0.4 | 7.6±1.1 | 23 | 9.1±0.5 | 47 | 9.7±0.6 | 56 |
| Whole lung | Y | 7.2±2.0 | 7.3±0.5 | 1 | 7.6±0.6 | 6 | 8.5±0.6 | 18 |
| | Z | 10.2±1.5 | 11.9±0.8 | 17 | 12.0±0.7 | 18 | 12.7±0.8 | 25 |
| | X | 8.3±0.5 | 10.0±1.2 | 20 | 11.6±0.6 | 40 | 12.7±0.8 | 53 |
| Right lung | Y | 7.3±0.4 | 7.3±0.4 | 0 | 7.3±0.4 | 0 | 8.9±0.5 | 22 |
| | Z | 11.3±0.8 | 11.3±0.8 | 0 | 11.3±0.8 | 0 | 12.6±0.9 | 12 |
| | X | 3.3±0.3 | 4.3±0.9 | 30 | 5.5±0.5 | 67 | 5.5±0.5 | 67 |
| Left lung | Y | 5.6±0.6 | 7.1±0.7 | 27 | 8.0±0.8 | 43 | 8.0±0.8 | 43 |
| | Z | 10.2±0.6 | 12.5±1.2 | 23 | 12.9±0.7 | 26 | 12.9±0.7 | 26 |

ΔL (%): percentage of length change compared with 0 cm $H_2O$ PEEP.

*Spatial heterogeneity.* The mean spatial CV of perfusion and ventilation for the different PEEP conditions are presented in Table 13. In general, unilateral PEEP to the left lung reduced perfusion but not ventilation heterogeneity in the left lung, most likely because of the reduced lung distortion caused by the increased FRC. This behavior was unrelated to blood flow or ventilation, neither of which changed with unilateral PEEP. Lung distortion was not the reason for the lower blood flow measured in the dependent left lung in the LLD posture than in the dependent right lung in the RLD posture.

Table 13. Perfusion and ventilation heterogeneity

| | PEEP cm $H_2O$ | 0 | 5S | 10S | 10B |
|---|---|---|---|---|---|
| $\dot{Q}$ CV | Left lung | 0.55±0.06 | 0.51±0.06* | 0.48±0.04* | 0.52±0.08 |
| | Right lung | 0.39±0.18† | 0.43±0.16 | 0.51±0.19 | 0.47±0.17*† |
| $\dot{V}_A$ CV | Left lung | 0.60±0.10 | 0.55±0.07 | 0.62±0.18 | 0.58±0.07 |
| | Right lung | 0.43±0.20† | 0.52±0.18 | 0.61±0.22 | 0.49±0.19* |

Values are presented as mean ± SD (n = 6). 5S and 10 S, 5 cm and 10 cm $H_2O$ selective dependent lung PEEP; 10B: 10 cm $H_2O$ PEEP to both lungs. CV: coefficient of variance.* Statistically different from 0 cm $H_2O$ PEEP in the same lung, $P < 0.05$; † Statistically different from left lung in the same PEEP condition.

Both perfusion and ventilation heterogeneity was greater in the dependent left lung than in the nondependent right lung without PEEP. Bilateral PEEP to the left lung reduced these differences in perfusion and ventilation heterogeneity between the dependent left and nondependent lungs. Bilateral PEEP increased perfusion and ventilation heterogeneity only in the right lung

*Regional distribution in* $\dot{Q}$. For the whole lung in the absence of PEEP, a negative (gravity dependent) vertical gradient (-0.61 $\dot{Q}\cdot ml^{-1}\cdot cm^{-1}$) in regional blood flow was present in the LLD posture, with the greater regional blood flow in the dependent regions (Table 14 and Fig 17). This gradient was reduced with unilateral PEEP of 5 cm $H_2O$ (-0.15) and 10 cm $H_2O$ (0.14) to the dependent left lung, and with 10 cm $H_2O$ bilateral PEEP (-0.37). Small, but significant, caudal-cranial gradient (-0.14 and –0.06) occurred

TABLE 14. Coefficients and $R^2$ of multiple linear regression equation† fit to $\dot{Q}$ data for whole, left and right lung, respectively

| lung | PEEP | Intercept | a | b | c | d | e | f | g | $R^2$ |
|---|---|---|---|---|---|---|---|---|---|---|
| | 0 | 4.8 | **-0.61** | -0.15 | -0.17 | 0.05 | -0.02 | **0.05** | **0.008** | 0.56 |
| Whole | | ±0.9 | **±0.19*** | ±0.25 | ±0.17 | ±0.08 | ±0.03 | **±0.03*** | **±0.006*** | ±0.11 |
| | 5s | 3.5 | **-0.15** | -0.04 | -0.13 | 0.01 | **-0.02** | 0.01 | **0.004** | 0.42 |
| | | ±0.7 | **±0.13*** | ±0.16 | ±0.13 | ±0.02 | **±0.01*** | ±0.02 | **±0.002*** | ±0.13 |
| | 10s | 3.4 | **0.14** | -0.02 | **-0.14** | -0.003 | **-0.02** | -0.01 | 0.001 | 0.39 |
| | | ±0.8 | **±0.11*** | ±0.13 | **±0.13*** | ±0.01 | **±0.01*** | ±0.02 | ±0.002 | ±0.18 |
| | 10 | 2.8 | **-0.37** | -0.11 | **-0.06** | 0.02 | **-0.01** | 0.007 | 0.003 | 0.64 |
| | | ±1.0 | **±0.24*** | ±0.12 | **±0.03*** | ±0.03 | **±0.006*** | ±0.009 | ±0.003 | ±0.19 |
| | 0 | 7.6 | **-0.83** | -0.28 | **-0.33** | **-0.38** | **-0.13** | 0.02 | **0.06** | 0.48 |
| Left | | ±1.6 | **±0.66*** | ±0.55 | **±0.24*** | **±0.29*** | **±0.05*** | ±0.13 | **±0.03*** | ±0.20 |
| | 5s | 3.8 | -0.27 | -0.12 | **-0.12** | **0.07** | **-0.04** | 0.05 | **0.012** | 0.46 |
| | | ±1.1 | ±0.33 | ±0.21 | **±0.06*** | **±0.07*** | **±0.01*** | ±0.02 | **±0.007*** | ±0.21 |
| | 10s | 2.5 | **-0.16** | -0.11 | -0.04 | 0.014 | **-0.014** | 0.002 | **0.004** | 0.48 |
| | | ±0.7 | **±0.09*** | ±0.12 | ±0.05 | ±0.018 | **±0.006*** | ±0.009 | **±0.003*** | ±0.24 |
| | 10 | 4.8 | -0.27 | -0.16 | **-0.13** | **0.05** | **-0.04** | 0.002 | **0.01** | 0.51 |
| | | ±2.1 | ±0.55 | ±0.26 | **±0.05*** | **±0.04*** | **±0.03*** | ±0.012 | **±0.009*** | ±0.16 |
| | 0 | 3.3 | **-0.28** | -0.04 | -0.07 | 0.001 | **-0.015** | **0.02** | 0.0002 | 0.42 |
| Right | | ±0.7 | **±0.15*** | ±0.11 | ±0.15 | ±0.03 | **±0.011*** | **±0.009*** | ±0.005 | ±0.22 |
| | 5s | 3.3 | **-0.24** | -0.03 | -0.12 | 0.007 | **-0.016** | **0.013** | 0.001 | 0.41 |
| | | ±0.8 | **±0.18*** | ±0.13 | ±0.19 | ±0.03 | **±0.016*** | **±0.011*** | ±0.007 | ±0.22 |
| | 10s | 4.2 | -0.03 | -0.03 | -0.18 | 0.003 | **-0.02** | **0.012** | -0.0002 | 0.36 |
| | | ±1.0 | ±0.29 | ±0.13 | ±0.20 | ±0.04 | **±0.01*** | **±0.008*** | ±0.006 | ±0.23 |
| | 10 | 1.4 | **-0.14** | **-0.04** | -0.02 | **-0.008** | **-0.003** | **0.006** | -0.0002 | 0.51 |
| | | ±0.3 | **±0.05*** | **±0.04*** | ±0.03 | **±0.006*** | **±0.002*** | **±0.003*** | ±0.001 | ±0.22 |

Values are presented as mean ± SD (n=6), * $P < 0.05$ Compared with zero by 1-tailed unpaired t test.

† Equation: $\dot{Q} = I + ax + by + cz + dxy + eyz + fzx + gxyz$. All intercepts are significant.

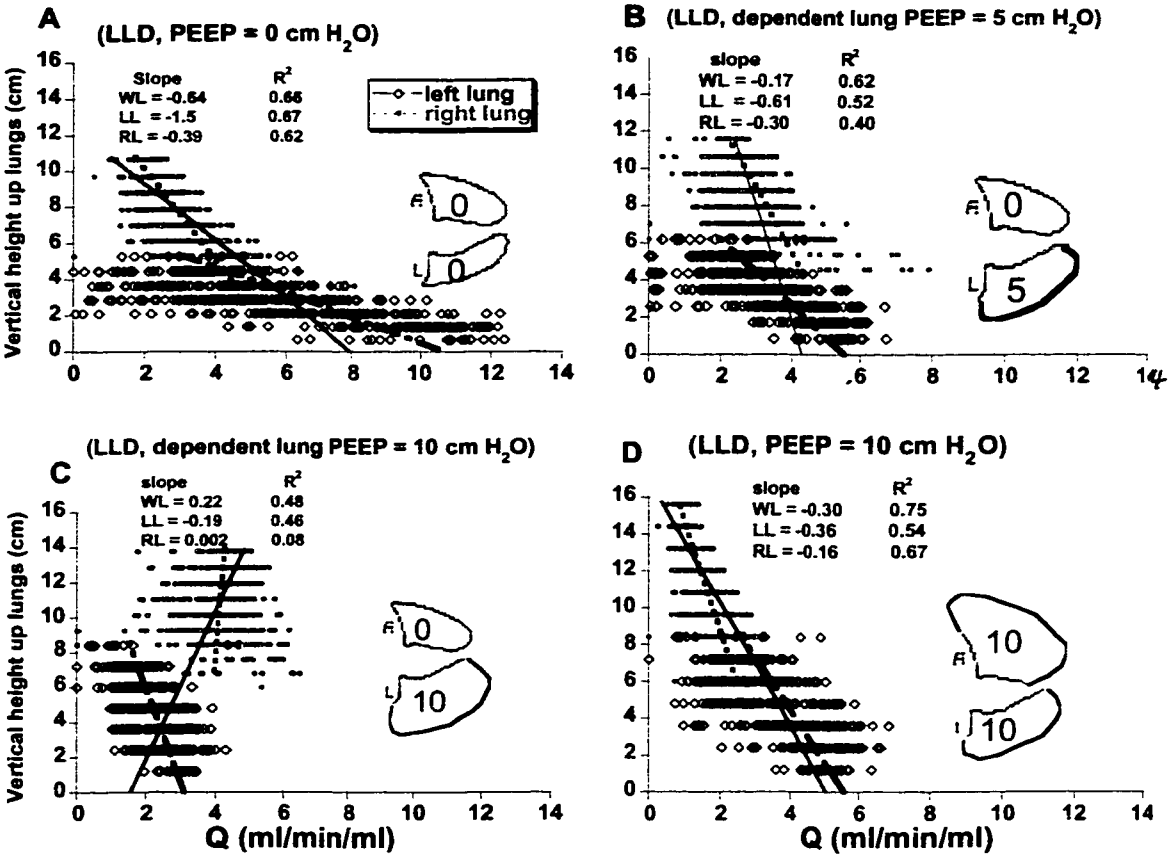


Fig 17. Blood flow per unit regional lung volume ($ml \cdot min^{-1} \cdot ml^{-1}$) vs. lung height for a representative dog in the LLD posture without PEEP (A), with 5 cm $H_2O$ unilateral dependent PEEP (B), with 10 cm $H_2O$ unilateral dependent PEEP (C) and with bilateral 10 cm $H_2O$ PEEP (D). R represents right lung (open points), L the left lung (solid points) and N, the number of lung pieces. The lines represent best-fit values from multiple linear regression analysis at center of mass.

with 10 cm $H_2O$ unilateral and bilateral PEEP, with the caudal region having a greater regional blood flow than the cranial region.

Similar to the whole lung, in the left lung the vertical gradient in $\dot{Q}$ without PEEP (-0.83) was accompanied with a negative caudal-cranial gradient (-0.33). Both gradients were reduced with 10 cm $H_2O$ unilateral PEEP and 10 cm $H_2O$ bilateral PEEP. In the right lung, the vertical gradient in $\dot{Q}$ and the effects of PEEP were generally smaller than

in the left lung. The reduction in the vertical gradient with unilateral and bilateral PEEP was associated with a decrease (40-90%) in the mean regional blood flow (intercept I).

Regional variation of the spatial gradients along an orthogonal coordinate was evident from the coefficients d, e, and f of the independent variables XY, YZ and ZX (Table 14). The largest regional variation occurred in the left lung without PEEP, where the vertical gradient ($\partial \dot{Q}/\partial X$) in blood flow decreased linearly with Y (coefficient d, -0.38):

$$\partial \dot{Q}/\partial X = -0.83-0.38Y$$

At the mid caudal-cranial region Z = 0, the vertical blood flow gradient became positive (0.31) in the dorsal region (Y = -3 cm) and more negative (-1.97) in the ventral region (Y = 3 cm). The variation of the vertical gradient along the Y coordinate was reduced (coefficient d, 0.07-0.05) with unilateral and bilateral PEEP.

***Regional distribution of*** $\dot{V}_A$. In the whole lung, a positive vertical gradient (0.37) in $\dot{V}_A$ was observed with 10 cm $H_2O$ unilateral PEEP to the left lung (Fig 18, Table 15). This was accompanied with a dorsal-ventral (0.12) and caudal-cranial (-0.27) gradient in $\dot{V}_A$. These gradients were reduced or eliminated with either 5 cm $H_2O$ unilateral PEEP or 10 cm $H_2O$ bilateral PEEP. In the left lung, the significant caudal-cranial gradient (-0.36) in $\dot{V}_A$ was eliminated with unilateral or bilateral PEEP. In the right lung, 10 cm $H_2O$ unilateral PEEP to the left lung produced a significant dorsal-ventral (0.15) and caudal-cranial (-0.39) gradient in $\dot{V}_A$. The positive dorsal-ventral gradient (0.12) became negative (-0.10) while the caudal-cranial gradient was abolished, with 10 cm $H_2O$ bilateral PEEP.

In the right lung, regional variation of the dorsal-ventral and caudal-ventral gradients in $\dot{V}_A$ with 10 cm $H_2O$ unilateral PEEP occurred in the caudal-cranial and dorsal-ventral directions (coefficient e, -0.07), respectively. Relatively small regional variations in the dorsal-ventral gradient in $\dot{V}_A$ were observed with 10 cm $H_2O$ bilateral PEEP in the two orthogonal directions.

Mean regional ventilation decreased with unilateral PEEP to the left lung and bilateral PEEP and this was associated with a PEEP-induced increase in lung volume (intercepts).

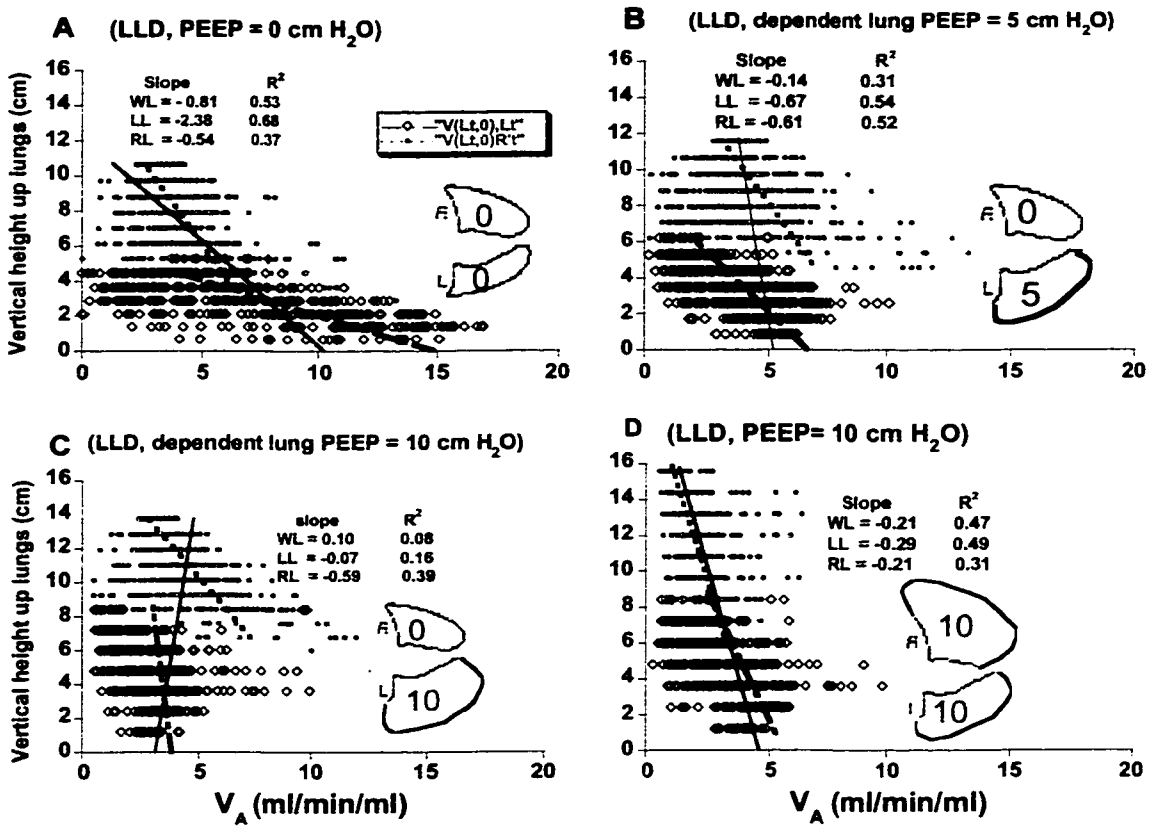


Fig 18. Ventilation per unit regional lung volume (ml· $min^{-1}$· $ml^{-1}$) *vs.* lung height for a representative dog in the LLD posture without PEEP (A), with 5 cm $H_2O$ unilateral dependent PEEP (B), with 10 cm $H_2O$ unilateral dependent PEEP (C) and with bilateral 10 cm $H_2O$ PEEP (D). R represents right lung (open points), L the left lung (solid points) and N, the number of lung pieces. The lines represent best-fit values from multiple linear regression analysis at center of mass.

TABLE 15. Coefficients and $R^2$ of multiple linear regression equation† fit to $\dot{V}_A$ data for whole, left and right lung, respectively

| lung | PEEP | Intercept | a | b | c | d | e | f | g | $R^2$ |
|---|---|---|---|---|---|---|---|---|---|---|
| | 0 | 6.2 | -0.44 | -0.03 | -0.31 | **0.05** | **-0.04** | **0.02** | 0.008 | 0.34 |
| Whole | | ±1.0 | ±0.50 | ±0.29 | ±0.30 | **±0.04*** | **±0.03*** | **±0.02*** | ±0.013 | ±0.19 |
| | 5s | 4.6 | 0.06± | 0.07 | -0.20 | 0.01 | -0.07 | -0.006 | 0.003 | 0.35 |
| | | ±0.7 | 0.29 | ±0.22 | ±0.20 | ±0.02 | ±0.07 | ±0.03 | ±0.005 | ±0.17 |
| | 10s | 4.9 | **0.37** | **0.12** | **-0.27** | -0.005 | **-0.07** | -0.03 | -0.004 | 0.36 |
| | | ±0.9 | **±0.29*** | **±0.05*** | **±0.21*** | ±0.02 | **±0.05*** | ±0.04 | ±0.004 | ±0.20 |
| | 10 | 3.0 | -0.12 | -0.07 | **-0.05** | -0.01 | **-0.01** | 0.009 | **0.003** | 0.35 |
| | | ±0.6 | ±0.17 | ±0.09 | **±0.03*** | ±0.02 | **±0.01*** | ±0.011 | **±0.002*** | ±0.23 |
| | 0 | 8.2 | -0.92 | -0.20 | **-0.36** | **0.38** | **-0.15** | 0.06 | **0.07** | 0.36 |
| Left | | ±2.5 | ±1.39 | ±0.28 | **±0.31*** | **±0.31*** | **±0.10*** | ±0.15 | **±0.04*** | ±0.20 |
| | 5s | 4.0 | -0.23 | -0.08 | -0.12 | 0.07 | **-0.05** | 0.01 | **0.04** | 0.37 |
| | | ±1.8 | ±0.49 | ±0.13 | ±0.14 | ±0.07 | **±0.03*** | ±0.03 | **±0.06*** | ±0.19 |
| | 10s | 2.8 | -0.13 | -0.04 | -0.05 | 0.02 | -0.015 | -0.001 | 0.007 | 0.28 |
| | | ±1.0 | ±0.20 | ±0.10 | ±0.10 | ±0.04 | ±0.022 | ±0.023 | ±0.01 | ±0.15 |
| | 10 | 3.7 | -0.09 | -0.07 | -0.09 | 0.05 | **-0.04** | -0.002 | 0.017 | 0.32 |
| | | ±1.7 | ±0.23 | ±0.09 | ±0.09 | ±0.05 | **±0.03*** | ±0.02 | ±0.021 | ±0.19 |
| Right | 0 | 5.2 | -0.18 | 0.04 | -0.17 | 0.02 | **-0.03** | -0.01 | 0.001 | 0.28 |
| | | ±0.8 | ±0.35 | ±0.19 | ±0.22 | ±0.08 | **±0.02*** | ±0.02 | ±0.01 | ±0.15 |
| | 5s | 5.2 | -0.23 | 0.11 | -0.25 | 0.04 | **-0.04** | -0.01 | 0.005 | 0.39 |
| | | ±0.9 | ±0.42 | ±0.20 | ±0.31 | ±0.08 | **±0.02*** | ±0.02 | ±0.015 | ±0.18 |
| | 10s | 6.5 | -0.01 | **0.15** | **-0.39** | 0.07 | **-0.07** | -0.02 | 0.002 | 0.40 |
| | | ±1.5 | ±0.63 | **±0.08*** | **±0.35*** | ±0.10 | **±0.03*** | ±0.03 | ±0.015 | ±0.11 |
| | 10 | 2.6 | -0.13 | **-0.10** | -0.03 | **-0.02** | **-0.01** | **0.014** | -0.001 | 0.43 |
| | | ±0.2 | ±0.17 | **±0.08*** | ±0.04 | **±0.01*** | **±0.002*** | **±0.011*** | ±0.002 | ±0.15 |

Values are presented as mean ± SD (n=6), * $P < 0.05$ Compared with zero by 1-tailed unpaired t test.

† Equation: $\dot{Q} = I + ax + by + cz + dxy + eyz + fzx + gxyz$. All intercepts are significant

*Regional distribution of* $\dot{V}_A/\dot{Q}$ *and* $P_RO_2$. Mean $P_RO_2$ was greatest in the nondependent lung (intercepts, 116-123 mmHg) and least in the dependent lung (100–110 mmHg). These $P_RO_2$ values did not vary with unilateral and bilateral PEEP. Thus the relatively low $P_RO_2$ observed in the dependent left lung in the LLD posture without PEEP was not affected by unilateral PEEP, consistent with the constant total blood flow measured in the dependent left lung without PEEP and with 5 and 10 cm $H_2O$ unilateral PEEP. The dependent-to-nondependent increase in $P_RO_2$ was demonstrated by large positive vertical gradients in $P_RO_2$ for the whole lung that was significant only with 10 cm $H_2O$ bilateral PEEP (2.18±1.75) (Fig 19, Table 16). Relatively smaller significant positive dorsal-ventral gradients in $P_RO_2$ for the whole lung was observed without PEEP (1.02±0.88) and with 5 (1.14±0.96) and 10 (1.10±0.82) cm $H_2O$ unilateral PEEP to the left lung. These dorsal-ventral gradients for the whole lung were associated with comparable gradients in the nondependent right lung and were reduced with 10 cm $H_2O$ bilateral PEEP.

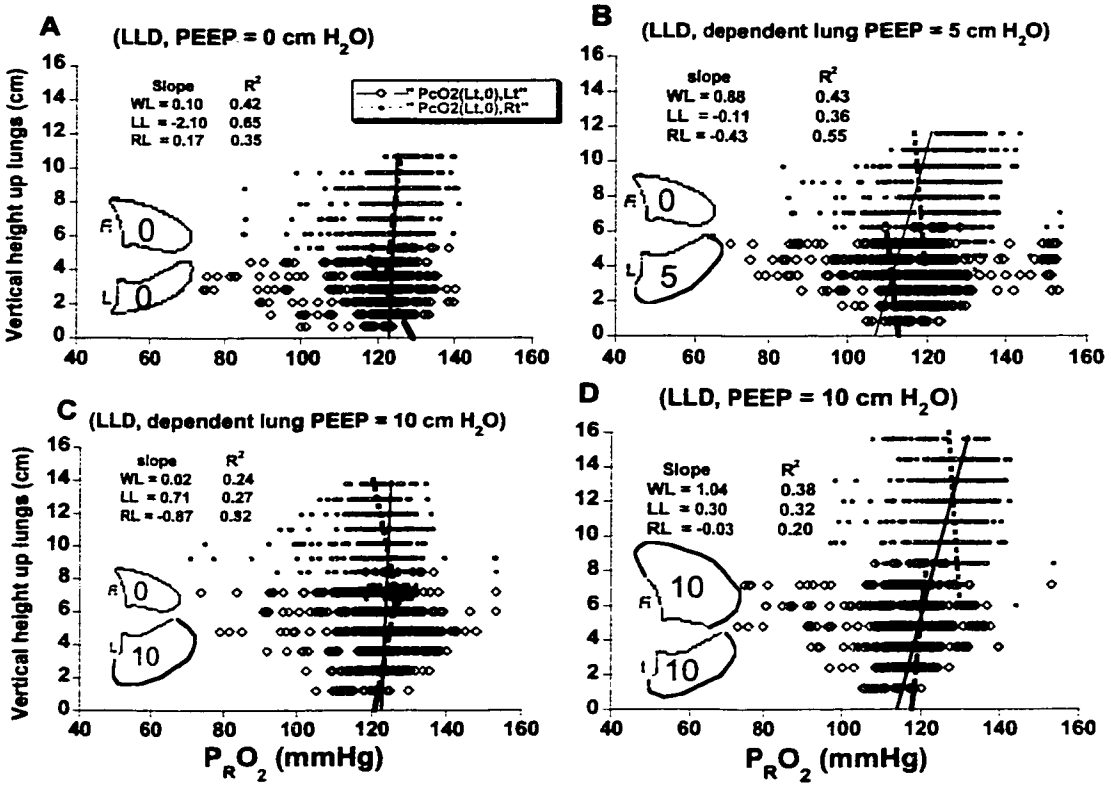


Fig 19. Regional $PO_2$ ($P_RO_2$) *vs.* lung height for a representative dog in the LLD posture without PEEP (A), with 5 cm $H_2O$ unilateral dependent PEEP (B), with 10 cm $H_2O$ unilateral dependent PEEP (C) and with bilateral 10 cm $H_2O$ PEEP (D). R represents right lung (open points), L the left lung (solid points) and N, the number of lung pieces. The lines represent best-fit values from multiple linear regression analysis at center of mass.

TABLE 16. Coefficients and $R^2$ of multiple linear regression equation† fit to $P_RO_2$ data for whole, left and right lung, respectively

| lung | PEEP | Intercept | a | b | c | d | e | f | g | $R^2$ |
|---|---|---|---|---|---|---|---|---|---|---|
| | 0 | 114.2 | 2.20 | **1.02** | -0.81 | 0.01 | -0.14 | -0.03 | 0.01 | 0.37 |
| Whole | | ±12.5 | ±2.10 | **±0.88*** | ±2.12 | ±0.33 | ±0.25 | ±0.16 | ±0.06 | ±0.22 |
| | 5s | 109.9 | 1.65 | **1.14** | -1.6 | -0.05 | **-0.16** | -0.17 | -0.03 | 0.46 |
| | | ±9.6 | ±2.68 | **±0.96*** | ±2.05 | ±0.21 | **±0.11*** | ±0.38 | ±0.05 | ±0.17 |
| | 10s | 114.9 | 1.16 | **1.10** | -1.05 | 0.04 | **-0.11** | **-0.11** | -0.006 | 0.34 |
| | | ±12.2 | ±1.85 | **±0.82*** | ±2.08 | ±0.28 | **±0.10*** | **±0.10*** | ±0.02 | ±0.18 |
| | 10 | 115.6 | **2.18** | 0.38 | 0.05 | **-0.13** | -0.04 | **0.10** | 0.01 | 0.43 |
| | | ±10.3 | **±1.75*** | ±1.00 | ±0.26 | **±0.12*** | ±0.07 | **±0.08*** | ±0.02 | ±0.15 |
| | 0 | 106.0 | -1.00 | 0.43 | 0.39 | 0.37 | 0.001 | 0.15 | 0.06 | 0.34 |
| Left | | ±19.9 | ±5.00 | ±1.91 | ±0.79 | ±1.12 | ±0.51 | ±0.36 | ±0.11 | ±0.17 |
| | 5s | 102.6 | -0.01 | 1.17 | -0.49 | 0.15 | -0.08 | 0.11 | 0.02 | 0.35 |
| | | ±18.5 | ±3.24 | ±1.46 | ±1.93 | ±0.58 | ±0.23 | ±0.15 | ±0.07 | ±0.13 |
| | 10s | 109.6 | 0.44 | 0.91 | -0.61 | 0.10 | -0.08 | 0.08 | -0.003 | 0.34 |
| | | ±18.8 | ±3.04 | ±1.45 | ±2.30 | ±0.25 | ±0.21 | ±0.17 | ±0.05 | ±0.19 |
| | 10 | 100.1 | -0.74 | 0.23 | 0.40 | 0.06 | 0.01 | 0.02 | 0.10 | 0.31 |
| | | ±19.1 | ±3.29 | ±1.09 | ±1.06 | ±0.50 | ±0.24 | ±0.17 | ±0.20 | ±0.11 |
| Right | 0 | 119.7 | **1.51** | **0.88** | -1.10 | 0.17 | -0.14 | -0.16 | 0.04 | 0.33 |
| | | ±1.5 | **±1.42*** | **±0.60*** | ±2.14 | ±0.22 | ±0.21 | ±0.18 | ±0.04 | ±0.16 |
| | 5s | 116.2 | 1.02 | **1.20** | -1.80 | 0.29 | **-0.27** | -0.19 | 0.05 | 0.47 |
| | | ±6.5 | ±1.22 | **±0.72*** | ±2.88 | ±0.41 | **±0.13*** | ±0.24 | ±0.06 | ±0.17 |
| | 10s | 119.9 | 0.23 | **1.33** | -1.46 | 0.26 | **-0.20** | -0.22 | 0.03 | 0.31 |
| | | ±10.1 | ±1.50 | **±1.21*** | ±2.32 | ±0.35 | **±0.10*** | ±0.25 | ±0.06 | ±0.15 |
| | 10 | 123.8 | 1.01 | -0.09 | 0.16 | **-0.07** | -0.05 | 0.07 | 0.02 | 0.19 |
| | | ±3.8 | ±1.78 | ±0.57 | ±0.29 | **±0.05*** | ±0.07 | ±0.10 | ±0.02 | ±0.10 |

Values are presented as mean ± SD (n=6), * $P < 0.05$ Compared with zero by 1-tailed unpaired t test. † Equation: $P_RO_2 = I + ax + by + cz + dxy + eyz + fzx + gxyz$. All intercepts are significant.

The dorsal-ventral gradients in $P_RO_2$ observed in the right lung with 5 and 10 cm $H_2O$ unilateral PEEP varied in the caudal-cranial direction, as evident from the significant coefficients of the YZ variable (coefficient e, -0.27 and –0.20).

The absence of an increase in $P_RO_2$ with unilateral and bilateral PEEP in the present study with constant ventilation to the dependent left lung was opposite to the PEEP-induced increase in $P_RO_2$ observed with conventional mechanical ventilation with single lumen tracheal tube intubation (Table 17). This indicated that PEEP did not improve gas exchange to the dependent left lung in the present study. The PEEP-induced improved gas exchange with conventional mechanical ventilation in the LLD posture was mostly likely caused by increased ventilation to the dependent left lung.

Table 17. Comparison conventional and differential ventilation in lateral decubitus posture without PEEP in regional $P_RO_2$ in Coefficients and $R^2$ of multiple linear regression equation† fit to $P_RO_2$ data for whole, left and right lung, respectively

| lung | mode | PEEP | Intercept | a | b | c | d | e | f | g | $R^2$ |
|---|---|---|---|---|---|---|---|---|---|---|---|
| Whole | CV | 0 | 113.4 | **1.30** | **1.15** | **0.5** | -0.14 | **-0.16** | -0.06 | 0.03 | 0.51 |
| | | | ±6.7 | **±1.2*** | **±0.89*** | **±0.26*** | ±0.19 | **±0.15*** | ±0.051 | ±0.04 | ±0.15 |
| | DV | 0 | 114.2 | 2.20 | **1.02** | -0.81 | 0.01 | -0.14 | -0.03 | 0.01 | 0.37 |
| | | | ±12.5 | ±2.10 | **±0.88*** | ±2.12 | ±0.33 | ±0.25 | ±0.16 | ±0.06 | ±0.22 |
| Left | CV | 0 | 104.9 | 0.21 | **2.8** | **0.85** | 0.50 | -0.42 | 0.079 | -0.04 | 0.52 |
| | | | ±12 | ±2.4 | **±2.6*** | **±0.67*** | ±0.57 | ±0.50 | ±0.32 | ±0.15 | ±0.16 |
| | DV | 0 | 106.0 | -1.00 | 0.43 | 0.39 | 0.37 | 0.001 | 0.15 | 0.06 | 0.34 |
| | | | ±20 | ±5.00 | ±1.91 | ±0.79 | ±1.12 | ±0.51 | ±0.36 | ±0.11 | ±0.17 |
| right | CV | 0 | 118.6 | -0.25 | 0.55 | 0.2 | 0.17 | -0.087 | -0.065 | 0.013 | 0.35 |
| | | | ±4.3 | ±0.36 | ±0.57 | ±0.3 | ±0.23 | ±0.11 | ±0.078 | ±0.028 | ±0.14 |
| | DV | 0 | 119.7 | **1.51** | **0.88** | -1.10 | 0.17 | -0.14 | -0.16 | 0.04 | 0.33 |
| | | | ±1.5 | **±1.42*** | **±0.60*** | ±2.14 | ±0.22 | ±0.21 | ±0.18 | ±0.04 | ±0.16 |

Values are presented as mean ± SD (n=6), CV: conventional ventilation. DV: differential ventilation.$P < 0.05$ Compared with zero by 1-tailed unpaired t test.

† Equation: $P_RO_2 = I + ax + by + cz + dxy + eyz + fzx + gxyz$. All intercepts are significant.

$P_RO_2$ of conventional ventilation in LLD without PEEP was adapted from (Chapter 3).

Consistent with the measured mean $P_RO_2$ values was a lower $\dot{V}_A/\dot{Q}$ in the left lung (1.1±0.4) than in the right lung (1.7±0.4) that was independent of the PEEP conditions. Positive vertical gradients in $\dot{V}_A/\dot{Q}$ in the whole lung were significant only without PEEP and with bilateral PEEP (0.08), and were associated with comparable gradients in the right lung (Fig 20 and Table 18). The vertical gradient in $\dot{V}_A/\dot{Q}$ in the whole lung and right lung without PEEP occurred in conjunction with significant dorsal-ventral gradients.

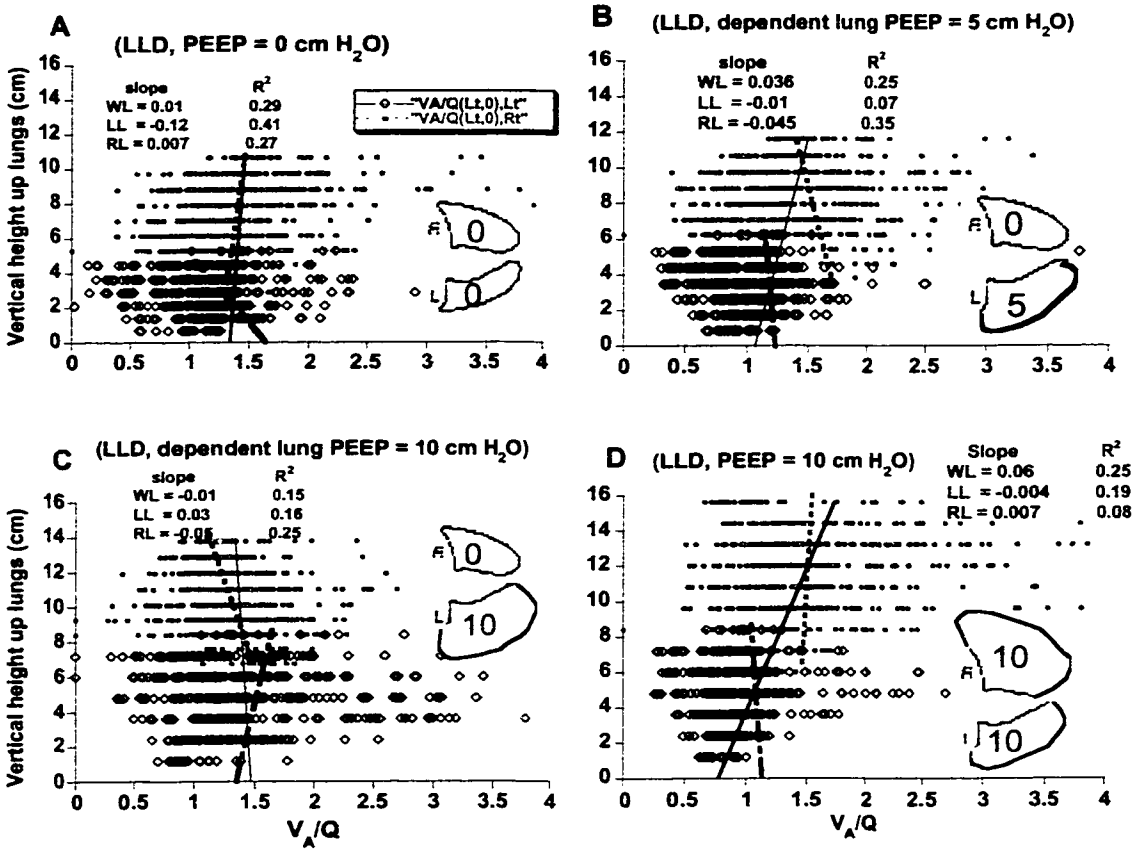


Fig 20. $\dot{V}_A/\dot{Q}$ *vs.* lung height for a representative dog in the LLD posture without PEEP (A), with 5 cm $H_2O$ unilateral dependent PEEP (B), with 10 cm $H_2O$ unilateral dependent PEEP (C) and with bilateral 10 cm $H_2O$ PEEP (D). R represents right lung (open points), L the left lung (solid points) and N, the number of lung pieces. The lines represent best-fit values from multiple linear regression analysis at center of mass.

TABLE 18. Coefficients and $R^2$ of multiple linear regression equation† fit to $\dot{V}_A/\dot{Q}$ data for whole, left and right lung, respectively

| lung | PEEP | Intercept | a | b | c | d | e | f | g | $R^2$ |
|---|---|---|---|---|---|---|---|---|---|---|
| | 0 | 1.5 | **0.09** | **0.05** | -0.02 | 0.006 | -0.001 | **-0.009** | -0.001 | 0.27 |
| Whole | | ±0.3 | **±0.08*** | **±0.04*** | ±0.04 | ±0.01 | ±0.007 | **±0.008*** | ±0.002 | ±0.16 |
| | 5s | 1.4 | 0.07 | 0.05 | -0.04 | 0.006 | -0.005 | **-0.004** | -0.002 | 0.27 |
| | | ±0.3 | ±0.09 | ±0.05 | ±0.05 | ±0.006 | ±0.01 | **±0.005*** | ±0.003 | ±0.16 |
| | 10s | 1.5 | 0.06 | **0.05** | -0.03 | 0.005 | **-0.003** | -0.002 | -0.001 | 0.18 |
| | | ±0.3 | ±0.06 | **±0.05*** | ±0.04 | ±0.01 | **±0.002*** | ±0.004 | ±0.001 | ±0.10 |
| | 10 | 1.6 | **0.08** | -0.01 | -0.0002 | -0.0005 | 0.001 | 0.001 | 0.001 | 0.22 |
| | | ±0.3 | **±0.04*** | ±0.05 | ±0.02 | ±0.02 | ±0.01 | ±0.014 | ±0.004 | ±0.13 |
| | 0 | 1.1 | -0.04 | -0.001 | 0.02 | 0.002 | 0.006 | 0.014 | 0.003 | 0.27 |
| Left | | ±0.4 | ±0.21 | ±0.08 | ±0.03 | ±0.042 | ±0.02 | ±0.023 | ±0.007 | ±0.10 |
| | 5s | 1.1 | 0.13 | 0.14 | -0.19 | -0.002 | -0.003 | 0.04 | 0.014 | 0.25 |
| | | ±0.4 | ±0.32 | ±0.29 | ±0.47 | ±0.02 | ±0.01 | ±0.09 | ±0.032 | ±0.11 |
| | 10s | 1.2 | 0.03 | 0.03 | -0.02 | 0.001 | 0.001 | -0.001 | 0.002 | 0.19 |
| | | ±0.4 | ±0.13 | ±0.05 | ±0.05 | ±0.01 | ±0.005 | ±0.01 | ±0.004 | ±0.17 |
| | 10 | 1.1 | -0.17 | -0.07 | 0.04 | 0.06 | -0.01 | -0.02 | 0.01 | 0.15 |
| | | ±0.4 | ±0.34 | ±0.14 | ±0.09 | ±0.15 | ±0.03 | ±0.05 | ±0.03 | ±0.09 |
| | 0 | 1.7 | **0.07** | **0.06** | **-0.05** | 0.01 | -0.002 | **-0.02** | 0.002 | 0.23 |
| Right | | ±0.4 | **±0.06*** | **±0.03*** | **±0.04*** | ±0.02 | ±0.005 | **±0.01*** | ±0.003 | ±0.13 |
| | 5s | 1.7 | 0.03 | **0.07** | -0.05 | 0.01 | **-0.01** | **-0.01** | 0.002 | 0.31 |
| | | ±0.4 | ±0.05 | **±0.06*** | ±0.06 | ±0.02 | **±0.004*** | **±0.008*** | ±0.002* | ±0.17 |
| | 10s | 1.7 | -0.01 | 0.07 | -0.04 | 0.01 | **-0.01** | -0.01 | -0.0004 | 0.23 |
| | | ±0.3 | ±0.04 | ±0.07 | ±0.05 | ±0.01 | **±0.004*** | ±0.02 | ±0.003 | ±0.10 |
| | 10 | 1.9 | **0.09** | -0.01 | -0.02 | -0.009 | 0.003 | 0.02 | -0.004 | 0.11 |
| | | ±0.3 | **±0.08*** | ±0.06 | ±0.08 | ±0.012 | ±0.02 | ±0.04 | ±0.01 | ±0.06 |

Values are presented as mean ± SD (n=6), * $P < 0.05$ Compared with zero by 1-tailed unpaired t test.

† Equation: $P_RO_2 = I + ax + by + cz + dxy + eyz + fzx + gxyz$. All intercepts are significant.

Notably absent were any significant gradients in $\dot{V}_A/\dot{Q}$ and $P_RO_2$ in the dependent left lung without and with PEEP. This is in contrast to a previous study (Chapter 3) with single endotracheal tube ventilation where small but significant gradients in $\dot{V}_A/\dot{Q}$ and $P_RO_2$ were observed. This suggests that differential ventilation with a double lumen tube changed the ventilation distribution in the left lung from that occurring with conventional ventilation with a single tube (see Discussion).

$\dot{V}_A$ *and* $\dot{Q}$ *matching.* The coefficient of correlation between $\dot{V}_A$ and $\dot{Q}$ with differential ventilation and 10 cm $H_2O$ bilateral PEEP was significantly less than that with 10 cm $H_2O$ unilateral PEEP to the dependent left lung (Table 19). Fig 21 shows that $\dot{V}_A$ and $\dot{Q}$ of individual lung pieces were highly correlated in the face of large heterogeneity. Lung pieces with lower (higher) $\dot{V}_A$ had lower (higher) $\dot{Q}$ without PEEP and with unilateral PEEP

Table 19. Coefficient of correlation (R) between $\dot{V}_A$ and $\dot{Q}$ during differential ventilation without PEEP and with selective PEEP to left lung and general PEEP to both right and left lung in the left lateral decubitus posture.

| Animal No | (LLD, 0) | (LLD, 5s) | (LLD, 10s) | (LLD, 10B) |
|---|---|---|---|---|
| 1 | 0.86 | 0.88 | 0.83 | 0.76 |
| 2 | 0.31 | 0.38 | 0.62 | 0.45 |
| 3 | 0.60 | 0.50 | 0.61 | 0.14 |
| 4 | 0.69 | 0.74 | 0.80 | 0.63 |
| 5 | 0.75 | 0.58 | 0.67 | 0.59 |
| 6 | 0.77 | 0.91 | 0.92 | 0.56 |
| Mean ± SD | 0.66±0.19 | 0.67±0.21 | 0.74±0.13 | 0.52±0.21* |

(LLD, 0): left lateral decubitus posture with 0 cm $H_2O$ PEEP
(LLD, 5s): left lateral decubitus posture with 5 cm $H_2O$ selective PEEP.
(LLD, 10s): left lateral decubitus posture with 10 cm $H_2O$ selective PEEP.
(LLD, 10B): left lateral decubitus posture with 10 cm $H_2O$ PEEP to both lungs. * $P < 0.05$, compared with 10 cm $H_2O$ selective PEEP

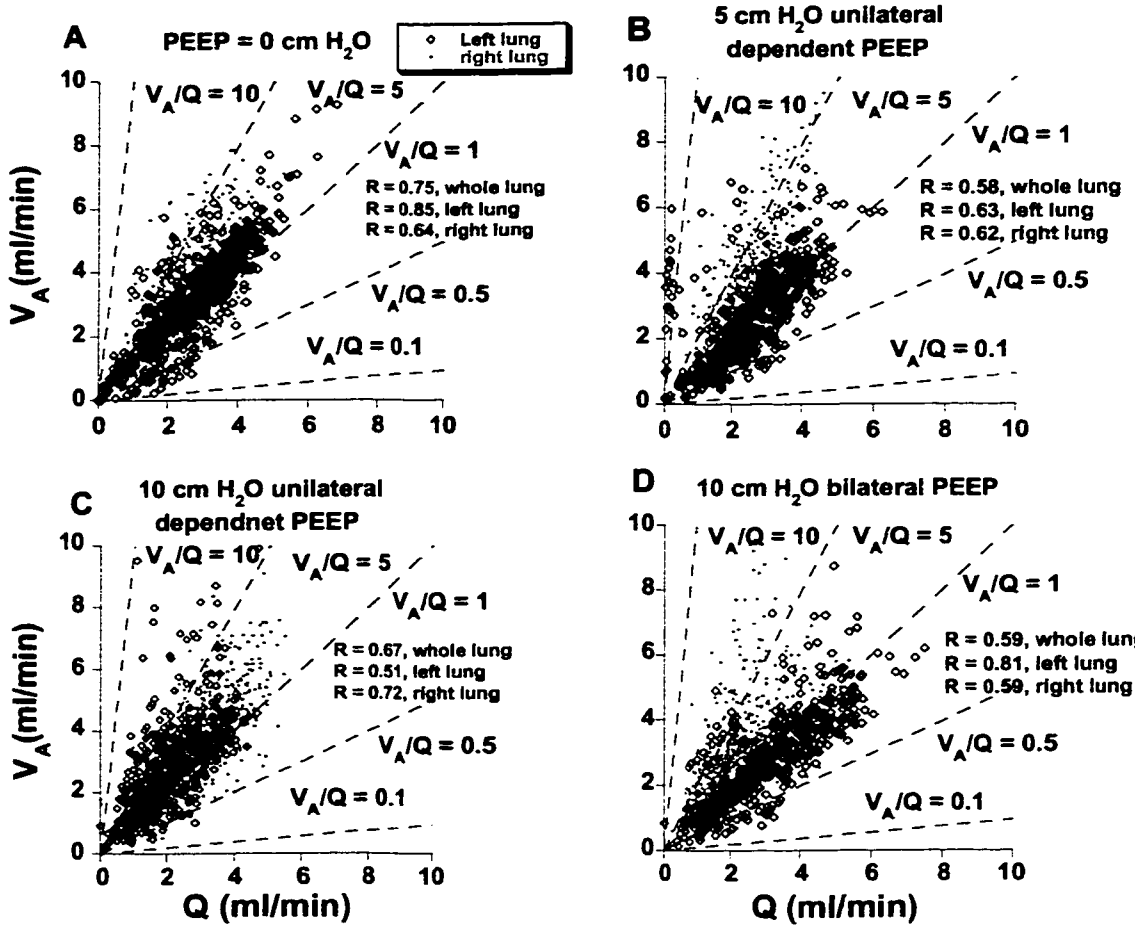


Fig 21. Scattergram of regional ventilation plot against regional perfusion for a representative animal in LLD posture without PEEP (A), with 5 cm $H_2O$ unilateral dependent PEEP (B), with 10 cm $H_2O$ unilateral dependent PEEP (C) and with bilateral 10 cm $H_2O$ PEEP (D).

***MIGET data.*** Gas exchange, evaluated using the multiple inert gas elimination technique (MIGET) showed similar unimodal distributions in $\dot{Q}$ and $\dot{V}_A$ without and with PEEP. The number of regions of $\dot{Q}$ with low $\dot{V}_A/\dot{Q}$ ($0.005 < \dot{V}_A/\dot{Q} < 0.1$) and shunt $\dot{V}_A/\dot{Q} < 0.005$) was small (< 2% of total) and unchanged without and with PEEP (Table 20). The distribution of $\dot{V}_A$ showed a similar behavior as $\dot{Q}$, that is, the number of regions of high $\dot{V}_A$ ($10 < \dot{V}_A/\dot{Q} < 100$) and deadspace $\dot{V}_A/\dot{Q} > 100$) were small (< 2% of total) and was unchanged without and with PEEP. These data support the evidence

provided by the regional data of $\dot{Q}$ and $\dot{V}_A$ measured by fluorescent microspheres that gas exchange in the LLD posture without PEEP was not improved by unilateral PEEP to the dependent left lung or by bilateral PEEP when ventilation to the dependent lung was kept constant.

Table 20. Distributions of ventilation and perfusion to regions with different $\dot{V}_A/\dot{Q}$ ratios from microsphere data during differential ventilation with selective and bilateral PEEP

| | ZEEP | 5cm $H_2O$ SPEEP | 10cm $H_2O$ SPEEP | 10cm $H_2O$ BPEEP |
|---|---|---|---|---|
| $\dot{V}$ mean | 1.58±0.31 | 1.52±0.21 | 1.61±0.25 | 1.54±0.25 |
| Log $\dot{V}$ SD | 0.45±0.18 | 0.46±0.16 | 0.43±0.14 | 0.56±0.16 |
| $\dot{V}$ high, % | 0.60±0.70 | 0.70±0.70 | 0.70±1.10 | 0.20±0.30 |
| $V_D$, % | 0.10±0.10 | 0.10±0.10 | 0.10±0.20 | 0.30±0.40 |
| $\dot{Q}$ mean | 1.25±0.29 | 1.17±0.25 | 1.28±0.26 | 1.08±0.31 |
| Log $\dot{Q}$ SD | 0.54±0.26 | 0.59±0.28 | 0.57±0.23 | 0.60±0.27 |
| $\dot{Q}$ low, % | 0.70±1.40 | 1.40±2.80 | 0.90±1.00 | 0.00±0.00 |
| $\dot{Q}$ S,% | 1.00±2.40 | 0.10±0.30 | 1.50±2.40 | 0.20±0.30 |

Values are means ± SD (n = 6). ZEEP: 0 cm $H_2O$ PEEP; SPEEP: selective PEEP to dependent lung in LLD posture; BPEEP: PEEP to both lungs; $\dot{V}$ mean and Log $\dot{V}$ SD; mean and log standard deviation of ventilation. $\dot{V}$ high and $V_D$; ventilation to regions with $10 < \dot{V}_A/\dot{Q} < 100$ and $\dot{V}_A/\dot{Q} > 100$, respectively; $\dot{Q}$ mean and log $\dot{V}$ SD: mean and log standard deviation of perfusion; $\dot{Q}$ low and $\dot{Q}$ S; perfusion of regions with $0.005 < \dot{V}_A/\dot{Q} < 0.1$ and shunt. * $P < 0.05$, significantly different from ZEEP.

**Discussion**

In this study, fluorescent microspheres were injected intravenously and aerosolized microspheres administered with ventilation to measure the effect of unilateral and bilateral PEEP on the regional distribution of flow and ventilation with constant differential ventilation to both lungs in the LLD posture.

## Methodological issue

The dog was chosen as animal model because the dog's pattern of lobar bronchial branching from the trachea allowed the differential ventilation to the left and right lungs with a double lumen tube (37), in contrast to other mammals such as the pigs.

We used the fluorescent microsphere technique to measure the regional distribution of $\dot{Q}$ and $\dot{V}_A$ because of its much greater resolution compared to other techniques. Three-dimensional data of the regional distribution of $\dot{Q}$, $\dot{V}_A$, $\dot{V}_A/\dot{Q}$ and regional $PO_2$ were obtained in 1.7 ml pieces of the isolated lung dried at TLC.

Both injected and aerosolized fluorescent microspheres were delivered in vivo near FRC, while the fluorescent intensity was measured in vitro in the dry lung pieces near total lung capacity. Several corrections were made to estimate the regional ventilation and perfusion in vivo near FRC. First, anisotropic reduction of the cubic lengths in the 3 dimension from TLC to FRC was made using previous measurements (56; 127). Second, we imposed a distortion to the vertical dimension (X) of each lung piece to account for the vertical Ptp gradient (1). No correction was made for the Ptp gradients in the other two axes (Y and Z) in the absence of reported data. The correction for the vertical Ptp gradient was only needed for the bilateral ventilation without PEEP and for unilateral ventilation with 5 cm $H_2O$ PEEP.

$\dot{Q}$ and $\dot{V}_A$ was normalized by dividing by regional volume, to conform with measurements using other techniques. This correction required the use of lung density of the inflated lung at FRC. Blood volume was excluded from the estimate of lung density because the dried lung pieces were blood-free.

### Conventional vs. differential mechanical ventilation

In the lateral posture, conventional mechanical ventilation in anesthetized human produced a mismatch between $\dot{Q}$ and $\dot{V}_A$ and impairment in gas exchange (86; 129; 130). This was the result of reduced regional ventilation to the dependent lung caused by a reduced FRC due to heart (73; 118) and abdominal compression (40; 135) and a reduced

lung compliance (129; 130) in conjunction with a gravity dependent regional blood flow distribution (7; 56; 82; 93; 127; 157; 159).

In the anesthetized dog ventilated with air in the LLD posture, blood flow, measured using the fluorescent microsphere technique (114), was lower in the dependent lung than in the nondependent lung, a behavior opposite to that expected due to gravity. The reduced blood flow was caused by a reduced $P_RO_2$ and $\dot{V}_A/\dot{Q}$, secondary to the reduced dependent lung FRC due to compression by the mediastinal content and reduced ventilation (Chapter 3). The relatively low flow in the dependent lung was increased either by a change to the RLD posture or by applying 10 cm $H_2O$ PEEP. Mechanical ventilation with 100% $O_2$ increased flow to the dependent lung in the LLD posture (Chapter 5), consistent with HPV as the mechanism for the reduced flow with air ventilation.

The rationale for differential ventilation in the left lateral posture was to ensure adequate ventilation to the dependent lung by matching the greater regional perfusion in the dependent lung with an equal ventilation, thus improving gas exchange (63). Previous studies in anesthetized humans using equal ventilation to both lungs showed improved gas exchange (9; 63). The explanation for the improved gas exchange was that differential ventilation caused more airways to open, resulting in a greater lung compliance and lower airway resistance in the dependent lung (85). However, an alternative explanation in this human study was the application of 50% of the total ventilation to the dependent left lung instead of the 35% measured with conventional ventilation.

The foregoing effects of differential ventilation on gas exchange are at odds with the present results. First, using the 35-65% left-right lung ventilation ratio measured with conventional ventilation, differential ventilation did not improve gas exchange, as measured by the A-a$DO_2$ ($O_2$ deficit). The reduced blood flow and reduced $P_RO_2$ to the dependent lung in the LLD posture measured with conventional ventilation (Chapter 3) was maintained with differential ventilation. The more uniform $P_RO_2$ distribution observed with differential ventilation was consistent with the elimination of the vertical

and dorsal-ventral gradients in $P_RO_2$ observed with conventional ventilation (Chapter 3). Thus, $\dot{V}_A/\dot{Q}$ inequalities as measured by spatial gradients in $\dot{V}_A/\dot{Q}$ did not contribute to the A-a$DO_2$.

The more uniform distribution of $P_RO_2$ observed with differential ventilation may be attributed to the increased flow velocity caused by the intrabronchial tube placed in the main stem bronchus of the left lung. The increased flow velocity might serve to redistribute gas more evenly in the lung periphery and result in more uniform ventilation and regional $P_RO_2$. In the left lung, $\dot{V}_A$ and $\dot{Q}$ measured by aerosolized microspheres were distributed similarly among lobes between differential and conventional ventilation. By contrast in the right lung, $\dot{V}_A$ and $\dot{V}_A/\dot{Q}$ in the caudal lobe were greater with the double lumen tube (53 and 50% total) than with the single lumen tube (38 and 35% total).

Consistent with the foregoing differences in $\dot{V}_A$ and $\dot{V}_A/\dot{Q}$, A-a$DO_2$ measured with differential ventilation averaged 23-28 mmHg, double the values (10-17 mmHg) measured previously with conventional ventilation (Chapter 3). The potential contribution of the double lumen tube to gas exchange impairment needs further study.

*Effect of unilateral and bilateral PEEP with differential ventilation in the LLD posture*

The application of PEEP to the dependent left lung with differential ventilation improved gas exchange in humans (9; 63; 86). In anesthetized humans, equal ventilation to both lungs with differential ventilation produced higher $PaO_2$ and a lower A-a$DO_2$, than with a single ventilator supplying a free distribution of ventilation between lungs either without or with 9 cm $H_2O$ PEEP (63). Similar studies in anesthetized humans showed a 30% reduction in A-a$DO_2$ with equal ventilation to both lungs and a further 13% reduction in A-a$DO_2$ with unilateral PEEP to the dependent lung (9). This behavior was attributed to the increased compliance, reduced airway resistance, and a more even ventilation distribution in the dependent lung as a result of the differential ventilation with unilateral PEEP (85).

In the present study with 35-65% left-right lung differential ventilation, no improvement in gas exchange as indicated by constant A-a$DO_2$ and mean $P_RO_2$ was observed with unilateral PEEP (5 and 10 cm $H_2O$) to the dependent left lung or with 10 cm $H_2O$ bilateral PEEP. This was consistent with the constant blood flow measured in the dependent left lung with unilateral PEEP compared to zero PEEP. The absence of the effect of PEEP on the oxygen deficit indicated that neither small airway closure nor lung nonuniform distortion was responsible for the lower $P_RO_2$ and oxygen deficit observed in the dependent lung, as these two factors would be reduced by the PEEP-induced increase in FRC.

Klingstedt et al (86) studied atelectasis and ventilation-perfusion distribution using multiple inert gas technique (MIGET) and CT scan in the supine and lateral position of human between conventional and differential ventilation with unilateral PEEP. They found that low $\dot{V}_A/\dot{Q}$ and shunt regions were decreased and oxygenation was improved with differential ventilation with unilateral PEEP. In addition, the atelectatic region was highly correlated with the shunt measured by MIGET, similar to our own studies in the anesthetized dog (Chapter 5). They reasoned that unilateral PEEP opened closed peripheral airways, increasing compliance and ventilation of the dependent lung and reducing shunt and low $\dot{V}_A/\dot{Q}$ regions. One difference between the human studies and ours is that cardiac output was maintained constant in our studies while it was allowed to change in the human studies. Thus in addition to the increased ventilation, a reduced blood flow to the dependent lung with differential ventilation might account for the increased $\dot{V}_A/\dot{Q}$ and reduced A-a$DO_2$ in the human studies. Another difference is the presence of the normal nonatelectatic lung in my study.

Consistent with the human studies (85), the greater the unilateral PEEP to the dependent lung, the greater the increase in the volume of the dependent lung (Table 11, Fig14), with no change in the volume of the nondependent lung. In the human studies, the compliance of dependent lung was increased and airway resistance was decreased by unilateral dependent PEEP, causing a more uniform gas distribution. In the present study

the spatial gradients in $\dot{V}_A$ observed without PEEP in the dependent left lung was reduced by unilateral or bilateral PEEP with differential ventilation, indicative of a more uniform ventilation distribution. Differential ventilation also reduced the positive dorsal-ventral gradient of $\dot{V}_A$ observed in the previous study with conventional mechanical ventilation (Chapter 3).

In the present study, all measures of gas exchange efficiency from MIGET analysis of microsphere data of $\dot{Q}$ and $\dot{V}_A$ were unchanged with unilateral and bilateral PEEP, opposite to previous studies in humans (63), in which shunt and low $\dot{V}_A/\dot{Q}$ regions were decreased by unilateral PEEP to the dependent lung. The latter was most likely caused by the PEEP-induced increased in ventilation that was constant in the present study.

The gravity dependent vertical gradients in $\dot{Q}$ observed with differential ventilation was consistent with the previous studies with conventional mechanical ventilation in dog (56; 127) and in human (7; 82; 93). That unilateral PEEP reduced the vertical gradient and eliminated the negative caudal-cranial gradient in $\dot{Q}$ was similar to the previous study (Chapter 3) with conventional ventilation with bilateral PEEP. However, the spatial distribution of $\dot{Q}$ in the nondependent right lung was not affected by the unilateral dependent PEEP (Table 14, Fig 16). Unilateral dependent PEEP reduced pulmonary vascular resistance (PVR) by opening closed airway and increased PVR by increasing alveolar pressure. These opposing effects might account for a small net effect on $\dot{Q}$ by unilateral dependent PEEP.

*Differential ventilation with unilateral dependent PEEP vs. differential ventilation with bilateral PEEP*

The lung volume of the dependent left lung with 10 cm $H_2O$ unilateral PEEP was greater than that of dependent lung with 10 cm $H_2O$ bilateral PEEP while the non-dependent lung volume with bilateral PEEP doubled that with unilateral 10 cm $H_2O$

PEEP. This behavior was similar to results found in humans studied in the LLD posture (85; 130).

While unilateral PEEP had no effect on blood flow to the dependent left lung, with the same differential ventilation bilateral PEEP diverted blood flow to the dependent left lung from the nondependent lung. This increased blood flow had no effect on the (A-a)$DO_2$ and was caused by the increased Ppa and Pcwp-induced increased vascular resistance in the nondependent lung. By contrast, bilateral PEEP with conventional ventilation increased $P_RO_2$, a reflection of an increased ventilation to the dependent left lung.

Differential ventilation with bilateral PEEP produced negative vertical and caudal-cranial gradients in $\dot{Q}$ but not the positive dorsal-ventral gradient observed with conventional ventilation. The difference might be due to the diversion of ventilation to the dependent left lung from the nondependent lung with conventional ventilation that was prevented with the differential ventilation. With conventional ventilation with air, the positive dorsal-ventral gradient in $\dot{Q}$ observed with conventional ventilation with air became negative with 100% $O_2$ ventilation, presumably a result of the removal of the HPV-induced reduced blood flow in the caudal regions, see studies described in (Chapter 5). With both modes of ventilation, the vertical gradient of $\dot{Q}$ varied along the caudal-cranial axis (Z), the vertical gradient of $\dot{Q}$ being more positive in the caudal regions and more negative in the cranial regions.

Differences in the spatial distribution of both $\dot{Q}$ and $\dot{V}_A$ occurred between unilateral PEEP and bilateral PEEP with differential ventilation. Bilateral PEEP abolished the positive dorsal-ventral gradient in $P_RO_2$ that occurred with unilateral PEEP in the nondependent right lung, the effect of the doubling of the nondependent lung volume with bilateral PEEP.

The increase in FRC of the nondependent lung with bilateral PEEP is associated with an increased risk of barotrauma, decreased venous return and decreased cardiac output (9; 63; 85). Previous studies (9; 10; 63) have demonstrated that equal ventilation to both lungs without and with unilateral PEEP improved gas exchange efficiency with a

lower risk of barotrauma and a smaller decrease in cardiac output. However, in the present study, unilateral PEEP with ventilation to the dependent lung similar to that without PEEP did not improve gas exchange. Similarly, bilateral PEEP produced no change in the (A-a)$DO_2$. Thus, the improved gas exchange in previous studies with differential ventilation was caused by the increased ventilation to the dependent lung and not by a PEEP-induced increased lung compliance, reduced airway resistance or reduced lung distortion.

# CHAPTER 5:

## Redistribution of Blood Flow and Lung Volume between Lungs in Lateral Decubitus Postures during Unilateral Atelectasis and PEEP

### Introduction

Several factors determine the regional distribution of blood flow and ventilation in the lung. These include the effects of gravity (7; 56; 82; 93; 127; 157; 159), regional lung volume distribution (15; 78), hypoxic pulmonary vasoconstriction (HPV) (13; 102; 103) and intrinsic vascular structure (16). In mechanically ventilated, anesthetized dogs studied in the lateral decubitus posture, blood flow in the left lateral decubitus (LLD) posture was lower in the dependent lung than in the nondependent lung, a behavior opposite to that expected due to gravity (114). This behavior in conjunction with a lower regional $PO_2$ ($P_RO_2$) in the dependent lung that was reversed with body inversion to the right lateral decubitis (RLD) posture, implicated HPV as a mechanism for the low dependent blood flow in the LLD posture (Chapter 3). The low $P_RO_2$ was attributed to a compression of the dependent left lung by the mediastinal contents and abdomen that reduced ventilation and lowered $\dot{V}_A/\dot{Q}$. The low $P_RO_2$ was abolished either by positioning the left lung nondependent in the RLD posture or by 10 cm $H_2O$ positive-end expiratory pressure (PEEP).

In this study, we addressed the question whether PEEP and posture in the lateral decubitus position affects the regional distribution of blood flow and ventilation and gas exchange after left lung atelectasis. We used intravenously injected and aerosolized fluorescent microspheres to study the spatial distribution in blood flow and ventilation. We studied the effects of changing from LLD to RLD posture to evaluate the influence of the weight of the heart, abdomen and left atelectatic lung on the ventilated right lung. We used ventilation with 100% $O_2$ to remove any HPV in the right ventilated lung. Thus any changes in blood flow of the ventilated lung with PEEP or a change in posture were attributed to lung volume-induced changes or gravity (height)-dependent changes in

vascular resistance. The goal was to provide a better understanding of the mechanisms responsible for gas exchange impairment in the lateral position and might be applicable to the optimal use of PEEP and body position in the ventilation of patients with unilateral lung disease or of patients after acute unilateral pneumonectomy.

**Methods**

The animal and separate lung preparation and general methods were described in Chapter 2. The right lung was ventilated with 100% $O_2$ throughout the study. The left lung was made atelectatic by ventilating it with 100% $O_2$ for ~ 5 min, occluding the left limb of the double lumen tube and allowing 30 minutes to achieve complete $O_2$ absorption. Before left lung atelectasis, the tidal volume of the right lung was measured by spirometry and subsequently used after left lung atelectasis. Intravenous normal saline (100-200 $ml \cdot hr^{-1}$) was administered to maintain constant cardiac output after left lung atelectasis and with 10 cm $H_2O$ positive end-expiratory pressure (PEEP). PEEP was generated by immersing the exhalation tube of the ventilator under 10 cm water. $NaHCO_3$ was given when necessary to correct metabolic acidosis with left lung atelectasis.

**Study protocol**

*Control studies.* We studied the effect of body position (left lateral decubitus (LLD) and right lateral decubitus (RLD) posture) and PEEP on the distribution of regional blood flow, ventilation and end-capillary $PO_2$ during hyperoxia (100% $O_2$). The dog was positioned in the LLD or RLD posture and PEEP was administered to both lungs in randomized order. Both lungs were ventilated with 100% $O_2$. After 20 min, the right and left tidal volumes were measured respectively. Cardiac output, pulmonary artery (Ppa), systemic arterial (Psa), airway (Paw), and capillary wedge pressure (Pcwp) were measured at end expiration. Arterial and mixed venous blood and exhaled gas were sampled for pH, $PCO_2$, and $PO_2$ analysis and the analysis of multiple inert gas elimination. One of four different colored 15 μm microspheres was randomly chosen and

intravenously injected over 5 min. The functional residual capacity (FRC) of both right and left lung was measured with by helium dilution.

*Left lung atelectasis.* We studied the effect of left lung atelectasis on the redistribution of regional blood flow and gas exchange in the LLD and RLD posture with and without PEEP to the right lung. Dogs were studied in the LLD and RLD posture in random order. After choosing the body posture, the right lung received 0 or 10 cm $H_2O$ PEEP determined in random order. Left lung atelectasis was induced by occluding the left bronchial tube of the double lumen tube and 30 min elapsed to ensure complete atelectasis. The right lung was ventilated with 100% $O_2$ throughout the study with the left lung atelectatic. After 20 minutes of stabilization blood gases, hemodynamic measurements, FRC and arterial, mixed venous and exhaled gas sample were obtained. Then aerosolized microspheres to the right lung and intravenous microspheres were delivered simultaneously for 5 min.

**Statistical analysis.** Volume-normalized blood flow and ventilation were used for all analysis. Values were presented as mean ± SD. A paired t test was used to test for a significant difference between two groups. ANOVA repeat measurement was used to evaluate differences among more than two groups. The coefficient of $R^2$ from a multiple linear regression model described how well the model explained the degree of variation in blood flow and ventilation due to spatial variation.

**Multiple linear regression analysis of spatial variation of $\dot{Q}$, $\dot{V}_A$, $\dot{V}_A/\dot{Q}$ and $P_RO_2$**

Data from the whole lung and from left and right lungs were analyzed using multiple linear regression analysis (StatView v. 5.0.1, SAS) as described in Chapter 2 to characterize the spatial distribution of regional blood flow and other variables in both the LLD and RLD posture, with and without PEEP, and with left lung atelectasis. No regression analysis of $\dot{V}_A/\dot{Q}$ and $P_RO_2$ was done on the atelectatic lung because $\dot{V}_A$ was absent. The intercepts, coefficients and $R^2$ values from the six animals were pooled and

their mean and SD were calculated. A single group one-tailed t test was used to test whether these coefficients were significantly different from zero.

## RESULTS

The hemodynamic data are shown in Table 21. The physiological variables, temperature, systemic arterial blood pressure and hemoglobin were constant throughout the study. Cardiac output (C.O.) did not change with the change in body position or left lung atelectasis, but decreased slightly with PEEP. PEEP, body posture, and left lung atelectasis produced changes in all of the measured physiological parameters in the lung.

### *Overall gas exchange*

For the control lung with 100% $O_2$ ventilation, $PaO_2$ was greater (559 Torr vs 493 Torr) in the LLD posture than in the RLD posture without PEEP but less (506 vs 594 Torr) without PEEP. With 10 cm $H_2O$ PEEP, (A-a)$DO_2$ in the control lung was greater (214 vs 124) in the LLD than the RLD posture, and increased in magnitude (486 vs 344) with left lung atelectasis (Table 22).

Left lung atelectasis decreased $PaO_2$, pH and $P\bar{v}O_2$ and increased $PaCO_2$ and (A-a)$DO_2$ in both postures. With 10 cm $H_2O$ PEEP, the atelectasis-induced reduction in $PaO_2$ was greater (373 vs 230 Torr) in the RLD than in the LLD posture.

With 100% $O_2$ ventilation, $P\bar{v}O_2$ averaged 63-68 mmHg in both LLD and RLD posture and decreased with PEEP and left lung atelectasis. With left lung atelectasis, $P\bar{v}O_2$ was similar in LLD and RLD postures (57 mmHg), but decreased with PEEP in the LLD posture (46 mmHg). Except for the LLD posture with PEEP, ventilation with 100 % $O_2$ with left lung atelectasis always increased $P\bar{v}O_2$ above the normal value measured with room air ventilation of both lungs (47 mmHg). With room air ventilation, $P\bar{v}O_2$ did not change with body posture or PEEP (Chapter 3).

The relatively high $PaO_2$ and $P\bar{v}O_2$ measured with left lung atelectasis and 100% $O_2$ ventilation to the right lung eliminated any hypoxic vasoconstriction in the right lung.

Table 21. Hemodynamic and pulmonary vascular resistance variable with and without left lung atelectasis

| | LLD | | | | RLD | | | | |
|---|---|---|---|---|---|---|---|---|---|
| | Non-atel | | Atel | | Non-atel | | Atel | | Significant Difference |
| PEEP, cm $H_2O$ | 0 | 10 | 0 | 10 | 0 | 10 | 0 | 10 | |
| Psa, cm $H_2O$ | 94 | 91 | 83 | 79 | 88 | 91 | 91 | 94 | |
| | ±5 | ±7 | ±6 | ±6 | ±7 | ±9 | ±6 | ±6 | |
| Ppa, cm $H_2O$ | 17 | 24 | 22 | 28 | 16 | 23 | 20 | 28 | PEEP***(P+:26±2, P-:19±2) |
| | ±2 | ±1 | ±4 | ±4 | ±2 | ±2 | ±2 | ±2 | Atel*(A+:25±3, A-:20±2) |
| Ppcw, cm $H_2O$ | 5.0 | 11.0 | 10.0 | 13.0 | 7.0 | 12.0 | 8.0 | 11.0 | PEEP**(P+:12±1, P-:8±1) |
| | ±0.8 | ±1.5 | ±2.6 | ±1.9 | ±0.8 | ±1.5 | ±2.3 | ±2.0 | |
| Paw.cm $H_2o$ | 10 | 21 | 10 | 25 | 10 | 20 | 11 | 21 | PEEP***(P+:22±2, P-:10±1) |
| | ±1 | ±1 | ±1 | ±6 | ±1 | ±1 | ±2 | ±2 | |
| $\dot{Q}_T$, $l \cdot min^{-1}$ | 3.3 | 3.2 | 3.2 | 2.9 | 3.4 | 3.0 | 3.1 | 3.0 | PEEP*(P+:3.05±0.11, |
| | ±0.2 | ±0.2 | ±0.3 | ±0.1 | ±0.2 | ±0.1 | ±0.1 | ±0.1 | P-:3.26±0.13) |
| $\dot{Q}_L$, % | 45 | 58 | 18 | 25 | 31 | 22 | 10 | 12 | Post***(L:37±3, R:19±2) |
| | ±3 | ±3 | ±4 | ±6 | ±2 | ±3 | ±3 | ±3 | PEEP*(P+:29±3, P-:26±2) |
| | | | | | | | | | Atel***(A+:16±3, A-:39±2) |
| $R_T$ | 3.5 | 3.8 | 4.7 | 6.0 | 2.8 | 3.7 | 3.7 | 5.8 | PEEP** (P+:4.8±1.6, P-:3.6±1.4) |
| $cmH_2O \cdot L^{-1} \cdot min^{-1}$ | ±1.0 | ±1.6 | ±0.8 | 0.9 | ±1.0 | ±0.8 | ±1.8 | ±1.5 | Atel** (A+: 5.0±1.5, A-: 3.5±1.3) |
| $R_L$ | 6.4 | 6.2 | 18.7 | 22.6 | 8.2 | 15.6 | 30.0 | 45.4 | Post* (L: 13.5±9.6, R:24.7±20.2) |
| $cmH_2O \cdot L^{-1} \cdot min^{-1}$ | ±2.2 | ±2.9 | ±8.5 | ±9.7 | ±4.1 | ±6.2 | ±10.1 | ±27.9 | Aetl** (A+:29.1±18.2, |
| | | | | | | | | | A-:9.1±5.4) |
| $R_R$ | 6.3 | 9.7 | 5.5 | 8.0 | 4.0 | 4.5 | 4.3 | 6.5 | Post** (L: 7.3±2.7, R: 4.9±1.8) |
| $cmH_2O \cdot L^{-1} \cdot min^{-1}$ | ±2.3 | ±3.5 | ±1.5 | ±0.5 | ±1.5 | ±1.5 | ±2.1 | ±1.2 | PEEP** (p+:7.2±2.7, p-:5.0±2.0) |

Values are means ± SE for 6 dogs. Non-atel:non-atelectasis; Atel: left lung atelectasis; Psa, means systemic arterial pressure; Ppa, mean pulmonary artery pressure; Ppcw, pulmonary capillary wedge pressure; Paw, peak airway pressure; VT:tidal volume; T, total cardiac output; L, left lung blood flow; R: pulmonary vascular resistance; R't, right lung; L't, left lung; post, position; L: LLD R: RLD; A+: with atelectasis; A-: no atelectasis; P+: with PEEP; P-: no PEEP.
* $P < 0.05$, ** $P < 0.01$, *** $P < 0.001$

Table 22. Tidal volume, functional residual capacity and arterial blood gas with and without left lung atelectasis

| | LLD | | | | RLD | | | | |
|---|---|---|---|---|---|---|---|---|---|
| | Non-atel | | Atel | | Non-atel | | Atel | | Significant Difference |
| PEEP, cm $H_2O$ | 0 | 10 | 0 | 10 | 0 | 10 | 0 | 10 | |
| $V_T$,right (ml) | 252 ±13 | 205 ±11 | 226 ±13 | 221 ±8 | 188 ±9 | 220 ±9 | 213 ±6 | 213 ±5 | |
| $Pao_2$, Torr | 559 ±24 | 506 ±35 | 367 ±63 | 230 ±73 | 493 ±60 | 594 ±10 | 401 ±42 | 373 ±61 | Atel**(A+:442±21, A-:387±31) Post* (L:415±42, R:465±32) |
| $Paco_2$, Torr | 40 ±0.7 | 36 ±0.3 | 39 ±1.3 | 40 ±0.9 | 37 ±0.3 | 37 ±1 | 40 ±1.8 | 39 ±1.6 | Atel*(A+:39±0.9, A-:37±0.4) |
| pH | 7.32 ±0.01 | 7.33 ±0.01 | 7.30 ±0.02 | 7.29 ±0.01 | 7.34 ±0.01 | 7.33 ±0.01 | 7.29 ±0.02 | 7.30 ±0.01 | Atel*(A+:7.3±0.01, A-:7.33±0.01) |
| $P\bar{v}o_2$, Torr | 68 ±6 | 65 ±5 | 57 ±4 | 46 ±4 | 67 ±5 | 63 ±3 | 59 ±3 | 55 ±3 | PEEP*(P+:57±3, P-:63±4) Atel**(A+:54±3, A-:67±5) |
| p(A-a)O2, Torr | 157 ±27 | 214 ±41 | 351 ±69 | 486 ±81 | 226 ±64 | 124 ±17 | 315 ±51 | 344 ±66 | Atel**(A+:374±62, A-:180±33) Post*(L:302±50, R:252±40) |
| FRC, R't (ml) | 463 ±90 | 894 ±168 | 513 ±229 | 963 ±335 | 281 ±93 | 542 ±51 | 365 ±101 | 751 ±221 | Post***(L:709±72, R:492±45) PEEP***(P+:787±59, P-:406±45) |
| FRC, L't (ml) | 143 ±45 | 306 ±72 | | | 286 ±130 | 547 ±160 | | | Post**(L:230±21, R:394±52) PEEP**(P+:430±51, P-:214±36) |

Values are means ± SE for 6 dogs. Non-atel:non-atelectasis; atel:left lung atelectasis; VT:tidal volume;Pao2, arterial PaO2; Paco2, arterial Paco2; Pvo2, mixed venous Po2;;P(A-a)o2, alveolar and arterial oxygen tension difference; FRC, functional residual capacity; R't, right lung; L't, left lung; post, position;L: LLD R: RLD; A+: with atelectasis; A-: no atelectasis; P+: with PEEP; P-: no PEEP. * $P < 0.05$, ** $P < 0.01$, *** $P < 0.001$

Thus any changes in $\dot{Q}$ observed in the right lung with PEEP and posture was attributed to factors other than hypoxic vasoconstriction

**MIGET data.**

Gas exchange data derived from the multiple inert-gas elimination technique (MIGET) are presented in Table 23. Left lung atelectasis increased the inert gas shunt in both LLD and RLD. The inert gas shunt fractions were identical to $\dot{Q}$ values measured in the left atelectatic lung by the fluorescent microsphere technique (Table 21). This was consistent with the absence of ventilation of the left atelectatic lung as verified by the negligibly small values of aerosolized microspheres detected (see below). Confirmation that the shunt fraction was produced by the blood flow of the atelectatic lung indicated that the $P_AO_2$ of the atelectatic lung was identical to the measured $P\bar{v}O_2$. This indicated that hypoxic vasoconstriction produced the reduced blood flow that occurred with left lung atelectasis.

PEEP increased dead space before and after left lung atelectasis. Both PEEP and left lung atelectasis increased mean $\dot{V}_A/\dot{Q}$. The fraction of ventilation to high $\dot{V}_A/\dot{Q}$ region was decreased by left lung atelectasis. The fraction of perfusion to low $\dot{V}_A/\dot{Q}$ regions was not affected by a change in posture, left lung atelectasis or PEEP. Ventilation distribution was broader in the LLD posture than in the RLD posture, as measured by a greater log $SD_{VA}$ in the LLD than RLD posture.

**Redistribution of *blood flow between right and left lung.***

*Effect of posture and PEEP, both lungs ventilated.* Without PEEP and with both lungs ventilated using 100% $O_2$ (control), total $\dot{Q}$ of the dependent left (right) lung was greater (45% vs. 31%) in the LLD (RLD) than in the RLD (LLD) posture (Fig 22, Table 24). This behavior was accentuated with 10 cm $H_2O$ PEEP. This behavior was also found with room air ventilation except for the LLD posture without PEEP where hypoxic vasoconstriction reduced blood flow in the dependent lung (see Discussion).

The greater flow in the dependent lung than in the nondependent lung in both postures was consistent

Table 23. Gas exchange of entire lung

| | LLD | | | | RLD | | | | Significant Difference |
|---|---|---|---|---|---|---|---|---|---|
| | Non-atel | | Atel | | Non-atel | | Atel | | |
| PEEP | 0 | 10 | 0 | 10 | 0 | 10 | 0 | 10 | |
| Mean $\dot{V}_A/\dot{Q}$ of $\dot{Q}$ | 0.7 ±0.1 | 0.8 ±0.1 | 0.8 ±0.2 | 1.5 ±0.3 | 0.6 ±0.1 | 0.8 ±0.1 | 0.8 ±0.1 | 1.0 ±0.1 | PEEP**(P+:1±0.1, P-:0.7±0.07) Atel*(A+:1±0.1, A-:0.7±0.08) |
| Mean $\dot{V}_A/\dot{Q}$ of $\dot{V}_A$ | 2.0 ±0.3 | 3.2 ±0.6 | 1.8 ±0.2 | 2.5 ±0.3 | 1.6 ±0.1 | 2.1 ±0.7 | 1.3 ±0.3 | 2.4 ±0.7 | |
| Log SD $\dot{Q}$ | 1.0 ±0.1 | 1.2 ±0.2 | 1.0 ±0.1 | 0.6 ±0.3 | 1.2 ±0.2 | 1.2 ±0.2 | 0.8 ±0.4 | 1.4 ±0.2 | |
| Log SD $\dot{V}_A$ | 1.2 ±0.2 | 1.4 ±0.2 | 1.6 ±0.2 | 1.4 ±0.4 | 1.2 ±0.4 | 0.8 ±0.4 | 1.0 ±0.1 | 0.8 ±0.4 | Post** (:L:1.3±0.1, R:1.1±0.2) |
| $\dot{Q}_S/\dot{Q}_T$ (%) | 6 ±4 | 5 ±3 | 13 ±5 | 25 ±7 | 2 ±0.6 | 0.3 ±0.2 | 9 ±3 | 11 ±3 | Atel*(A+:14±4, A-:3±2) |
| $V_D/V_T$(%) | 40 ±3 | 45 ±1 | 45 ±4 | 54 ±5 | 44 ±3 | 48 ±2 | 49 ±3 | 50 ±4 | PEEP**(P+:49±2, P-:45±2) |
| $\dot{Q}$ of low $\dot{V}_A/\dot{Q}$ (%) | 2.3 ±1.8 | 2 ±1.2 | 5.5 ±2.7 | 0.9 ±0.9 | 4.5 ±3.6 | 1.9 ±1.2 | 5.1 ±1.7 | 4.7 ±2.9 | |
| $\dot{V}_A$ of high $\dot{V}_A/\dot{Q}$ (%) | 8 ±4 | 14 ±2 | 5 ±2 | 3 ±1 | 7 ±3 | 8 ±3 | 3 ±2 | 3 ±3 | Atel**(A+:4±1, A-:10±2) |

Values are presented as means ± SE (n=5). Mean $\dot{V}_A/\dot{Q}$ of $\dot{Q}$ and mean $\dot{V}_A/\dot{Q}$ of $\dot{V}_A$ : mean ventilation-perfusion ratio of perfusion and ventilation distributions, respectively; $\dot{Q}_S/\dot{Q}_T$, inert gas shunt; $V_D/V_T$, inert gas dead space; corrected for shunt; $\dot{Q}$ of low $\dot{V}_A/\dot{Q}$, $\dot{Q}$ to low $\dot{V}_A/\dot{Q}$ units $\dot{V}_A/\dot{Q}$ ratio <0.1); $\dot{V}_A$ of high $\dot{V}_A/\dot{Q}$, $\dot{V}_A$ to high $\dot{V}_A/\dot{Q}$ units $\dot{V}_A/\dot{Q}$ ratio 10-100). Atel, atelectasis; A+, with atelectasis; A-, no atelectasis; P+, with PEEP; P-: no PEEP;Post, position; L, LLD, R: RLD, *P < 0.05, **P < 0.01.

with the gravity dependent vertical gradient in regional blood flow measured by a multiple linear regression analysis of the data (see below, Table 25).

Table 24. Cardiac output (%) to left and right lung between breathing room air and 100% $O_2$ from microsphere data

| | | LLD | | RLD | |
|---|---|---|---|---|---|
| | PEEP, cm $H_2O$ | 0 | 10 | 0 | 10 |
| $\dot{Q}_R$ (%) | Left lung | 37±6 | 49±8 | 36±4 | 32±5 |
| $\dot{Q}_H$(%) | Left lung | 45±7* | 58±6* | 31±5 | 22±6* |
| $\dot{Q}_A$(%) | Left lung | 18±4† | 25±6† | 10±3† | 12±3† |
| $\dot{Q}_R$(%) | Right lung | 63±6 | 51±8 | 64±4 | 68±5 |
| $\dot{Q}_H$(%) | Right lung | 55±7* | 42±6* | 69±9 | 78±6* |
| $\dot{Q}_A$(%) | Right lung | 82±10† | 75±14† | 90±7† | 88±6† |

Values are means ± SD (n = 6). * significant difference between breathing 100% $O_2$ and room air ($P < 0.05$). † significant difference between left lung atelectasis and both lung ventilation with 100% $O_2$ ($P < 0.05$) $\dot{Q}_R$: blood flow during breathing room air (obtained from experiment in (Chapter 3). $\dot{Q}_H$: blood flow during breathing 100% $O_2$. $\dot{Q}_A$: blood flow during left lung atelectasis.

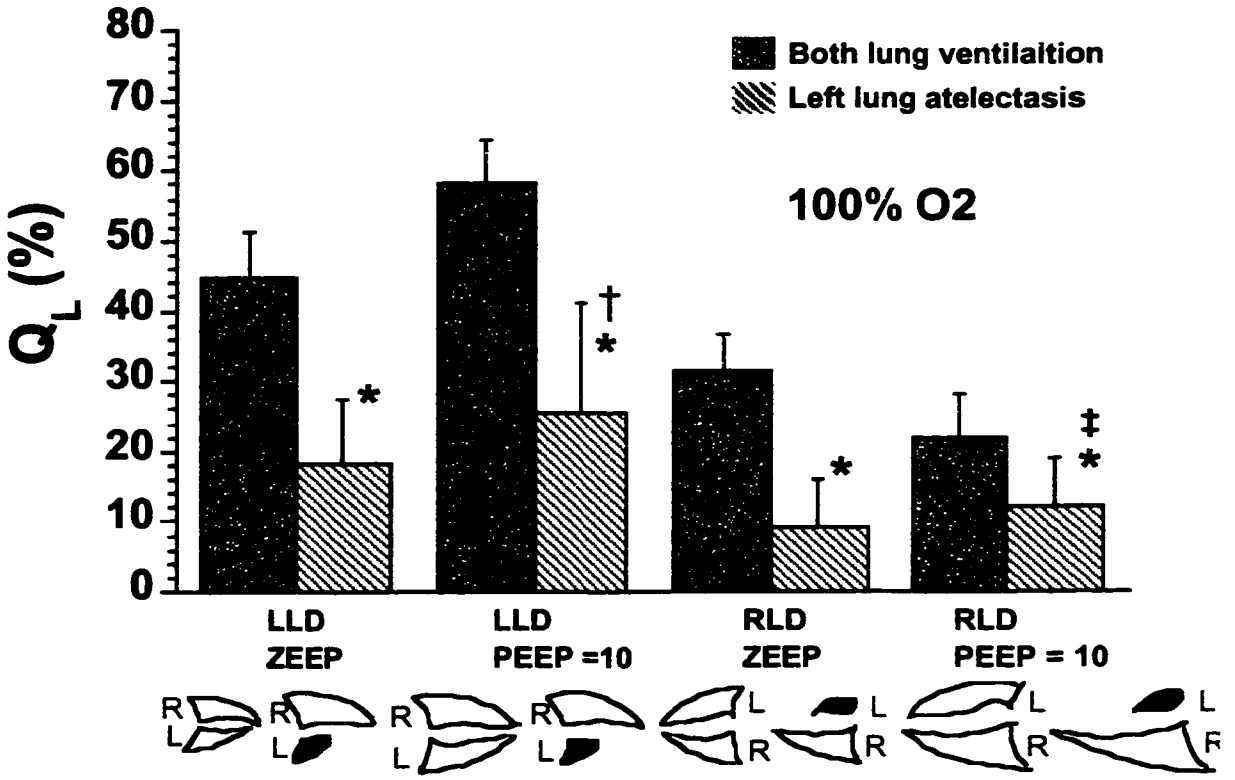


Fig 22. Effect of position and PEEP on the left lung blood flow during bilateral ventilation and left lung atelectasis. Values are mean ± SD. *P < 0.05, left atelectatic lung compared with control at the same position and PEEP condition. †P < 0.05, left atelectatic lung between 0 and 10 cm $H_2O$ PEEP. ‡P < 0.05, left atelectatic lung with 10 cm $H_2O$ PEEP between LLD and RLD posture.

*Effect of left lung atelectasis.* Left lung atelectasis produced a small but significant reduction in cardiac output. The largest effect of left lung atelectasis was to reduce $\dot{Q}$ in the left lung by 60% in the LLD posture and 45% in the RLD posture, with a simultaneous increase in $\dot{Q}$ in the right lung. This behavior occurred with and without 10 cm $H_2O$ PEEP. This reduction in flow in the left atelectatic lung was most likely due to pulmonary hypoxic vasoconstriction, since the $P\bar{v}O_2$ was was ~55 mmHg and in the absence of ventilation blood $PO_2$ did not change as blood crossed the circulation (see below). The posture-induced differences in $\dot{Q}$ caused by left lung atelectasis was attributed to changes in PVR as defined by the zonal conditions. This behavior in $\dot{Q}$ was

supported by measured changes in pulmonary vascular resistance (PVR, [Ppa-Ppcw]/$\dot{Q}$), and was consistent with the interrelationship among Ppa, Ppcw and Palv that produced changes in PVR, as discussed below.

***Pulmonary vascular pressures and airway pressure: zone 2 and zone 3.***

*Effect of gravity on* $\dot{Q}$ *and PVR.* The effect of height on PVR was used to interpret the changes in blood flow with body posture and PEEP. The effect of gravity on blood flow distribution along the height of the lung has been described in terms of the relation between Ppa, Ppv and Palv (159). By this theory, PVR depends on Ppa – Palv in zone 2 (Ppa>Palv>Ppv) and Ppa – Ppv in zone 3 (Ppa>Ppv>Palv). At a constant Palv, PVR decreases and $\dot{Q}$ increases down the height of the lung with the increase in Ppa in zone 2. When Ppv becomes greater than Palv in zone 3, PVR decreases and $\dot{Q}$ increases down the lung as a result of increased vascular recruitment and distention. In general, at constant zonal conditions PVR changes with lung volume (15). $\dot{Q}$ is greater and PVR is smaller in zone 3 than in zone 2. In the atelectatic left lung vascular resistance was assumed to depend on Ppa - Ppv (zone 3) as Palv was not involved.

*Effect of PEEP.* With both lungs ventilated with 100% $O_2$ (control), in both LLD and RLD postures, Ppa increased from 16 to 23 cm $H_2O$ with 10 cm $H_2O$ PEEP, while Ppv (Ppcw, referenced to the mid chest level) and Palv increased from 6 and 5 cm $H_2O$ to 11 and 15 cm $H_2O$ with 10 cm $H_2O$ PEEP, respectively (Table 21). Thus without PEEP, the dependent lung was in zone 3 and the nondependent was in zone 2. PEEP located part of the dependent lung in zone 2 with the nondependent lung remaining in zone 2. Since the changes in PVR and $\dot{Q}$ are greater in zone 2 than zone 3 and $\dot{Q}$ increases and PVR decreases down the lung, the PEEP-induced greater lung regions in zone 2 produced a shift in $\dot{Q}$ from the nondependent to the dependent lung.

In the LLD posture, PEEP caused a shift of $\dot{Q}$ from the nondependent right lung (55 to 42%, Table 7) to the dependent left lung (45 to 58%). This behavior was

consistent with the PEEP-induced increase (30%) in PVR (Table 21) in the nondependent right lung in the LLD. Similarly, in the RLD posture, PEEP caused a shift of $\dot{Q}$ from the nondependent left lung (31 to 22%) to the dependent right lung (69 to 78%). This behavior was consistent with the PEEP-induced 90% increased PVR in the nondependent left lung in the RLD posture.

*Effect of left lung atelectasis and body position.* Left lung atelectasis increased Ppa and Ppv by 5 and 3 cm $H_2O$, respectively. With left lung atelectasis, Ppa increased from 21 to 28 cm $H_2O$ with 10 cm $H_2O$ PEEP in both postures, while Ppv and Palv increased from 9 and 5 cm $H_2O$ without PEEP to 12 and 16 cm $H_2O$ with 10 cm $H_2O$ PEEP.

Inversion from the LLD to the RLD posture produced a reduction in blood flow in the atelectatic lung from 18 to 10% without PEEP and from 25 to 12 % with 10 cm $H_2O$ PEEP (Table 24, Fig. 22). This behavior was consistent with a reduced PVR in the right lung positioned dependent in the RLD posture with the atelectatic lung in nondependent position.

***Lung volumes***

*Both lungs ventilation (control).* In the control lung ventilated with 100% $O_2$ with and without 10 cm $H_2O$ PEEP, FRC of the right lung was 3 fold greater than that of the left lung in the LLD posture, but was similar to left lung FRC in the RLD posture (Fig. 23, Table 22). This behavior indicated a shift in gas volume from the nondependent to the dependent lung with inversion from the LLD to the RLD posture. This effect, observed in a previous study with room air ventilation (chapter 3), was most likely due to the compression of the smaller dependent left lung by the heart and abdominal weight in the LLD posture. The foregoing fractional differences in FRC between the left and right lung in the LLD and RLD posture observed without PEEP was maintained with 10 cm $H_2O$ PEEP, in the face of a doubling of the lung volumes.

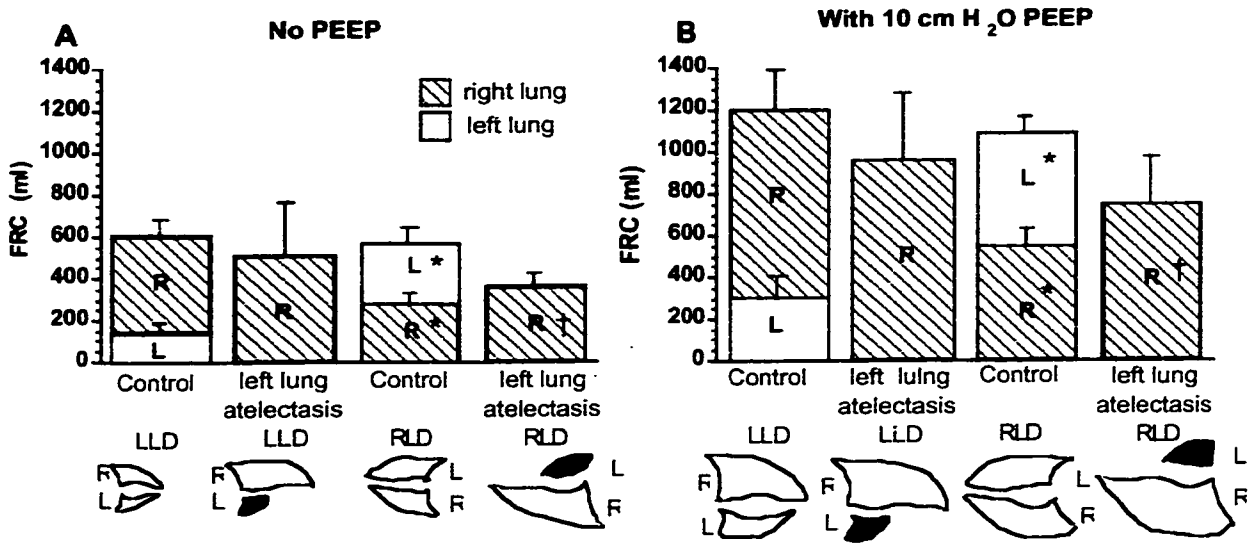


Fig 23. Left and right lung volume changes with bilateral ventilation and after left lung atelectasis with and without PEEP in both LLD and RLD postures. Values are mean ± SD (n = 6). *P < 0.05 comparison of same lung between LLD and RLD during bilateral ventilation. † P < 0.05 comparison of right lung between LLD and RLD with left lung atelectasis.

*Effect of left lung atelectasis*. Without PEEP, left lung atelectasis in the LLD posture caused an increase in FRC of the right nondependent lung compensating exactly for the atelactasis-induced gas loss from the left lung (Fig. 23). This behavior was also observed with 10 cm $H_2O$ PEEP. However, the left lung atelectasis-induced increased in FRC of the right lung in the LLD posture was reduced with inversion to the RLD posture. This behavior was most likely due to lung compression of the dependent right lung in the RLD and expansion in the LLD posture, by the weight of the atelectatic lung, heart and abdomen.

**Microspheres data**

For each animal, 1110-1562 lung pieces were processed for regional blood flow and ventilation. An average of 126 ± 46 lung pieces (9 ± 3%) with > 25% pulmonary airways and 15 ± 13 lung pieces (1±1%) with fluorescent intensity outside the range of the mean ± 4 SD were discarded. Regional blood flow and ventilation analysis was done on 90 ± 3% of the total lung pieces, consisting of 523 ± 74 pieces in the left lung and 674

± 127 pieces in the right lung. For the analysis of $V_A/\dot{Q}$ and $P_RO_2$ in the control lung and the right lung with left lung atelectasis, we discarded pieces outside the range of mean ± 3SD of ln ($\dot{V}_A/\dot{Q}$). This procedure eliminated right lung pieces (1 ± 0.3%) with deadspace (infinite or very large $\dot{V}_A/\dot{Q}$) and with shunt (very low $\dot{V}_A/\dot{Q}$).

Table 25 described the X, Y, Z coordinate distances of the center of mass of left, right and whole lung, referenced to the original coordinate axes (Xo, Yo, Zo) oriented at the edges of the lung during whole lung and right lung ventilation. PEEP increased lung volume and the distances between the center of mass and original coordinate axes. The increase in distance with PEEP was greatest (~ 60 %) in the left lung in the LLD posture and least (~10%) in the RLD posture. Left lung atelectasis did not change the PEEP-induced change in distance between the center of mass and original coordinate.

Table 25. x, y, z coordinate distances between center of mass and original coordinate system at caudal edge ($z_0 = 0$), left edge ($x_0 = 0$), dorsal edge ($y_0 = 0$) of the lung

| | | LLD | | ΔL (%) | RLD | | ΔL (%) |
|---|---|---|---|---|---|---|---|
| PEEP,cm $H_2O$ | | 0 | 10 | | 0 | 10 | |
| Whole lung | X | 6.1±0.2 | 9.5±0.5 | 56 | 8.0±0.4 | 9.9±0.5 | 24 |
| | Y | 6.6±0.8 | 8.7±1.1 | 32 | 6.7±0.9 | 8.9±1.1 | 33 |
| | Z | 11.7±0.9 | 13.9±1.1 | 19 | 11.8±0.9 | 13.9±1.1 | 18 |
| Right lung | X | 8.4±0.3 | 12.8±0.6 | 52 | 5.2±0.2 | 6.6±0.4 | 27 |
| | Y | 7.3±0.8 | 9.1±0.9 | 25 | 6.6±0.7 | 9.1±0.9 | 38 |
| | Z | 12.2±0.4 | 13.8±1.0 | 13 | 11±0.8 | 13.8±1.0 | 25 |
| Left lung | X | 3.2±0.2 | 5.3±0.5 | 66 | 11.8±0.5 | 14.1±0.7 | 20 |
| | Y | 5.7±1.0 | 8.2±1.5 | 44 | 6.8±1.2 | 8.2±0.5 | 21 |
| | Z | 10.9±1.0 | 14.1±1.2 | 29 | 12.8±1.1 | 14.1±1.2 | 10 |
| Right lung atelectasis | X | 13.4±1.2 | 14.0±1.6 | 4 | 6.3±0.6 | 6.7±0.3 | 6 |
| | Y | 8.8±1.1 | 9.1±0.9 | 3 | 8.5±1.2 | 9.1±0.9 | 7 |
| | Z | 13.3±1.3 | 13.8±1.0 | 4 | 13.0±1.4 | 13.8±1.0 | 6 |
| Left lung atelectasis | X | 2.8±0.4 | 2.9±0.6 | 4 | 16.0±0.9 | 16.9±0.9 | 6 |
| | Y | 4.0±0.5 | 4.1±0.7 | 3 | 3.9±0.6 | 4.1±0.6 | 5 |
| | Z | 6.9±1.3 | 7.6±1.3 | 10 | 6.7±1.1 | 6.8±1.1 | 2 |

**Spatial gradients in $\dot{Q}$, $\dot{V}_A$, $\dot{V}_A/\dot{Q}$ and $P_RO_2$**

An important finding in the analysis of $\dot{Q}$ and $\dot{V}_A$ using multiple linear regression analysis in the present study using 100% $O_2$ ventilation was the relatively high degree of spatial correlation as measured by the coefficient $R^2$. Values for $R^2$ averaged 0.67 ± 19, 0.59 ± 19 and 0.58 ± 17 for the whole lung, left lung and right lung, respectively. These values were substantially greater than those (~0.4) obtained with room air ventilation (Chapter 3), indicating that ventilation with 100% $O_2$ served to reduced the spatial nonuniformity in regional blood flow observed with room air ventilation (see Discussion). The high degree of spatial correlation justified the use of the full multiple linear regression analysis and indicated that blood flow variation due to inter-regional heterogeneity was less than that caused by spatial gradients.

**Spatial gradient in $\dot{Q}$: whole lung ventilation with 100% $O_2$.**

A significant negative (gravity dependent) vertical gradient (coefficient a, -0.45 and –0.66 $\dot{Q}\cdot ml^{-1}\cdot cm^{-1}$ height) in regional blood flow occurred in the whole lung in both LLD and RLD postures (Fig. 24, Table 26). The vertical gradient of $\dot{Q}$ in the whole lung in LLD (-0.45) was less than that in RLD (-0.66) indicated that the dependent lung in the LLD posture had less blood flow than the dependent lung in the RLD posture (Table 24). PEEP diminished the vertical gradient of $\dot{Q}$ in both LLD (-0.16) and RLD (-0.27) postures. Total blood flow was lower (45%) in the dependent lung than in the nondependent lung in the LLD posture (Table 24). In contrast, inversion from the LLD to the RLD posture increased blood flow in the dependent lung (from 45 to 69%). PEEP increased blood flow of the dependent lung (58%) in the LLD posture. The reduced vertical gradient of $\dot{Q}$ with PEEP was associated with a reduced (50%) mean regional blood flow (intercept) in both postures.

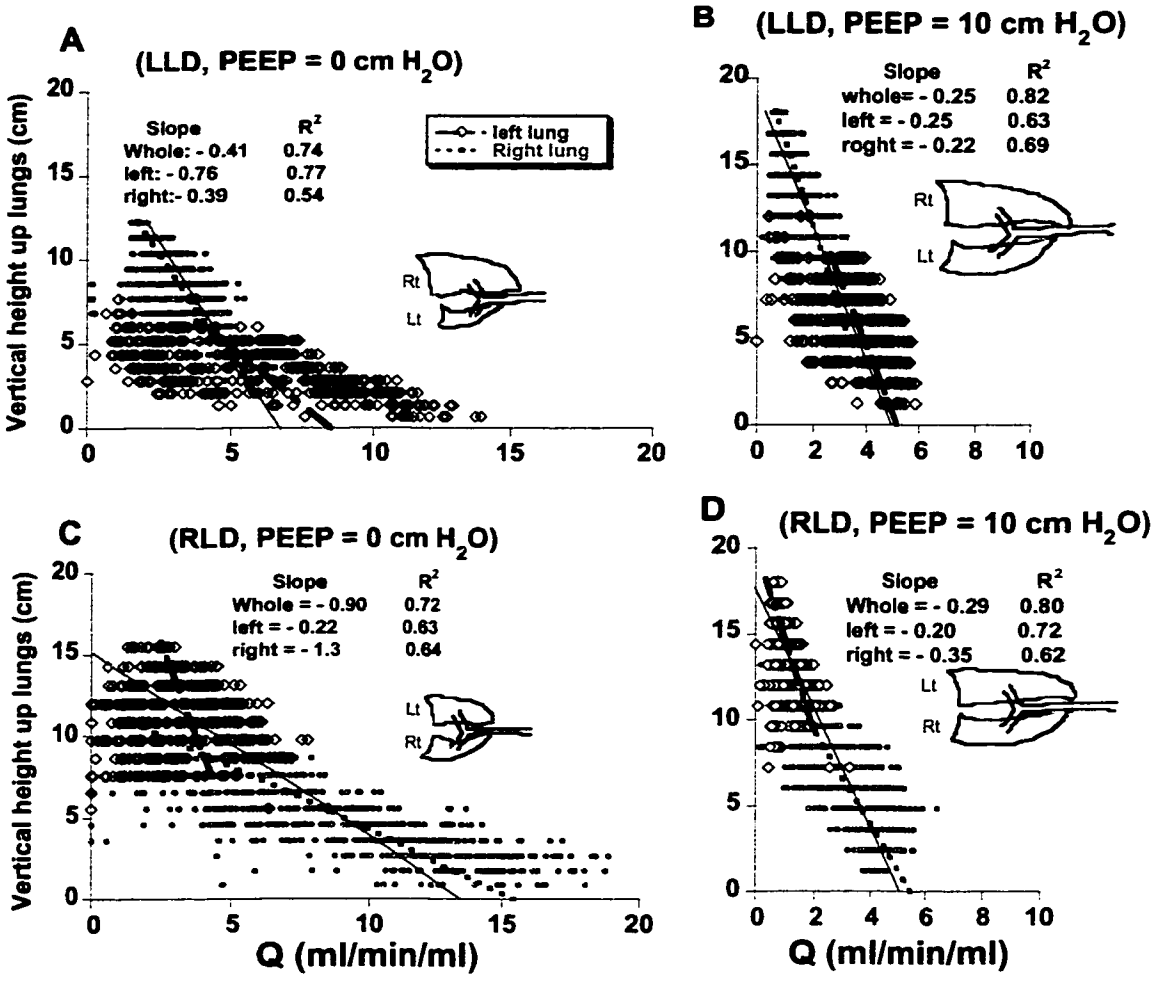


Fig 24. Blood flow per unit regional lung volume (ml. $min^{-1}$. $ml^{-1}$) vs. lung height for a representative dog, in the LLD (posture) without PEEP (A), LLD with 10 cm $H_20$ PEEP (B), RLD posture without PEEP (C) and RLD with 10 cm $H_2O$ PEEP (D). R represents right lung (open points), L the left lung (solid points) and N, the number of lung pieces. The lines represent best-fit values from multiple linear regression analysis at center of mass. $R^2$ indicated that ~70% of the variability in blood flow was spatially determined.

The vertical gradient in $\dot{Q}$ observed in the LLD posture occurred in conjunction with significant but relatively small dorsal-ventral (coefficient b,-0.15) and caudal-cranial (-0.21) gradients. These gradients were either reduced or eliminated with PEEP. The negative dorsal-ventral gradient in $\dot{Q}$ indicated a greater blood flow in the dorsal regions, opposite to the behavior observed with room air ventilation (Chapter 3).

TABLE 26. Coefficients and $R^2$ of multiple linear regression equation† fit to $\dot{Q}$ data for whole, left and right lung, respectively

| lung | Position | PEEP | Intercept | a | b | c | d | e | f | g | $R^2$ |
|---|---|---|---|---|---|---|---|---|---|---|---|
| | LLD | 0 | 5.1 | **-0.45** | **-0.15** | **-0.21** | 0.01 | -0.02 | **0.07** | 0.003 | 0.64 |
| Whole | | | ±0.6 | **±0.36*** | **±0.11*** | **±0.14*** | ±0.03 | ±0.03 | **±0.05*** | ±0.004 | ±0.19 |
| | LLD | 10 | 2.9 | **-0.16** | **-0.08** | -0.10 | 0.003 | -0.01 | 0.02 | 0.001 | 0.69 |
| | | | ±2.2 | **±0.10*** | **±0.06*** | ±0.13 | ±0.008 | ±0.013 | ±0.03 | ±0.002 | ±0.18 |
| | RLD | 0 | 5.3 | **-0.66** | -0.12 | **-0.19** | **0.04** | **-0.04** | -0.005 | 0.003 | 0.70 |
| | | | ±3.3 | **±0.50*** | ±0.17 | **±0.14*** | **±0.04*** | **±0.03*** | ±0.04 | ±0.004 | ±0.19 |
| | RLD | 10 | 2.6 | **-0.27** | -0.08 | -0.04 | **0.02** | **-0.007** | -0.01 | 0.000 | 0.69 |
| | | | ±0.4 | **±0.12*** | ±0.08 | ±0.04 | **±0.01*** | **±0.005*** | ±0.01 | ±0.001 | ±0.23 |
| | LLD | 0 | 6.9 | **-1.01** | **-0.28** | **-0.40** | **0.10** | **-0.07** | 0.08 | 0.024 | 0.66 |
| Left | | | ±1.1 | **±0.74*** | **±0.16*** | **±0.35*** | **±0.08*** | **±0.03*** | ±0.11 | ±0.026 | ±0.20 |
| | LLD | 10 | 3.5 | -0.23 | **-0.14** | -0.16 | 0.011 | -0.01 | 0.02 | 0.003 | 0.62 |
| | | | ±2.1 | ±0.22 | **±0.09*** | ±0.24 | ±0.016 | ±0.01 | ±0.03 | ±0.007 | ±0.18 |
| | RLD | 0 | 3.1 | **-0.21** | -0.06 | -0.19 | -0.002 | -0.01 | **0.02** | -0.001 | 0.52 |
| | | | ±1.9 | **±0.19*** | ±0.11 | ±0.24 | ±0.03 | ±0.04 | **±0.01*** | ±0.006 | ±0.19 |
| | RLD | 10 | 1.5 | **-0.17** | -0.008 | -0.04 | -0.001 | **-0.006** | 0.001 | 0.001 | 0.59 |
| | | | ±0.6 | **±0.09*** | ±0.05 | ±0.04 | ±0.009 | **±0.003*** | ±0.007 | ±0.003 | ±0.20 |
| | LLD | 0 | 4.1 | **-0.47** | **-0.11** | **-0.07** | -0.03 | -0.03 | 0.03 | 0.001 | 0.52 |
| Right | | | ±1.3 | **±0.20*** | **±0.10*** | **±0.06*** | ±0.07 | ±0.02 | ±0.02 | ±0.006 | ±0.18 |
| | LLD | 10 | 2.4 | **-0.23** | **-0.06** | -0.04 | -0.02 | **-0.012** | 0.006 | 0.001 | 0.60 |
| | | | ±2.4 | **±0.20*** | **±0.05*** | ±0.06 | ±0.02 | **±0.011*** | ±0.007 | ±0.002 | ±0.18 |
| | RLD | 0 | 7.3 | **-0.90** | -0.21 | -0.14 | 0.08 | **-0.06** | 0.02 | 0.008 | 0.63 |
| | | | ±4.8 | **±0.68*** | ±0.25 | ±0.15 | ±0.08 | **±0.04*** | ±0.04 | ±0.011 | ±0.18 |
| | RLD | 10 | 3.4 | **-0.28** | **-0.12** | -0.01 | 0.02 | **-0.006** | **-0.008** | 0.001 | 0.53 |
| | | | ±0.9 | **±0.10*** | **±0.09*** | ±0.05 | ±0.02 | **±0.005*** | **±0.006*** | ±0.002 | ±0.19 |

Values are presented as mean ± SD (n=6), * $P < 0.05$ Compared with zero by 1-tailed unpaired t test.

† Equation: $Q = I + ax + by + cz + dxy + eyz + fzx + gxyz$. All intercepts are significant.

Both left and right lungs showed vertical, ventral-dorsal and caudal-cranial gradients in $\dot{Q}$ of the LLD and RLD postures with and without PEEP similar to those observed for the whole lung.

*Regional variations in spatial gradients in* $\dot{Q}$. The coefficients d, e, and f of the XY, YZ and XZ variables in the multiple linear regression equation represented the change in the spatial gradients with respect to an orthogonal coordinate. In the control lung in the LLD posture without PEEP, the vertical gradient ($\partial \dot{Q}/\partial X$) of regional blood flow increased linearly in the caudal-cranial direction (coefficient f, 0.07):

$$\partial \dot{Q}/\partial X = -0.45 + 0.07Z$$

Thus, at the mid dorsal-ventral regions (Y = 0), the vertical gradient in $\dot{Q}$ increased from the caudal region (-0.94 $\dot{Q} \cdot ml^{-1} \cdot cm^{-1}$, Z = -7 cm) to the cranial region (0.05, Z = 7 cm). This variation in the vertical gradient in the Z direction was eliminated by PEEP or by inversion to the RLD posture.

In the dependent left lung in the LLD posture, the vertical gradient in $\dot{Q}$ (coefficient a, -1.0) varied linearly in the dorsal-ventral direction (coefficient d, 0.10):

$$\partial \dot{Q}/\partial X = -1.0 + 0.10\ Y$$

At the middle caudal-cranial region (Z= 0), the vertical gradient was more negative (-1.7) in the dorsal region (Y = -7) and became more positive (-0.3) in the ventral region (Y = 7 cm). This variation in the vertical gradient in the Y direction was eliminated by PEEP or by inversion to the RLD posture.

In the dependent lung in the LLD posture, the significant dorsal-ventral gradient in $\dot{Q}$ (coefficient b, -0.28) also changed linearly with Z (coefficient e, -0.07).

$$\partial \dot{Q}/\partial Y = -0.28 - 0.07Z$$

At the mid left-right region (X = 0), the dorsal-ventral gradient was positive (+0.19) in the caudal region (Z = -7 cm) and became more negative (-0.77) in the cranial region (Z = 7 cm). This variation in the dorsal-ventral gradient in the Z direction was eliminated by PEEP or by inversion to the RLD posture.

In general, the largest nonuniformities in $\dot{Q}$ were associated with the left lung in the LLD posture. PEEP and inversion to the RLD posture eliminated these spatial uniformities. This was accomplished by shifts of flow from the dependent, dorsal and cranial regions to the nondependent, ventral and caudal regions with PEEP and from the dependent, dorsal and cranial regions in the LLD posture to dependent, ventral and caudal regions in the RLD posture, without PEEP.

**Regional distribution of $\dot{Q}$ and $\dot{V}_A$ in the right lung with left lung atelectasis.**

Without PEEP, the gradient of $\dot{Q}$ in the right lung (Fig 25) fell to about half of control in both LLD and RLD postures (Fig 24, table 27). With PEEP, the gradient of $\dot{Q}$ in the right lung fell only slightly compared to control. In summary, perfusion became more uniform after application of PEEP. After one-lung atelectasis, the open lung is even more expanded by PEEP, and perfusion was more uniform.

Aerosolized microspheres measured in the left atelectatic lung averaged $1.5 \pm 1.9$ % of that used to measure ventilation in the right lung, confirming little or no ventilation to the left atectatic lung. In one dog ventilated with 10 cm $H_2O$ PEEP, ventilation of the left atelectatic lung was 26 % of the right lung ventilation. The resulting gas exchange data were excluded from the pooled data.

Regional distribution of ventilation measured by fluorescent microspheres was limited to the right lung with left lung atelectasis. The largest vertical gradient in $\dot{V}_A$ was observed in the LLD posture (coefficient a, -0.34, Table 27) with PEEP and was accompanied by a negative dorsal-ventral gradient (coefficient b, -0.25). The vertical gradient persisted with inversion from the LLD to RLD posture (coefficient a, -0.24). Both vertical gradients in $\dot{V}_A$ in LLD and RLD postures with PEEP were absent without PEEP. In other words, position had no effect on the vertical gradient of $\dot{V}_A$ in both LLD and RLD postures. In addition, PEEP produced a significant negative dorsal-ventral gradient in $\dot{V}_A$ in the LLD posture. The only significant gradient in $\dot{V}_A$ in the LLD posture without PEEP occurred in the caudal-cranial direction (coefficient c, 0.17), and it varied linearly in the dorsal-ventral direction (coefficient e, -0.04), changing to negative

values in the ventral regions. The distribution of $\dot{V}_A$ in right lung during one-lung atelectasis was shown in fig 26 in one dog. The gradient of $\dot{V}_A$ was increased when right lung was dependent with and without PEEP. The mean $\dot{V}_A$ was decreased after addition of PEEP. This was resulted from regional ventilation normalized with larger piece volume.

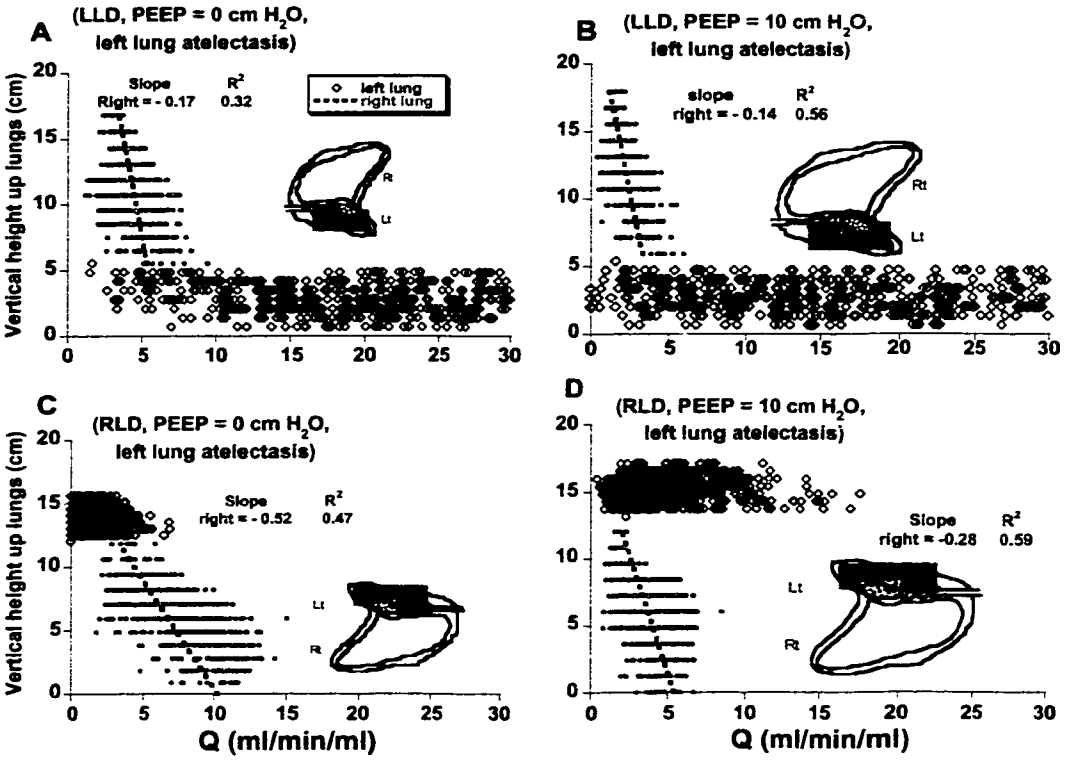


Fig 25. Blood flow per unit regional lung volume (ml. $min^{-1}$. $ml^{-1}$) vs. lung height with left lung atelectasis for a representative dog, in the LLD (posture) without PEEP (A), LLD with 10 cm $H_2O$ PEEP (B), RLD without PEEP (C) and RLD with 10 cm $H_2O$ PEEP (D). R represents right lung (open points), L the left lung (solid points) and N, the number of lung pieces. The lines represent best-fit values from multiple linear regression analysis at the center of mass.

TABLE 27. Coefficients and $R^2$ of multiple linear regression equation† fit to $\dot{Q}$ data for left lung sand and both $\dot{Q}$ and $\dot{V}_A$ for right lung, respectively during left lung atelectasis

| | Lung | position | PEEP | Intercept | a | b | c | d | e | f | g | $R^2$ |
|---|---|---|---|---|---|---|---|---|---|---|---|---|
| | | LLD | 0 | 13.4 | 0.73 | -0.34 | **-1.0** | 0.20 | -0.20 | -0.05 | 0.07 | 0.44 |
| | | | | ±7.8 | ±2.10 | ±1.62 | **±0.64*** | ±1.11 | ±0.28 | ±0.44 | ±0.16 | ±0.21 |
| $\dot{Q}$ | left | LLD | 10 | 21.0 | 0.03 | -1.88 | **-1.28** | -0.32 | -0.25 | 0.06 | 0.19 | 0.40 |
| | | | | ±7.1 | ±2.39 | ±2.25 | **±0.94*** | ±1.15 | ±0.19 | ±0.42 | ±0.27 | ±0.16 |
| | | RLD | 0 | 6.7 | -0.02 | -0.50 | -0.57 | 0.08 | 0.05 | 0.10 | -0.10 | 0.28 |
| | | | | ±5.1 | ±1.00 | ±1.32 | ±0.49 | ±0.95 | ±0.22 | ±0.31 | ±0.19 | ±0.19 |
| | | RLD | 10 | 7.6 | -0.33 | -0.91 | **-0.71** | 0.53 | 0.16 | -0.44 | -0.000 | 0.34 |
| | | | | ±4.7 | ±1.10 | ±1.70 | **±0.57*** | ±1.10 | ±0.32 | ±0.40 | ±0.14 | ±0.20 |
| | | LLD | 0 | 5.5 | -0.07 | -0.25 | -0.05 | -0.03 | **-0.024** | **0.025** | -0.002 | 0.40 |
| | | | | ±2.1 | ±0.14 | ±0.28 | ±0.07 | ±0.04 | **±0.016*** | **±0.02*** | ±0.006 | ±0.10 |
| $\dot{Q}$ | right | LLD | 10 | 2.5 | **-0.16** | **-0.08** | -0.03 | **-0.01** | **-0.01** | 0.008 | -0.000 | 0.55 |
| | | | | ±0.7 | **±0.07*** | **±0.03*** | ±0.04 | **±0.004*** | **±0.005*** | ±0.007 | ±0.001 | ±0.03 |
| | | RLD | 0 | 8.6 | **-0.54** | **-0.47** | -0.01 | 0.05 | **-0.03** | **-0.04** | 0.005 | 0.50 |
| | | | | ±2.0 | **±0.14*** | **±0.24*** | ±0.12 | ±0.07 | **±0.02*** | **±0.01*** | ±0.007 | ±0.11 |
| | | RLD | 10 | 3.6 | **-0.26** | **-0.23** | -.005 | 0.02 | **-0.007** | **-0.01** | 0.001 | 0.56 |
| | | | | ±1.0 | **±0.10*** | **±0.12*** | ±0.06 | ±0.03 | **±0.006*** | **±0.004*** | ±0.002 | ±0.13 |
| | | LLD | 0 | 8.1 | -0.19 | 0.03 | **-0.17** | 0.03 | **-0.04** | -0.01 | 0.000 | 0.27 |
| | | | | ±1.5 | ±0.26 | ±0.29 | **±0.07*** | ±0.04 | **±0.03*** | ±0.02 | ±0.005 | ±0.10 |
| $\dot{V}_A$ | right | LLD | 10 | 4.3 | **-0.34** | **-0.25** | -0.05 | -0.02 | -0.02 | 0.013 | -0.003 | 0.46 |
| | | | | ±1.0 | **±0.13*** | **±0.11*** | ±0.15 | ±0.03 | ±0.02 | ±0.019 | ±0.005 | ±0.14 |
| | | RLD | 0 | 10.9 | -0.13 | -0.02 | 0.04 | -0.03 | **-0.06** | -0.04 | 0.006 | 0.31 |
| | | | | ±2.0 | ±0.68 | ±0.39 | ±0.17 | ±0.08 | **±0.01*** | ±0.06 | ±0.01 | ±0.16 |
| | | RLD | 10 | 5.2 | **-0.24** | -0.13 | 0.04 | -0.02 | -0.01 | -0.01 | 0.001 | 0.28 |
| | | | | ±1.4 | **±0.15*** | ±0.14 | ±0.08 | ±0.03 | ±0.02 | ±0.02 | ±0.005 | ±0.22 |

Values are presented as mean ± SD (n=6), * $P < 0.05$ Compared with zero by 1-tailed unpaired t test. †
Equation: $Q = I + ax + by + cz + dxy + eyz + fzx + gxyz$. All intercepts are significant.

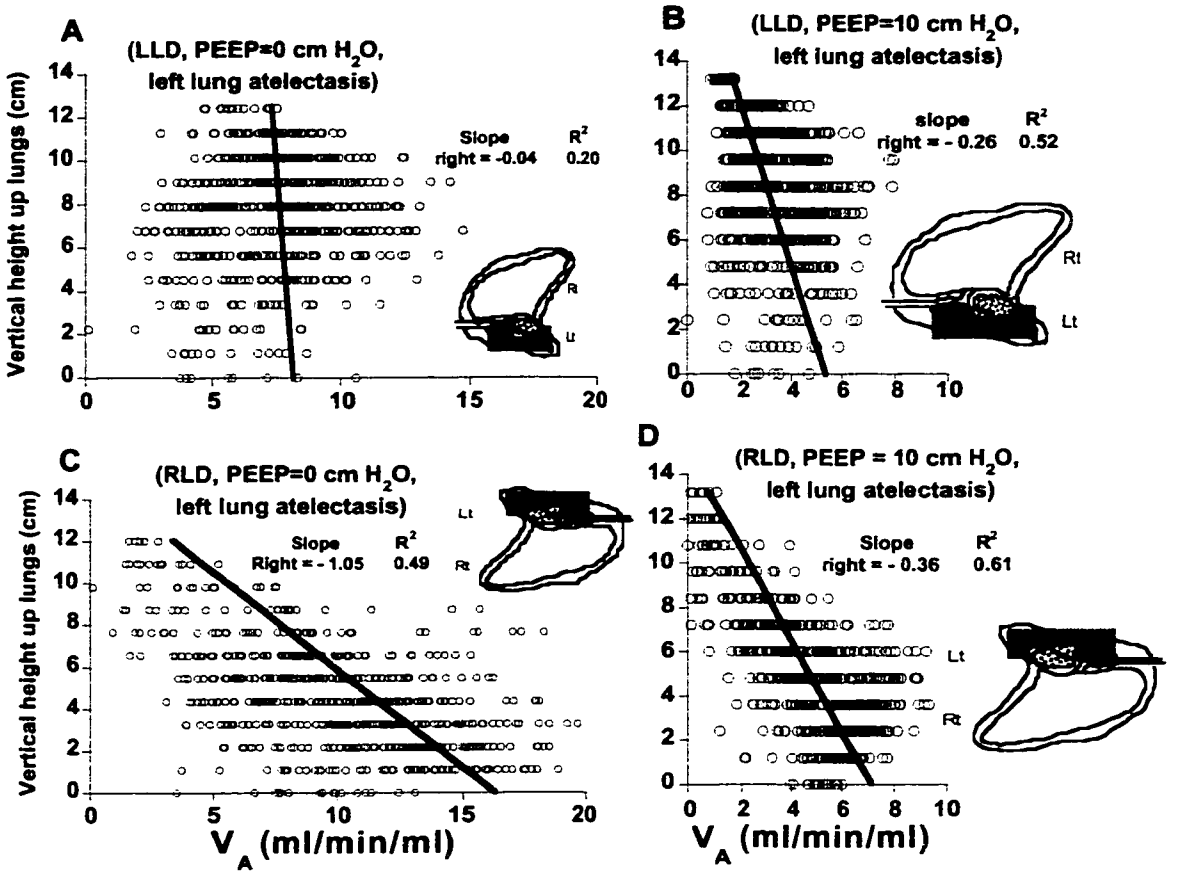


Fig 26. Ventilation per unit regional lung volume (ml· $min^{-1}$· $ml^{-1}$) of right lung with left lung atelectasis vs. lung height for the representative animal in LLD without PEEP (A), LLD with 10 cm $H_2O$ PEEP (B), RLD without PEEP (C), and RLD with 10 cm $H_2O$ PEEP. The lines represent the best-fit values at center of mass from multiple linear regression analysis.

**Regional distribution of $\dot{V}_A/\dot{Q}$ and $P_RO_2$ in the right lung with left lung atelectasis**

Consistent with the microsphere measurements of ventilation, regional variations in $\dot{V}_A/\dot{Q}$ and $P_RO_2$ were available only for the right lung with left lung atelectasis. The only significant gradient in $\dot{V}_A/\dot{Q}$ (coefficient a, -0.04) and $P_RO_2$ (-0.27) were observed in the right lung in the LLD posture with PEEP (Fig. 27 and 28, Table 28). These gradients were abolished by inversion to the RLD posture and by removing PEEP. A dorsal-ventral gradient in $\dot{V}_A/\dot{Q}$ (0.08±0.02) and $P_RO_2$ (coefficient b, 0.45±0.22)

occurred in the RLD posture without PEEP. Inversion to the LLD posture produced a similar dorsal-ventral gradient in $P_RO_2$, in conjunction with a linear variation in the vertical direction (coefficient d, 0.07), indicating a reduced gradient in the dependent regions of the left lung and an increased gradient in the nondependent region of the right lung.

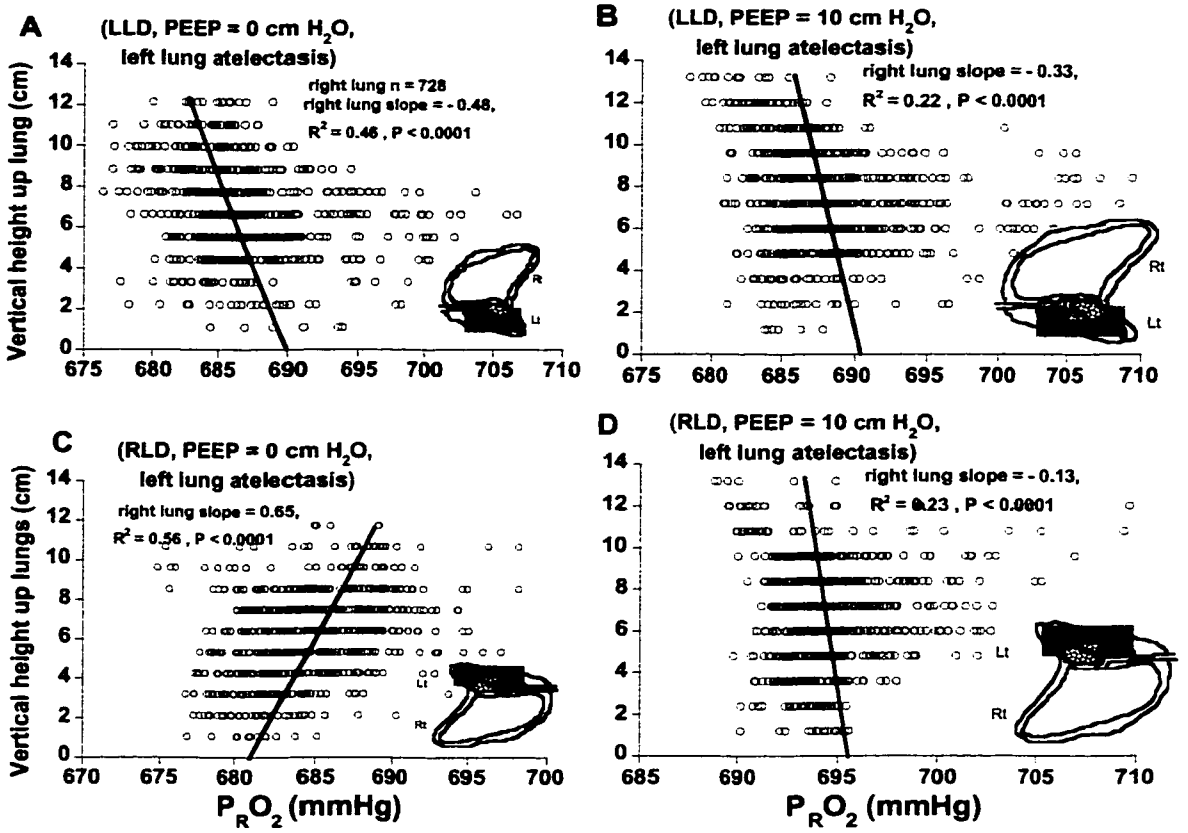


Fig 27. Regional $PO_2$ ($P_RO_2$) of the right lung during left lung atelectasis vs. lung height for the representative animal in LLD without PEEP (*A*), LLD with 10 cm $H_2O$ cm PEEP (*B*), RLD without PEEP (*C*), and RLD with 10 cm $H_2O$ PEEP (*D*). The lines represent the best-fit values from multiple linear regression analysis.

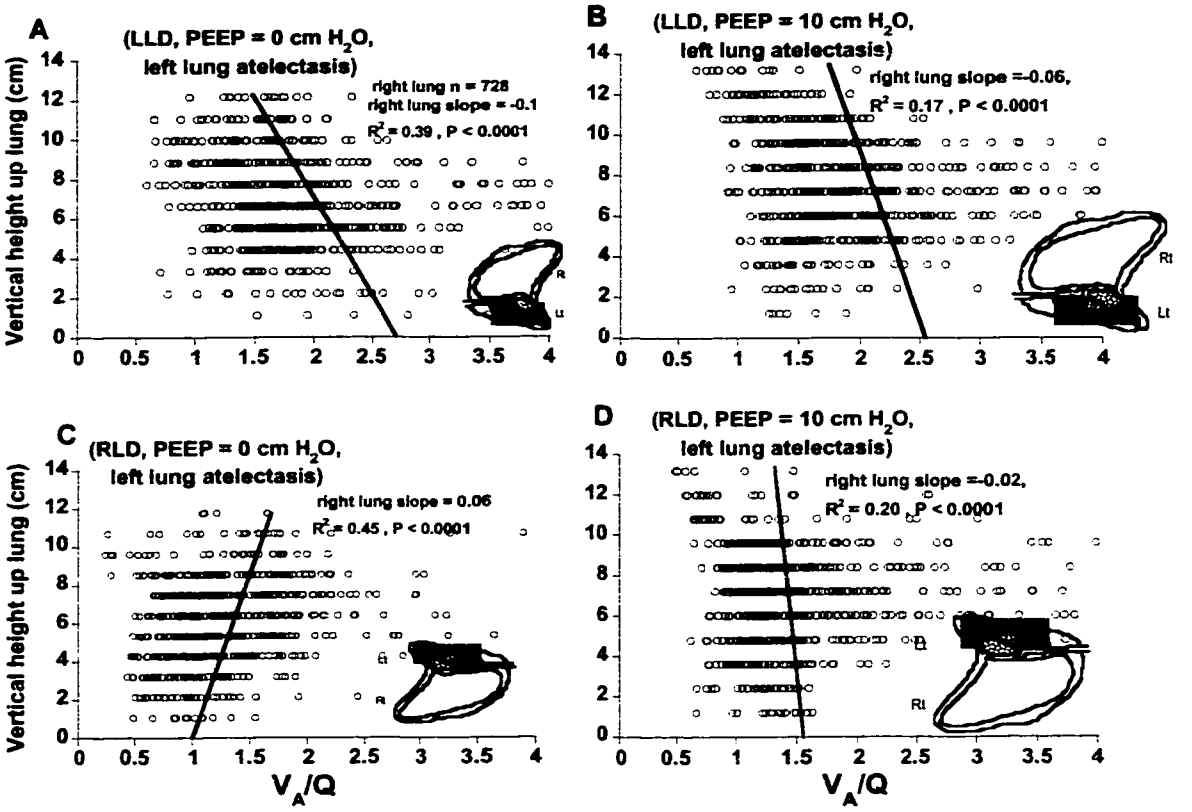


Fig 28. $\dot{V}_A/\dot{Q}$ vs. lung height of the right lung with left lung atelectasis for the representative animal in LLD without PEEP (*A*), LLD with 10 cm $H_2O$ PEEP (*B*), RLD without PEEP (*C*) and RLD with 10 cm $H_2O$ PEEP (*D*). The lines represent the best-fit values at the center of mass from multiple linear regression analysis.

### $\dot{V}_A$ and $\dot{Q}$ matching in the right lung after left lung atelectasis

Despite considerable $\dot{V}_A$ and $\dot{Q}$ heterogeneity, $\dot{V}_A$ and $\dot{Q}$ were still matched in the ventilated lung in both LLD and RLD postures (Fig 29). Addition of PEEP did not alter $\dot{V}_A$ and $\dot{Q}$ matching. As shown in fig 8, $\dot{V}_A/\dot{Q}$ was centered around $\dot{V}_A/\dot{Q} = 2$ in LLD, but between 1 and 2 in RLD. The probable cause was that total $\dot{Q}$ to the ventilated lung was increased in RLD, because the redistribution of blood flow during left lung atelectasis. The coefficient of correlation (R) between $\dot{V}_A$ and $\dot{Q}$ in the right lung during left lung atelectasis were no different between LLD and RLD with and without PEEP (Table 8).

TABLE 28. Coefficients and $R^2$ of multiple linear regression equation† fit to $P_{RO_2}$ and $\dot{V}_A / \dot{Q}$ data for right lung during left lung atelectasis

| | Lung | position | PEEP | Intercept | a | b | c | d | e | f | g | $R^2$ |
|---|---|---|---|---|---|---|---|---|---|---|---|---|
| | | LLD | 0 | 3.6 | -0.13 | 0.23 | -0.06 | -0.01 | -0.01 | -0.02 | -0.001 | 0.35 |
| | | | | ±4.4 | ±0.32 | ±0.33 | ±0.07 | ±0.06 | ±0.03 | ±0.02 | ±0.003 | ±0.17 |
| $\dot{V}_A / \dot{Q}$ | right | LLD | 10 | 1.8 | **-0.04** | -0.05 | -0.004 | -0.01 | 0.003 | -0.003 | -0.001 | 0.25 |
| | | | | ±0.5 | **±0.03*** | ±0.05 | ±0.03 | ±0.007 | ±0.009 | ±0.01 | ±0.001 | ±0.09 |
| | | RLD | 0 | 1.4 | 0.07 | **0.08** | 0.000 | 0.00 | -0.004 | 0.001 | 0.0004 | 0.36 |
| | | | | ±0.1 | ±0.10 | **±0.02*** | ±0.02 | ±0.02 | ±0.004 | ±0.008 | ±0.002 | ±0.11 |
| | | RLD | 10 | 1.4 | 0.06 | 0.08 | -0.001 | **-0.01** | 0.004 | 0.004 | -0.0002 | 0.34 |
| | | | | ±0.3 | ±0.11 | ±0.08 | ±0.03 | **±0.009*** | ±0.008 | ±0.005 | ±0.001 | ±0.20 |
| | | LLD | 0 | 684 | -0.08 | **0.47** | -0.15 | **0.07** | -0.02 | **-0.06** | 0.0002 | 0.38 |
| | | | | ±14 | ±0.44 | **±0.23*** | ±0.18 | **±0.05*** | ±0.03 | **±0.05*** | ±0.01 | ±0.20 |
| $P_{RO_2}$ | right | LLD | 10 | 678 | **-0.27** | -0.29 | -0.04 | -0.01 | 0.01 | -0.02 | -0.003 | 0.29 |
| | | | | ±8 | **±0.17*** | ±0.27 | ±0.18 | ±0.05 | ±0.04 | ±0.05 | ±0.01 | ±0.09 |
| | | RLD | 0 | 680 | 0.52 | **0.45** | 0.02 | -0.03 | **-0.03** | 0.01 | 0.001 | 0.43 |
| | | | | ±4 | ±0.65 | **±0.22*** | ±0.11 | ±0.1 | **±0.02*** | ±0.06 | ±0.01 | ±0.13 |

* $P < 0.05$ Compared with zero by 1-tailed unpaired t test. † Equation: $P_{RO_2} = I + ax + by + cz + dxy + eyz + fzx + gxyz$. All intercepts are significant.

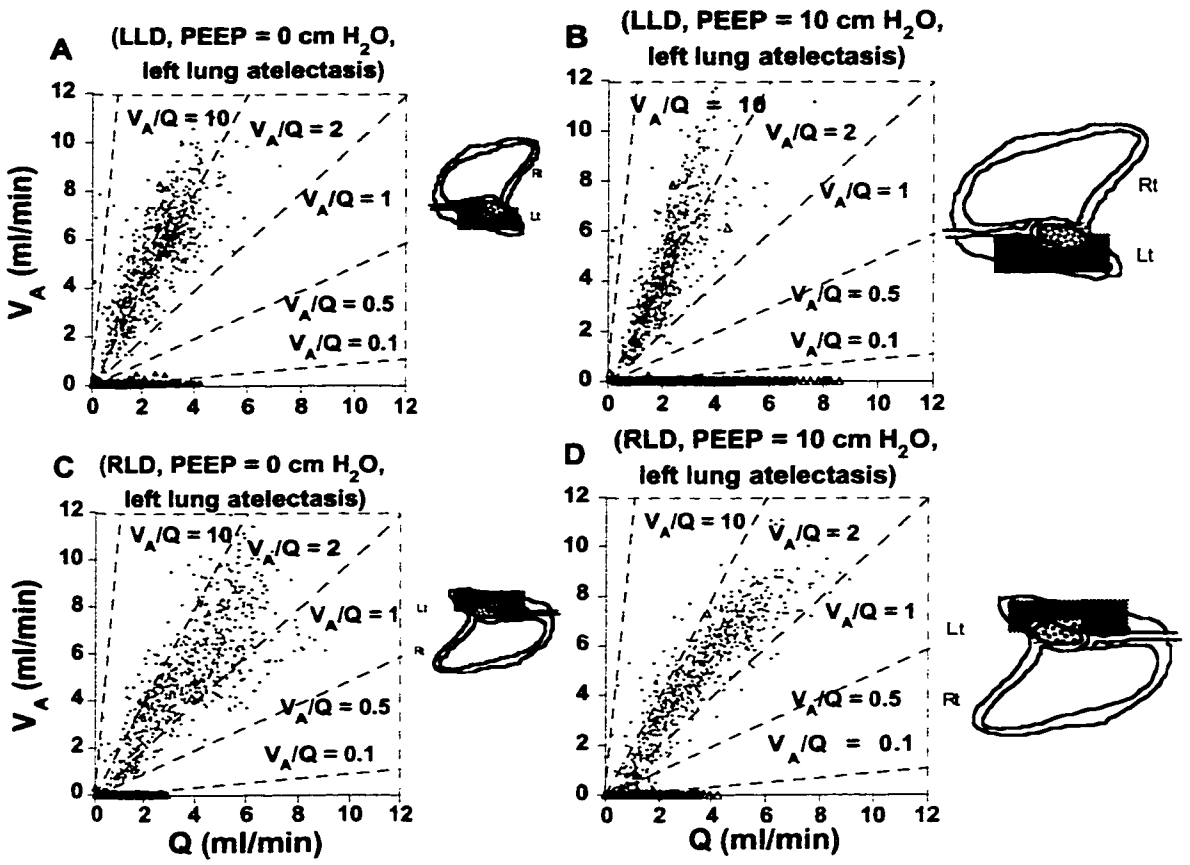


Fig 29. Scattergram of regional ventilation plot against regional perfusion for a representative animal in LLD and RLD with and without PEEP during left lung atelectasis.

## Discussion

### Methodological issues

On isolation from the chest cavity, the atelectatic left lung showed no visual evidence of edema and was easily expanded by ventilation with 5 cm $H_2O$ PEEP and by inflation to TLC with 25 cm $H_2O$ inflation pressure. Cardiac output was maintained nearly constant by administering normal saline intravenously during the experiment. This was done to eliminate the cardiac output-induced effects on regional blood flow distribution. The accurate measurement of total ventilation to the ventilated right lung by

the fluorescent microspheres with the absence of ventilation to the atelectatic left lung depended on the complete isolation of the two lungs by the double lumen intubation. Aerosolized microspheres administered to the right lung and detected in the atelectatic lung was only substantial (> 5% of total) in the RLD posture with 10 cm $H_2O$ PEEP in one animal. These data were not included in any of the pooled data.

The use of 100% $O_2$ ventilation to the right lung with left lung atelectasis allowed the evaluation of the shift of $\dot{Q}$ to the right lung caused by changes in vascular pressure (zonal conditions) and distortion of the right lung by the weight of the atelectatic lung, independent of the effects of pulmonary hypoxic vasoconstriction.

The atelectatic lung was gas free and had a density of 1 $g \cdot ml^{-1}$. Like the abdominal contents the atelectatic lung has a low shear modulus (43) and is incompressible. The distortion due to the heart and abdominal weight on the atelectatic lung is unknown and we assumed that it is isotropically expanded. Because it is incompressible and cannot change volume, a nonuniform distortion cannot affect blood flow. Thus the change in blood flow with position and PEEP must be due to changes in zonal conditions.

*The fluorescent microsphere technique.* The fluorescent microsphere technique produced high-resolution maps of $\dot{Q}$ and $\dot{V}_A$ distributions within 1.7 ml volume pieces of lung dried after inflation to TLC (47; 132). The location of these lung pieces within the lung was adjusted to values appropriate for FRC and corrected for the vertical Ptp gradient. In the atelectatic lung, no correction for a vertical Ptp gradient was done because the atelectatic lung was gas free and had a volume below that of RV and it volume consisted of tissue and blood and was incompressible.

***Volume adjustment to FRC and for vertical Ptp gradient during bilateral ventilation.*** Both injected and aerosolized microspheres were delivered in vivo near FRC, while the fluorescent signal was read in vitro in dried lung piece inflated to TLC. Therefore, several corrections were made to express the regional ventilation and perfusion as $\dot{Q}$ and $\dot{V}_A$ per unit regional volume at FRC. As in a previous study (Chapter 3) for the control ventilation of both lung, the dimensions of the lung was reduced along

each axis according to the previous measurements of the borders of the lung at FRC and TLC (56). This produced an anisotropic lung expansion at FRC and a constant (homogeneous) deformation in each coordinate. Next, we distorted the vertical dimension of each lung cube to account for the vertical Ptp gradient measured in the dog in the lateral decubitus posture (1). This distortion to the X-dimension of the cubes at each vertical height was applied to the Y- and Z-dimensions of the cubes. This adjustment preserved the homogeneous deformation in the Y and Z coordinates and produced top-to-bottom changes in regional lung volume identical to that based on the PV curve. The changes in regional lung volume imposed by the vertical Ptp gradient resulted in a 3 fold top-to-bottom increase in lung density and 3 fold top-to-bottom increase in $\dot{Q}$ and $\dot{V}_A$ per unit regional lung volume.

***Volume adjustment to FRC and for vertical Ptp gradient with left lung atelectasis.*** In the absence of reported data, we assumed that the atelectatic lung was isotropically expanded and each spatial dimension was reduced equally from TLC to FRC. The volume of the atelectatic lung was the sum of the tissue and blood. The blood volume was based on the cardiac output and transit time across a normally expanded lung. Transit time in the atelectatic lung might be greater than that of the normally expanded lung since transit time increases as flow decreases (154). Thus we may have underestimated the blood volume and lung volume of the atelectatic lung. We included the blood volume in the estimate of lung volume in the atelectatic lung. We did not include the blood volume in the correction for regional volume (eq. 6) in the normalization for $\dot{Q}$ and $\dot{V}_A$. This was justified because we used the dried tissue mass from a blood-free lung to calculate regional volume. The lung density based on blood-free lung was appropriate to the dried tissue mass without blood.

In addition to wet tissue mass, blood volume varied with posture and PEEP in the left atelectatic lung and represented a major part of the atelectatic lung volume.

**Effect of posture on lung volume**

FRC of the dependent lung was smaller than that of the nondependent lung in the LLD posture, but equal in the RLD posture after correcting for the smaller weight of the

left lung, a behavior consistent with previous results in the anesthetized dog ventilated with air (Chapter 3) and in anesthetized humans (129; 130). This behavior indicated that lung compression due to heart and abdominal weight in conjunction with the vertical Ptp gradient was greater on the smaller dependent left lung in the LLD posture than on the dependent right lung in the RLD posture.

The application of 10 cm $H_2O$ PEEP doubled the FRC of both left and right lung but maintained the left-right differences in FRC observed without PEEP, consistent with results in anesthetized humans in the lateral posture (130). This behavior in conjunction with the elimination of the vertical Ptp gradient with PEEP (2) suggests that nonuniform lung distortion independent of the vertical Ptp gradient was involved, and this occurred in spite of the PEEP-induced stiffer lung (130; 135). A role for the abdomen with a passive diaphragm has been implicated (40). Studies of lung deformation using finite element models have implicated the weight of the lung (160), the heart (12) and abdomen (43) as a contributor to the vertical Ptp gradient. Similar effects in the lateral decubitis posture need to be evaluated.

**Effect of left lung atelectasis and posture on the right lung volume**

FRC of either the left or right lung was reduced with inversion from the nondependent to dependent position. A similar effect occurred in the right lung with left lung atelectasis. With left lung atelectasis, the right lung expanded to fill the space in the thoracic cavity previously occupied by the expanded left lung, the result of a reduced pleural pressure (27). Right lung expansion was reduced with the lung positioned dependent because of compression by the weight of the atelectatic left lung, heart and abdomen. This behavior observed with unilateral atelectasis was similar to that which occurred in left lung pneumonectomized rabbits studied in the LLD and RLD postures (117) and in the pneumonectomized dogs (80).

**The effect of PEEP, left lung atelectasis and posture on blood flow and pulmonary vascular resistance**

*Effect of PEEP on PVR.* That PEEP caused a shift of blood flow from the nondependent lung to the dependent lung in the LLD and RLD posture in the control lung

ventilated with 100% $O_2$ is in line with previous studies in dogs (56; 127) and humans (93; 130). The major effect of PEEP on the blood flow distribution in the absence of hypoxic vasoconstriction was attributed to the increased vascular resistance in the nondependent regions relative to dependent regions.

*Effect of left lung atelectasis on* $\dot{Q}$ *and PVR.* Previous studies (18; 45; 107; 111; 121) have demonstrated that the diversion in blood flow from a lung made atelectatic was caused primarily by the increased vascular resistance due to hypoxic pulmonary vasoconstriction (HPV). That HPV was involved was supported by our experimental results.

First, in the absence of ventilation, the blood flowing through the atelectatic lung maintained a $P_RO_2$ equal to $P\bar{v}O_2$ (60 mmHg) that was below the level (100 mmHg) needed to trigger a HPV response (34). The absence of ventilation to the atelectatic lung was indicated by the absence of aerosolized microspheres in the atelectatic lung and confirmed by the blood flow to the atelectatic lung detected as shunt by the MIGET data for the whole lung.

Second, studies of hypoxia to one lung indicated a shift (40%) of blood flow from the hypoxic lung to the other lung (102; 103) and an increase in perfusion pressure of 30%. This shift in blood flow was somewhat less that the 60% observed with left lung atelectasis. The greater reduction in blood flow caused by left lung atelectasis might be related to the dynamic response of the hypoxic vasoconstriction response (35; 147) or the lung nonuniform distortion caused by lung atelectasis per se and by the weight of the mediastinal contents and the abdomen in the intact chest.

*Effect of posture on* $\dot{Q}$ *and PVR to atelectatic left lung.* Blood flow to the dependent atelectatic left lung was reduced by half when it was positioned nondependent. This reduced blood flow to the atelectatic lung was consistent with increased vascular resistance and zone 2 conditions in the nondependent position. By contrast, the greater blood flow to the atelectatic lung in the dependent than in the nondependent position was opposite to that expected from the greater nonuniform lung distortion in the dependent position. Accordingly, the differences in blood flow to the atelectatic lung between the

LLD and RLD posture was primarily due to changes in the zonal conditions. The contribution of lung distortion to the reduction of blood flow to an atelectatic lung has been invoked in previous studies (25; 112; 126; 144) and its importance needs to be evaluated.

*Effect of PEEP on* $\dot{Q}$ *and HPV in the atelectatic lung.* With PEEP applied to the right lung ventilated with 100% $O_2$, blood flow (7%) shifted from the right lung to the atelectatic left lung in the LLD posture but not in the RLD posture. The reduced flow to the right lung with inversion from the RLD to LLD posture with PEEP was consistent with the fact that the nondependent right lung is positioned lower relative to the mid chest level. The latter was exacerbated by the smaller FRC of the right lung in the RLD posture due to compression by the nondependent atelectatic lung and mediastinal contents. These effects on flow to the right lung were greater than any increase in HPV in the dependent atelectatic lung caused by the reduction of $P\bar{v}O_2$ with PEEP (from 57 to 46 mmHg). A similar inhibitory effect on the increased HPV response with PEEP has been reported in open chest dogs (33).

Without PEEP, PVR to the whole lung ventilated with 100% $O_2$ increased with left lung atelectasis due to increased Ppa and Pcwp with cardiac output remaining constant. Similarly, with left lung atelectasis, PEEP increased PVR. This effect of PEEP with left lung atelectasis was similar to the results in dogs ventilated bilaterally with 40% $O_2$ (96) or with 100% $O_2$ (33). In the latter studies PEEP had no inhibitory effect on the hypoxia-induced increase in PVR. Therefore, the effect of lung atelectasis and PEEP on pulmonary vascular resistance was additive.

**Regional distribution of perfusion**

*Effect of gravity.* Similar to previous studies in humans (7; 82; 93) and in dogs (56; 127), gravity dependent (negative) vertical gradients were observed in the whole lung and in both left and right lungs in both LLD and RLD postures. These vertical gradients occurred in conjunction with relatively smaller dorsal-ventral and caudal-cranial gradients. According to gravitational zone theory, the vertical gradient of $\dot{Q}$ in the upper

lung was greater than that in lower lung (gradient of $\dot{Q}$ in zone 2 was greater in zone 3) (Fig 30, line a). After addition of PEEP, the lung volume was increased and the gradient of $\dot{Q}$ in upper lung should be much less than that in lower lung (Fig 30, line c). However, our finding demonstrated that gradient of $\dot{Q}$ in upper lung was less than that in lower lung (Fig 30, line b). Moreover, the gradient of $\dot{Q}$ in both lungs was close after addition of PEEP (Fig 30, line d). This finding was also seen in weight normalized blood flow analysis before data correction based on observed pleural pressure gradient. We did not have good explanation for this unique finding. This might result from different observation from high and low-resolution technique or use of 100% $O_2$ which eliminates the hypoxic pulmonary vasoconstriction in the dependent lung. Further study was needed to elucidate the mechanism regarding where this unique finding deviated from gravitational zone model prediction.

*Vertical gradients with left lung atelectasis.* The vertical gradient of $\dot{Q}$ in the right lung was significantly reduced with left lung atelectasis. This behavior was caused by the increased right lung volume that eliminated the vertical gradient in Ptp and regional lung volume, similar to the effects observed with PEEP applied to the normal lung without atelectasis. Moreover, the vertical gradient of $\dot{Q}$ in the right lung with left lung atelectasis was greater in the nondependent position than in the dependent position, a reflection of the greater fraction of the right lung in zone 3 in the dependent position.

*Nongravitational gradients.* In the present study in both the LLD and RLD posture, a negative dorsal-ventral gradient of $\dot{Q}$ was observed in the left, right and whole

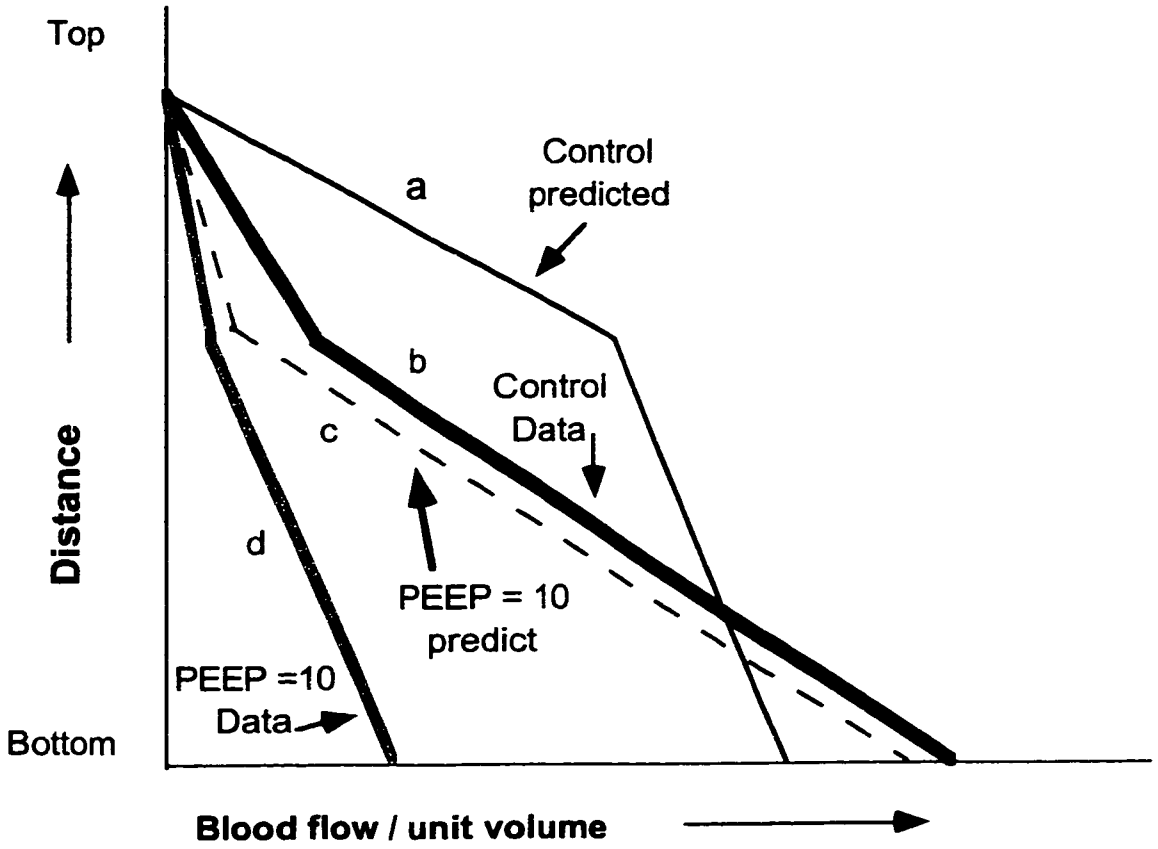


Fig 30. Schematic diagram illustrating the gravitational zone model predicted and regional blood flow distribution in upper and lower lung compared with $\dot{Q}$ measured in this present study. A. predicted $\dot{Q}$ without PEEP. b, measured $\dot{Q}$ without PEEP; c ,predicted $\dot{Q}$ with 10 cm $H_2O$ PEEP; d, measured $\dot{Q}$ with 10 cm $H_2O$ PEEP.

lung with 100% $O_2$ ventilation, with the dorsal regions having a greater blood flow. By contrast, with air ventilation the dorsal-ventral gradient of $\dot{Q}$ was positive, with the dorsal regions having the lower $\dot{Q}$ (Chapter 3). The positive dorsal-ventral gradient in $\dot{Q}$ was accompanied with a positive gradient in $P_RO_2$, with the dorsal regions having the lowest $P_RO_2$ (Chapter 3). This difference between air and 100% $O_2$ ventilation is consistent with HPV occurring in the dorsal regions with air ventilation that was eliminated with 100% $O_2$ ventilation, resulting in a shift of $\dot{Q}$ from ventral to dorsal regions. The greater $\dot{Q}$ in the dorsal lung regions with 100% $O_2$ ventilation was similar to the finding in isolated dog lung ventilated with 95% $O_2$ (16). In the latter study, the

greater $\dot{Q}$ in the dorsal lung region was attributed to a greater intrinsic vascular conductance.

Because of the uncertainty regarding nonuniform lung distortion in the atelectatic left lung and the assumption that lung volume was uniform, the spatial gradients measured by the regression analysis are of questionable value in the atelectatic lung.

*Effect of hyperoxia.* In a previous study (114) with room air ventilation, blood flow was lower in the dependent left lung than in the nondependent right lung in the LLD posture, opposite to the behavior expected from the effect of gravity. In Chapter 3, simultaneous measurements of regional blood flow and ventilation indicated a positive vertical gradient in regional $P_RO_2$, with the dependent lung regions having a $P_RO_2$ value low enough to invoke an hypoxic vasoconstriction response. The present experiments showed that blood flow measured with 100% $O_2$ ventilation was greater than that measured with air ventilation, supporting the conclusion that HPV was responsible for the reduced flow in the dependent lung ventilated with air. A similar conclusion was reached in studies of blood flow distribution measured using xenon-131 in supine humans breathing air and oxygen-enriched gas (122). In these studies, blood flow in the human subjects breathing air was uniform up the lung, but shifted from the nondependent to dependent lung regions while breathing 100% $O_2$. The lower blood flow to the dependent lung region while breathing air was attributed to a dependent lung closing volume above FRC, a reduced ventilation, and hypoxic vasoconstriction in the dependent lung. Breathing 100% $O_2$ abolished the hypoxic vasoconstriction, shifting flow to the dependent lung regions.

Other factors might decrease blood flow to the dependent lung region (zone 4). These include increases in vascular resistance due to a reduced lung volume arising from the vertical Ptp gradient, to nonuniform lung distortion caused by the weight of the mediastinal contents, and to the compression of extra-alveolar vessels by an increased perivascular interstitial pressure (78).

The variability in $\dot{Q}$ and $\dot{V}_A$ measured by a higher $R^2$ of the multiple linear regression fit to the data was lower with 100% $O_2$ ventilation than with air ventilation

(Chapter 3), indicating that HPV present with air ventilation contributed to a spatial variation that was reduced with 100% $O_2$ ventilation. Similar effects of 100% $O_2$ on the heterogeneity in $\dot{Q}$ were measured in anesthetized and hemodiluted dogs (84).

*Effect of PEEP.* In general with 100% $O_2$ ventilation, PEEP increased lung volume and reduced spatial nonuniformities in $\dot{Q}$ by redistributing blood flow from dependent and caudal regions to nondependent and cranial regions, confirming previous findings with air ventilation (Chapter 3). However, the PEEP-induced shift in blood flow from ventral to dorsal regions measured previously with air ventilation was reversed with 100% $O_2$ ventilation. The PEEP-induced reduction in spatial nonuniformities in $\dot{Q}$ and $\dot{V}_A$ was most striking in the dependent left lung.

**Regional distribution of ventilation in the right lung with left lung atelectasis.**

Regional ventilation measured by the aerosolized microsphere technique was observed only with left lung atelectasis in the right lung. In previous studies of the whole lung ventilated with air (hung), vertical gradients in $\dot{V}_A$ occurred in the right lung in both LLD and RLD postures. Left lung atelectasis with 100% $O_2$ ventilation reduced or abolished these gradients in the present study, similar to the effect of PEEP in the previous study. This effect of left lung atelectasis (or PEEP) was attributed to the increased right lung volume that abolished the vertical Ptp gradient.

Without PEEP in the LLD posture, a negative caudal-cranial gradient in $\dot{V}_A$ that became more negative in the dorsal-ventral direction was observed, indicating better ventilation in the caudal-dorsal regions. In the LLD posture, PEEP produced a negative vertical gradient in $\dot{V}_A$ together with a negative dorsal-ventral gradient, indicating a better ventilation in the dependent-dorsal regions. Thus, in the LLD posture, PEEP caused a shift in ventilation form the caudal to the dependent lung regions.

In the RLD posture without PEEP, the most negative dorsal-ventral gradient was observed in the caudal regions and the most negative caudal-cranial gradients were observed in the dorsal regions, indicating a better ventilation in the caudal-dorsal regions. Without PEEP, the negative vertical gradient in $\dot{V}_A$ implied better ventilation in the

dependent region. Thus in the RLD posture, PEEP caused a shift in ventilation from the caudal-dorsal to the dependent lung region. The major effect of PEEP in both postures was to shift ventilation to the dependent regions from the caudal regions.

In the absence of a vertical Ptp gradient, the foregoing gradients might be associated with lung distortion by the atelectatic left lung, heart and abdomen. Unlike awake breathing, mechanical ventilation with anesthesia caused a diaphragm shape change (40) with a caudal movement of the nondependent diaphragm resulting in an expansion of the nondependent lung. This might account for the negative caudal-cranial gradient of $\dot{V}_A$ in the nondependent right lung with left lung atelectasis in the LLD posture. In the RLD posture, the dependent right lung was compressed by the atelectatic lung, heart, and the less mobile dependent diaphragm, resulting in a reduced caudal-cranial gradient of $\dot{V}_A$.

The greater ventilation in the caudal than in cranial region of the right lung ventilated with 100% $O_2$ with left lung atelectasis was similar in behavior to that measured with the whole lung ventilated with air (Chapter 3) and opposite to the that measured in conscious humans in the lateral decubitus posture (8).

In the absence of a vertical Ptp gradient, PEEP produced negative vertical and dorsal-ventral gradients in $\dot{V}_A$ in both the LLD and RLD posture. The mechanism involved requires further study.

**Ventilation and perfusion matching**

With conventional ventilation with 100% $O_2$, $\dot{V}_A/\dot{Q}$ heterogeneity was an important factor responsible for the $O_2$ deficit as measured by A-a$DO_2$. Left lung atelectasis increased the A-a$DO_2$ because of shunt represented by the blood flow to the atelectatic lung. With left lung atelectasis, the A-a$DO_2$ in the LLD posture with 10 cm $H_2O$ PEEP was greater than that in the LLD posture without PEEP and in the RLD posture with and without PEEP. This increased A-a$DO_2$ was caused by an increased shunt as represented by the increased blood flow to the atelectatic lung. The effect of shunt on the A-a$DO_2$ was unrelated to the coefficient of correlation between $\dot{V}_A/\dot{Q}$ and

$\dot{Q}$ which remained constant with a change in posture and with PEEP (Table 28). In the right lung, $\dot{V}_A/\dot{Q}$ inequality attributed to hypoxic pulmonary vasoconstriction, a mechanism for matching perfusion to ventilation to optimize gas exchange in the normal lung (13; 108), was eliminated with the 100% $O_2$ ventilation.

**Regional distribution of $\dot{V}_A/\dot{Q}$ and $P_RO_2$ in the right lung with left lung atelectasis.**

In the right lung with left lung atelectasis, significant vertical and dorsal-ventral gradients in $\dot{V}_A/\dot{Q}$ and $P_RO_2$ were observed. These spatial gradients in $\dot{V}_A/\dot{Q}$ and $P_RO_2$ were much smaller (as % mean $\dot{V}_A/\dot{Q}$ and $P_RO_2$ values, 0.06) than values measured with air ventilation (0.9, chapter 3), indicating a reduction in $\dot{V}_A/\dot{Q}$ inequality with 100% $O_2$ ventilation.

In conclusion, in the lateral decubitis posture, ventilation of the right lung with 100% $O_2$ with the left lung atelectatic maintained adequate oxygenation by a HPV-induced shift of blood flow from the atelectatic lung to the ventilated lung. The small shift in blood flow from the atelectatic left lung positioned from the LLD to RLD posture produced no improvement in gas exchange. The application of 10 cm $H_2O$ PEEP to the nondependent right lung in the LLD posture produced an increased A-a$DO_2$ that was eliminated with inversion to the RLD posture. This might be due to the increased fraction of the right lung with reduced vascular resistance, resulting in a greater blood flow to the right lung in the RLD posture. The effects of ventilation using lower $O_2$ levels need to be evaluated.

# CHAPTER 6: GENERAL CONCLUSION

The design of the studies described in this dissertation were tailored to obtain a better understanding of mechanisms involving the distribution of regional blood flow, ventilation and gas exchange in the lateral decubitus posture. The lateral decubitus posture with unilateral lung ventilation is common practice during thoracic surgery. Gravity has long been considered to be a major determinant of regional blood flow and ventilation and has been substantiated by many human and animal studies. However, with the development of high-resolution techniques, the innate vascular and bronchus branching structure has emerged as an important additional factor governing regional blood flow and ventilation. In addition, one study (114) demonstrated that regional blood flow did not redistribute with a change from the LLD to the supine posture. These findings challenged the concept that gravity determined regional blood flow in the lateral decubitus posture.

Differential ventilation with unilateral dependent PEEP in the lateral posture has been considered to be a useful strategy to reduce shunt and improve gas exchange. However, the evidence of gas exchange improvement and reduced atelectasis obtained from data using MIGET and CT yielded no spatial information of regional perfusion, ventilation and gas exchange. Hypoxia occurred in some patients with unilateral lung atelectasis with PEEP provided to the ventilated lung. Although the redistribution of $\dot{V}_A$ and $\dot{Q}$ between the atelectatic and ventilated lung has been studied, spatial information about $\dot{V}_A$, $\dot{Q}$ and gas exchange in the ventilated lung with unilateral lung atelectasis remains unknown.

These studies are the first to use a high-resolution technique to examine the distribution of $\dot{Q}$, $\dot{V}_A$, $\dot{V}_A/\dot{Q}$ and $P_RO_2$ in the lateral decubitus posture. The high resolution in conjunction with multiple linear regression analysis allowed the spatial description of these variables at any arbitrary position relative to the 3 rectangular coordinate axes.

The major findings of the effect of lateral posture and PEEP on regional blood flow, ventilation, and gas exchange (Chapter 3) are as follows. First, the vertical gradient in $\dot{Q}$ was greater in the RLD than LLD posture. This was attributed to a reduced blood flow in the dependent left lung in the LLD posture. Second, PEEP reduced the vertical gradient in

both postures and eliminated the difference between postures. PEEP or body inversion from the LLD to the RLD posture abolished the positive vertical, dorsal-ventral and caudal-cranial gradients in $P_RO_2$ observed in the LLD posture. Third, a positive vertical gradient in $P_RO_2$ was observed in the LLD posture with the dependent dorsal-caudal regions of the dependent lung having values below that (100 mm Hg) needed to invoke a hypoxic vasoconstriction response. This behavior was consistent with the reduced blood flow to the dependent lung in the LLD posture.

The major findings of the effect of differential ventilation with unilateral dependent PEEP on the regional blood flow, ventilation, lung volume and gas exchange (Chapter 4) are listed as follows. First, with constant (35- 65%, left-right lung) differential ventilation in the LLD posture, neither unilateral PEEP (5 and 10cm $H_2O$) to the dependent lung nor bilateral PEEP improved gas exchange efficiency, as indicated by A-a$DO_2$ or $P_RO_2$. Therefore, a PEEP-induced increase in ventilation was most likely responsible for the improved gas exchange observed previously with conventional mechanical ventilation. Second, compared to the supine posture, unilateral dependent PEEP in the LLD posture did not increase $\dot{Q}$ to the dependent lung. Bilateral PEEP increased blood flow to the dependent left lung due to an increase in Pcwp locating the dependent lung deeper in zone 3. Third, FRC of the dependent lung was reduced when the animal was positioned from the supine to the LLD posture. Fourth, the PEEP-induced increase in FRC to the dependent left lung with unilateral PEEP and bilateral PEEP produced no change in the (A-a)$DO_2$. This indicated that the relatively low blood flow in the dependent left lung compared to that in the nondependent lung observed without PEEP was not caused predominantly by non-uniform lung distortion.

The effects of left lung atelectasis in the lateral posture on $\dot{Q}$, $\dot{V}_A$, lung volume and gas exchange in right lung with 100% $O_2$ with and without PEEP (Chapter 5) were as follows. First, compared to previous results with air ventilation (Chapter 3), ventilation with 100% $O_2$ increased $\dot{Q}$ to the dependent left lung in the LLD posture (control). This supported the conclusion that HPV occurred in the dependent left lung in the LLD posture with air ventilation. Second, with left lung atelectasis, HPV caused a shift of

blood flow from the atelectatic lung to the ventilated lung. Blood flow to the atelectatic left lung was greater with the left lung in the dependent position with and without PEEP. This was attributed to a lower vascular resistance in the dependent position than in the nondependent position. Third, left and right lung volume ratio was 1:3 in LLD and close to 1:1 in RLD and the ratios of FRC were not altered by the addition of PEEP. Fourth, left lung atelectasis caused a compensatory volume expansion in the right lung that was greater in the LLD than RLD posture. This was evidence that compression of the dependent right lung resulted from the weight of the atelectatic left lung, heart and abdomen in the RLD posture. Fifth, vertical, dorsal-ventral and caudal-cranial gradients in $\dot{Q}$ were observed in the right lung with left lung atelectasis in both LLD and RLD posture. PEEP reduced these gradients. Sixth, any impairment in gas exchange associated with left lung atelectasis was reduced with ventilation of the right lung with 100% $O_2$. However, PEEP increased the $O_2$ deficit (A-a$DO_2$) in the LLD posture, a result of an increased shunt measured as an increased blood flow to the atelectatic lung. Seventh, despite the heterogeneity of $\dot{Q}$ and $\dot{V}_A$, the ventilation and perfusion was still matched with and without PEEP in the right lung.

We conclude that mediastinal shift combined with individual lung volume changes and vertical vascular pressure gradients determine blood flow distribution in the lateral decubitus posture. Hypoxic pulmonary vasoconstriction occurred in the dependent lung in LLD posture due to reduced ventilation resulting from the heart and abdominal weight-induced reduction in the dependent lung volume. This phenomenon was abolished either by turning the animal from the LLD to the RLD posture or by the application of bilateral PEEP. The improvement of gas exchange during differential ventilation with unilateral dependent PEEP was mainly due to increased ventilation to the dependent lung rather than an increased dependent lung volume. Shunt was the principal contributor to impairment of gas exchange during left lung atelectasis. In addition, $\dot{V}_A$ and $\dot{Q}$ in the right lung were still well matched during left lung atelectasis. Despite spatial inequalities in $\dot{V}_A$ and $\dot{Q}$, individual lung volume change induced by mediastinal shift and hypoxic pulmonary vasoconstriction accounted for parts of regional blood flow and ventilation

variability. Factors other than gravity (innate pulmonary vascular and bronchus branching structure) also contributed to the regional blood flow and ventilation distributions.

**Advantages and limitations of multiple linear regression analysis**

*Advantages.* The rationale for exploring the spatial distributions of regional ventilation, blood flow and gas exchange is as follows. First, many studies have demonstrated that blood flow distribution was influenced by gravity in the vertical direction. In addition, lung distortion caused by the vertical pleural pressure gradient also affected the lung volume and ventilation distributions. Second, a greater regional blood flow in the dorsal lung region due to greater intrinsic vascular conductance in the supine posture has been documented. This behavior suggests a ventral-dorsal gradient in blood flow. Third, abdominal compression of the caudal lung and diaphragmatic compliance also affected regional blood flow and ventilation in the cranial-caudal direction. This behavior might produce caudal-cranial gradients. Fourth, hypoxic pulmonary vasoconstriction related to reduced regional ventilation and lung volume might affect the blood flow distribution resulting in regional differences in $\dot{V}_A/\dot{Q}$ and $P_RO_2$. Fifth, the branching structure of the pulmonary vasculature and airways might result in spatially ordered regional blood flow and ventilation distributions. The first three factors suggest that in the lateral posture, blood flow and ventilation be distributed along not only the vertical direction (left-right) but also along the ventral-dorsal and caudal-cranial directions. In addition, the appearance of heart and changing shape of diaphragm between non-dependent and dependent lung after anesthesia in the lateral decubitus posture may cause vertical gradient of $\dot{Q}$ and $\dot{V}_A$ changing in dorsal-ventral and caudal-cranial directions. Accordingly we used a multiple linear regression analysis in these three orthogonal coordinate directions to describe regional blood flow and ventilation.

In the present study, the multiple linear regression analysis detected spatial gradients of $\dot{Q}$, $\dot{V}_A$, $\dot{V}_A/\dot{Q}$ and $P_RO_2$ in the three coordinate axes and changes in the spatial gradients along orthogonal directions. By contrast in the present and previous studies the use of linear one-dimensional regression analysis often failed to detect any significant

gradients, most likely because the ignored spatial variation in the other two directions was lumped into the residual part (random variation) of the variability by the analysis.

*Test for significance.* Multiple regression analysis proved to be successful in describing spatial gradients in flow and ventilation that changed with body position and with PEEP. Spatial gradients were calculated for each animal and averaged over several animals to determine the spatial gradients that were present over the group of animals. Spatial gradients of $\dot{Q}$, $\dot{V}_A$, $\dot{V}_A/\dot{Q}$ and $P_RO_2$ for each animal are given in the Appendix. The significance of each spatial gradient of each animal was given by the regression analysis and the pooled gradients were tested for significance. This is a common method used to evaluate physiological data. The other method of pooling the data before the regression analysis might hide any inter-animal variability that is great enough to produce insignificance in the pooled data. Accordingly, the data as presented in this thesis represent a conservative estimate of variability in terms of spatial gradients. The main rationale for the study is to describe the spatial variation of $\dot{Q}$, $\dot{V}_A$ and $\dot{V}_A/\dot{Q}$ in the lateral posture. Therefore the behavior that applied for a group of animals was the primary focus. Characteristics found in one animal but not reproduced in a group of animals were of secondary importance.

*Limitations.* A limitation of the multiple linear regression analysis is its failure to describe the total heterogeneity in blood flow and ventilation, as given by the coefficient of determination ($R^2$). The multiple linear regression equation represents a best-fit average over each volume element consistent with flow that varies linearly with respect to the spatial dimensions. Any variation of flow that is not linear is lumped in the residual (non-spatial) part of the variability. The addition of higher order terms to the regression equation increases the estimate of the spatial variability ($R^2$) by fitting the variation at a smaller scale and is equivalent to averaging over a smaller volume. The size of the volume element sets the limit of spatial resolution of the variability. Accordingly, multiple linear regression always underestimates the spatial variability and overestimates the residual part of the variability. In addition, multiple linear regression can not accurately predict the regional blood flow or ventilation between individual

neighbor pieces. Instead, a gradually shifting and approximately changing of blood flow can be detected by the multiple linear regression fitting.

A better estimate of the total spatial variability is afforded by a fractal analysis in which both the total variability and the random part of the variability are calculated (49). Such an analysis requires a much smaller volume resolution than is available in the present study and is beyond the scope of this study. Fractal analysis separates the variability into an ordered part and a random part but does not specify any particular type of spatial variation. Although the fractal nature of the branching vascular tree might suggest a relationship to the fractal nature of the flow heterogeneity (49), the actual part of the flow heterogeneity that is attributed to vascular branching remains to be determined. By contrast, multiple linear regression analysis is able to describe the part of the variability associated with spatial gradients and its variation in the chosen 3-dimensional coordinate system. The spatial variability measured by $R^2$ is independent of translation and rotation of the coordinate system, even though the coefficients and their significance would change.

Although multiple linear regression analysis in the chosen coordinate system proved to be a good model for the description of blood flow in the lung in the lateral posture, it might not be optimal for other studies. For example, for a radial distribution of blood flow, a cylindrical or spherical set of coordinates might be more appropriate.

**Future directions**

All studies were performed in the anesthetized dog in the lateral posture. The findings and conclusions may not apply to humans. In addition, the correction of the regional blood flow and ventilation data measured at TLC to *in vivo* values at FRC, although reasonable, produced spatial gradients in ventilation and perfusion that require verification by measurements *in vivo*. Thus, the use of non-invasive technology such as high-resolution Xenon CT and PET would be useful particularly in humans.

On account of the complexity of the present studies, anatomical shift of the mediastinal and abdominal contents were not measured. It will be useful to examine the movement of the heart and diaphragm between the LLD and RLD posture using CT.

The present studies focused use healthy dogs rather than humans with lung disease. Spatial information of regional blood flow and ventilation in pathological conditions such as unilateral pneumonectomy and unilateral pneumothorax (pleural pressure positive in one chest cavity) will be of interest. Other studies in the lateral position might include gas exchange after lung transplantation, regional distribution of $\dot{V}_A$ and $\dot{Q}$ in patient with diaphragmatic paralysis after cervical spine injury and the optimal PEEP level and $FiO_2$ in the ventilated lung during unilateral lung atelectasis.

**REFERENCE**

1. **Agostoni E and D'Angelo E.** Comparative features of the transpulmonary pressure. *Respir Physiol* 11: 76-83, 1970.

2. **Agostoni E, D'Angelo E and Bonanni MV.** Topography of pleural surface pressure above resting volume in relaxed animals. *J Appl Physiol* 29: 297-306, 1970.

3. **Albert RK and Hubmayr RD.** The prone position eliminates compression of the lungs by the heart . *Am J Respir Crit Care Med* 161: 1660-1665, 2000.

4. **Altemeier WA, McKinney S and Glenny RW.** Fractal nature of regional ventilation distribution. *J Appl Physiol* 88: 1551-1557, 2000.

5. **Altemeier WA, Robertson HT and Glenny RW.** Pulmonary gas-exchange analysis by using simultaneous deposition of aerosolized and injected microspheres. *J Appl Physiol* 85: 2344-2351, 1998.

6. **Altemeier WA, Robertson HT, McKinney S and Glenny RW.** Pulmonary embolization causes hypoxemia by redistributing regional blood flow without changing ventilation. *J Appl Physiol* 85: 2337-2343, 1998.

7. **Amis TC, Jones HA and Hughes JM.** Effect of posture on inter-regional distribution of pulmonary perfusion and $\dot{V}_A/\dot{Q}$ ratios in man. *Respir Physiol* 56: 169-182, 1984.

8. **Amis TC, Jones HA and Hughes JM.** Effect of posture on inter-regional distribution of pulmonary ventilation in man. *Respir Physiol* 56: 145-167, 1984.

9. **Baehrendtz S and Klingstedt C.** Differential ventilation and selective PEEP during anaesthesia in the lateral decubitus posture. *Acta Anaesthesiol Scand* 28: 252-259, 1984.

10. **Baehrendtz S, Santesson J, Bindslev L, Hedenstierna G and Matell G.** Differential ventilation in acute bilateral lung disease. Influence on gas exchange and central haemodynamics. *Acta Anaesthesiol Scand* 27: 270-277, 1983.

11. **Banchero N, Schwartz PE, Tsakiris AG and Wood EH.** Pleural and esophageal pressures in the upright body position. *J Appl Physiol* 23: 228-234, 1967.

12. **Bar-Yishay E, Hyatt RE and Rodarte JR.** Effect of heart weight on distribution of lung surface pressures in vertical dogs. *J Appl Physiol* 61: 712-718, 1986.

13. **Barer GR, Howard P and Shaw JW**. Stimulus-response curves for the pulmonary vascular bed to hypoxia and hypercapnia. *J Physiol (Lond)* 211: 139-155, 1970.

14. **Bassingthwaighte JB and Ackerman FH**. Mathematical linearity of circulatory transport. *J. Appl. Physiol* 22: 879-888, 1967.

15. **Beck KC and Lai-Fook SJ**. Pulmonary blood flow vs. gas volume at various perfusion pressures in rabbit lung. *J Appl Physiol* 58: 2004-2010, 1985.

16. **Beck KC and Rehder K**. Differences in regional vascular conductances in isolated dog lungs. *J Appl Physiol* 61: 530-538, 1986.

17. **Beck KC, Vettermann J and Rehder K**. Gas exchange in dogs in the prone and supine positions. *J Appl Physiol* 72: 2292-2297, 1992.

18. **Benumof JL**. Mechanism of decreased blood flow to atelectatic lung. *J Appl Physiol* 46: 1047-1048, 1979.

19. **Benumof JL and Wahrenbrock EA**. Blunted hypoxic pulmonary vasoconstriction by increased lung vascular pressures. *J Appl Physiol* 38: 846-850, 1975.

20. **Bindslev L, Hedenstierna G, Santesson J, Gottlieb I and Carvallhas A**. Ventilation-perfusion distribution during inhalation anaesthesia. Effects of spontaneous breathing, mechanical ventilation and positive end-expiratory pressure. *Acta Anaesthesiol Scand* 25: 360-371, 1981.

21. **Brimioulle S, Vachiery JL, Lejeune P, Leeman M, Melot C and Naeije R**. Acid-base status affects gas exchange in canine oleic acid pulmonary edema. *Am J Physiol* 260: H1080-1086, 1991.

22. **Brismar B, Hedenstierna G, Lundquist H, Strandberg A, Svensson L and Tokics L**. Pulmonary densities during anesthesia with muscular relaxation--a proposal of atelectasis. *Anesthesiology* 62: 422-428, 1985.

23. **Bryan AC, Bentivoglio LG, Beerel f, macleish M, Zidulka A and Bates DV**. Factors affecting regional distribution of ventilation and perfusion in the lung. *J. Appl. Physiol.* 19: 395-402, 1966.

24. **Bryan AC, Milic-Emili J and Pengelly LD**. Effect of gravity on the distribution of pulmonary ventilation. *J. Appl. Physiol.* 21: 778-784, 1966.

25. **Burton AC and Patel DJ**. Effect on pulmonary vascular resistance of inflation of the rabbit lungs. *A. Appl. Physiol* 12: 239, 1958.

26. **Carlsson AJ, Bindslev L, Santesson J, Gottlieb I and Hedenstierna G**. Hypoxic pulmonary vasoconstriction in the human lung: the effect of prolonged unilateral hypoxic challenge during anaesthesia. *Acta Anaesthesiol Scand* 29: 346-351, 1985.

27. **Chen L, Williams JJ, Alexander CM, Ray RJ, Marshall C and Marshall BE**. The effect of pleural pressure on the hypoxic pulmonary vasoconstrictor response in closed chest dogs. *Anesth Analg* 67: 763-769, 1988.

28. **Choe KH, Kim YT, Shim TS, Lim CM, Lee SD, Koh Y, Kim WS, Kim DS, Ryu JS and Kim WD**. Closing volume influences the postural effect on oxygenation in unilateral lung disease. *Am J Respir Crit Care Med* 161: 1957-1962, 2000.

29. **Dawson CA, Grimm DJ and Linehan JH**. Lung inflation and longitudinal distribution of pulmonary vascular resistance during hypoxia. *J Appl Physiol* 47: 532-536, 1979.

30. **Domino KB, Chen L, Alexander CM, Williams JJ, Marshall C and Marshall BE**. Time course and responses of sustained hypoxic pulmonary vasoconstriction in the dog. *Anesthesiology* 60: 562-566, 1984.

31. **Domino KB, Hlastala MP, Eisenstein BL and Cheney FW**. Effect of regional alveolar hypoxia on gas exchange in dogs. *J Appl Physiol* 67: 730-735, 1989.

32. **Domino KB, Lu Y, Eisenstein BL and Hlastala MP**. Hypocapnia worsens arterial blood oxygenation and increases $\dot{V}_A/\dot{Q}$ heterogeneity in canine pulmonary edema. *Anesthesiology* 78: 91-99, 1993.

33. **Domino KB and Pinsky MR**. Effect of positive end-expiratory pressure on hypoxic pulmonary vasoconstriction in the dog. *Am J Physiol* 259: H697-705, 1990.

34. **Domino KB, Wetstein L, Glasser SA, Lindgren L, Marshall C, Harken A and Marshall BE**. Influence of mixed venous oxygen tension ($PvO_2$) on blood flow to atelectatic lung. *Anesthesiology* 59: 428-434, 1983.

35. **Dorrington KL, Clar C, Young JD, Jonas M, Tansley JG and Robbins PA.** Time course of the human pulmonary vascular response to 8 hours of isocapnic hypoxia. *Am J Physiol* 273: H1126-1134, 1997.

36. **Dueck R, Wagner PD and West JB.** Effects of positive end-expiratory pressure on gas exchange in dogs with normal and edematous lungs. *Anesthesiology* 47: 359-366, 1977.

37. **Evans JW and Wagner PD.** Limits on $\dot{V}_A/\dot{Q}$ distributions from analysis of experimental inert gas elimination. *J Appl Physiol* 42: 889-898, 1977.

38. **Farrukh IS and Michael JR.** Cellular mechanisms that control pulmonary vascular tone during hypoxia and normoxia. Possible role of Ca2+ATPases. *Am Rev Respir Dis* 145: 1389-1397, 1992.

39. **Fowler WS.** Lung function studies II. The respiratory dead space. *Am. J. Physiol.* 154: 405-416, 1948.

40. **Froese AB and Bryan AC.** Effects of anesthesia and paralysis on diaphragmatic mechanics in man. *Anesthesiology* 41: 242-255, 1974.

41. **Frostell CG, Blomqvist H, Hedenstierna G, Lundberg J and Zapol WM.** Inhaled nitric oxide selectively reverses human hypoxic pulmonary vasoconstriction without causing systemic vasodilation. *Anesthesiology* 78: 427-435, 1993.

42. **Gale GE, Torre-Bueno JR, Moon RE, Saltzman HA and Wagner PD.** Ventilation-perfusion inequality in normal humans during exercise at sea level and simulated altitude. *J Appl Physiol* 58: 978-988, 1985.

43. **Ganesan S, Rouch KE and Lai-Fook SJ.** A finite element analysis of the effects of the abdomen on regional lung expansion. *Respir Physiol* 99: 341-353, 1995.

44. **Gerbino AJ, McKinney S and Glenny RW.** Correlation between ventilation and perfusion determines $\dot{V}_A/\dot{Q}$ heterogeneity in endotoxemia. *J Appl Physiol* 88: 1933-1942.2000.

45. **Glasser SA, Domino KB, Lindgren L, Parcella P, Marshall C and Marshall BE.** Pulmonary blood pressure and flow during atelectasis in the dog. *Anesthesiology* 58: 225-231, 1983.

46. **Glazier JB, Hughes JM, Maloney JE and West JB**. Vertical gradient of alveolar size in lungs of dogs frozen intact. *J Appl Physiol* 23: 694-705, 1967.

47. **Glenny RW, Bernard S and Brinkley M**. Validation of fluorescent-labeled microspheres for measurement of regional organ perfusion. *J Appl Physiol* 74: 2585-2597, 1993.

48. **Glenny RW, Bernard S, Robertson HT and Hlastala MP**. Gravity is an important but secondary determinant of regional pulmonary blood flow in upright primates. *J Appl Physiol* 86: 623-632, 1999.

49. **Glenny RW, Bernard SL and Robertson HT**. Pulmonary blood flow remains fractal down to the level of gas exchange. *J Appl Physiol* 89: 742-748, 2000.

50. **Glenny RW, Lamm WJ, Albert RK and Robertson HT**. Gravity is a minor determinant of pulmonary blood flow distribution . *J Appl Physiol* 71: 620-629, 1991.

51. **Glenny RW, Lamm WJ, Bernard SL, An D, Chornuk M, Pool SL, Wagner WW, Jr., Hlastala MP and Robertson HT**. Selected contribution: redistribution of pulmonary perfusion during weightlessness and increased gravity. *J Appl Physiol* 89: 1239-1248, 2000.

52. **Glenny RW, McKinney S and Robertson HT**. Spatial pattern of pulmonary blood flow distribution is stable over days. *J Appl Physiol* 82: 902-907, 1997.

53. **Glenny RW and Robertson HT**. Fractal properties of pulmonary blood flow: characterization of spatial heterogeneity. *J Appl Physiol* 69: 532-545, 1990.

54. **Glenny RW, Robertson HT and Hlastala MP**. Vasomotor tone does not affect perfusion heterogeneity and gas exchange in normal primate lungs during normoxia. *J Appl Physiol* 89: 2263-2267, 2000.

55. **Glenny RW, Robertson HT, Yamashiro S and Bassingthwaighte JB**. Applications of fractal analysis to physiology. *J Appl Physiol* 70: 2351-2367, 1991.

56. **Greenleaf JF, Ritman EL, Sass DJ and Wood EH**. Spatial distribution of pulmonary blood flow in dogs in left decubitus position. *Am J Physiol* 227: 230-244, 1974.

57. **Groh J, Kuhnle GE, Kuebler WM and Goetz AE.** An experimental model for simultaneous quantitative analysis of pulmonary micro- and macrocirculation during unilateral hypoxia in vivo. *Res Exp Med* 192: 431-441, 1992.

58. **Groh J, Kuhnle GE, Ney L, Sckell A and Goetz AE.** The effect of mechanical ventilation, thoracotomy, and one-lung respiration on intrapulmonary perfusion distribution. An animal experimental study. *Anaesthesist* 44: 319-327, 1995.

59. **Groh J, Kuhnle GE, Ney L, Sckell A and Goetz AE.** Effects of isoflurane on regional pulmonary blood flow during one-lung ventilation. *Br J Anaesth* 74: 209-216, 1995.

60. **Hakim TS, Dean GW and Lisbona R.** Effect of body posture on spatial distribution of pulmonary blood flow. *J Appl Physiol* 64: 1160-1170.1988.

61. **Hakim TS, Lisbona R and Dean GW.** Gravity-independent inequality in pulmonary blood flow in humans. *J Appl Physiol* 63: 1114-1121.1987.

62. **Hakim TS, Lisbona R and Dean GW.** Effect of cardiac output on gravity-dependent and nondependent inequality in pulmonary blood flow. *J Appl Physiol* 66: 1570-1578, 1989.

63. **Hedenstierna G, Baehrendtz S, Klingstedt C, Santesson J, Soderborg B, Dahlborn M and Bindslev L.** Ventilation and perfusion of each lung during differential ventilation with selective PEEP. *Anesthesiology* 61: 369-376, 1984.

64. **Hedenstierna G, Bindslev L and Santesson J.** Pressure-volume and airway closure relationships in each lung in anaesthetized man. *Clin Physiol* 1: 479-493, 1981.

65. **Hedenstierna G, Lundquist H, Lundh B, Tokics L, Strandberg A, Brismar B and Frostell C.** Pulmonary densities during anaesthesia. An experimental study on lung morphology and gas exchange. *Eur Respir J* 2: 528-535, 1989.

66. **Hedenstierna G, White FC, Mazzone R and Wagner PD.** Redistribution of pulmonary blood flow in the dog with PEEP ventilation. *J Appl Physiol* 46: 278-287, 1979.

67. **Hedenstierna G, White FC and Wagner PD.** Spatial distribution of pulmonary blood flow in the dog with PEEP ventilation. *J Appl Physiol* 47: 938-946, 1979.

68. **Hlastala M and Berger A.** *Physiology of Respiration.* New York: Oxford University Press, 1996.

69. **Hlastala MP and Berger AJ.** *Physiology of Respiration*: Oxford University Press, 2001.

70. **Hlastala MP, Bernard SL, Erickson HH, Fedde MR, Gaughan EM, McMurphy R, Emery MJ, Polissar N and Glenny RW.** Pulmonary blood flow distribution in standing horses is not dominated by gravity. *J Appl Physiol* 81: 1051-1061, 1996.

71. **Hlastala MP, Chornuk MA, Self DA, Kallas HJ, Burns JW, Bernard S, Polissar NL and Glenny RW.** Pulmonary blood flow redistribution by increased gravitational force. *J Appl Physiol* 84: 1278-1288, 1998.

72. **Hlastala MP and Robertson HT.** Inert gas elimination characteristics of the normal and abnormal lung. *J Appl Physiol* 44: 258-266, 1978.

73. **Hoffman EA and Ritman EL.** Effect of body orientation on regional lung expansion in dog and sloth. *J Appl Physiol* 59: 481-491, 1985.

74. **Hogg JC, Holst P, Corry P, Ruff F, Housley E and Morris E.** Effect of regional lung expansion and body position on pulmonary perfusion in dogs. *J Appl Physiol* 31: 97-101, 1971.

75. **Hoppin FG, Jr., Green ID and Mead J.** Distribution of pleural surface pressure in dogs. *J Appl Physiol* 27: 863-873, 1969.

76. **Hubmayr RD, Walters BJ, Chevalier PA, Rodarte JR and Olson LE.** Topographical distribution of regional lung volume in anesthetized dogs. *J Appl Physiol* 54: 1048-1056.1983.

77. **Hughes JM.** Pulmonary blood flow distribution in exercising and in resting horses. *J Appl Physiol* 81: 1049-1050.1996.

78. **Hughes JMB, Glazier JB, Maloney JE and West JB.** Effect of lung volume on the distribution of pulmonary blood flow in man. *Respiratory physiology* 4: 58-72, 1968.

79. **Hyatt RE, Bar-Yishay E and Abel MD.** Influence of the heart on the vertical gradient of transpulmonary pressure in dogs. *J Appl Physiol* 58: 52-57, 1985.

80. **Johnson RL, Jr., Cassidy SS, Grover R, Ramanathan M, Estrera A, Reynolds RC, Epstein R and Schutte J**. Effect of pneumonectomy on the remaining lung in dogs. *J Appl Physiol* 70: 849-858, 1991.

81. **Kallas HJ, Domino KB, Glenny RW, Anderson EA and Hlastala MP**. Pulmonary blood flow redistribution with low levels of positive end- expiratory pressure. *Anesthesiology* 88: 1291-1299, 1998.

82. **Kaneko K, Milic-Emili J, Dolovich MB, Dawson A and Bates DV**. Regional distribution of ventilation and perfusion as a function of body position. *J Appl Physiol* 21: 767-777, 1966.

83. **Katori R, Amorim D, Theye RA and Wood EH**. Influence of body position on regional pulmonary arterial-venous shunts in intact dogs. *J Appl Physiol* 29: 288-296, 1970.

84. **Kleen M, Habler O, Hutter J, Kemming G, Podtschaske A, Tiede M, Welte M, Keipert PE, Batra S, Faithfull NS, Corso C, Zwissler B and Messmer K.** Hemodilution and hyperoxia locally change distribution of regional pulmonary perfusion in dogs. *Am J Physiol* 274: H520-528, 1998.

85. **Klingstedt C, Baehrendtz S, Bindslev L and Hedenstierna G**. Lung and chest wall mechanics during differential ventilation with selective PEEP. *Acta Anaesthesiol Scand* 29: 716-721, 1985.

86. **Klingstedt C, Hedenstierna G, Baehrendtz S, Lundqvist H, Strandberg A, Tokics L and Brismar B**. Ventilation-perfusion relationships and atelectasis formation in the supine and lateral positions during conventional mechanical and differential ventilation. *Acta Anaesthesiol Scand* 34: 421-429, 1990.

87. **Koyama S, Lamm WJ, Hildebrandt J and Albert RK**. Flow characteristics of open vessels in zone 1 rabbit lungs. *J Appl Physiol* 66: 1817-1823.1989.

88. **Krayer S, Rehder K, Vettermann J, Didier EP and Ritman EL**. Position and motion of the human diaphragm during anesthesia-paralysis. *Anesthesiology* 70: 891-898, 1989.

89. **Kruger JJ, Baine T and J. L. Patterson J**. elevation gradient of intrathoracic pressure. *J. Appl. Physiol* 16: 465-468, 1961.

90. **Kuriyama T, Latham LP, Horwitz LD, Reeves JT and Wagner WW, Jr.** Role of collateral ventilation in ventilation-perfusion balance. *J Appl Physiol* 56: 1500-1506, 1984.

91. **Lai-Fook SJ, Hyatt RE and Rodarte JR.** Effect of parenchymal shear modulus and lung volume on bronchial pressure-diameter behavior. *J Appl Physiol* 44: 859-868, 1978.

92. **Lamm WJ, Obermiller T, Hlastala MP and Albert RK.** Perfusion through vessels open in zone 1 contributes to gas exchange in rabbit lungs in situ. *J Appl Physiol* 79: 1895-1899, 1995.

93. **Landmark SJ, Knopp TJ, Rehder K and Sessler AD.** Regional pulmonary perfusion and $\dot{V}_A/\dot{Q}$ in awake and anesthetized- paralyzed man. *J Appl Physiol* 43: 993-1000, 1977.

94. **Larsson A, Malmkvist G and Werner O.** Variations in lung volume and compliance during pulmonary surgery. *Br J Anaesth* 59: 585-591, 1987.

95. **Lejeune P, De Smet JM, de Francquen P, Leeman M, Brimioulle S, Hallemans R, Melot C and Naeije R.** Inhibition of hypoxic pulmonary vasoconstriction by increased left atrial pressure in dogs. *Am J Physiol* 259: H93-100, 1990.

96. **Lejeune P, Vachiery JL, De Smet JM, Leeman M, Brimioulle S, Delcroix M, Melot C and Naeije R.** PEEP inhibits hypoxic pulmonary vasoconstriction in dogs. *J Appl Physiol* 70: 1867-1873, 1991.

97. **Liu S, Margulies SS and Wilson TA.** Deformation of the dog lung in the chest wall. *J Appl Physiol* 68: 1979-1987, 1990.

98. **Madden JA, Dawson CA and Harder DR.** Hypoxia-induced activation in small isolated pulmonary arteries from the cat. *J Appl Physiol* 59: 113-118, 1985.

99. **Mann CM, Domino KB, Walther SM, Glenny RW, Polissar NL and Hlastala MP.** Redistribution of pulmonary blood flow during unilateral hypoxia in prone and supine dogs. *J Appl Physiol* 84: 2010-2019, 1998.

100. **Marshall BE.** Hypoxic pulmonary vasoconstriction. *Acta Anaesthesiol Scand Suppl* 94: 37-41, 1990.

101. **Marshall BE, Clarke WR, Costarino AT, Chen L, Miller F and Marshall C.** The dose-response relationship for hypoxic pulmonary vasoconstriction. *Respir Physiol* 96: 231-247, 1994.

102. **Marshall BE and Marshall C.** Continuity of response to hypoxic pulmonary vasoconstriction. *J Appl Physiol* 49: 189-196, 1980.

103. **Marshall BE, Marshall C, Benumof J and Saidman LJ.** Hypoxic pulmonary vasoconstriction in dogs: effects of lung segment size and oxygen tension. *J Appl Physiol* 51: 1543-1551, 1981.

104. **Marshall BE, Marshall C, Frasch F and Hanson CW.** Role of hypoxic pulmonary vasoconstriction in pulmonary gas exchange and blood flow distribution. 1. Physiologic concepts. *Intensive Care Med* 20: 291-297, 1994.

105. **Marshall BE, Marshall C, Magno M, Lilagan P and Pietra GG.** Influence of bronchial arterial $PO_2$ on pulmonary vascular resistance. *J Appl Physiol* 70: 405-415, 1991.

106. **Marshall C and Marshall BE.** Hypoxic pulmonary vasoconstriction is not endothelium dependent. *Proc Soc Exp Biol Med* 201: 267-270, 1992.

107. **McFarlane PA, Gardaz JP and Sykes MK.** $CO_2$ and mechanical factors reduce blood flow in a collapsed lung lobe. *J Appl Physiol* 57: 739-743, 1984.

108. **Melsom MN, Flatebo T and Nicolaysen G.** Hypoxia and hyperoxia both transiently affect distribution of pulmonary perfusion but not ventilation in awake sheep. *Acta Physiol Scand* 166: 151-158, 1999.

109. **Melsom MN, Kramer-Johansen J, Flatebo T, Muller C and Nicolaysen G.** Distribution of pulmonary ventilation and perfusion measured simultaneously in awake goats. *Acta Physiol Scand* 159: 199-208, 1997.

110. **Milic-Emili J, Henderson JA, Dolovich MB, Trop D and Kaneko K.** Regional distribution of inspired gas in the lung. *J Appl Physiol* 21: 749-759, 1966.

111. **Miller FL, Chen L, Malmkvist G, Marshall C and Marshall BE.** Mechanical factors do not influence blood flow distribution in atelectasis. *Anesthesiology* 70: 481-488, 1989.

112. **Morgan BC and Guntheroth WG**. Pulmonary blood flow and resistance during acute atelectasis in intact dogs. *J Appl Physiol* 28: 609-613, 1970.

113. **Mure M, Domino KB, Lindahl SG, Hlastala MP, Altemeier WA and Glenny RW**. Regional ventilation-perfusion distribution is more uniform in the prone position. *J Appl Physiol* 88: 1076-1083, 2000.

114. **Mure M, Domino KB, Robertson T, Hlastala MP and Glenny RW**. Pulmonary blood flow does not redistribute in dogs with reposition from supine to left lateral position. *Anesthesiology* 89: 483-492, 1998.

115. **Murray TR, Chen L, Marshall BE and Macarak EJ**. Hypoxic contraction of cultured pulmonary vascular smooth muscle cells. *Am J Respir Cell Mol Biol* 3: 457-465, 1990.

116. **Nicolaysen G, Shepard J, Onizuka M, Tanita T, Hattner RS and Staub NC**. No gravity-independent gradient of blood flow distribution in dog lung. *J Appl Physiol* 63: 540-545, 1987.

117. **Olson LE**. Effect of posture on static lung volumes and pulmonary mechanics in pneumonectomized rabbits. *J Appl Physiol* 74: 415-422, 1993.

118. **Olson LE and Hoffman EA**. Heart-lung interactions determined by electron beam X-ray CT in laterally recumbent rabbits. *J Appl Physiol* 78: 417-427, 1995.

119. **Orphanidou D, Hughes JM, Myers MJ, Al-Suhali AR and Henderson B**. Tomography of regional ventilation and perfusion using krypton 81m in normal subjects and asthmatic patients. *Thorax* 41: 542-551, 1986.

120. **Parker JC, Ardell JL, Hamm CR, Barman SA and Coker PJ**. Regional pulmonary blood flow during rest, tilt, and exercise in unanesthetized dogs. *J Appl Physiol* 78: 838-846, 1995.

121. **Pirlo AF, Benumof JL and Trousdale FR**. Atelectatic lobe blood flow: open vs. closed chest, positive pressure vs. spontaneous ventilation. *J Appl Physiol* 50: 1022-1026, 1981.

122. **Prefaut C and Engel LA**. Vertical distribution of perfusion and inspired gas in supine man. *Respir Physiol* 43: 209-219, 1981.

123. **Prisk GK, Elliott AR, Guy HJ, Kosonen JM and West JB**. Pulmonary gas exchange and its determinants during sustained microgravity on Spacelabs SLS-1 and SLS-2. *J Appl Physiol* 79: 1290-1298.1995.

124. **Prisk GK, Guy HJ, Elliott AR, Paiva M and West JB**. Ventilatory inhomogeneity determined from multiple-breath washouts during sustained microgravity on Spacelab SLS-1. *J Appl Physiol* 78: 597-607, 1995.

125. **Prisk GK, Guy HJ, Elliott AR and West JB**. Inhomogeneity of pulmonary perfusion during sustained microgravity on SLS-1. *J Appl Physiol* 76: 1730-1738, 1994.

126. **Quebbeman EJ and Dawson CA**. Influence of inflation and atelectasis on the hypoxic pressor response in isolated dog lung lobes. *Cardiovasc Res* 10: 672-677, 1976.

127. **Reed JH, Jr. and Wood EH**. Effect of body position on vertical distribution of pulmonary blood flow. *J Appl Physiol* 28: 303-311, 1970.

128. **Rees DI and Wansbrough SR**. One-lung anesthesia: percent shunt and arterial oxygen tension during continuous insufflation of oxygen to the nonventilated lung. *Anesth Analg* 61: 507-512, 1982.

129. **Rehder K and Sessler AD**. Function of each lung in spontaneously breathing man anesthetized with thiopental-meperidine. *Anesthesiology* 38: 320-327, 1973.

130. **Rehder K, Wenthe FM and Sessler AD**. Function of each lung during mechanical ventilation with ZEEP and with PEEP in man anesthetized with thiopental-meperidine. *Anesthesiology* 39: 597-606, 1973.

131. **Robertson HT, Altemeier WA and Glenny RW**. Physiological implications of the fractal distribution of ventilation and perfusion in the lung. *Ann Biomed Eng* 28: 1028-1031, 2000.

132. **Robertson HT, Glenny RW, Stanford D, McInnes LM, Luchtel DL and Covert D**. High-resolution maps of regional ventilation utilizing inhaled fluorescent microspheres. *J Appl Physiol* 82: 943-953, 1997.

133. **Rodarte JR, Chaniotakis M and Wilson TA**. Variability of parenchymal expansion measured by computed tomography. *J Appl Physiol* 67: 226-231, 1989.

134. **Ross DJ, Wu P and Mohsenifar Z.** Assessment of postural differences in regional pulmonary perfusion in man by single-photon emission computerized tomography. *Clin Sci (Colch)* 92: 81-85, 1997.

135. **Roussos CS, Martin RR and Engel LA.** Diaphragmatic contraction and the gradient of alveolar expansion in the lateral posture. *J Appl Physiol* 43: 32-38, 1977.

136. **Schimmel C, D. Frazer SR and Gleny RW.** Extending fluorescent microsphere method for regional organ blood flow to 13 simultaneous colors. *Am J. Physiol*, 2001.

137. **Schimmel C, Frazer D, Huckins SR and Glenny RW.** Validation of automated spectrofluroimetry for measurement of regional organ perfusion using fluorescent microspheres. *Computer Methods and Programs in Biomedicine* 62: 115-125, 2000.

138. **Sprague RS, Stephenson AH and Lonigro AJ.** Prostaglandin I2 supports blood flow to hypoxic alveoli in anesthetized dogs. *J Appl Physiol* 56: 1246-1251, 1984.

139. **Staub NC.** Pulmonary edema. *Physiol Rev* 54: 678-811, 1974.

140. **Surprenant EL and Rodbard. S.** A hydrostatic pressure gradient in the pleural sac. *Am. Heart J* 66: 215-220, 1963.

141. **Swenson ER, Robertson HT and Hlastala MP.** Effects of inspired carbon dioxide on ventilation-perfusion matching in normoxia, hypoxia, and hyperoxia. *Am J Respir Crit Care Med* 149: 1563-1569, 1994.

142. **Sylvester JT, Harabin AL, Peake MD and Frank RS.** Vasodilator and constrictor responses to hypoxia in isolated pig lungs. *J Appl Physiol* 49: 820-825, 1980.

143. **Sylvester JT, Mitzner W, Ngeow Y and Permutt S.** Hypoxic constriction of alveolar and extra-alveolar vessels in isolated pig lungs. *J Appl Physiol* 54: 1660-1666, 1983.

144. **Thomas LJ, JR., Griffo ZJ and Roos A.** Effect of negative-pressure inflation of the lung on pulmonary vascular resistance. *J. Appl. Physiol* 16: 451, 1961.

145. **Tokics L, Hedenstierna G, Svensson L, Brismar B, Cederlund T, Lundquist H and Strandberg A.** $\dot{V}_A/\dot{Q}$ distribution and correlation to atelectasis in anesthetized paralyzed humans. *J Appl Physiol* 81: 1822-1833, 1996.

146. **Tolins M, Weir EK, Chesler E, Nelson DP and From AH.** Pulmonary vascular tone is increased by a voltage-dependent calcium channel potentiator. *J Appl Physiol* 60: 942-948, 1986.

147. **Vejlstrup NG, O'Neill M, Nagyova B and Dorrington KL.** Time course of hypoxic pulmonary vasoconstriction: a rabbit model of regional hypoxia. *Am J Respir Crit Care Med* 155: 216-221, 1997.

148. **Wagner PD, Laravuso RB, Uhl RR and West JB.** Continuous distributions of ventilation-perfusion ratios in normal subjects breathing air and 100 per cent $O_2$. *J Clin Invest* 54: 54-68, 1974.

149. **Wagner PD, Naumann PF and Laravuso RB.** Simultaneous measurement of eight foreign gases in blood by gas chromatography. *J Appl Physiol* 36: 600-605, 1974.

150. **Wagner PD, Saltzman HA and West JB.** Measurement of continuous distributions of ventilation-perfusion ratios: theory. *J Appl Physiol* 36: 588-599, 1974.

151. **Walther SM, Domino KB, Glenny RW and Hlastala MP.** Pulmonary blood flow distribution in sheep: effects of anesthesia, mechanical ventilation, and change in posture. *Anesthesiology* 87: 335-342, 1997.

152. **Walther SM, Domino KB, Glenny RW, Polissar NL and Hlastala MP.** Pulmonary blood flow distribution has a hilar-to-peripheral gradient in awake, prone sheep. *J Appl Physiol* 82: 678-685, 1997.

153. **Walther SM, Domino KB and Hlastala MP.** Effects of posture on blood flow diversion by hypoxic pulmonary vasoconstriction in dogs. *Br J Anaesth* 81: 425-429, 1998.

154. **Wang PM, Fike CD, Kaplowitz MR, Brown LV, Ayappa I, Jahed M and Lai-Fook SJ.** Effects of lung inflation and blood flow on capillary transit time in isolated rabbit lungs. *J Appl Physiol* 72: 2420-2427, 1992.

155. **Warner DO, Warner MA and Ritman EL.** Human chest wall function while awake and during halothane anesthesia. I. Quiet breathing. *Anesthesiology* 82: 6-19, 1995.

156. **Weir EK and Archer SL.** The mechanism of acute hypoxic pulmonary vasoconstriction: the tale of two channels. *Faseb J* 9: 183-189, 1995.

157. **West J, B. and Dollery CT**. Distribution of blood flow and ventilation-perfusion in the lung measured with radioacitve $CO_2$. *J. Appl. Physiol* 15: 405-410, 1960.

158. **West JB**. Regional differences in gas exchange in the lung of erect man. *J. Appl. Physiol* 17: 893-898, 1962.

159. **West JB and Dollery CT**. Distribution of blood flow in isolated lung:relation to vascular and alveolar pressures. *J. Apl. Physiol* 55: 1341-1348, 1964.

160. **West JB and Matthews FL**. Stresses, strains, and surface pressures in the lung caused by its weight. *J Appl Physiol* 32: 332-345, 1972.

161. **Wiener CM, McKenna WJ, Myers MJ, Lavender JP and Hughes JM**. Left lower lobe ventilation is reduced in patients with cardiomegaly in the supine but not the prone position. *Am Rev Respir Dis* 141: 150-155, 1990.

162. **Wilson TA and Beck KC**. Contributions of ventilation and perfusion inhomogeneities to the $\dot{V}_A/\dot{Q}$ distribution. *J Appl Physiol* 72: 2298-2304, 1992.

163. **Yuan XJ, Tod ML, Rubin LJ and Blaustein MP**. Hypoxic and metabolic regulation of voltage-gated K+ channels in rat pulmonary artery smooth muscle cells. *Exp Physiol* 80: 803-813, 1995.

Table A1. Coefficients and $R^2$ of multiple linear regression equation † fit to $\dot{Q}$, $\dot{V}_A$, $\dot{V}_A/\dot{Q}$ and $P_RO_2$ data for whole lung of dog 1

| | Post | PEEP | Int | a | | b | | c | | d | | e | | f | | g | | $R^2$ |
|---|---|---|---|---|---|---|---|---|---|---|---|---|---|---|---|---|---|---|
| | LLD | 0 | 7.9 | -0.30 | * | 0.09 | * | -0.08 | * | -0.098 | * | -0.026 | * | 0.058 | * | -0.003 | | 0.29 |
| | LLD | 10 | 3.8 | -0.18 | * | -0.04 | * | -0.03 | * | 0.002 | | 0.001 | | 0.006 | * | 0.001 | * | 0.49 |
| Q | RLD | 0 | 7.4 | -0.87 | * | -0.06 | * | -0.04 | | 0.086 | | -0.071 | * | 0.018 | * | 0.010 | * | 0.71 |
| | RLD | 10 | 2.5 | -0.20 | * | 0.00 | | -0.01 | * | -0.000 | | 0.000 | | -0.003 | * | -0.001 | * | 0.75 |
| | LLD | 0 | 5.0 | 0.26 | * | 0.24 | * | 0.10 | * | -0.093 | * | -0.000 | | 0.043 | * | -0.001 | | 0.36 |
| $V_A$ | LLD | 10 | 2.6 | -0.07 | * | 0.00 | | 0.02 | * | -0.001 | | 0.001 | | 0.006 | * | 0.001 | * | 0.12 |
| | RLD | 0 | 4.6 | -0.68 | * | 0.09 | * | 0.10 | * | 0.082 | * | -0.058 | * | -0.009 | * | 0.010 | * | 0.61 |
| | RLD | 10 | 2.8 | -0.17 | * | -0.00 | | 0.04 | * | 0.004 | * | 0.003 | * | -0.010 | * | -0.001 | * | 0.51 |
| | LLD | 0 | 0.7 | 0.06 | * | 0.04 | * | 0.01 | * | 0.001 | | 0.002 | * | 0.002 | * | 0.001 | * | 0.57 |
| | LLD | 10 | 0.7 | 0.01 | * | 0.01 | * | 0.01 | * | -0.000 | | 0.000 | | 0.001 | * | 0.000 | | 0.18 |
| $V_A/Q$ | RLD | 0 | 0.6 | -0.02 | * | 0.03 | * | 0.02 | * | 0.008 | * | -0.002 | * | -0.001 | * | -0.000 | | 0.56 |
| | RLD | 10 | 1.2 | 0.02 | * | -0.00 | | 0.02 | * | 0.002 | * | 0.001 | | -0.001 | * | -0.000 | | 0.15 |
| | LLD | 0 | 104.8 | 3.00 | * | 1.44 | * | 0.65 | * | -0.290 | * | 0.033 | * | 0.026 | | -0.001 | | 0.70 |
| $P_RO_2$ | LLD | 10 | 109.5 | 0.64 | * | 0.25 | * | 0.39 | * | 0.002 | | 0.009 | | 0.037 | * | 0.000 | | 0.19 |
| | RLD | 0 | 98.3 | -1.53 | * | 1.93 | * | 1.37 | * | 0.520 | * | -0.300 | * | 0.010 | | -0.007 | | 0.65 |
| | RLD | 10 | 108.7 | 0.38 | * | -0.06 | | 0.43 | * | 0.026 | | 0.017 | | -0.043 | * | -0.002 | | 0.15 |

* $P < 0.05$ compared with zero by 1-tailed unpaired t test.

† Equation: variable = I + ax + by +cz + dxy + eyz +fzx + gxyz . All intercepts are significant

Post:posture; Int:intercept.

Table A2. Coefficients and $R^2$ of multiple linear regression equation † fit to $\dot{Q}$, $\dot{V}_A$, $\dot{V}_A/\dot{Q}$ and $P_RO_2$ data for right lung of dog 1

| | Post | PEEP | Int | a | b | c | d | e | f | g | $R^2$ |
|---|---|---|---|---|---|---|---|---|---|---|---|
| | LLD | 0 | 7.46 | -0.72 * | -0.24 * | 0.02 | -0.03 * | -0.04 * | 0.03 * | 0.01 * | 0.46 |
| | LLD | 10 | 3.20 | -0.18 * | -0.13 * | 0.00 | -0.01 * | -0.01 * | 0.01 * | 0.00 | 0.48 |
| $\dot{Q}$ | RLD | 0 | 9.85 | -1.30 * | -0.34 * | -0.07 * | 0.13 * | -0.13 * | 0.06 * | 0.02 * | 0.67 |
| | RLD | 10 | 3.24 | -0.24 * | -0.06 * | 0.00 | 0.01 * | -0.01 * | -0.01 * | 0.00 * | 0.65 |
| | LLD | 0 | 6.45 | -0.50 * | -0.04 | 0.15 * | 0.04 * | -0.01 * | 0.03 * | 0.02 * | 0.39 |
| $\dot{V}_A$ | LLD | 10 | 2.64 | -0.25 * | -0.12 * | 0.04 * | -0.02 * | -0.01 * | 0.02 * | 0.00 * | 0.59 |
| | RLD | 0 | 6.50 | -0.79 * | -0.21 * | 0.13 * | 0.11 * | -0.13 * | 0.06 * | 0.01 * | 0.48 |
| | RLD | 10 | 3.64 | -0.15 * | -0.08 * | 0.08 * | 0.01 | -0.02 * | 0.00 | 0.00 * | 0.35 |
| | LLD | 0 | 1.00 | 0.04 | 0.12 * | 0.01 | 0.02 | 0.01 | 0.00 | 0.00 | 0.05 |
| | LLD | 10 | 0.83 | -0.03 * | -0.01 * | 0.02 * | 0.00 * | 0.00 | 0.00 * | 0.00 | 0.31 |
| $\dot{V}_A/\dot{Q}$ | RLD | 0 | 0.64 | 0.01 | 0.00 | 0.02 * | 0.01 * | -0.01 * | 0.01 * | 0.00 | 0.50 |
| | RLD | 10 | 1.15 | 0.04 * | 0.00 | 0.03 * | 0.00 | 0.00 * | 0.00 * | 0.00 | 0.39 |
| | LLD | 0 | 115.50 | 0.30 * | 0.78 * | 0.48 * | 0.23 * | 0.02 | -0.01 | 0.04 * | 0.33 |
| $P_RO_2$ | LLD | 10 | 114.10 | -0.84 * | -0.35 * | 0.55 * | -0.12 * | -0.01 | 0.19 * | 0.01 | 0.35 |
| | RLD | 0 | 103.40 | -0.05 | -0.19 | 1.22 * | 0.40 * | -0.52 * | 0.45 * | -0.01 | 0.55 |
| | RLD | 10 | 108.00 | 0.93 * | -0.13 | 0.60 * | -0.07 * | -0.10 * | 0.10 * | 0.01 * | 0.45 |

* $P < 0.05$ compared with zero by 1-tailed unpaired t test.

† Equation: variable = I + ax + by +cz + dxy + eyz +fzx + gxyz . All intercepts are significant

Post:posture; Int:intercept.

Table A3. Coefficients and $R^2$ of multiple linear regression equation † fit to $\dot{Q}$, $\dot{V}_A$, $\dot{V}_A/\dot{Q}$ and $P_RO_2$ data for left lung of dog 1

| | Post | PEEP | Int | a | b | c | d | e | f | g | $R^2$ |
|---|---|---|---|---|---|---|---|---|---|---|---|
| | LLD | 0 | 8.80 | -0.37 * | 0.54 * | -0.24 * | 0.31 * | -0.03 * | 0.05 * | 0.00 | 0.26 |
| | LLD | 10 | 5.10 | -0.14 * | -0.02 | -0.01 | 0.04 * | -0.03 * | 0.00 | 0.01 * | 0.32 |
| Q | RLD | 0 | 4.41 | -0.24 * | 0.18 * | 0.03 * | -0.06 * | -0.03 * | 0.00 | 0.00 | 0.42 |
| | RLD | 10 | 1.60 | -0.10 * | 0.06 * | -0.04 * | -0.01 * | 0.00 * | 0.00 * | 0.00 * | 0.44 |
| | LLD | 0 | 3.30 | 0.33 * | 0.48 * | -0.03 | 0.12 * | 0.02 * | 0.05 * | -0.02 * | 0.30 |
| $V_A$ | LLD | 10 | 2.95 | 0.13 * | 0.18 * | -0.01 | 0.01 | -0.02 * | 0.01 * | 0.00 | 0.37 |
| | RLD | 0 | 2.10 | -0.14 * | 0.24 * | 0.07 * | -0.02 * | -0.02 * | -0.01 * | 0.00 | 0.67 |
| | RLD | 10 | 2.06 | -0.11 * | -0.01 | 0.00 | 0.00 | -0.01 * | 0.01 * | 0.00 * | 0.28 |
| | LLD | 0 | 0.37 | 0.07 * | 0.04 * | 0.01 * | 0.00 | 0.00 * | 0.01 * | 0.00 * | 0.52 |
| | LLD | 10 | 0.58 | 0.04 * | 0.04 * | 0.00 | -0.01 * | 0.00 * | 0.00 * | 0.00 * | 0.45 |
| $V_A/Q$ | RLD | 0 | 0.46 | 0.00 | 0.04 * | 0.02 * | 0.01 * | 0.00 * | 0.00 * | 0.00 | 0.73 |
| | RLD | 10 | 1.31 | 0.01 | -0.05 | 0.03 | 0.01 | 0.00 | 0.01 | -0.01 | 0.25 |
| | LLD | 0 | 90.30 | 4.95 * | 2.55 * | 0.24 * | 0.51 * | 0.09 * | 0.42 * | -0.15 * | 0.45 |
| $P_RO_2$ | LLD | 10 | 105.80 | 2.15 * | 2.10 * | 0.05 | -0.11 * | -0.18 * | 0.06 * | -0.02 * | 0.50 |
| | RLD | 0 | 92.70 | 0.08 | 3.40 * | 1.54 * | 0.04 | -0.36 * | 0.01 | -0.02 | 0.83 |
| | RLD | 10 | 111.30 | 0.05 | -1.25 * | 0.72 * | 0.11 * | -0.12 * | 0.19 * | -0.02 | 0.33 |

* $P < 0.05$ compared with zero by 1-tailed unpaired t test.

† Equation: variable = I + ax + by +cz + dxy + eyz +fzx + gxyz . All intercepts are significant

Post:posture; Int:intercept.

Table A4. Coefficients and $R^2$ of multiple linear regression equation † fit to $\dot{Q}$, $\dot{V}_A$, $\dot{V}_A/\dot{Q}$ and $P_RO_2$ data for whole lung of dog 2

| | Post | PEEP | Int | a | b | c | d | e | f | g | $R^2$ |
|---|---|---|---|---|---|---|---|---|---|---|---|
| | LLD | 0 | 2.36 | -0.10 * | 0.04 * | -0.05 * | -0.02 * | -0.02 | 0.02 * | 0.01 * | 0.45 |
| | LLD | 10 | 1.91 | 0.01 * | 0.00 | -0.02 * | -0.01 * | -0.01 * | 0.00 * | 0.00 * | 0.31 |
| Q | RLD | 0 | 3.10 | -0.13 * | 0.07 * | -0.06 * | 0.03 * | -0.01 * | 0.02 * | 0.00 * | 0.38 |
| | RLD | 10 | 1.50 | -0.02 | -0.04 | -0.03 | 0.00 | 0.00 | 0.00 | 0.00 | 0.27 |
| | LLD | 0 | 4.59 | 0.17 * | 0.01 | 0.06 * | -0.05 * | -0.07 * | 0.04 * | 0.03 * | 0.31 |
| $V_A$ | LLD | 10 | 2.45 | 0.02 * | -0.05 * | 0.02 * | -0.03 * | -0.02 * | 0.01 * | 0.00 * | 0.39 |
| | RLD | 0 | 4.60 | -0.29 * | 0.21 * | 0.05 * | 0.05 * | -0.05 * | 0.01 * | 0.00 | 0.33 |
| | RLD | 10 | 2.40 | 0.07 * | -0.07 * | 0.00 | -0.01 * | -0.01 * | 0.01 * | 0.00 * | 0.35 |
| | LLD | 0 | 2.08 | 0.13 * | -0.02 * | 0.07 * | -0.01 * | -0.01 * | 0.00 | 0.00 * | 0.29 |
| | LLD | 10 | 1.28 | -0.02 | -0.02 * | 0.03 * | -0.01 * | -0.01 * | 0.00 | 0.00 * | 0.30 |
| $V_A/Q$ | RLD | 0 | 1.44 | -0.05 * | 0.04 * | 0.06 * | 0.01 * | -0.01 * | 0.00 | 0.00 | 0.52 |
| | RLD | 10 | 1.72 | 0.07 * | -0.01 * | 0.04 * | -0.01 * | -0.01 * | 0.00 * | 0.00 | 0.30 |
| | LLD | 0 | 117.64 | 1.76 * | 0.07 | 0.82 * | -0.19 * | -0.23 * | -0.08 * | 0.09 * | 0.27 |
| $P_RO_2$ | LLD | 10 | 114.80 | -0.16 * | -0.49 * | 0.63 * | -0.23 * | -0.10 * | 0.00 | 0.03 * | 0.36 |
| | RLD | 0 | 116.70 | -0.76 * | 0.90 * | 1.11 * | 0.19 * | -0.31 * | 0.02 | 0.00 | 0.61 |
| | RLD | 10 | 110.90 | 1.11 * | -0.18 * | 0.63 * | -0.16 * | -0.10 * | -0.01 | 0.02 * | 0.40 |

* $P < 0.05$ compared with zero by 1-tailed unpaired t test.

† Equation: variable = I + ax + by +cz + dxy + eyz +fzx + gxyz . All intercepts are significant

Post:posture; Int:intercept.

Table A5. Coefficients and $R^2$ of multiple linear regression equation † fit to $\dot{Q}$, $\dot{V}_A$, $\dot{V}_A/\dot{Q}$ and $P_RO_2$ data for right lung of dog 2

| | Post | PEEP | Int | a | b | c | d | e | f | g | $R^2$ |
|---|---|---|---|---|---|---|---|---|---|---|---|
| | LLD | 0 | 2.21 | -0.14 * | -0.02 * | -0.01 * | 0.01 | 0.00 | 0.03 * | 0.01 * | 0.38 |
| | LLD | 10 | 1.98 | -0.03 * | -0.04 * | -0.01 * | -0.01 * | 0.00 * | 0.01 * | 0.00 * | 0.30 |
| Q | RLD | 0 | 3.63 | 0.05 | -0.04 * | -0.12 * | 0.01 | -0.01 * | 0.08 * | -0.01 * | 0.31 |
| | RLD | 10 | 1.57 | 0.01 | -0.04 | -0.04 | 0.00 | 0.00 | 0.01 | 0.00 | 0.29 |
| | LLD | 0 | 5.52 | -0.53 * | -0.18 * | 0.12 * | 0.14 * | -0.02 * | 0.02 | 0.02 * | 0.32 |
| $V_A$ | LLD | 10 | 2.69 | -0.25 * | -0.16 * | 0.03 * | -0.01 * | -0.01 * | 0.01 * | 0.00 * | 0.58 |
| | RLD | 0 | 5.60 | 0.25 * | 0.05 | 0.02 | -0.01 | -0.07 * | 0.15 * | -0.02 * | 0.22 |
| | RLD | 10 | 2.17 | 0.10 | -0.03 | -0.01 | -0.02 | -0.02 | 0.02 | 0.00 | 0.25 |
| | LLD | 0 | 2.51 | -0.09 * | -0.05 * | 0.07 * | 0.05 * | -0.01 * | -0.01 | 0.01 * | 0.25 |
| | LLD | 10 | 1.35 | -0.10 * | -0.06 * | 0.03 * | 0.00 | 0.00 * | 0.00 | 0.00 * | 0.54 |
| $V_A/Q$ | RLD | 0 | 1.56 | 0.04 * | 0.02 * | 0.06 * | 0.00 | -0.01 * | 0.01 * | 0.00 | 0.48 |
| | RLD | 10 | 1.48 | 0.05 | 0.02 | 0.03 | -0.02 | -0.01 | 0.00 | 0.00 | 0.27 |
| | LLD | 0 | 123.70 | -0.67 * | -0.52 * | 0.55 * | 0.49 * | -0.06 * | -0.02 | 0.04 * | 0.18 |
| $P_RO_2$ | LLD | 10 | 115.60 | -1.84 * | -1.33 * | 0.50 * | -0.11 * | -0.03 | 0.05 * | 0.01 | 0.53 |
| | RLD | 0 | 117.50 | 0.68 * | -0.23 * | 1.18 * | 0.22 | -0.40 * | 0.34 * | -0.01 | 0.36 |
| | RLD | 10 | 107.20 | 1.00 | 0.37 | 0.71 | -0.35 | -0.12 | 0.08 | -0.01 | 0.32 |

* $P < 0.05$ compared with zero by 1-tailed unpaired t test.

† Equation: variable = I + ax + by +cz + dxy + eyz +fzx + gxyz . All intercepts are significant

Post:posture; Int:intercept.

Table A6. Coefficients and $R^2$ of multiple linear regression equation † fit to $\dot{Q}$, $\dot{V}_A$, $\dot{V}_A/\dot{Q}$ and $P_RO_2$ data for left lung of dog 2

| | Post | PEEP | Int | a | b | c | d | e | f | g | $R^2$ |
|---|---|---|---|---|---|---|---|---|---|---|---|
| | LLD | 0 | 2.67 | -0.13 * | 0.18 * | -0.09 * | 0.02 | -0.08 * | 0.01 | 0.02 * | 0.57 |
| | LLD | 10 | 1.88 | 0.07 * | 0.07 * | -0.03 * | 0.01 | -0.03 * | 0.00 | 0.00 * | 0.36 |
| Q | RLD | 0 | 2.59 | 0.00 | 0.19 * | -0.01 | -0.02 * | -0.02 * | 0.01 * | 0.01 * | 0.49 |
| | RLD | 10 | 1.42 | -0.01 | -0.03 * | -0.02 * | -0.01 | 0.00 | 0.01 * | 0.00 * | 0.26 |
| | LLD | 0 | 3.48 | -0.11 | 0.35 * | 0.06 * | 0.07 | -0.15 * | 0.00 | 0.02 * | 0.45 |
| $V_A$ | LLD | 10 | 2.23 | 0.05 * | 0.10 * | 0.01 | 0.00 | -0.04 * | -0.01 * | 0.00 | 0.60 |
| | RLD | 0 | 3.30 | -0.17 * | 0.37 * | 0.09 * | 0.02 | -0.03 * | 0.00 | 0.02 * | 0.68 |
| | RLD | 10 | 2.76 | -0.04 * | -0.09 * | 0.00 | 0.00 | 0.00 | 0.01 * | 0.01 * | 0.40 |
| | LLD | 0 | 1.40 | 0.01 | 0.08 * | 0.11 * | 0.05 * | -0.04 * | 0.00 | 0.01 | 0.40 |
| | LLD | 10 | 1.21 | 0.01 | 0.02 * | 0.04 * | -0.01 * | -0.01 * | 0.00 | 0.00 * | 0.52 |
| $V_A/Q$ | RLD | 0 | 1.27 | -0.07 * | 0.06 * | 0.05 * | 0.02 * | -0.01 * | -0.01 * | 0.00 * | 0.67 |
| | RLD | 10 | 2.06 | -0.01 | -0.02 * | 0.04 * | 0.02 * | 0.00 | -0.01 * | 0.00 * | 0.15 |
| | LLD | 0 | 107.70 | -0.08 | 2.87 * | 2.17 * | 1.36 * | -1.22 * | -0.49 * | 0.27 * | 0.34 |
| $P_RO_2$ | LLD | 10 | 114.30 | 0.09 | 0.59 * | 0.83 * | -0.04 | -0.27 * | -0.03 | -0.02 * | 0.61 |
| | RLD | 0 | 114.80 | -1.10 * | 1.46 * | 1.03 * | 0.19 * | -0.33 * | 0.02 | 0.05 * | 0.76 |
| | RLD | 10 | 116.70 | -0.20 | -0.26 * | 0.38 * | 0.12 | 0.00 | -0.06 | 0.05 * | 0.14 |

* $P < 0.05$ compared with zero by 1-tailed unpaired t test.

† Equation: variable = I + ax + by +cz + dxy + eyz +fzx + gxyz . All intercepts are significant

Post:posture; Int:intercept.

Table A7. Coefficients and $R^2$ of multiple linear regression equation † fit to $\dot{Q}$, $\dot{V}_A$, $\dot{V}_A/\dot{Q}$ and $P_RO_2$ data for whole lung of dog 3

| | Post | PEEP | Int | a | b | c | d | e | f | g | $R^2$ |
|---|---|---|---|---|---|---|---|---|---|---|---|
| | LLD | 0 | 3.87 | -0.17 * | -0.02 | -0.08 * | 0.00 | -0.02 * | 0.03 * | 0.00 * | 0.47 |
| | LLD | 10 | 2.20 | -0.14 * | -0.02 * | -0.01 * | 0.00 * | -0.01 * | 0.00 | 0.00 * | 0.71 |
| Q | RLD | 0 | 5.80 | -0.47 * | 0.03 | -0.12 * | 0.04 * | -0.05 * | 0.03 * | 0.00 * | 0.55 |
| | RLD | 10 | 2.16 | -0.12 * | -0.04 * | -0.03 * | 0.00 * | -0.01 * | 0.00 * | 0.00 * | 0.60 |
| | LLD | 0 | 4.83 | -0.02 | 0.03 * | -0.06 * | 0.01 * | -0.04 * | 0.03 * | 0.01 * | 0.21 |
| $V_A$ | LLD | 10 | 2.84 | -0.15 * | -0.07 * | 0.00 | 0.00 | -0.01 * | 0.00 | 0.00 * | 0.56 |
| | RLD | 0 | 4.72 | -0.50 * | 0.25 * | 0.02 | 0.03 * | -0.05 * | 0.00 | 0.00 * | 0.44 |
| | RLD | 10 | 2.10 | -0.05 * | -0.02 * | 0.02 * | -0.01 * | -0.01 * | 0.00 | 0.00 | 0.27 |
| | LLD | 0 | 1.31 | 0.05 * | 0.02 * | 0.01 * | 0.01 * | 0.00 * | 0.00 | 0.00 * | 0.24 |
| | LLD | 10 | 1.32 | 0.01 * | 0.00 | 0.01 * | 0.00 | 0.00 * | 0.00 * | 0.00 | 0.07 |
| $V_A/Q$ | RLD | 0 | 0.75 | -0.03 * | 0.06 * | 0.03 * | 0.01 * | 0.00 * | 0.00 * | 0.00 * | 0.50 |
| | RLD | 10 | 1.10 | 0.03 * | 0.01 * | 0.03 * | 0.00 * | 0.00 * | 0.00 * | 0.00 * | 0.29 |
| | LLD | 0 | 113.84 | 1.01 * | 0.33 * | 0.23 * | 0.09 * | -0.10 * | 0.00 | 0.03 * | 0.37 |
| $P_RO_2$ | LLD | 10 | 114.80 | 0.13 * | -0.01 | 0.17 * | -0.01 | -0.03 * | 0.03 * | 0.00 | 0.05 |
| | RLD | 0 | 105.20 | -1.50 * | 2.53 * | 1.20 * | 0.44 * | -0.37 * | 0.01 | -0.01 * | 0.64 |
| | RLD | 10 | 116.97 | 0.80 * | 0.16 * | 0.72 * | 0.02 | 0.00 | -0.06 * | -0.01 * | 0.37 |

* $P < 0.05$ compared with zero by 1-tailed unpaired t test.

† Equation: variable = I + ax + by +cz + dxy + eyz +fzx + gxyz . All intercepts are significant

Post:posture; Int:intercept.

Table A8. Coefficients and $R^2$ of multiple linear regression equation † fit to $\dot{Q}$, $\dot{V}_A$, $\dot{V}_A/\dot{Q}$ and $P_RO_2$ data for right lung of dog 3

| | Post | PEEP | Int | a | b | c | d | e | f | g | $R^2$ |
|---|---|---|---|---|---|---|---|---|---|---|---|
| | LLD | 0 | 3.46 | -0.21 * | -0.04 * | -0.03 * | 0.00 | -0.01 * | 0.02 * | 0.00 | 0.43 |
| | LLD | 10 | 1.65 | -0.11 * | -0.04 * | -0.01 * | -0.01 * | 0.00 * | 0.01 * | 0.00 | 0.58 |
| Q | RLD | 0 | 7.51 | -0.54 * | -0.01 | -0.20 * | 0.01 | -0.09 * | 0.17 * | 0.01 * | 0.42 |
| | RLD | 10 | 2.63 | -0.10 * | -0.05 * | -0.03 * | 0.00 | -0.01 * | 0.01 * | 0.00 | 0.43 |
| | LLD | 0 | 5.00 | -0.31 * | 0.04 * | -0.02 * | 0.09 * | -0.01 * | 0.00 | 0.01 * | 0.24 |
| $V_A$ | LLD | 10 | 2.28 | -0.24 * | -0.09 * | 0.01 * | -0.01 * | -0.01 * | 0.01 * | 0.00 | 0.65 |
| | RLD | 0 | 6.22 | -0.25 * | 0.24 * | 0.06 * | 0.00 | -0.08 * | 0.20 * | 0.01 | 0.29 |
| | RLD | 10 | 2.28 | 0.02 | 0.03 * | 0.03 * | -0.03 * | -0.01 * | 0.01 * | 0.00 * | 0.31 |
| | LLD | 0 | 1.49 | -0.01 | 0.04 * | 0.01 * | 0.03 * | 0.00 | -0.01 * | 0.00 * | 0.27 |
| | LLD | 10 | 1.37 | -0.04 * | -0.01 * | 0.01 * | 0.00 | 0.00 | 0.00 | 0.00 | 0.16 |
| $V_A/Q$ | RLD | 0 | 0.80 | 0.03 * | 0.04 * | 0.04 * | 0.01 * | 0.00 | 0.02 * | 0.00 | 0.54 |
| | RLD | 10 | 0.92 | 0.03 * | 0.01 * | 0.04 * | 0.00 | 0.00 | 0.00 * | 0.00 * | 0.39 |
| | LLD | 0 | 117.50 | -0.03 | 0.45 * | 0.17 * | 0.38 * | 0.01 | -0.12 * | 0.01 | 0.25 |
| $P_RO_2$ | LLD | 10 | 115.80 | -0.97 * | -0.19 * | 0.24 * | 0.04 | 0.00 | 0.01 | -0.01 | 0.18 |
| | RLD | 0 | 109.30 | 0.43 * | 1.46 * | 1.22 * | 0.17 * | -0.29 * | 0.59 * | -0.03 | 0.54 |
| | RLD | 10 | 113.00 | 0.86 * | 0.17 * | 1.14 * | 0.02 | 0.03 | 0.05 | -0.03 * | 0.43 |

* $P < 0.05$ compared with zero by 1-tailed unpaired t test.

† Equation: variable = I + ax + by +cz + dxy + eyz +fzx + gxyz . All intercepts are significant

Post:posture; Int:intercept.

Table A9. Coefficients and $R^2$ of multiple linear regression equation † fit to $\dot{Q}$, $\dot{V}_A$, $\dot{V}_A/\dot{Q}$ and $P_RO_2$ data for left lung of dog 3

| | Post | PEEP | Int | a | b | c | d | e | f | g | $R^2$ |
|---|---|---|---|---|---|---|---|---|---|---|---|
| | LLD | 0 | 4.59 | -0.39 * | 0.00 | -0.12 * | 0.10 * | -0.06 * | 0.02 | 0.01 * | 0.47 |
| | LLD | 10 | 3.02 | -0.18 * | -0.02 * | 0.01 | 0.02 * | -0.01 * | -0.01 * | 0.00 * | 0.50 |
| Q | RLD | 0 | 3.75 | -0.18 * | 0.19 * | -0.04 * | -0.06 * | -0.05 * | 0.02 * | 0.00 | 0.36 |
| | RLD | 10 | 1.58 | -0.10 * | -0.01 | -0.05 * | -0.01 * | -0.01 * | 0.00 | 0.00 | 0.48 |
| | LLD | 0 | 4.72 | -0.36 * | 0.08 * | -0.07 * | 0.09 * | -0.08 * | 0.04 * | 0.01 * | 0.41 |
| $V_A$ | LLD | 10 | 3.79 | -0.08 * | -0.04 * | 0.01 | 0.08 * | -0.03 * | -0.02 * | 0.00 * | 0.49 |
| | RLD | 0 | 2.23 | -0.24 * | 0.32 * | 0.01 | 0.01 | -0.03 * | -0.01 * | 0.01 * | 0.60 |
| | RLD | 10 | 1.92 | -0.12 * | -0.04 * | 0.00 | -0.02 * | -0.01 * | 0.01 * | 0.00 * | 0.34 |
| | LLD | 0 | 1.10 | 0.02 | 0.02 * | 0.02 * | 0.01 | -0.01 * | 0.00 * | 0.00 * | 0.31 |
| | LLD | 10 | 1.29 | 0.03 * | 0.00 | 0.00 | 0.00 * | 0.00 * | 0.00 * | 0.00 * | 0.08 |
| $V_A/Q$ | RLD | 0 | 0.59 | -0.03 * | 0.07 * | 0.02 * | 0.01 * | 0.00 | 0.00 * | 0.00 * | 0.68 |
| | RLD | 10 | 1.28 | -0.05 | 0.02 | 0.01 * | 0.00 | 0.00 | 0.01 * | 0.00 * | 0.24 |
| | LLD | 0 | 108.97 | 0.30 | 0.73 * | 0.50 * | 0.53 * | -0.21 * | 0.08 | -0.06 * | 0.32 |
| $P_RO_2$ | LLD | 10 | 113.20 | 0.51 * | -0.06 | 0.06 | 0.02 * | -0.02 * | -0.01 * | 0.00 * | 0.03 |
| | RLD | 0 | 99.00 | -1.74 * | 4.30 * | 1.08 * | 0.34 * | -0.37 * | -0.07 | 0.06 * | 0.78 |
| | RLD | 10 | 123.20 | -1.10 | 0.48 * | 0.23 * | 0.03 * | 0.00 | 0.07 * | 0.03 * | 0.26 |

* $P < 0.05$ compared with zero by 1-tailed unpaired t test.

† Equation: variable = I + ax + by +cz + dxy + eyz +fzx + gxyz . All intercepts are significant

Post:posture; Int:intercept.

Table A 10. Coefficients and $R^2$ of multiple linear regression equation † fit to $\dot{Q}$, $\dot{V}_A$, $\dot{V}_A/\dot{Q}$ and $P_RO_2$ data for whole lung of dog 4

| | Post | PEEP | Int | a | b | c | d | e | f | g | $R^2$ |
|---|---|---|---|---|---|---|---|---|---|---|---|
| | LLD | 0 | 5.95 | -0.33 * | 0.17 * | -0.14 * | -0.04 * | -0.03 * | 0.08 * | 0.01 * | 0.36 |
| | LLD | 10 | 3.45 | -0.12 * | -0.03 * | 0.00 | -0.02 * | -0.01 * | 0.01 * | 0.00 * | 0.33 |
| Q | RLD | 0 | 5.67 | 0.13 * | 0.35 * | -0.14 * | 0.03 * | -0.04 * | 0.00 | 0.00 * | 0.36 |
| | RLD | 10 | 3.70 | -0.12 * | 0.08 * | -0.05 * | 0.00 | -0.02 * | 0.01 * | 0.00 * | 0.30 |
| | LLD | 0 | 7.56 | -0.48 * | 0.64 * | -0.20 * | -0.07 * | -0.07 * | 0.08 * | 0.01 * | 0.50 |
| $V_A$ | LLD | 10 | 4.18 | -0.14 * | 0.01 | 0.05 * | -0.03 * | -0.02 * | 0.01 * | 0.00 * | 0.35 |
| | RLD | 0 | 8.11 | -1.13 * | 0.68 * | -0.29 * | 0.00 | -0.08 * | 0.04 * | 0.01 * | 0.61 |
| | RLD | 10 | 4.10 | -0.05 * | 0.14 * | -0.04 * | -0.01 * | -0.02 * | 0.00 | 0.00 | 0.27 |
| | LLD | 0 | 1.30 | -0.02 * | 0.08 * | 0.01 * | 0.00 | -0.01 * | -0.01 * | 0.00 * | 0.38 |
| | LLD | 10 | 1.23 | 0.00 | 0.01 * | 0.02 * | 0.00 * | 0.00 * | 0.00 | 0.00 * | 0.28 |
| $V_A/Q$ | RLD | 0 | 1.27 | -0.05 * | 0.06 * | 0.00 | 0.00 * | -0.01 * | 0.00 * | 0.00 * | 0.46 |
| | RLD | 10 | 1.10 | 0.02 * | 0.02 * | 0.01 * | 0.00 | 0.00 * | 0.00 * | 0.00 * | 0.24 |
| | LLD | 0 | 123.60 | -0.43 * | 1.12 * | 0.36 * | 0.06 * | -0.17 * | -0.07 * | -0.01 | 0.58 |
| $P_RO_2$ | LLD | 10 | 121.10 | 0.03 | 0.21 * | 0.43 * | -0.03 * | -0.08 * | 0.00 | 0.00 | 0.35 |
| | RLD | 0 | 120.15 | -0.90 * | 1.14 * | 0.07 | 0.08 * | -0.15 * | -0.02 | -0.02 * | 0.51 |
| | RLD | 10 | 121.00 | 0.40 * | 0.36 * | 0.19 * | -0.03 * | -0.04 * | -0.02 * | 0.00 | 0.34 |

* $P < 0.05$ compared with zero by 1-tailed unpaired t test.

† Equation: variable = I + ax + by +cz + dxy + eyz +fzx + gxyz . All intercepts are significant

Post:posture; Int:intercept.

Table A 11. Coefficients and $R^2$ of multiple linear regression equation † fit to $\dot{Q}$, $\dot{V}_A$, $\dot{V}_A/\dot{Q}$ and $P_RO_2$ data for right lung of dog 4

| | Post | PEEP | Int | a | b | c | d | e | f | g | $R^2$ |
|---|---|---|---|---|---|---|---|---|---|---|---|
| | LLD | 0 | 5.66 | -0.47 * | -0.02 | 0.02 | 0.03 * | -0.02 * | 0.00 | 0.01 * | 0.28 |
| | LLD | 10 | 3.14 | -0.14 * | -0.10 * | 0.02 * | 0.00 | 0.00 | 0.01 * | 0.00 * | 0.29 |
| Q | RLD | 0 | 5.74 | 0.29 * | 0.19 * | -0.13 * | 0.00 | -0.05 * | 0.06 * | 0.00 | 0.32 |
| | RLD | 10 | 4.16 | -0.06 * | 0.06 * | -0.07 * | 0.00 | -0.02 * | 0.02 * | 0.00 | 0.20 |
| | LLD | 0 | 7.48 | -0.86 * | 0.35 * | -0.08 * | -0.03 * | -0.07 * | 0.00 | 0.01 * | 0.67 |
| $V_A$ | LLD | 10 | 4.00 | -0.27 * | -0.11 * | 0.05 * | 0.00 | -0.02 * | 0.01 * | 0.00 * | 0.32 |
| | RLD | 0 | 11.40 | -1.19 * | 0.64 * | -0.34 * | 0.01 | -0.15 * | 0.19 * | 0.01 * | 0.42 |
| | RLD | 10 | 4.43 | 0.03 | 0.13 * | -0.04 * | -0.01 * | -0.03 * | 0.02 * | 0.00 | 0.26 |
| | LLD | 0 | 1.36 | -0.02 | 0.08 * | -0.03 * | -0.01 | -0.01 * | 0.00 | 0.00 * | 0.02 |
| | LLD | 10 | 1.25 | -0.03 * | 0.00 | 0.01 * | 0.00 | 0.00 * | 0.00 | 0.00 | 0.24 |
| $V_A/Q$ | RLD | 0 | 1.41 | -0.01 | 0.04 * | 0.01 * | 0.00 | -0.01 * | 0.00 * | 0.00 | 0.30 |
| | RLD | 10 | 1.10 | 0.02 * | 0.02 * | 0.01 * | 0.00 | 0.00 | 0.00 | 0.00 | 0.30 |
| | LLD | 0 | 124.30 | -0.53 * | 1.03 * | -0.10 * | 0.04 | -0.17 * | -0.03 | -0.04 * | 0.60 |
| $P_RO_2$ | LLD | 10 | 122.20 | -0.46 * | -0.01 | 0.26 * | 0.04 * | -0.08 * | -0.01 | -0.01 * | 0.31 |
| | RLD | 0 | 123.20 | -0.22 * | 0.68 * | 0.18 * | 0.00 | -0.11 * | 0.10 * | 0.00 | 0.34 |
| | RLD | 10 | 120.30 | 0.38 * | 0.44 * | 0.28 * | -0.04 * | -0.04 * | 0.02 | 0.00 | 0.38 |

* $P < 0.05$ compared with zero by 1-tailed unpaired t test.

† Equation: variable = I + ax + by +cz + dxy + eyz +fzx + gxyz . All intercepts are significant

Post:posture; Int:intercept.

Table A 12. Coefficients and $R^2$ of multiple linear regression equation † fit to $\dot{Q}$, $\dot{V}_A$, $\dot{V}_A/\dot{Q}$ and $P_RO_2$ data for left lung of dog 4

| | Post | PEEP | Int | a | b | c | d | e | f | g | $R^2$ |
|---|---|---|---|---|---|---|---|---|---|---|---|
| | LLD | 0 | 6.97 | -0.58 * | 0.44 * | -0.38 * | 0.21 * | -0.13 * | 0.13 * | 0.02 * | 0.56 |
| | LLD | 10 | 4.10 | -0.14 * | 0.13 * | -0.05 * | 0.03 * | -0.03 * | 0.00 | 0.00 * | 0.44 |
| Q | RLD | 0 | 5.98 | 0.29 * | 0.45 * | -0.15 * | -0.05 * | -0.06 * | 0.00 | -0.01 * | 0.49 |
| | RLD | 10 | 3.23 | -0.10 * | 0.06 * | -0.03 * | -0.04 * | -0.02 * | 0.01 * | 0.00 * | 0.21 |
| | LLD | 0 | 8.10 | -0.88 * | 0.65 * | -0.29 * | 0.27 * | -0.18 * | 0.11 * | 0.04 * | 0.54 |
| $V_A$ | LLD | 10 | 4.80 | -0.05 | 0.26 * | -0.02 | 0.06 * | -0.04 * | 0.00 | 0.00 | 0.55 |
| | RLD | 0 | 3.93 | -0.50 * | 0.46 * | -0.14 * | -0.06 * | -0.06 * | 0.00 | 0.01 * | 0.43 |
| | RLD | 10 | 3.87 | -0.06 * | 0.10 * | -0.02 * | -0.04 * | -0.03 * | 0.01 * | 0.00 | 0.25 |
| | LLD | 0 | 1.22 | -0.06 * | 0.03 * | 0.04 * | 0.02 * | -0.01 * | -0.05 * | 0.00 | 0.30 |
| | LLD | 10 | 1.30 | 0.03 * | 0.03 * | 0.02 * | 0.01 * | 0.00 * | 0.00 | 0.00 * | 0.49 |
| $V_A/Q$ | RLD | 0 | 1.10 | -0.06 * | 0.05 * | -0.01 * | 0.00 | -0.01 * | 0.00 | 0.00 * | 0.39 |
| | RLD | 10 | 1.21 | 0.02 | 0.02 * | 0.00 | 0.00 | 0.00 * | 0.00 | 0.00 * | 0.13 |
| | LLD | 0 | 122.90 | -1.16 * | 0.84 * | 0.79 * | 0.71 * | -0.26 * | -0.04 | 0.01 | 0.67 |
| $P_RO_2$ | LLD | 10 | 121.60 | 0.42 * | 0.77 * | 0.46 * | 0.29 * | -0.15 * | 0.01 | -0.02 * | 0.61 |
| | RLD | 0 | 117.60 | -1.36 * | 1.46 * | -0.06 | -0.12 | -0.27 * | 0.08 * | 0.02 | 0.49 |
| | RLD | 10 | 122.50 | 0.20 | 0.29 * | 0.09 * | 0.00 | -0.07 * | 0.00 | -0.01 * | 0.19 |

* $P < 0.05$ compared with zero by 1-tailed unpaired t test.

† Equation: variable = I + ax + by +cz + dxy + eyz +fzx + gxyz . All intercepts are significant

Post:posture; Int:intercept.

Table A 13. Coefficients and $R^2$ of multiple linear regression equation † fit to $\dot{Q}$, $\dot{V}_A$, $\dot{V}_A/\dot{Q}$ and $P_RO_2$ data for whole lung of dog 5

| | Post | PEEP | Int | a | b | c | d | e | f | g | $R^2$ |
|---|---|---|---|---|---|---|---|---|---|---|---|
| | LLD | 0 | 6.41 | -0.28 * | 0.20 * | -0.05 * | -0.063 * | -0.023 * | 0.063 * | 0.006 * | 0.44 |
| | LLD | 10 | 2.82 | -0.06 * | -0.03 * | -0.01 * | -0.018 * | -0.009 * | 0.009 * | 0.001 * | 0.35 |
| Q | RLD | 0 | 7.00 | -0.84 * | 0.20 * | -0.01 * | 0.010 * | -0.026 * | -0.012 * | 0.002 | 0.68 |
| | RLD | 10 | 3.18 | -0.18 * | -0.03 * | 0.02 * | -0.002 | -0.005 * | -0.009 * | 0.000 | 0.65 |
| | LLD | 0 | 5.06 | -0.10 * | 0.51 * | -0.05 * | -0.070 * | -0.032 * | 0.034 * | 0.003 * | 0.49 |
| $V_A$ | LLD | 10 | 2.76 | -0.04 * | 0.00 | 0.03 * | -0.036 * | -0.003 * | 0.009 * | 0.001 * | 0.32 |
| | RLD | 0 | 5.71 | -0.70 * | 0.57 * | -0.09 * | -0.017 * | -0.030 * | -0.009 * | -0.002 | 0.63 |
| | RLD | 10 | 2.58 | -0.14 * | 0.02 * | 0.02 * | -0.015 * | 0.004 * | -0.011 * | -0.002 * | 0.41 |
| | LLD | 0 | 0.81 | 0.02 * | 0.05 * | 0.00 | 0.000 | -0.002 * | -0.005 * | 0.000 | 0.42 |
| | LLD | 10 | 0.98 | 0.03 | 0.01 * | 0.02 * | -0.005 * | 0.002 * | 0.000 | 0.000 * | 0.30 |
| $V_A/Q$ | RLD | 0 | 0.80 | 0.00 | 0.01 * | -0.01 * | 0.001 | -0.001 * | -0.001 * | 0.000 * | 0.47 |
| | RLD | 10 | 0.84 | 0.01 * | 0.02 * | 0.00 | -0.004 * | 0.003 * | -0.001 | 0.000 | 0.13 |
| | LLD | 0 | 113.01 | 0.65 * | 1.37 * | 0.20 * | -0.110 * | -0.090 * | -0.110 * | 0.007 | 0.49 |
| $P_RO_2$ | LLD | 10 | 117.70 | 0.10 * | 0.22 * | 0.37 * | -0.140 * | 0.035 * | 0.007 | 0.006 | 0.32 |
| | RLD | 0 | 108.00 | -0.21 * | 1.53 * | -0.20 * | 0.034 * | -0.075 * | -0.042 * | -0.004 | 0.43 |
| | RLD | 10 | 108.90 | 0.04 | 0.30 * | 0.03 | -0.110 * | 0.066 * | -0.020 | -0.004 | 0.09 |

* $P < 0.05$ compared with zero by 1-tailed unpaired t test.

† Equation: variable = I + ax + by +cz + dxy + eyz +fzx + gxyz . All intercepts are significant

Post:posture; Int:intercept.

Table A 14. Coefficients and $R^2$ of multiple linear regression equation † fit to $\dot{Q}$, $\dot{V}_A$, $\dot{V}_A/\dot{Q}$ and $P_RO_2$ data for right lung of dog 5

| | Post | PEEP | Int | a | b | c | d | e | f | g | $R^2$ |
|---|---|---|---|---|---|---|---|---|---|---|---|
| | LLD | 0 | 6.27 | -0.46 * | 0.02 | 0.06 * | 0.004 | -0.013 * | 0.006 | 0.006 * | 0.41 |
| | LLD | 10 | 2.70 | -0.09 * | -0.10 * | 0.01 | -0.004 | -0.002 * | 0.013 * | 0.000 | 0.49 |
| Q | RLD | 0 | 8.43 | -1.50 * | 0.25 * | 0.11 * | 0.044 * | -0.032 * | 0.006 | 0.000 | 0.64 |
| | RLD | 10 | 3.74 | -0.23 * | -0.03 * | 0.06 * | -0.005 | -0.002 | -0.018 * | 0.000 | 0.52 |
| | LLD | 0 | 5.64 | -0.54 * | 0.31 * | -0.03 * | 0.002 | -0.025 * | -0.043 * | 0.012 * | 0.50 |
| $V_A$ | LLD | 10 | 2.78 | -0.20 * | -0.13 * | 0.03 * | 0.001 | 0.004 * | 0.005 | 0.002 * | 0.46 |
| | RLD | 0 | 6.73 | -1.30 * | 0.71 * | 0.00 | 0.031 * | -0.012 * | -0.005 | -0.013 * | 0.59 |
| | RLD | 10 | 3.10 | -0.07 * | 0.07 * | 0.07 * | -0.030 * | 0.006 * | 0.006 | -0.004 * | 0.30 |
| | LLD | 0 | 0.90 | -0.01 * | 0.05 * | -0.01 * | 0.001 | -0.002 * | -0.009 * | 0.001 * | 0.36 |
| | LLD | 10 | 1.02 | -0.04 * | -0.01 * | 0.01 * | 0.001 | 0.003 * | -0.003 * | 0.001 * | 0.22 |
| $V_A/Q$ | RLD | 0 | 0.79 | -0.01 | 0.06 * | 0.00 | 0.003 * | 0.001 | 0.001 | -0.002 * | 0.50 |
| | RLD | 10 | 0.84 | 0.04 * | 0.03 * | 0.01 * | -0.005 * | 0.002 * | 0.006 * | -0.001 * | 0.34 |
| | LLD | 0 | 116.50 | -0.50 * | 0.89 * | -0.20 * | 0.058 * | -0.053 * | -0.200 * | 0.021 * | 0.36 |
| $P_RO_2$ | LLD | 10 | 118.80 | -0.82 * | -0.26 * | 0.26 * | 0.015 | 0.063 * | -0.034 | 0.011 * | 0.26 |
| | RLD | 0 | 107.40 | -0.72 * | 1.56 * | -0.03 | 0.120 * | -0.029 * | 0.019 | -0.035 * | 0.47 |
| | RLD | 10 | 109.20 | 0.80 * | 0.71 * | 0.16 * | -0.140 * | 0.040 * | 0.150 * | -0.020 * | 0.30 |

* $P < 0.05$ compared with zero by 1-tailed unpaired t test.

† Equation: variable = I + ax + by +cz + dxy + eyz +fzx + gxyz . All intercepts are significant

Post:posture; Int:intercept.

Table A 15. Coefficients and $R^2$ of multiple linear regression equation † fit to $\dot{Q}$, $\dot{V}_A$, $\dot{V}_A/\dot{Q}$ and $P_RO_2$ data for left lung of dog 5

| | Post | PEEP | Int | a | b | c | d | e | f | g | $R^2$ |
|---|---|---|---|---|---|---|---|---|---|---|---|
| | LLD | 0 | 6.85 | -1.15 * | 0.41 * | -0.16 * | -0.086 * | -0.055 * | 0.021 | 0.041 * | 0.60 |
| | LLD | 10 | 3.02 | -0.19 * | 0.06 * | -0.03 * | 0.015 * | -0.016 * | 0.003 | 0.004 * | 0.41 |
| Q | RLD | 0 | 4.47 | 0.03 | 0.08 * | -0.05 * | -0.012 | -0.008 * | 0.000 | 0.000 | 0.14 |
| | RLD | 10 | 2.44 | -0.05 * | -0.05 * | 0.00 | -0.005 | -0.005 * | 0.008 * | -0.003 * | 0.34 |
| | LLD | 0 | 4.26 | -0.89 * | 0.64 * | -0.11 * | -0.120 * | -0.024 * | 0.087 * | 0.007 | 0.66 |
| $V_A$ | LLD | 10 | 2.70 | -0.09 * | 0.18 * | 0.00 | -0.002 | -0.007 * | 0.023 * | 0.004 * | 0.52 |
| | RLD | 0 | 3.50 | -0.07 | 0.34 * | -0.17 * | -0.015 | -0.006 | -0.045 * | 0.010 * | 0.52 |
| | RLD | 10 | 2.02 | -0.14 * | -0.03 * | -0.03 * | -0.005 | -0.003 | 0.007 | -0.002 | 0.26 |
| | LLD | 0 | 0.65 | -0.03 * | 0.05 * | 0.02 * | 0.004 | 0.001 | 0.007 * | -0.004 * | 0.54 |
| | LLD | 10 | 0.92 | 0.03 * | 0.04 * | 0.01 * | -0.002 | 0.002 * | 0.007 * | 0.000 | 0.54 |
| $V_A/Q$ | RLD | 0 | 0.86 | -0.04 * | 0.01 * | -0.01 * | -0.002 | 0.001 | 0.000 * | 0.000 * | 0.09 |
| | RLD | 10 | 0.83 | -0.04 * | 0.00 | -0.01 * | -0.002 | 0.000 | 0.001 | 0.000 | 0.09 |
| | LLD | 0 | 106.80 | -2.21 * | 1.80 * | 0.79 * | 0.420 * | -0.075 * | 0.350 * | -0.120 * | 0.67 |
| $P_RO_2$ | LLD | 10 | 116.00 | 0.47 * | 0.98 * | 0.27 * | -0.022 | 0.019 | 0.140 * | -0.008 | 0.55 |
| | RLD | 0 | 107.50 | -0.41 * | 1.57 * | -0.71 * | -0.022 | -0.014 | -0.290 * | 0.080 * | 0.53 |
| | RLD | 10 | 109.10 | -1.36 * | 0.09 | -0.40 * | -0.130 | 0.015 | 0.030 | 0.006 | 0.10 |

* $P < 0.05$ compared with zero by 1-tailed unpaired t test.

† Equation: variable = I + ax + by +cz + dxy + eyz +fzx + gxyz . All intercepts are significant

Post:posture;Int:intercept

Table A 16. Coefficients and $R^2$ of multiple linear regression equation † fit to $\dot{Q}$, $\dot{V}_A$, $\dot{V}_A/\dot{Q}$ and $P_RO_2$ data for whole lung of dog 6

| | Post | PEEP | Int | a | b | c | d | e | f | g | $R^2$ |
|---|---|---|---|---|---|---|---|---|---|---|---|
| | LLD | 0 | 3.38 | -0.41 * | -0.01 | -0.08 * | 0.002 | -0.021 * | 0.028 * | 0.009 * | 0.65 |
| | LLD | 10 | 2.37 | -0.22 * | -0.04 * | -0.05 * | 0.002 | -0.006 * | 0.001 | 0.003 * | 0.74 |
| Q | RLD | 0 | 3.37 | -0.32 * | 0.01 | -0.08 * | 0.008 * | -0.012 * | 0.014 * | -0.002 * | 0.66 |
| | RLD | 10 | 1.90 | -0.19 * | 0.02 * | -0.01 * | 0.003 * | -0.011 | -0.004 * | -0.002 * | 0.62 |
| | LLD | 0 | 3.39 | -0.24 * | 0.22 * | -0.01 * | -0.047 * | -0.045 * | 0.018 * | 0.011 * | 0.44 |
| $V_A$ | LLD | 10 | 2.45 | -0.05 * | 0.02 * | -0.02 * | -0.025 * | -0.011 * | -0.001 | 0.003 * | 0.30 |
| | RLD | 0 | 5.00 | -0.19 * | 0.09 * | -0.11 * | -0.008 | -0.026 * | 0.002 | 0.008 * | 0.21 |
| | RLD | 10 | 2.70 | -0.14 * | 0.02 * | -0.03 * | 0.003 | -0.007 * | -0.003 * | 0.000 | 0.75 |
| | LLD | 0 | 1.09 | 0.05 * | 0.08 * | 0.02 * | -0.009 * | -0.007 * | 0.000 | -0.003 | 0.50 |
| | LLD | 10 | 1.18 | 0.08 * | 0.03 * | 0.01 * | -0.010 * | -0.003 * | 0.002 * | 0.000 | 0.53 |
| $V_A/Q$ | RLD | 0 | 1.64 | 0.11 * | 0.02 * | -0.01 * | 0.001 | 0.000 | 0.000 | 0.004 * | 0.48 |
| | RLD | 10 | 1.50 | 0.07 * | -0.01 * | -0.01 * | -0.002 * | -0.001 | 0.003 * | 0.001 * | 0.41 |
| | LLD | 0 | 107.80 | 1.80 * | 2.54 * | 0.70 * | -0.400 * | -0.410 * | -0.040 | 0.060 * | 0.61 |
| $P_RO_2$ | LLD | 10 | 112.94 | 2.01 * | 0.93 * | 0.42 * | -0.290 * | -0.140 * | 0.004 | 0.026 * | 0.63 |
| | RLD | 0 | 118.90 | 1.40 * | 0.54 * | 0.01 | -0.079 * | -0.077 * | -0.048 * | 0.060 * | 0.58 |
| | RLD | 10 | 116.10 | 1.18 * | -0.19 * | -0.09 * | -0.036 * | -0.046 * | 0.039 * | 0.023 * | 0.40 |

* $P < 0.05$ compared with zero by 1-tailed unpaired t test.

† Equation: variable = I + ax + by +cz + dxy + eyz +fzx + gxyz . All intercepts are significant

Post:posture; Int:intercept.

Table A 17. Coefficients and $R^2$ of multiple linear regression equation † fit to $\dot{Q}$, $\dot{V}_A$, $\dot{V}_A/\dot{Q}$ and $P_RO_2$ data for right lung of dog 6

| | Post | PEEP | Int | a | b | c | d | e | f | g | $R^2$ |
|---|---|---|---|---|---|---|---|---|---|---|---|
| | LLD | 0 | 2.44 | -0.22 * | -0.04 * | -0.02 * | -0.017 * | -0.002 | 0.009 * | 0.000 | 0.39 |
| | LLD | 10 | 1.61 | -0.14 * | -0.05 * | -0.04 * | -0.004 * | 0.002 * | 0.000 | 0.000 | 0.53 |
| Q | RLD | 0 | 4.11 | -0.51 * | -0.01 | -0.09 * | 0.024 * | -0.015 * | 0.033 * | 0.001 | 0.58 |
| | RLD | 10 | 2.39 | -0.23 * | 0.00 | 0.01 * | 0.008 * | 0.003 * | -0.005 * | -0.001 * | 0.50 |
| | LLD | 0 | 3.09 | -0.28 * | 0.06 * | -0.01 | -0.052 * | -0.025 * | 0.011 * | 0.002 | 0.42 |
| $V_A$ | LLD | 10 | 2.33 | -0.14 * | -0.09 * | -0.04 * | -0.025 * | -0.002 | 0.006 * | 0.001 | 0.42 |
| | RLD | 0 | 5.19 | -0.55 * | 0.18 * | -0.05 * | 0.092 * | -0.060 * | 0.003 | 0.008 * | 0.29 |
| | RLD | 10 | 3.04 | -0.14 * | -0.01 | -0.02 * | 0.020 * | -0.007 * | -0.012 * | 0.000 | 0.21 |
| | LLD | 0 | 1.27 | -0.01 | 0.04 * | 0.01 * | -0.007 * | -0.009 * | -0.002 | 0.000 | 0.30 |
| | LLD | 10 | 1.47 | 0.04 * | -0.01 * | 0.01 * | -0.012 * | -0.002 * | 0.004 * | 0.000 | 0.11 |
| $V_A/Q$ | RLD | 0 | 1.30 | 0.04 * | 0.06 * | 0.01 * | 0.028 * | -0.012 * | -0.005 * | 0.001 | 0.54 |
| | RLD | 10 | 1.32 | 0.07 * | 0.00 | -0.02 * | 0.008 * | -0.005 * | -0.001 | 0.001 * | 0.38 |
| | LLD | 0 | 114.70 | -0.03 | 0.91 * | 0.22 * | -0.140 * | -0.270 * | -0.030 | 0.000 | 0.37 |
| $P_RO_2$ | LLD | 10 | 120.90 | 0.49 * | -0.26 * | 0.20 * | -0.190 * | -0.023 | 0.094 * | 0.009 | 0.14 |
| | RLD | 0 | 113.73 | 0.18 | 1.22 * | 0.41 * | 0.380 * | -0.300 * | -0.085 * | 0.033 * | 0.56 |
| | RLD | 10 | 112.80 | 1.43 * | -0.09 | -0.28 * | 0.140 * | -0.125 * | -0.044 * | 0.018 * | 0.34 |

* $P < 0.05$ compared with zero by 1-tailed unpaired t test.

† Equation: variable = I + ax + by +cz + dxy + eyz +fzx + gxyz . All intercepts are significant

Post:posture; Int:intercept.

Table A 18. Coefficients and $R^2$ of multiple linear regression equation † fit to $\dot{Q}$, $\dot{V}_A$, $\dot{V}_A/\dot{Q}$ and $P_RO_2$ data for left lung of dog 6

| | Post | PEEP | Int | a | b | c | d | e | f | g | $R^2$ |
|---|---|---|---|---|---|---|---|---|---|---|---|
| | LLD | 0 | 4.71 | -1.00 * | 0.00 | -0.09 * | 0.112 * | -0.080 * | 0.018 * | 0.030 * | 0.67 |
| | LLD | 10 | 3.30 | -0.30 * | -0.05 * | -0.04 * | 0.014 | -0.023 * | -0.005 | 0.003 * | 0.63 |
| Q | RLD | 0 | 2.36 | -0.13 * | -0.01 | -0.04 * | -0.021 * | -0.020 * | 0.013 * | 0.000 | 0.43 |
| | RLD | 10 | 1.20 | -0.08 * | 0.01 * | -0.01 * | -0.001 | -0.006 * | 0.001 | 0.000 | 0.30 |
| | LLD | 0 | 3.67 | -0.78 * | 0.29 * | 0.03 * | 0.070 * | -0.110 * | 0.002 | 0.036 * | 0.63 |
| $V_A$ | LLD | 10 | 2.53 | -0.11 * | 0.10 * | 0.01 | 0.011 | -0.032 * | -0.004 | 0.000 | 0.36 |
| | RLD | 0 | 4.40 | -0.07 * | -0.10 * | -0.09 * | 0.045 * | 0.000 | 0.030 * | 0.004 | 0.41 |
| | RLD | 10 | 2.08 | -0.05 * | -0.04 * | -0.01 * | 0.010 | -0.006 * | 0.012 * | 0.003 * | 0.37 |
| | LLD | 0 | 0.84 | -0.02 * | 0.11 * | 0.03 * | -0.004 | -0.013 * | 0.000 | 0.001 | 0.55 |
| | LLD | 10 | 0.78 | 0.04 * | 0.05 * | 0.01 * | 0.001 | -0.003 * | 0.001 * | -0.002 * | 0.53 |
| $V_A/Q$ | RLD | 0 | 1.91 | 0.09 * | -0.03 * | 0.00 | 0.040 * | 0.017 * | 0.002 | 0.003 * | 0.22 |
| | RLD | 10 | 1.80 | 0.08 * | -0.04 * | 0.01 * | 0.004 | 0.003 * | 0.008 * | 0.003 * | 0.17 |
| | LLD | 0 | 93.00 | -0.33 | 7.86 * | 0.54 | -0.420 * | -0.840 * | 0.190 * | 0.024 | 0.64 |
| $P_RO_2$ | LLD | 10 | 102.90 | 1.35 * | 2.13 * | 0.70 * | 0.120 | -0.290 * | -0.034 | -0.058 * | 0.58 |
| | RLD | 0 | 123.50 | 0.89 * | -0.36 * | -0.11 * | 0.380 * | 0.140 * | 0.014 | 0.034 * | 0.26 |
| | RLD | 10 | 120.80 | 0.88 * | -0.72 * | 0.11 * | 0.008 | 0.020 | 0.150 * | 0.058 * | 0.23 |

* $P < 0.05$ compared with zero by 1-tailed unpaired t test.

† Equation: variable = I + ax + by +cz + dxy + eyz +fzx + gxyz . All intercepts are significant

Post:posture; Int:intercept.

Table A19. Coefficients and $R^2$ of multiple linear regression equation † fit to $\dot{Q}$, $\dot{V}_A$, $\dot{V}_A/\dot{Q}$ and $P_RO_2$ data for whole lung of dog 7 with and without unilateral dependent PEEP in left lateral decubitus posture

| | PEEP | Int | a | b | c | d | e | f | g | $R^2$ |
|---|---|---|---|---|---|---|---|---|---|---|
| | 0 | 3.74 | -0.39 * | -0.27 * | -0.10 * | 0.065 * | 0.024 | 0.031 * | 0.000 | 0.60 |
| | 5s | 3.26 | -0.15 * | -0.18 * | -0.08 * | 0.031 * | -0.008 * | 0.015 * | 0.002 | 0.52 |
| Q | 10s | 2.60 | -0.03 * | -0.02 | -0.16 * | 0.012 * | -0.018 * | -0.020 * | -0.001 | 0.35 |
| | 10 | 2.32 | -0.29 * | -0.14 * | -0.03 * | 0.024 * | -0.009 * | 0.000 | 0.002 * | 0.78 |
| | 0 | 6.76 | -0.57 * | -0.55 * | -0.76 * | 0.120 * | -0.006 | 0.010 | -0.001 | 0.43 |
| $V_A$ | 5s | 5.35 | -0.23 * | -0.35 * | -0.16 * | 0.054 * | -0.200 * | -0.001 | 0.001 | 0.41 |
| | 10s | 5.26 | 0.09 * | 0.12 * | -0.32 * | 0.045 * | -0.060 * | -0.036 * | -0.006 * | 0.30 |
| | 10 | 3.83 | -0.32 * | -0.24 * | -0.04 * | 0.022 * | -0.014 * | 0.015 * | 0.004 * | 0.56 |
| | 0 | 1.90 | 0.03 * | 0.00 | 0.02 * | 0.006 * | 0.002 | -0.015 * | -0.001 | 0.14 |
| | 5s | 1.65 | -0.05 | 0.00 | -0.01 * | 0.001 | -0.001 | -0.013 * | -0.002 * | 0.14 |
| $V_A/Q$ | 10s | 1.90 | 0.03 * | 0.10 * | -0.05 * | 0.011 * | -0.004 * | -0.002 | -0.001 | 0.12 |
| | 10 | 1.89 | 0.09 * | 0.00 | 0.01 | -0.009 * | 0.002 * | 0.012 * | 0.001 * | 0.41 |
| | 0 | 126.60 | 0.42 * | -0.14 * | 0.11 * | 0.087 * | -0.002 | -0.093 * | -0.002 | 0.15 |
| $P_RO_2$ | 5s | 122.00 | -0.12 | -0.09 | -0.33 * | 0.048 * | -0.048 * | -0.200 * | -0.023 * | 0.23 |
| | 10s | 119.00 | -0.51 * | 1.24 * | -1.34 * | 0.280 * | -0.040 | -0.240 * | -0.010 | 0.20 |
| | 10 | 124.10 | 1.03 * | 0.01 | -0.04 | -0.065 * | 0.030 * | 0.150 * | 0.020 * | 0.50 |

* $P < 0.05$ compared with zero by 1-tailed unpaired t test.

† Equation: variable = I + ax + by +cz + dxy + eyz +fzx + gxyz . All intercepts are significant

Int: intercept. 5s: 5 cm $H_2O$ selective unilateral dependent PEEP. 10s:10 cm $H_2O$ selective unilateral dependent PEEP. 10: 10 cm $H_2O$ bilateral PEEP.

Table A20. Coefficients and $R^2$ of multiple linear regression equation † fit to $\dot{Q}$, $\dot{V}_A$, $\dot{V}_A/\dot{Q}$ and $P_RO_2$ data for right lung of dog 7 with and without unilateral dependent PEEP in left lateral decubitus posture

| | PEEP | Int | a | b | c | d | e | f | g | $R^2$ |
|---|---|---|---|---|---|---|---|---|---|---|
| | 0 | 2.64 | -0.24 * | -0.11 * | -0.02 * | 0.025 * | -0.011 * | 0.010 * | -0.001 | 0.51 |
| | 5s | 2.90 | -0.21 * | -0.12 * | -0.06 * | 0.045 * | -0.008 * | 0.012 * | -0.002 | 0.50 |
| Q | 10s | 3.10 | -0.28 * | 0.01 | -0.27 * | 0.063 * | -0.035 * | 0.018 * | 0.003 | 0.53 |
| | 10 | 1.11 | -0.11 * | -0.05 * | -0.02 * | -0.001 | -0.005 * | 0.002 | -0.001 * | 0.59 |
| | 0 | 4.92 | -0.29 * | -0.20 * | -0.08 * | 0.038 * | -0.022 * | 0.007 | -0.006 * | 0.33 |
| $V_A$ | 5s | 4.70 | -0.25 * | -0.20 * | -0.19 * | 0.085 * | -0.024 * | -0.008 | -0.007 * | 0.42 |
| | 10s | 6.40 | -0.49 * | 0.27 * | -0.51 * | 0.200 * | -0.110 * | -0.006 | 0.010 | 0.40 |
| | 10 | 2.35 | -0.15 * | -0.15 * | 0.02 * | -0.019 * | -0.007 * | 0.011 * | -0.003 * | 0.49 |
| | 0 | 1.90 | 0.06 * | 0.02 * | -0.02 * | -0.004 | 0.000 | -0.005 * | -0.001 | 0.10 |
| | 5s | 1.60 | 0.04 * | 0.01 * | -0.05 * | 0.000 | -0.006 * | -0.011 * | -0.001 | 0.29 |
| $V_A/Q$ | 10s | 1.90 | 0.05 * | 0.15 * | -0.07 * | 0.026 * | -0.013 * | 0.005 | 0.003 | 0.27 |
| | 10 | 2.17 | 0.05 * | -0.03 * | 0.04 * | -0.016 * | 0.004 * | 0.011 * | 0.001 | 0.13 |
| | 0 | 127.40 | 0.56 * | 0.14 * | -0.18 * | -0.011 | -0.014 | -0.048 * | -0.007 | 0.13 |
| $P_RO_2$ | 5s | 121.40 | 0.57 * | 0.20 * | -0.94 * | -0.010 | -0.100 * | -0.150 * | -0.040 * | 0.36 |
| | 10s | 118.10 | 0.97 * | 2.37 * | -2.46 * | 0.320 * | -0.180 * | 0.200 * | 0.050 | 0.37 |
| | 10 | 127.40 | 0.30 * | -0.30 * | 0.35 * | -0.130 * | 0.047 * | 0.088 * | 0.010 * | 0.19 |

* $P < 0.05$ compared with zero by 1-tailed unpaired t test.

† Equation: variable = I + ax + by +cz + dxy + eyz +fzx + gxyz . All intercepts are significant

Int: intercept. 5s: 5 cm $H_2O$ selective unilateral dependent PEEP. 10s:10 cm $H_2O$ selective unilateral dependent PEEP. 10: 10 cm $H_2O$ bilateral PEEP.

Table A21. Coefficients and $R^2$ of multiple linear regression equation † fit to $\dot{Q}$, $\dot{V}_A$, $\dot{V}_A/\dot{Q}$ and $P_RO_2$ data for left lung of dog 7 with and without unilateral dependent PEEP in left lateral decubitus posture

| | PEEP | Int | a | b | c | d | e | f | g | $R^2$ |
|---|---|---|---|---|---|---|---|---|---|---|
| | 0 | 6.20 | 0.09 | -0.30 * | -0.33 * | 0.310 * | -0.073 * | 0.160 | 0.023 * | 0.44 |
| | 5s | 4.19 | 0.09 | -0.20 * | -0.17 * | 0.140 * | -0.040 * | 0.005 | 0.010 * | 0.50 |
| Q | 10s | 2.20 | -0.20 * | -0.13 * | -0.01 * | 0.002 | -0.010 * | 0.000 | 0.003 * | 0.64 |
| | 10 | 4.20 | -0.12 * | -0.18 * | -0.07 * | 0.040 * | -0.031 * | -0.010 * | 0.006 * | 0.56 |
| | 0 | 10.80 | 0.87 * | -0.61 * | -0.45 * | 0.470 * | -0.140 * | 0.090 * | 0.066 * | 0.31 |
| $V_A$ | 5s | 6.98 | 0.57 * | -0.32 * | -0.31 * | 0.120 * | -0.075 * | 0.049 * | 0.027 * | 0.40 |
| | 10s | 4.00 | 0.01 | -0.13 * | -0.12 * | -0.028 | -0.033 * | 0.010 | 0.007 * | 0.37 |
| | 10 | 6.20 | 0.21 * | -0.21 * | -0.21 * | 0.068 * | -0.066 * | 0.005 | 0.010 * | 0.47 |
| | 0 | 1.80 | 0.12 * | -0.02 | 0.04 | 0.007 | -0.002 | 0.022 * | 0.012 * | 0.34 |
| | 5s | 1.68 | 0.11 * | 0.02 | 0.00 | -0.021 | -0.001 | 0.020 * | 0.005 * | 0.27 |
| $V_A/Q$ | 10s | 1.90 | 0.21 * | 0.10 * | -0.07 * | -0.005 | -0.006 * | 0.009 * | 0.002 | 0.21 |
| | 10 | 1.40 | 0.11 * | 0.02 * | -0.04 * | 0.007 | -0.007 * | 0.010 * | 0.003 * | 0.27 |
| | 0 | 125.60 | 1.47 * | -0.47 * | 0.15 * | 0.180 | -0.100 | 0.210 * | 0.099 * | 0.32 |
| $P_RO_2$ | 5s | 122.80 | 1.29 * | 0.06 | -0.06 | -0.220 * | -0.038 | 0.230 * | 0.048 * | 0.24 |
| | 10s | 121.90 | 1.97 * | 0.80 * | -0.91 * | -0.004 | -0.083 * | 0.110 * | 0.030 * | 0.30 |
| | 10 | 119.20 | 1.91 * | 0.18 | -0.80 * | 0.180 * | -0.140 * | 0.210 * | 0.500 * | 0.42 |

* $P < 0.05$ compared with zero by 1-tailed unpaired t test.

† Equation: variable = I + ax + by +cz + dxy + eyz +fzx + gxyz . All intercepts are significant

Int: intercept. 5s: 5 cm $H_2O$ selective unilateral dependent PEEP. 10s:10 cm $H_2O$ selective unilateral dependent PEEP. 10: 10 cm $H_2O$ bilateral PEEP.

Table A22. Coefficients and $R^2$ of multiple linear regression equation † fit to $\dot{Q}$, $\dot{V}_A$, $\dot{V}_A/\dot{Q}$ and $P_RO_2$ data for whole lung of dog 8 with and without unilateral dependent PEEP in left lateral decubitus posture

| | PEEP | Int | a | b | c | d | e | f | g | $R^2$ |
|---|---|---|---|---|---|---|---|---|---|---|
| | 0 | 6.20 | -0.91 * | -0.19 * | -0.18 * | -0.050 * | -0.004 | 0.060 * | 0.003 | 0.58 |
| | 5s | 4.30 | -0.31 * | 0.00 | -0.20 * | 0.004 | -0.020 * | -0.018 * | 0.007 * | 0.46 |
| Q | 10s | 4.30 | 0.17 * | -0.03 | -0.22 * | -0.003 | -0.016 * | -0.036 * | 0.002 * | 0.50 |
| | 10 | 4.45 | -0.79 * | -0.13 * | -0.10 * | 0.020 * | -0.020 * | 0.020 * | 0.008 * | 0.73 |
| | 0 | 7.78 | -1.10 * | 0.09 | -0.29 * | 0.050 * | -0.020 * | 0.049 * | 0.009 | 0.40 |
| $V_A$ | 5s | 5.40 | -0.11 * | 0.19 * | -0.47 * | 0.006 | -0.044 * | -0.050 * | 0.001 | 0.40 |
| | 10s | 5.74 | 0.39 * | 0.07 * | -0.51 * | 0.003 | -0.030 * | -0.100 * | -0.002 | 0.49 |
| | 10 | 3.65 | -0.28 * | -0.09 * | -0.07 * | -0.006 | -0.010 * | 0.025 * | 0.004 * | 0.51 |
| | 0 | 1.28 | 0.03 * | 0.07 * | -0.03 * | 0.011 * | 0.000 | -0.012 * | -0.001 | 0.21 |
| | 5s | 1.20 | 0.01 | 0.03 * | -0.13 * | 0.011 | 0.002 | -0.006 | -0.007 * | 0.13 |
| $V_A/Q$ | 10s | 1.43 | 0.08 * | 0.02 * | -0.02 * | -0.005 * | -0.002 | 0.003 * | -0.001 * | 0.23 |
| | 10 | 1.25 | 0.09 * | 0.01 * | -0.01 * | -0.007 * | 0.000 | 0.006 * | -0.001 * | 0.29 |
| | 0 | 125.20 | 0.42 * | 0.96 * | -0.60 * | 0.150 * | 0.033 | -0.140 * | -0.001 | 0.18 |
| $P_RO_2$ | 5s | 107.50 | -1.83 * | 1.07 * | -4.10 * | 0.210 * | -0.072 | -0.930 * | -0.087 * | 0.53 |
| | 10s | 132.20 | 0.74 * | 0.33 * | -0.26 * | -0.037 | 0.000 | 0.030 * | -0.006 | 0.22 |
| | 10 | 118.90 | 1.99 * | 0.45 * | -0.36 * | -0.120 * | 0.020 | 0.180 * | 0.001 | 0.47 |

* $P < 0.05$ compared with zero by 1-tailed unpaired t test.

† Equation: variable = I + ax + by +cz + dxy + eyz +fzx + gxyz . All intercepts are significant

Int: intercept. 5s: 5 cm $H_2O$ selective unilateral dependent PEEP. 10s:10 cm $H_2O$ selective unilateral dependent PEEP. 10: 10 cm $H_2O$ bilateral PEEP.

Table A23. Coefficients and $R^2$ of multiple linear regression equation † fit to $\dot{Q}$, $\dot{V}_A$, $\dot{V}_A/\dot{Q}$ and $P_RO_2$ data for right lung of dog 8 with and without unilateral dependent PEEP in left lateral decubitus posture

| | PEEP | Int | a | b | c | d | e | f | g | $R^2$ |
|---|---|---|---|---|---|---|---|---|---|---|
| | 0 | 4.10 | -0.29 * | -0.12 * | -0.02 * | -0.042 * | -0.005 | 0.016 * | -0.008 * | 0.39 |
| | 5s | 3.93 | -0.40 * | -0.03 | -0.27 * | -0.002 | -0.017 * | 0.018 * | -0.003 | 0.59 |
| Q | 10s | 5.18 | 0.10 * | -0.06 * | -0.35 * | 0.001 | -0.020 * | 0.006 | -0.007 | 0.51 |
| | 10 | 1.90 | -0.23 * | -0.08 * | -0.02 * | -0.018 * | -0.003 * | 0.010 * | -0.002 * | 0.64 |
| | 0 | 5.20 | -0.11 | 0.18 * | -0.20 * | 0.015 | -0.009 | -0.028 * | 0.001 | 0.16 |
| $V_A$ | 5s | 6.06 | -0.51 * | 0.21 * | -0.68 * | 0.130 * | -0.068 * | -0.001 | 0.018 * | 0.56 |
| | 10s | 7.64 | 0.29 * | 0.07 | -0.84 * | 0.150 * | -0.062 * | -0.081 * | 0.004 | 0.51 |
| | 10 | 2.86 | -0.27 * | -0.14 * | -0.02 * | -0.039 * | -0.009 * | 0.018 * | -0.003 * | 0.52 |
| | 0 | 1.33 | 0.06 * | 0.10 * | -0.05 * | 0.020 * | -0.002 | -0.019 * | 0.002 * | 0.39 |
| | 5s | 1.32 | 0.01 | 0.08 * | -0.15 * | 0.036 * | -0.016 * | -0.021 * | 0.004 * | 0.58 |
| $V_A/Q$ | 10s | 1.72 | -0.04 * | 0.00 | 0.03 * | 0.013 * | -0.005 * | -0.035 * | 0.000 | 0.28 |
| | 10 | 1.56 | 0.03 * | -0.01 * | 0.00 | -0.007 * | -0.004 * | 0.003 | -0.001 | 0.03 |
| | 0 | 125.90 | 0.96 * | 1.34 * | -0.94 * | 0.220 * | 0.030 | -0.220 * | 0.032 * | 0.39 |
| $P_RO_2$ | 5s | 108.60 | -0.04 | 2.10 * | -6.77 * | 1.060 * | -0.410 * | -0.380 * | 0.120 * | 0.70 |
| | 10s | 135.10 | -0.39 | 0.08 | 0.03 | 0.150 | -0.053 | -0.330 * | -0.005 | 0.12 |
| | 10 | 126.10 | 0.24 | -0.14 * | -0.06 | -0.062 * | -0.037 * | 0.020 | -0.008 | 0.03 |

* $P < 0.05$ compared with zero by 1-tailed unpaired t test.

† Equation: variable = I + ax + by +cz + dxy + eyz +fzx + gxyz . All intercepts are significant

Int: intercept. 5s: 5 cm $H_2O$ selective unilateral dependent PEEP. 10s:10 cm $H_2O$ selective unilateral dependent PEEP. 10: 10 cm $H_2O$ bilateral PEEP.

Table A24. Coefficients and $R^2$ of multiple linear regression equation † fit to $\dot{Q}$, $\dot{V}_A$, $\dot{V}_A/\dot{Q}$ and $P_{RO2}$ data for left lung of dog 8 with and without unilateral dependent PEEP in left lateral decubitus posture

| | PEEP | Int | a | b | c | d | e | f | g | $R^2$ |
|---|---|---|---|---|---|---|---|---|---|---|
| | 0 | 10.46 | -1.20 * | -0.20 * | -0.45 * | 0.580 * | -0.130 * | -0.073 | 0.054 * | 0.41 |
| | 5s | 5.10 | -0.56 * | -0.13 * | -0.10 * | 0.100 * | -0.060 * | 0.010 | 0.017 * | 0.46 |
| Q | 10s | 3.29 | -0.21 * | -0.12 * | -0.03 * | 0.032 * | -0.024 * | -0.003 | 0.004 * | 0.47 |
| | 10 | 8.40 | -1.21 * | -0.25 * | -0.20 * | 0.110 * | -0.086 * | 0.019 | 0.026 * | 0.61 |
| | 0 | 11.70 | -1.34 * | 0.10 | -0.58 * | 0.220 | -0.170 * | 0.280 * | 0.090 * | 0.33 |
| $V_A$ | 5s | 4.90 | -0.56 * | -0.03 | -0.21 * | 0.050 | -0.060 * | 0.040 * | 0.026 * | 0.47 |
| | 10s | 3.74 | -0.23 * | -0.07 * | -0.08 * | 0.040 * | -0.026 * | -0.005 | 0.005 * | 0.32 |
| | 10 | 5.06 | -0.36 * | -0.12 * | -0.17 * | 0.080 * | -0.055 * | 0.009 | 0.016 * | 0.43 |
| | 0 | 1.06 | 0.04 | 0.04 * | -0.01 | -0.055 * | 0.008 * | 0.049 * | 0.001 | 0.27 |
| | 5s | 0.94 | 0.75 | 0.73 * | -1.14 * | -0.015 | -0.008 * | 0.230 * | 0.080 * | 0.22 |
| $V_A/Q$ | 10s | 1.13 | 0.00 | 0.03 * | -0.02 * | -0.003 | 0.005 * | -0.001 | 0.000 | 0.05 |
| | 10 | 0.76 | -0.02 | 0.01 | -0.02 * | -0.003 | 0.005 * | 0.005 | 0.000 | 0.05 |
| | 0 | 122.50 | 0.71 | 0.50 * | -0.51 * | -0.480 * | 0.026 | 0.710 * | 0.043 | 0.15 |
| $P_{RO2}$ | 5s | 113.00 | 0.75 | 0.73 * | -1.14 * | -0.150 | -0.008 | 0.230 * | 0.080 * | 0.22 |
| | 10s | 129.50 | 0.15 | 0.46 * | -0.36 * | 0.092 | 0.010 | 0.016 | 0.006 | 0.11 |
| | 10 | 108.60 | 0.08 | 0.03 | -0.79 * | 0.140 | -0.014 | 0.130 | 0.043 | 0.14 |

* $P < 0.05$ compared with zero by 1-tailed unpaired t test.

† Equation: variable = I + ax + by +cz + dxy + eyz +fzx + gxyz . All intercepts are significant

Int: intercept. 5s: 5 cm $H_2O$ selective unilateral dependent PEEP. 10s:10 cm $H_2O$ selective unilateral dependent PEEP. 10: 10 cm $H_2O$ bilateral PEEP

Table A25. Coefficients and $R^2$ of multiple linear regression equation † fit to $\dot{Q}$, $\dot{V}_A$, $\dot{V}_A/\dot{Q}$ and $P_RO_2$ data for whole lung of dog 9 with and without unilateral dependent PEEP in left lateral decubitus posture

| | PEEP | Int | a | b | c | d | e | f | g | $R^2$ |
|---|---|---|---|---|---|---|---|---|---|---|
| | 0 | 4.36 | -0.64 * | 0.10 * | -0.16 * | -0.010 | -0.043 * | 0.061 * | 0.014 * | 0.66 |
| | 5s | 3.25 | -0.17 * | 0.10 * | -0.07 * | -0.016 * | -0.023 * | 0.028 * | 0.005 * | 0.38 |
| Q | 10s | 3.37 | 0.22 * | 0.01 | -0.06 * | -0.017 * | -0.014 * | 0.016 * | 0.003 * | 0.48 |
| | 10 | 2.52 | -0.30 * | 0.01 * | -0.05 * | -0.001 | -0.014 * | 0.003 * | 0.004 * | 0.75 |
| | 0 | 5.73 | -0.81 * | 0.23 * | -0.13 * | 0.010 | -0.088 * | 0.034 * | 0.030 * | 0.53 |
| $V_A$ | 5s | 4.30 | -0.14 * | 0.25 * | -0.08 * | 0.023 * | -0.053 * | 0.020 * | 0.013 * | 0.31 |
| | 10s | 3.95 | 0.10 * | 0.10 * | -0.03 * | -0.016 * | -0.019 * | 0.010 * | 0.000 | 0.08 |
| | 10 | 2.86 | -0.21 * | 0.00 | -0.03 * | -0.001 | -0.023 * | 0.002 | 0.006 * | 0.47 |
| | 0 | 1.37 | 0.01 | 0.03 * | 0.01 * | 0.013 * | -0.009 * | -0.012 * | 0.002 * | 0.29 |
| | 5s | 1.32 | 0.04 * | 0.06 * | 0.00 | 0.012 * | -0.009 * | -0.003 * | 0.002 * | 0.25 |
| $V_A/Q$ | 10s | 1.38 | -0.01 * | 0.03 * | 0.02 * | 0.000 | -0.004 * | -0.005 * | -0.001 | 0.15 |
| | 10 | 1.31 | 0.06 * | 0.00 | 0.01 * | 0.000 | -0.005 * | 0.002 | 0.001 * | 0.25 |
| | 0 | 124.20 | 0.10 | 0.82 * | 0.43 * | 0.08 * | -0.26 * | -0.19 * | 0.05 * | 0.42 |
| $P_RO_2$ | 5s | 122.00 | 0.88 * | 1.33 * | 0.15 * | 0.05 | -0.28 * | 0.01 | 0.04 * | 0.43 |
| | 10s | 122.90 | 0.02 | 0.63 * | 0.35 * | -0.01 | -0.15 * | -0.08 * | 0.00 | 0.24 |
| | 10 | 123.20 | 1.04 * | 0.21 * | 0.37 * | -0.03 | -0.13 * | 0.03 * | 0.03 * | 0.38 |

* $P < 0.05$ compared with zero by 1-tailed unpaired t test.

† Equation: variable = I + ax + by +cz + dxy + eyz +fzx + gxyz . All intercepts are significant

Int: intercept. 5s: 5 cm $H_2O$ selective unilateral dependent PEEP. 10s:10 cm $H_2O$ selective unilateral dependent PEEP. 10: 10 cm $H_2O$ bilateral PEEP.

Table A26. Coefficients and $R^2$ of multiple linear regression equation † fit to $\dot{Q}$, $\dot{V}_A$, $\dot{V}_A/\dot{Q}$ and $P_RO_2$ data for right lung of dog 9 with and without unilateral dependent PEEP in left lateral decubitus posture

| | PEEP | Int | a | b | c | d | e | f | g | $R^2$ |
|---|---|---|---|---|---|---|---|---|---|---|
| | 0 | 3.09 | -0.39 * | 0.03 * | -0.05 * | -0.025 * | -0.015 * | 0.029 * | 0.004 * | 0.62 |
| | 5s | 3.10 | -0.30 * | 0.07 * | -0.02 * | -0.024 * | -0.019 * | 0.019 * | 0.003 | 0.40 |
| Q | 10s | 4.23 | 0.00 | -0.02 | -0.01 | -0.035 * | -0.010 * | 0.019 * | 0.001 | 0.08 |
| | 10 | 1.56 | -0.16 * | -0.01 | -0.04 * | -0.007 * | -0.003 * | 0.009 * | 0.000 | 0.67 |
| | 0 | 4.30 | -0.54 * | 0.16 * | -0.08 * | -0.100 | -0.033 * | -0.011 | 0.018 * | 0.37 |
| $V_A$ | 5s | 4.56 | -0.61 * | 0.37 * | -0.06 * | -0.073 * | -0.045 * | -0.009 | 0.016 * | 0.52 |
| | 10s | 4.67 | -0.59 * | 0.10 * | 0.00 | -0.047 * | -0.025 * | -0.009 | 0.006 | 0.39 |
| | 10 | 2.30 | -0.21 * | -0.03 * | -0.02 * | -0.011 * | -0.011 * | -0.004 | 0.002 * | 0.31 |
| | 0 | 1.43 | 0.01 | 0.05 * | -0.01 * | 0.014 * | -0.005 * | -0.022 * | 0.004 * | 0.27 |
| | 5s | 1.48 | -0.05 * | 0.10 * | -0.01 * | -0.002 | -0.008 * | -0.018 * | 0.004 * | 0.35 |
| $V_A/Q$ | 10s | 1.34 | -0.05 | 0.03 | 0.01 | -0.001 | -0.004 | -0.009 | 0.000 | 0.25 |
| | 10 | 1.54 | 0.01 | -0.01 | 0.02 | 0.001 | -0.004 | -0.007 | 0.001 | 0.08 |
| | 0 | 125.20 | 0.17 | 0.75 * | -0.05 | 0.079 | -0.180 * | -0.390 * | 0.040 * | 0.35 |
| $P_RO_2$ | 5s | 125.10 | -0.43 * | 1.47 * | 0.18 * | -0.043 | -0.240 * | -0.380 * | 0.032 * | 0.55 |
| | 10s | 123.10 | -0.87 * | 0.64 * | 0.26 * | -0.064 | -0.150 * | -0.190 * | -0.004 | 0.32 |
| | 10 | 127.50 | -0.03 | 0.02 | 0.45 * | -0.020 | -0.074 * | -0.097 * | 0.021 * | 0.20 |

* $P < 0.05$ compared with zero by 1-tailed unpaired t test.

† Equation: variable = I + ax + by +cz + dxy + eyz +fzx + gxyz . All intercepts are significant

Int: intercept. 5s: 5 cm $H_2O$ selective unilateral dependent PEEP. 10s:10 cm $H_2O$ selective unilateral dependent PEEP. 10: 10 cm $H_2O$ bilateral PEEP.

Table A27. Coefficients and $R^2$ of multiple linear regression equation † fit to $\dot{Q}$, $\dot{V}_A$, $\dot{V}_A/\dot{Q}$ and $P_RO_2$ data for left lung of dog 9 with and without unilateral dependent PEEP in left lateral decubitus posture

| | PEEP | Int | a | b | c | d | e | f | g | $R^2$ |
|---|---|---|---|---|---|---|---|---|---|---|
| | 0 | 6.50 | -1.50 * | 0.06 | -0.25 * | 0.230 * | -0.150 * | 0.048 * | 0.068 * | 0.67 |
| | 5s | 3.55 | -0.61 * | 0.08 * | -0.09 * | 0.023 | -0.034 * | 0.015 | 0.011 * | 0.52 |
| Q | 10s | 2.26 | -0.19 * | -0.02 * | -0.05 * | 0.015 * | -0.015 * | -0.002 | 0.003 * | 0.46 |
| | 10 | 3.88 | -0.36 * | 0.02 | -0.07 * | 0.038 * | -0.039 * | -0.002 | 0.008 * | 0.54 |
| | 0 | 8.20 | -2.38 * | 0.06 | -0.56 | 0.450 * | -0.280 * | -0.060 * | 0.130 * | 0.68 |
| $V_A$ | 5s | 4.31 | -0.67 * | 0.03 | -0.03 | 0.140 * | -0.087 * | -0.038 * | 0.025 * | 0.54 |
| | 10s | 3.42 | -0.07 | 0.14 * | -0.02 | 0.076 * | -0.015 * | -0.045 * | -0.004 | 0.16 |
| | 10 | 3.92 | -0.29 * | -0.02 | -0.04 * | 0.100 * | -0.060 * | -0.027 * | 0.010 * | 0.49 |
| | 0 | 1.32 | -0.12 * | -0.01 | 0.06 * | 0.046 * | -0.021 * | -0.015 * | 0.010 * | 0.41 |
| | 5s | 1.18 | -0.01 | 0.00 | 0.02 | 0.029 * | -0.014 * | -0.011 | 0.003 | 0.07 |
| $V_A/Q$ | 10s | 1.52 | 0.03 | 0.04 * | 0.02 * | 0.015 * | -0.003 | -0.014 * | -0.002 * | 0.16 |
| | 10 | 1.07 | 0.00 | -0.02 * | 0.02 * | 0.020 * | -0.010 * | -0.008 * | 0.002 * | 0.19 |
| | 0 | 123.60 | -2.10 * | 0.58 * | 1.17 * | 1.440 * | -0.680 * | -0.270 * | 0.190 * | 0.65 |
| $P_RO_2$ | 5s | 119.60 | -0.11 | 1.25 * | 0.11 | 1.200 * | -0.490 * | -0.140 | 0.055 * | 0.36 |
| | 10s | 124.80 | 0.71 * | 0.86 * | 0.34 * | 0.450 * | -0.190 * | -0.200 * | -0.025 | 0.27 |
| | 10 | 119.60 | 0.30 | 0.18 | 0.34 | 0.640 | -0.330 | -0.140 | 0.023 | 0.32 |

* $P < 0.05$ compared with zero by 1-tailed unpaired t test.

† Equation: variable = I + ax + by +cz + dxy + eyz +fzx + gxyz . All intercepts are significant

Int: intercept. 5s: 5 cm $H_2O$ selective unilateral dependent PEEP. 10s:10 cm $H_2O$ selective unilateral dependent PEEP. 10: 10 cm $H_2O$ bilateral PEEP.

Table A28. Coefficients and $R^2$ of multiple linear regression equation † fit to $\dot{Q}$, $\dot{V}_A$, $\dot{V}_A/\dot{Q}$ and $P_RO_2$ data for whole lung of dog 10 with and without unilateral dependent PEEP in left lateral decubitus posture

| | PEEP | Int | a | b | c | d | e | f | g | $R^2$ |
|---|---|---|---|---|---|---|---|---|---|---|
| | 0 | 4.32 | -0.63 * | 0.02 | -0.06 * | 0.020 * | -0.039 * | 0.002 | 0.013 * | 0.34 |
| | 5s | 2.50 | -0.18 * | 0.02 | -0.03 * | 0.003 | -0.008 * | 0.000 | 0.002 * | 0.18 |
| Q | 10s | 2.60 | 0.03 * | 0.05 * | -0.05 * | 0.005 | -0.007 * | -0.008 * | 0.000 | 0.05 |
| | 10 | 2.34 | -0.22 * | -0.03 * | -0.02 * | 0.006 * | -0.007 * | -0.004 | 0.002 * | 0.28 |
| | 0 | 5.65 | -0.44 * | 0.08 | -0.03 | 0.050 * | -0.025 * | 0.015 | -0.007 * | 0.15 |
| $V_A$ | 5s | 3.81 | 0.05 * | 0.09 * | -0.03 * | 0.005 | -0.014 * | -0.002 | -0.003 * | 0.04 |
| | 10s | 3.87 | 0.33 * | 0.12 * | -0.13 * | 0.010 | -0.170 * | -0.020 * | -0.008 * | 0.20 |
| | 10 | 2.56 | 0.01 | 0.02 | -0.02 | -0.002 | -0.009 * | -0.007 * | -0.001 * | 0.03 |
| | 0 | 1.80 | 0.13 * | 0.03 | -0.01 | 0.016 * | 0.005 | 0.002 | -0.004 * | 0.06 |
| | 5s | 1.80 | 0.15 * | 0.02 * | 0.02 * | 0.000 | -0.005 * | 0.001 | -0.001 | 0.17 |
| $V_A/Q$ | 10s | 1.56 | 0.11 * | 0.01 | -0.01 | 0.000 | -0.002 | -0.002 | -0.001 * | 0.09 |
| | 10 | 1.78 | 0.15 * | 0.03 * | -0.01 | 0.000 | -0.007 * | 0.000 | -0.001 * | 0.17 |
| | 0 | 98.40 | 3.40 * | 0.51 * | 0.58 * | 0.090 | -0.008 | 0.120 * | -0.090 * | 0.20 |
| $P_RO_2$ | 5s | 101.00 | 3.52 * | 0.62 * | 0.47 * | -0.110 * | -0.110 * | 0.015 | -0.030 * | 0.31 |
| | 10s | 99.40 | 3.10 * | 0.36 | -0.12 | -0.080 | -0.070 * | -0.060 | -0.049 * | 0.22 |
| | 10 | 106.00 | 3.27 * | 0.62 * | 0.20 | -0.089 * | -0.110 * | 0.010 | -0.024 * | 0.30 |

* $P < 0.05$ compared with zero by 1-tailed unpaired t test.

† Equation: variable = I + ax + by +cz + dxy + eyz +fzx + gxyz . All intercepts are significant

Int: intercept. 5s: 5 cm $H_2O$ selective unilateral dependent PEEP. 10s:10 cm $H_2O$ selective unilateral dependent PEEP. 10: 10 cm $H_2O$ bilateral PEEP.

Table A29. Coefficients and $R^2$ of multiple linear regression equation † fit to $\dot{Q}$, $\dot{V}_A$, $\dot{V}_A/\dot{Q}$ and $P_RO_2$ data for right lung of dog 10 with and without unilateral dependent PEEP in left lateral decubitus posture

| | PEEP | Int | a | b | c | d | e | f | g | $R^2$ |
|---|---|---|---|---|---|---|---|---|---|---|
| | 0 | 2.49 | -0.06 | 0.06 * | -0.03 * | -0.013 | -0.007 * | 0.030 * | 0.002 | 0.09 |
| | 5s | 2.00 | -0.01 | 0.04 * | -0.03 * | -0.014 | -0.003 | 0.027 * | 0.001 | 0.08 |
| Q | 10s | 2.72 | 0.16 * | 0.08 * | -0.08 * | -0.020 * | -0.012 * | 0.020 * | 0.000 | 0.15 |
| | 10 | 1.34 | -0.08 * | 0.01 | -0.02 * | -0.004 | 0.001 | 0.004 | 0.001 | 0.10 |
| | 0 | 4.52 | 0.32 * | 0.16 * | -0.01 | 0.005 | -0.027 * | 0.024 * | 0.000 | 0.16 |
| $V_A$ | 5s | 4.00 | 0.24 * | 0.12 * | -0.04 * | -0.005 | -0.020 * | 0.031 * | 0.003 | 0.14 |
| | 10s | 5.14 | 0.50 * | 0.18 * | -0.21 * | -0.013 | -0.054 * | 0.012 | -0.004 | 0.23 |
| | 10 | 2.51 | 0.20 * | 0.03 * | -0.03 * | -0.017 * | -0.012 * | 0.011 * | 0.001 | 0.19 |
| | 0 | 2.22 | 0.09 | 0.07 * | -0.01 | 0.033 * | -0.002 | -0.017 | 0.006 | 0.04 |
| | 5s | 2.30 | 0.05 | 0.03 * | 0.01 | 0.022 * | -0.007 * | -0.014 * | 0.005 * | 0.06 |
| $V_A/Q$ | 10s | 1.97 | 0.03 | 0.01 | -0.03 * | 0.015 | -0.009 * | -0.022 * | 0.001 | 0.04 |
| | 10 | 2.37 | 0.20 * | 0.03 * | -0.01 | -0.001 | -0.010 * | 0.009 | 0.000 | 0.12 |
| | 0 | 108.20 | 4.12 * | 0.56 * | 0.73 * | 0.160 | -0.180 * | -0.190 | 0.060 | 0.22 |
| $P_RO_2$ | 5s | 111.80 | 2.67 * | 0.47 * | 0.45 * | 0.140 | -0.180 * | -0.190 * | 0.083 * | 0.20 |
| | 10s | 110.80 | 2.72 * | 0.37 | -0.43 * | 0.072 | -0.310 * | -0.490 * | 0.043 | 0.19 |
| | 10 | 118.40 | 4.62 * | 0.49 * | 0.33 * | -0.080 | -0.150 * | 0.062 | 0.058 * | 0.33 |

* $P < 0.05$ compared with zero by 1-tailed unpaired t test.

† Equation: variable = I + ax + by +cz + dxy + eyz +fzx + gxyz . All intercepts are significant

Int: intercept. 5s: 5 cm $H_2O$ selective unilateral dependent PEEP. 10s:10 cm $H_2O$ selective unilateral dependent PEEP. 10: 10 cm $H_2O$ bilateral PEEP.

Table A30. Coefficients and $R^2$ of multiple linear regression equation † fit to $\dot{Q}$, $\dot{V}_A$, $\dot{V}_A/\dot{Q}$ and $P_RO_2$ data for left lung of dog 10 with and without unilateral dependent PEEP in left lateral decubitus posture

| | PEEP | Int | a | b | c | d | e | f | g | $R^2$ |
|---|---|---|---|---|---|---|---|---|---|---|
| | 0 | 6.70 | -0.33 | 0.14 | -0.06 | -0.084 | -0.110 * | 0.050 | 0.033 * | 0.13 |
| | 5s | 3.27 | 0.03 | 0.02 | -0.05 * | -0.025 | -0.019 * | 0.020 | 0.005 | 0.06 |
| Q | 10s | 2.41 | -0.03 | -0.01 | 0.00 | -0.014 | -0.005 | 0.009 | 0.003 * | 0.02 |
| | 10 | 3.82 | 0.48 * | 0.09 * | -0.11 * | 0.002 | -0.030 * | 0.009 | -0.001 | 0.19 |
| | 0 | 6.75 | -2.50 * | -0.35 * | 0.14 * | -0.130 | 0.029 | 0.130 * | 0.025 | 0.22 |
| $V_A$ | 5s | 3.31 | -0.61 * | -0.09 * | 0.07 * | -0.061 | 0.007 | 0.030 * | 0.007 | 0.12 |
| | 10s | 1.96 | -0.48 * | -0.13 * | 0.09 * | -0.021 | 0.028 * | 0.016 | 0.004 | 0.13 |
| | 10 | 2.39 | -0.19 * | -0.03 | 0.05 * | -0.022 | 0.000 | 0.019 * | 0.004 * | 0.07 |
| | 0 | 1.18 | -0.43 * | -0.13 * | 0.03 | -0.022 | 0.040 * | 0.025 | -0.006 | 0.13 |
| | 5s | 1.10 | -0.17 * | -0.02 | 0.04 * | -0.004 | 0.011 * | 0.003 | -0.001 | 0.19 |
| $V_A/Q$ | 10s | 0.92 | -0.19 * | -0.05 * | 0.04 * | 0.000 | 0.009 * | 0.003 | 0.001 | 0.10 |
| | 10 | 0.89 | -0.27 * | -0.06 * | 0.05 * | 0.001 | 0.008 * | 0.002 | 0.002 | 0.13 |
| | 0 | 83.60 | -10.62 * | -2.20 * | 1.53 * | -0.450 | 0.680 * | 0.380 * | -0.059 | 0.33 |
| $P_RO_2$ | 5s | 84.00 | -6.10 * | -0.64 * | 1.54 * | -0.280 | 0.220 * | 0.170 | -0.016 | 0.27 |
| | 10s | 81.40 | -5.10 * | -1.11 * | 1.26 * | -0.210 | 0.300 * | 0.150 | 0.010 | 0.22 |
| | 10 | 85.00 | -7.30 * | -1.29 * | 1.72 * | -0.300 | 0.270 * | 0.190 | 0.027 | 0.31 |

* $P < 0.05$ compared with zero by 1-tailed unpaired t test.

† Equation: variable = I + ax + by +cz + dxy + eyz +fzx + gxyz . All intercepts are significant

Int: intercept. 5s: 5 cm $H_2O$ selective unilateral dependent PEEP. 10s:10 cm $H_2O$ selective unilateral dependent PEEP. 10: 10 cm $H_2O$ bilateral PEEP.

Table A31. Coefficients and $R^2$ of multiple linear regression equation † fit to $\dot{Q}$, $\dot{V}_A$, $\dot{V}_A/\dot{Q}$ and $P_RO_2$ data for whole lung of dog 11 with and without unilateral dependent PEEP in left lateral decubitus posture

| | PEEP | Int | a | b | c | d | e | f | g | $R^2$ |
|---|---|---|---|---|---|---|---|---|---|---|
| | 0 | 5.10 | -0.43 * | 0.01 | -0.50 * | 0.063 * | -0.055 * | 0.089 * | 0.013 * | 0.58 |
| | 5s | 3.16 | 0.10 * | 0.12 * | -0.35 * | 0.005 | -0.035 * | -0.014 * | 0.003 * | 0.54 |
| Q | 10s | 3.33 | 0.24 * | 0.14 * | -0.34 * | -0.002 | -0.034 * | -0.020 * | 0.002 | 0.52 |
| | 10 | 1.68 | -0.12 * | -0.04 * | -0.09 * | 0.006 * | -0.008 * | 0.010 * | 0.002 * | 0.61 |
| | 0 | 4.99 | 0.13 * | 0.15 * | -0.59 * | 0.050 * | -0.065 * | 0.032 * | 0.011 * | 0.42 |
| $V_A$ | 5s | 3.84 | 0.26 * | 0.18 * | -0.43 * | 0.010 | -0.047 * | -0.031 * | 0.002 | 0.48 |
| | 10s | 4.46 | 0.39 * | 0.22 * | -0.50 * | 0.009 | -0.054 * | -0.043 * | 0.001 | 0.48 |
| | 10 | 2.17 | 0.07 * | -0.06 * | -0.10 * | -0.031 * | -0.006 * | 0.012 * | 0.001 * | 0.41 |
| | 0 | 0.99 | 0.12 * | 0.05 * | -0.08 * | 0.004 | -0.012 * | 0.000 | 0.001 | 0.47 |
| | 5s | 1.03 | 0.06 * | 0.03 * | -0.06 * | 0.000 | -0.008 * | 0.000 * | -0.001 | 0.39 |
| $V_A/Q$ | 10s | 1.06 | 0.02 | 0.04 | -0.10 * | 0.013 * | -0.001 | -0.003 | -0.001 | 0.12 |
| | 10 | 1.83 | 0.06 * | -0.11 * | 0.02 * | -0.025 * | -0.002 | 0.013 * | -0.002 | 0.19 |
| | 0 | 104.80 | 3.78 * | 1.57 * | -5.04 * | 0.280 * | -0.590 * | 0.196 * | 0.070 * | 0.60 |
| $P_RO_2$ | 5s | 105.00 | 1.74 * | 1.07 * | -3.64 * | -0.100 | -0.297 * | 0.040 | -0.064 * | 0.56 |
| | 10s | 104.50 | -0.22 | 1.68 * | -5.12 * | 0.450 * | -0.290 * | -0.190 * | 0.008 | 0.52 |
| | 10 | 121.70 | 0.58 * | -1.05 * | 0.18 * | -0.130 * | -0.027 | 0.170 * | -0.001 | 0.25 |

* $P < 0.05$ compared with zero by 1-tailed unpaired t test.

† Equation: variable = I + ax + by +cz + dxy + eyz +fzx + gxyz . All intercepts are significant

Int: intercept. 5s: 5 cm $H_2O$ selective unilateral dependent PEEP. 10s:10 cm $H_2O$ selective unilateral dependent PEEP. 10: 10 cm $H_2O$ bilateral PEEP.

Table A32. Coefficients and $R^2$ of multiple linear regression equation † fit to $\dot{Q}$, $\dot{V}_A$, $\dot{V}_A/\dot{Q}$ and $P_RO_2$ data for right lung of dog 11 with and without unilateral dependent PEEP in left lateral decubitus posture

| | PEEP | Int | a | b | c | d | e | f | g | $R^2$ |
|---|---|---|---|---|---|---|---|---|---|---|
| | 0 | 4.17 | -0.49 * | 0.07 * | -0.35 * | 0.040 * | -0.036 * | 0.023 * | 0.007 * | 0.64 |
| | 5s | 4.10 | -0.47 * | 0.10 * | -0.44 * | 0.040 * | -0.045 * | 0.006 | 0.013 * | 0.66 |
| Q | 10s | 4.74 | -0.46 * | 0.09 * | -0.45 * | 0.042 * | -0.047 * | 0.009 | 0.009 * | 0.63 |
| | 10 | 1.32 | -0.12 * | -0.03 * | -0.06 * | -0.006 * | -0.005 * | 0.004 * | 0.000 | 0.63 |
| | 0 | 5.56 | -0.56 * | 0.14 * | -0.60 * | 0.150 * | -0.060 * | -0.020 | 0.009 | 0.53 |
| $V_A$ | 5s | 5.45 | -0.57 * | 0.17 * | -0.58 * | 0.102 * | -0.064 * | -0.016 | 0.016 * | 0.52 |
| | 10s | 6.63 | -0.61 * | 0.20 * | -0.71 * | 0.110 * | -0.080 * | -0.015 | 0.016 * | 0.51 |
| | 10 | 2.48 | -0.15 * | -0.17 * | -0.09 * | -0.025 * | -0.006 * | 0.019 * | -0.001 | 0.55 |
| | 0 | 1.25 | 0.05 | 0.04 | -0.10 | 0.014 | -0.012 | 0.000 | 0.000 | 0.33 |
| | 5s | 1.25 | 0.03 | 0.04 * | -0.07 * | 0.012 | -0.011 * | 0.003 | 0.001 | 0.22 |
| $V_A/Q$ | 10s | 1.18 | -0.03 | 0.08 * | -0.11 * | 0.018 * | -0.007 * | -0.011 * | 0.002 | 0.32 |
| | 10 | 1.83 | 0.06 * | -0.11 * | 0.02 * | -0.025 * | -0.002 | 0.013 * | -0.002 | 0.19 |
| | 0 | 112.00 | 1.28 * | 1.82 * | -5.27 * | 0.570 * | -0.520 * | 0.130 | 0.086 * | 0.60 |
| $P_RO_2$ | 5s | 111.60 | 1.22 * | 1.35 * | -3.74 * | 0.420 * | -0.440 * | 0.260 * | 0.090 * | 0.52 |
| | 10s | 107.50 | -1.58 * | 3.13 * | -5.76 * | 0.930 * | -0.290 * | -0.410 * | 0.130 * | 0.54 |
| | 10 | 121.70 | 0.58 * | -1.05 * | 0.18 * | -0.130 * | -0.027 | 0.170 * | -0.001 | 0.25 |

* $P < 0.05$ compared with zero by 1-tailed unpaired t test.

† Equation: variable = I + ax + by +cz + dxy + eyz +fzx + gxyz . All intercepts are significant

Int: intercept. 5s: 5 cm $H_2O$ selective unilateral dependent PEEP. 10s:10 cm $H_2O$ selective unilateral dependent PEEP. 10: 10 cm $H_2O$ bilateral PEEP.

Table A33. Coefficients and $R^2$ of multiple linear regression equation † fit to $\dot{Q}$, $\dot{V}_A$, $\dot{V}_A/\dot{Q}$ and $P_RO_2$ data for left lung of dog 11 with and without unilateral dependent PEEP in left lateral decubitus posture

| | PEEP | Int | a | b | c | d | e | f | g | $R^2$ |
|---|---|---|---|---|---|---|---|---|---|---|
| | 0 | 7.54 | -0.53 * | -0.03 | -0.74 * | 0.510 * | -0.220 * | 0.110 * | 0.060 * | 0.58 |
| | 5s | 2.10 | -0.02 | 0.01 | -0.21 * | 0.048 * | -0.025 * | 0.016 * | 0.005 * | 0.62 |
| Q | 10s | 1.47 | -0.06 * | -0.04 * | -0.13 * | 0.032 * | -0.012 * | 0.016 * | 0.002 * | 0.64 |
| | 10 | 2.30 | -0.09 * | -0.05 * | -0.13 * | 0.037 * | -0.025 * | 0.005 | 0.006 * | 0.55 |
| | 0 | 5.26 | 0.22 | -0.05 | -0.61 * | 0.450 * | -0.180 * | 0.023 | 0.047 * | 0.47 |
| $V_A$ | 5s | 1.88 | 0.09 * | 0.02 | -0.21 * | 0.043 * | -0.025 * | 0.008 | 0.003 | 0.56 |
| | 10s | 1.70 | 0.03 | -0.03 | -0.18 * | 0.035 * | -0.017 * | 0.010 | 0.027 | 0.51 |
| | 10 | 1.62 | -0.06 * | -0.08 * | -0.07 * | -0.007 | -0.007 * | -0.001 | 0.004 * | 0.37 |
| | 0 | 0.65 | 0.05 * | 0.02 | 0.00 | -0.018 * | 0.014 * | -0.001 | -0.002 * | 0.19 |
| | 5s | 0.73 | 0.09 * | 0.03 * | -0.06 * | -0.004 | -0.002 | 0.001 | -0.002 * | 0.35 |
| $V_A/Q$ | 10s | 0.91 | 0.09 | -0.01 | -0.08 * | -0.011 | 0.002 | -0.013 | 0.009 * | 0.12 |
| | 10 | 0.77 | 0.00 | 0.01 | 0.02 * | -0.023 * | 0.010 * | -0.005 | -0.002 * | 0.19 |
| | 0 | 92.00 | 1.70 * | 0.50 | -0.15 | -0.530 * | 0.470 * | 0.050 | -0.069 * | 0.27 |
| $P_RO_2$ | 5s | 96.00 | 3.58 * | 2.21 * | -4.00 * | -0.120 | -0.038 | 0.140 | -0.100 * | 0.52 |
| | 10s | 101.60 | 4.02 * | 1.04 * | -4.99 * | -0.080 | -0.250 * | 0.320 * | -0.088 * | 0.54 |
| | 10 | 96.00 | 0.47 | 0.15 | 0.55 * | -0.720 * | 0.310 * | -0.080 | -0.069 * | 0.27 |

* $P < 0.05$ compared with zero by 1-tailed unpaired t test.

† Equation: variable = I + ax + by +cz + dxy + eyz +fzx + gxyz . All intercepts are significant

Int: intercept. 5s: 5 cm $H_2O$ selective unilateral dependent PEEP. 10s:10 cm $H_2O$ selective unilateral dependent PEEP. 10: 10 cm $H_2O$ bilateral PEEP.

Table A34. Coefficients and $R^2$ of multiple linear regression equation † fit to $\dot{Q}$, $\dot{V}_A$, $\dot{V}_A/\dot{Q}$ and $P_RO_2$ data for whole lung of dog 12 with and without unilateral dependent PEEP in left lateral decubitus posture

| | PEEP | Int | a | b | c | d | e | f | g | $R^2$ |
|---|---|---|---|---|---|---|---|---|---|---|
| | 0 | 4.91 | -0.63 * | -0.56 * | -0.04 * | 0.190 * | -0.014 * | 0.045 * | 0.003 | 0.62 |
| | 5s | 4.10 | -0.19 * | -0.29 * | -0.03 * | 0.028 * | -0.014 * | 0.030 * | 0.005 * | 0.45 |
| Q | 10s | 4.30 | 0.20 * | -0.24 * | -0.01 | -0.011 * | -0.023 * | 0.025 * | 0.001 | 0.41 |
| | 10 | 3.45 | -0.50 * | -0.33 * | -0.05 * | 0.070 * | -0.002 | 0.011 * | -0.001 | 0.68 |
| | 0 | 6.10 | 0.13 * | -0.18 * | -0.05 * | 0.028 | -0.024 * | 0.008 | 0.005 | 0.04 |
| $V_A$ | 5s | 4.75 | 0.54 * | 0.03 | -0.04 * | -0.017 * | -0.037 * | 0.030 * | 0.003 | 0.46 |
| | 10s | 5.81 | 0.89 * | 0.11 * | -0.09 * | -0.023 * | -0.063 * | 0.004 | -0.007 * | 0.62 |
| | 10 | 2.77 | -0.01 | -0.04 * | -0.03 * | -0.023 * | -0.013 * | 0.009 * | 0.003 * | 0.08 |
| | 0 | 1.62 | 0.21 * | 0.11 * | -0.05 * | -0.012 * | 0.005 * | -0.018 * | 0.000 | 0.42 |
| | 5s | 1.40 | 0.19 * | 0.14 * | -0.03 * | 0.011 * | -0.008 * | -0.005 * | -0.001 | 0.54 |
| $V_A/Q$ | 10s | 1.41 | 0.15 * | 0.12 * | -0.03 * | 0.008 * | -0.003 * | -0.008 * | -0.001 | 0.34 |
| | 10 | 1.71 | 0.03 | 0.02 | -0.02 | 0.038 | 0.019 | -0.027 | 0.008 | 0.01 |
| | 0 | 106.10 | 5.10 * | 2.39 * | -0.36 * | -0.640 * | 0.005 | -0.100 * | 0.020 | 0.63 |
| $P_RO_2$ | 5s | 102.00 | 5.72 * | 2.81 * | -0.10 | -0.400 * | -0.120 * | 0.030 | 0.002 | 0.70 |
| | 10s | 111.20 | 3.82 * | 2.38 * | 0.21 * | -0.350 * | -0.120 * | -0.130 * | 0.022 * | 0.62 |
| | 10 | 99.50 | 5.16 * | 2.03 * | -0.08 | -0.370 * | -0.046 | 0.031 | 0.028 * | 0.67 |

* $P < 0.05$ compared with zero by 1-tailed unpaired t test.

† Equation: variable = I + ax + by +cz + dxy + eyz +fzx + gxyz . All intercepts are significant

Int: intercept. 5s: 5 cm $H_2O$ selective unilateral dependent PEEP. 10s:10 cm $H_2O$ selective unilateral dependent PEEP. 10: 10 cm $H_2O$ bilateral PEEP.

Table A35. Coefficients and $R^2$ of multiple linear regression equation † fit to $\dot{Q}$, $\dot{V}_A$, $\dot{V}_A/\dot{Q}$ and $P_RO_2$ data for right lung of dog 12 with and without unilateral dependent PEEP in left lateral decubitus posture

| | PEEP | Int | a | b | c | d | e | f | g | $R^2$ |
|---|---|---|---|---|---|---|---|---|---|---|
| | 0 | 3.40 | -0.21 * | -0.19 * | 0.08 * | 0.021 | -0.017 * | 0.010 | -0.003 | 0.26 |
| | 5s | 3.65 | -0.08 * | -0.25 * | 0.08 * | -0.003 | -0.004 | -0.004 | -0.006 * | 0.25 |
| Q | 10s | 4.94 | 0.31 * | -0.26 * | 0.08 * | -0.032 | -0.021 * | 0.001 | -0.007 | 0.24 |
| | 10 | 1.47 | -0.13 * | -0.09 * | 0.01 * | -0.013 * | -0.005 * | 0.004 | 0.000 | 0.41 |
| | 0 | 6.43 | 0.11 | -0.20 * | -0.03 | 0.023 | -0.020 * | -0.033 * | -0.014 * | 0.15 |
| $V_A$ | 5s | 6.37 | 0.32 * | -0.04 | 0.07 * | 0.007 | -0.044 * | -0.041 * | -0.018 * | 0.19 |
| | 10s | 8.58 | 0.82 * | 0.09 * | -0.06 * | 0.028 | -0.095 * | -0.042 * | -0.024 * | 0.33 |
| | 10 | 2.82 | -0.18 * | -0.13 * | -0.02 * | -0.026 * | -0.008 * | 0.028 * | -0.002 | 0.52 |
| | 0 | 2.14 | 0.18 * | 0.08 * | -0.09 * | -0.024 * | 0.005 | -0.030 * | 0.003 | 0.22 |
| | 5s | 1.97 | 0.11 * | 0.17 * | -0.04 * | 0.007 | -0.014 * | -0.018 * | 0.001 | 0.35 |
| $V_A/Q$ | 10s | 1.97 | -0.01 | 0.16 * | -0.07 * | -0.007 | -0.014 * | 0.010 | -0.006 * | 0.21 |
| | 10 | 2.11 | 0.17 | 0.07 | -0.18 * | -0.003 | 0.034 * | 0.094 * | -0.024 * | 0.04 |
| | 0 | 119.70 | 1.98 * | 0.67 * | -0.65 * | -0.019 | 0.031 | -0.260 * | 0.002 | 0.31 |
| $P_RO_2$ | 5s | 118.60 | 2.15 * | 1.62 * | 0.02 | 0.190 * | -0.220 * | -0.300 * | -0.006 | 0.49 |
| | 10s | 124.80 | 0.50 * | 1.38 * | -0.39 * | 0.150 * | -0.190 * | -0.090 | -0.040 * | 0.33 |
| | 10 | 121.40 | 0.35 * | 0.47 * | -0.31 * | -0.013 | -0.023 | 0.180 * | 0.020 * | 0.15 |

* $P < 0.05$ compared with zero by 1-tailed unpaired t test.

† Equation: variable = I + ax + by +cz + dxy + eyz +fzx + gxyz . All intercepts are significant

Int: intercept. 5s: 5 cm $H_2O$ selective unilateral dependent PEEP. 10s:10 cm $H_2O$ selective unilateral dependent PEEP. 10: 10 cm $H_2O$ bilateral PEEP.

Table A36. Coefficients and $R^2$ of multiple linear regression equation † fit to $\dot{Q}$, $\dot{V}_A$, $\dot{V}_A/\dot{Q}$ and $P_RO_2$ data for left lung of dog 12 with and without unilateral dependent PEEP in left lateral decubitus posture

| | PEEP | Int | a | b | c | d | e | f | g | $R^2$ |
|---|---|---|---|---|---|---|---|---|---|---|
| | 0 | 8.20 | -1.48 * | -1.35 * | -0.15 * | 0.710 * | -0.110 * | -0.180 * | 0.100 * | 0.62 |
| | 5s | 4.62 | -0.56 * | -0.49 * | -0.10 * | 0.130 * | -0.037 * | -0.035 * | 0.023 * | 0.62 |
| Q | 10s | 3.23 | -0.26 * | -0.32 * | -0.04 * | 0.015 | -0.016 * | -0.008 | 0.009 * | 0.62 |
| | 10 | 6.00 | -0.29 * | -0.62 * | -0.18 * | 0.070 * | -0.008 | -0.011 | 0.013 * | 0.59 |
| | 0 | 6.60 | -0.36 | -0.37 * | -0.10 | 0.810 * | -0.180 * | -0.130 * | 0.085 * | 0.12 |
| $V_A$ | 5s | 2.65 | -0.18 * | -0.07 * | -0.04 * | 0.098 * | -0.050 * | -0.004 | 0.160 * | 0.15 |
| | 10s | 2.10 | -0.05 | 0.00 | 0.02 | 0.014 | -0.029 * | 0.010 | 0.005 * | 0.16 |
| | 10 | 3.00 | 0.15 * | 0.06 | -0.08 * | 0.100 * | -0.048 * | -0.017 | 0.060 | 0.08 |
| | 0 | 0.88 | 0.11 * | 0.10 * | 0.00 | 0.052 * | -0.005 | 0.004 | 0.003 | 0.25 |
| | 5s | 0.64 | 0.02 | 0.06 * | 0.01 * | 0.005 * | -0.001 | 0.002 | 0.001 | 0.37 |
| $V_A/Q$ | 10s | 0.77 | 0.05 * | 0.07 * | 0.02 * | 0.010 * | 0.000 | 0.008 * | 0.002 * | 0.51 |
| | 10 | 1.87 | -0.82 * | -0.35 | 0.21 | 0.370 * | -0.066 | -0.120 * | 0.063 * | 0.04 |
| | 0 | 88.40 | 2.84 * | 3.68 * | 0.12 | 2.07 * | -0.39 * | -0.16 | 0.16 * | 0.34 |
| $P_RO_2$ | 5s | 80.00 | 0.51 | 3.38 * | 0.59 * | 0.44 | -0.12 * | 0.01 | 0.06 * | 0.49 |
| | 10s | 98.10 | 0.88 * | 3.40 * | 1.03 * | 0.33 * | -0.27 * | 0.05 | 0.05 * | 0.61 |
| | 10 | 72.40 | 0.08 | 2.12 * | 1.39 * | 0.43 * | -0.04 | -0.17 * | 0.06 * | 0.42 |

* $P < 0.05$ compared with zero by 1-tailed unpaired t test.

† Equation: variable = I + ax + by +cz + dxy + eyz +fzx + gxyz . All intercepts are significant

Int: intercept. 5s: 5 cm $H_2O$ selective unilateral dependent PEEP. 10s:10 cm $H_2O$ selective unilateral dependent PEEP. 10: 10 cm $H_2O$ bilateral PEEP.

Table A37. Coefficients and $R^2$ of multiple linear regression equation † fit to $\dot{Q}$ for whole, right and left lung of dog 13 during two-lung ventilation with hyperoxia

| | Post | PEEP | Int | a | | b | | c | | d | | e | | f | | g | $R^2$ |
|---|---|---|---|---|---|---|---|---|---|---|---|---|---|---|---|---|---|
| | LLD | 0 | 5.81 | -0.81 | * | -0.23 | * | -0.14 | * | 0.02 | | -0.07 | * | 0.03 | * | 0.01 | 0.44 |
| Whole | LLD | 10 | 2.97 | -0.26 | * | -0.14 | * | -0.04 | * | -0.01 | * | -0.02 | * | 0.00 | | 0.00 | 0.38 |
| | RLD | 0 | 4.92 | -0.58 | * | -0.27 | * | -0.08 | * | 0.13 | * | -0.05 | * | 0.04 | * | 0.00 | 0.45 |
| | RLD | 10 | 2.53 | -0.22 | * | -0.08 | * | -0.02 | * | 0.03 | * | -0.01 | | 0.00 | | 0.00 | 0.34 |
| | LLD | 0 | 4.90 | -0.29 | * | 0.32 | * | -0.18 | * | -0.15 | * | -0.07 | * | 0.04 | * | 0.005 | 0.28 |
| | LLD | 10 | 2.10 | -0.14 | * | -0.14 | * | -0.04 | * | -0.05 | * | -0.02 | * | 0.02 | * | -0.002 | 0.28 |
| Right | RLD | 0 | 6.60 | -0.81 | * | -0.61 | * | -0.18 | * | 0.24 | * | -0.06 | * | 0.05 | * | -0.004 | 0.35 |
| | RLD | 10 | 3.10 | -0.24 | * | -0.15 | * | -0.05 | * | 0.05 | * | -0.01 | | -0.00 | | 0.003 | 0.20 |
| | LLD | 0 | 8.45 | -2.15 | * | -0.60 | * | 0.02 | | 0.12 | | -0.10 | * | -0.07 | * | 0.04 | * | 0.37 |
| | LLD | 10 | 4.04 | -0.53 | * | -0.24 | * | 0.03 | | 0.01 | | -0.02 | * | -0.02 | * | 0.00 | | 0.29 |
| Left | RLD | 0 | 3.01 | -0.11 | * | -0.04 | | 0.08 | * | 0.01 | | -0.04 | * | 0.03 | * | 0.01 | * | 0.20 |
| | RLD | 10 | 1.69 | -0.28 | * | 0.02 | | -0.02 | * | 0.01 | | -0.01 | | -0.01 | | 0.01 | * | 0.28 |

* $P < 0.05$ compared with zero by 1-tailed unpaired t test.

† Equation: variable = I + ax + by +cz + dxy + eyz +fzx + gxyz .

All intercepts are significant. Post:posture; Int:intercept.

Table A38. Coefficients and $R^2$ of multiple linear regression equation † fit to $\dot{Q}$, $\dot{V}_A$, $\dot{V}_A/\dot{Q}$, and $P_RO_2$ for right lung of dog 13 during one-lung ventilation with left lung atelectasis and hyperoxia

| | Post | PEEP | Int | x | y | z | xy | yz | zx | xyz | R2 |
|---|---|---|---|---|---|---|---|---|---|---|---|
| | LLD | 0 | 9.00 | 0.14 | -0.81 * | -0.05 | -0.106 * | -0.052 * | 0.063 * | -0.010 | 0.26 |
| $\dot{Q}$,atel | LLD | 10 | 3.20 | -0.04 | -0.29 * | -0.02 | -0.032 * | -0.018 * | 0.017 * | -0.002 | 0.28 |
| | RLD | 0 | 7.02 | -0.65 * | -0.69 * | -0.12 * | 0.160 * | -0.040 * | -0.030 | 0.010 | 0.34 |
| | RLD | 10 | 4.30 | -0.40 * | -0.40 * | -0.06 * | 0.084 * | -0.014 * | -0.018 * | 0.004 | 0.35 |
| | LLD | 0 | 10.06 | -0.45 * | -0.47 * | -0.15 * | 0.013 | -0.071 * | -0.003 | 0.002 | 0.14 |
| $\dot{V}_A$,atel | LLD | 10 | 5.80 | -0.38 * | -0.25 * | -0.01 | -0.015 | -0.032 * | 0.023 * | 0.008 * | 0.17 |
| | RLD | 0 | 8.19 | -0.23 * | -0.32 * | -0.20 * | 0.013 | -0.070 * | 0.031 | -0.004 | 0.19 |
| | RLD | 10 | 6.80 | -0.02 | -0.22 * | -0.03 | -0.024 | -0.030 * | 0.009 | 0.000 | 0.08 |
| | LLD | 0 | 12.60 | -0.77 * | 0.90 * | -0.19 * | -0.120 * | -0.070 * | -0.060 | -0.002 | 0.21 |
| | LLD | 10 | 2.20 | -0.10 * | 0.15 * | 0.04 * | -0.034 * | -0.002 | 0.019 * | 0.007 * | 0.17 |
| $\dot{V}_A/\dot{Q}$ | RLD | 0 | 1.45 | 0.11 * | 0.11 * | -0.01 | 0.002 | -0.010 * | 0.007 | -0.001 | 0.19 |
| | RLD | 10 | 1.20 | 0.19 * | 0.19 * | -0.01 | -0.012 | 0.002 | 0.010 | -0.001 | 0.19 |
| | LLD | 0 | 708.80 | -0.49 * | 0.37 * | -0.08 * | 0.084 * | -0.026 | -0.069 * | 0.012 | 0.13 |
| $P_RO_2$ | LLD | 10 | 693.80 | -0.48 * | 0.47 * | 0.11 * | -0.030 | -0.002 | 0.041 | 0.024 * | 0.19 |
| | RLD | 0 | 679.90 | 0.77 * | 0.63 * | -0.08 | -0.040 * | -0.064 * | 0.073 * | -0.010 * | 0.25 |
| | RLD | 10 | 682.90 | 0.97 * | 1.28 * | -0.16 | -0.136 * | 0.023 | 0.066 * | -0.007 | 0.31 |

* $P < 0.05$ compared with zero by 1-tailed unpaired t test.

† Equation: variable = I + ax + by +cz + dxy + eyz +fzx + gxyz .

All intercepts are significant. Post:posture; Int:intercept. Atel:atelectasis

Table A39. Coefficients and $R^2$ of multiple linear regression equation † fit to $\dot{Q}$ for whole, right and left lung of dog 14 during two-lung ventilation with hyperoxia

| | Post | PEEP | Int | a | | b | | c | | d | | e | | f | | g | | $R^2$ |
|---|---|---|---|---|---|---|---|---|---|---|---|---|---|---|---|---|---|---|
| | LLD | 0 | 5.25 | -0.58 | * | -0.04 | * | -0.09 | * | 0.010 | | -0.012 | * | 0.066 | * | 0.003 | * | 0.73 |
| Whole | LLD | 10 | 2.87 | -0.20 | * | -0.03 | * | -0.06 | * | 0.009 | * | 0.000 | | 0.017 | * | 0.002 | * | 0.65 |
| | RLD | 0 | 8.30 | -1.14 | * | -0.12 | * | -0.19 | * | 0.037 | * | -0.040 | * | -0.039 | * | 0.003 | | 0.83 |
| | RLD | 10 | 3.01 | -0.37 | * | -0.09 | * | -0.01 | * | 0.013 | * | -0.006 | * | -0.026 | * | 0.000 | | 0.83 |
| | LLD | 0 | 3.97 | -0.56 | * | -0.03 | * | 0.02 | | 0.015 | * | -0.008 | * | -0.007 | | 0.002 | | 0.55 |
| | LLD | 10 | 2.22 | -0.27 | * | -0.01 | | -0.01 | * | -0.005 | * | 0.000 | | 0.001 | | 0.001 | | 0.63 |
| Right | RLD | 0 | 11.40 | -1.54 | * | -0.24 | * | -0.02 | | 0.062 | * | -0.066 | * | 0.018 | | 0.016 | * | 0.74 |
| | RLD | 10 | 4.17 | -0.37 | * | -0.14 | * | 0.08 | * | 0.007 | | -0.006 | * | -0.013 | * | 0.001 | | 0.67 |
| | LLD | 0 | 7.30 | -0.91 | * | -0.08 | * | -0.29 | * | 0.077 | * | -0.060 | * | 0.107 | * | 0.017 | * | 0.71 |
| | LLD | 10 | 3.83 | -0.12 | * | -0.08 | * | -0.14 | * | 0.029 | * | -0.016 | * | 0.024 | * | 0.002 | * | 0.60 |
| Left | RLD | 0 | 3.92 | -0.43 | * | -0.07 | * | -0.33 | * | -0.047 | * | -0.036 | * | 0.020 | * | -0.007 | * | 0.73 |
| | RLD | 10 | 1.44 | -0.15 | * | -0.04 | * | -0.10 | * | -0.003 | | -0.006 | * | 0.010 | * | -0.003 | * | 0.77 |

* $P < 0.05$ compared with zero by 1-tailed unpaired t test.

† Equation: variable = I + ax + by +cz + dxy + eyz +fzx + gxyz .

All intercepts are significant. Post:posture; Int:intercept.

Table A40. Coefficients and $R^2$ of multiple linear regression equation † fit to $\dot{Q}$, $\dot{V}_A$, $\dot{V}_A/\dot{Q}$, and $P_{RO2}$ of right lung of dog 14 during one-lung ventilation with left lung atelectasis and hyperoxia

| | Post | PEEP | Int | x | y | z | xy | yz | zx | xyz | R2 |
|---|---|---|---|---|---|---|---|---|---|---|---|
| | LLD | 0 | 4.68 | -0.07 * | -0.14 * | 0.03 * | -0.013 * | -0.016 * | 0.023 * | -0.003 * | 0.33 |
| $\dot{Q}$,atel | LLD | 10 | 2.32 | -0.20 * | -0.07 * | 0.00 | -0.012 * | -0.009 * | 0.005 * | 0.000 | 0.53 |
| | RLD | 0 | 8.29 | -0.54 * | -0.30 * | 0.13 * | 0.012 * | -0.037 * | -0.054 * | 0.007 * | 0.56 |
| | RLD | 10 | 3.96 | -0.24 * | -0.22 * | 0.08 * | 0.011 * | -0.006 * | -0.008 * | 0.001 | 0.64 |
| | LLD | 0 | 9.19 | -0.53 * | 0.29 * | -0.13 * | 0.012 | -0.080 * | -0.030 * | -0.003 | 0.36 |
| $V_A$,atel | LLD | 10 | 5.63 | -0.50 * | -0.41 * | 0.20 * | -0.064 * | -0.060 * | 0.045 * | -0.010 * | 0.28 |
| | RLD | 0 | 10.65 | -0.22 * | 0.20 * | 0.02 | -0.150 * | -0.070 * | -0.068 * | 0.004 | 0.44 |
| | RLD | 10 | 5.98 | -0.34 * | -0.22 * | 0.17 * | 0.005 | -0.028 * | -0.031 * | 0.008 * | 0.20 |
| | LLD | 0 | 2.03 | -0.10 * | 0.14 * | -0.05 * | 0.018 * | -0.009 * | -0.017 * | 0.001 | 0.39 |
| | LLD | 10 | 2.10 | -0.06 * | -0.08 * | 0.05 * | 0.000 | -0.009 * | 0.010 * | -0.001 | 0.17 |
| $V_A/Q$ | RLD | 0 | 1.36 | 0.06 * | 0.09 * | -0.02 * | -0.019 * | -0.003 * | -0.001 | -0.001 * | 0.45 |
| | RLD | 10 | 1.44 | -0.02 * | 0.04 * | 0.00 | -0.012 * | -0.001 | 0.001 | 0.001 | 0.20 |
| | LLD | 0 | 686.80 | -0.48 * | 0.64 * | -0.18 * | 0.105 * | -0.057 * | -0.082 * | -0.001 | 0.46 |
| $P_{RO2}$ | LLD | 10 | 688.00 | -0.33 * | -0.33 * | 0.24 * | -0.002 | -0.032 * | 0.058 * | -0.005 | 0.22 |
| | RLD | 0 | 685.00 | 0.65 * | 0.57 * | -0.12 * | -0.170 * | -0.036 * | -0.016 | -0.004 * | 0.56 |
| | RLD | 10 | 694.50 | -0.13 * | 0.19 * | 0.03 | -0.055 * | -0.006 | -0.001 | 0.004 * | 0.23 |

* $P < 0.05$ compared with zero by 1-tailed unpaired t test.

† Equation: variable = I + ax + by +cz + dxy + eyz +fzx + gxyz .

All intercepts are significant. Post:posture; Int:intercept. Atel:atelectasis

Table A41. Coefficients and $R^2$ of multiple linear regression equation † fit to $\dot{Q}$ for whole, right and left lung of dog 14 during two-lung ventilation with hyperoxia

| | Post | PEEP | Int | a | | b | | c | | d | | e | | f | | g | | $R^2$ |
|---|---|---|---|---|---|---|---|---|---|---|---|---|---|---|---|---|---|---|
| | LLD | 0 | 6.07 | -0.01 | | -0.29 | * | -0.46 | * | -0.010 | | -0.039 | * | 0.155 | * | 0.004 | | 0.59 |
| Whole | LLD | 10 | 6.87 | -0.09 | * | -0.15 | * | -0.36 | * | -0.006 | | -0.030 | * | 0.067 | * | 0.004 | * | 0.58 |
| | RLD | 0 | 8.49 | -1.25 | * | -0.41 | * | -0.37 | * | 0.072 | * | -0.070 | * | -0.049 | * | 0.006 | * | 0.85 |
| | RLD | 10 | 3.06 | -0.42 | * | -0.18 | * | -0.11 | * | 0.016 | * | -0.015 | * | -0.022 | * | 0.000 | | 0.85 |
| | LLD | 0 | 6.46 | -0.73 | * | -0.12 | * | -0.14 | * | -0.011 | | -0.048 | * | 0.062 | * | -0.008 | * | 0.61 |
| | LLD | 10 | 7.05 | -0.60 | * | -0.07 | * | -0.15 | * | -0.033 | * | -0.028 | * | 0.014 | * | 0.002 | | 0.68 |
| Right | RLD | 0 | 13.02 | -1.65 | * | -0.53 | * | -0.08 | * | 0.102 | * | -0.103 | * | -0.015 | | 0.027 | * | 0.71 |
| | RLD | 10 | 4.77 | -0.34 | * | -0.23 | * | -0.02 | * | 0.002 | | -0.014 | * | -0.014 | * | 0.000 | | 0.67 |
| | LLD | 0 | 6.07 | -0.86 | * | -0.49 | * | -0.92 | * | 0.081 | | -0.093 | * | 0.163 | * | 0.067 | * | 0.71 |
| | LLD | 10 | 6.54 | -0.44 | * | -0.23 | * | -0.62 | * | 0.018 | | -0.039 | * | 0.064 | * | 0.017 | * | 0.68 |
| Left | RLD | 0 | 3.21 | -0.43 | * | -0.27 | * | -0.41 | * | 0.056 | * | -0.004 | | 0.003 | | -0.003 | | 0.59 |
| | RLD | 10 | 1.24 | -0.13 | * | -0.09 | * | -0.14 | * | 0.012 | | 0.001 | | 0.007 | * | -0.002 | | 0.66 |

* $P < 0.05$ compared with zero by 1-tailed unpaired t test.

† Equation: variable = I + ax + by +cz + dxy + eyz +fzx + gxyz .

All intercepts are significant. Post:posture; Int:intercept.

Table A42. Coefficients and $R^2$ of multiple linear regression equation † fit to $\dot{Q}$, $\dot{V}_A$, $\dot{V}_A/\dot{Q}$, and $P_{RO_2}$ of right lung of dog 15 during one-lung ventilation with left lung atelectasis and hyperoxia

| | Post | PEEP | Int | x | y | z | xy | yz | zx | xyz | R2 |
|---|---|---|---|---|---|---|---|---|---|---|---|
| | LLD | 0 | 7.20 | -0.26 * | -0.18 * | -0.17 * | -0.015 | -0.035 * | 0.021 * | -0.006 * | 0.50 |
| $\dot{Q}$,atel | LLD | 10 | 3.55 | -0.25 * | -0.08 * | -0.09 * | -0.007 | -0.020 * | 0.006 | -0.001 | 0.58 |
| | RLD | 0 | 11.94 | -0.32 * | -0.59 * | -0.13 | -0.014 * | -0.052 * | -0.042 * | 0.007 | 0.50 |
| | RLD | 10 | 4.62 | -0.13 * | -0.30 * | -0.06 * | -0.008 | -0.012 * | -0.009 | 0.003 | 0.56 |
| | LLD | 0 | 8.70 | 0.16 * | 0.24 * | -0.08 * | 0.095 * | -0.017 * | -0.003 | 0.009 * | 0.22 |
| $\dot{V}_A$,atel | LLD | 10 | 4.13 | -0.46 * | -0.11 * | -0.17 * | -0.007 | -0.010 * | -0.001 | 0.000 | 0.66 |
| | RLD | 0 | 13.83 | -0.22 * | 0.20 * | 0.05 * | -0.079 | -0.066 * | -0.030 * | 0.007 | 0.13 |
| | RLD | 10 | 5.08 | -0.31 * | -0.01 | 0.07 * | -0.065 * | 0.029 * | -0.024 * | -0.005 * | 0.41 |
| | LLD | 0 | 1.28 | 0.07 * | 0.09 * | 0.02 * | 0.026 * | 0.008 * | -0.006 * | 0.004 * | 0.59 |
| | LLD | 10 | 1.13 | -0.06 * | -0.01 * | -0.03 * | -0.001 | 0.003 * | -0.003 * | 0.000 | 0.36 |
| $\dot{V}_A/\dot{Q}$ | RLD | 0 | 1.23 | 0.03 * | 0.09 * | 0.03 * | -0.006 * | 0.005 * | 0.005 * | -0.001 | 0.42 |
| | RLD | 10 | 1.15 | -0.03 * | 0.09 * | 0.04 * | -0.023 * | 0.017 * | 0.000 | -0.002 * | 0.61 |
| | LLD | 0 | 671.94 | 0.42 * | 0.45 * | 0.13 * | 0.130 * | 0.030 * | -0.038 * | 0.017 * | 0.62 |
| $P_{RO_2}$ | LLD | 10 | 666.40 | -0.44 * | -0.08 * | -0.20 * | -0.011 | 0.025 * | -0.026 * | 0.004 | 0.39 |
| | RLD | 0 | 673.20 | 0.13 * | 0.48 * | 0.15 * | -0.028 * | 0.014 * | 0.018 | -0.002 | 0.41 |
| | RLD | 10 | 678.10 | -0.22 * | 0.42 * | 0.18 * | -0.110 * | 0.070 * | -0.006 | -0.005 | 0.60 |

* $P < 0.05$ compared with zero by 1-tailed unpaired t test.

† Equation: variable = I + ax + by +cz + dxy + eyz +fzx + gxyz .

All intercepts are significant. Post:posture; Int:intercept. Atel:atelectasis

Table A43. Coefficients and $R^2$ of multiple linear regression equation † fit to $\dot{Q}$ for whole, right and left lung of dog 16 during two-lung ventilation with hyperoxia

| | Post | PEEP | Int | a | | b | | c | | d | | e | | f | | g | | $R^2$ |
|---|---|---|---|---|---|---|---|---|---|---|---|---|---|---|---|---|---|---|
| | LLD | 0 | 4.86 | -0.15 | * | -0.13 | * | -0.24 | * | 0.023 | * | 0.006 | * | 0.095 | * | -0.004 | * | 0.63 |
| Whole | LLD | 10 | 1.93 | -0.14 | * | -0.07 | * | -0.06 | * | 0.010 | * | 0.001 | | 0.017 | * | -0.001 | * | 0.72 |
| | RLD | 0 | 3.16 | -0.26 | * | -0.03 | * | -0.20 | * | 0.001 | | -0.011 | * | 0.054 | * | -0.001 | * | 0.76 |
| | RLD | 10 | 1.85 | -0.23 | * | -0.06 | * | -0.03 | * | 0.015 | * | -0.003 | * | 0.000 | | 0.000 | | 0.78 |
| | LLD | 0 | 4.48 | -0.32 | * | -0.11 | * | -0.05 | * | -0.001 | | -0.012 | * | 0.035 | * | -0.001 | | 0.37 |
| | LLD | 10 | 1.39 | -0.17 | * | -0.04 | * | -0.01 | * | -0.008 | * | -0.007 | * | 0.008 | * | 0.000 | | 0.52 |
| Right | RLD | 0 | 4.25 | -0.38 | * | -0.02 | | -0.40 | * | -0.016 | | -0.019 | * | 0.088 | * | 0.003 | | 0.75 |
| | RLD | 10 | 2.59 | -0.24 | * | -0.12 | * | -0.03 | * | 0.009 | * | -0.002 | | 0.004 | | 0.001 | | 0.63 |
| | LLD | 0 | 6.10 | 0.01 | | -0.19 | * | -0.61 | * | 0.25 | * | -0.02 | * | 0.18 | * | -0.01 | | 0.71 |
| | LLD | 10 | 2.61 | 0.00 | | -0.11 | * | -0.16 | * | 0.02 | * | 0.00 | * | 0.04 | * | 0.00 | * | 0.71 |
| Left | RLD | 0 | 2.19 | -0.21 | * | -0.03 | * | -0.03 | * | 0.00 | | -0.02 | * | 0.01 | * | 0.00 | * | 0.53 |
| | RLD | 10 | 0.85 | -0.16 | * | 0.02 | * | -0.03 | * | -0.01 | * | -0.01 | * | 0.00 | * | 0.00 | | 0.60 |

* $P < 0.05$ compared with zero by 1-tailed unpaired t test.

† Equation: variable = I + ax + by +cz + dxy + eyz +fzx + gxyz .

All intercepts are significant. Post:posture; Int:intercept.

Table A44. Coefficients and $R^2$ of multiple linear regression equation † fit to $\dot{Q}$, $\dot{V}_A$, $\dot{V}_A/\dot{Q}$, and $P_{RO2}$ of right lung of dog 16 during one-lung ventilation with left lung atelectasis and hyperoxia

| | Post | PEEP | Int | x | y | z | xy | yz | zx | xyz | R2 |
|---|---|---|---|---|---|---|---|---|---|---|---|
| | LLD | 0 | 3.97 | 0.00 | -0.14 * | -0.03 * | -0.008 * | -0.007 * | 0.023 * | -0.001 * | 0.49 |
| $Q$,atel | LLD | 10 | 2.46 | -0.13 * | -0.13 * | -0.02 * | -0.012 * | -0.011 * | 0.017 * | -0.001 * | 0.57 |
| | RLD | 0 | 4.61 | -0.32 * | -0.13 * | 0.02 * | 0.006 | 0.001 | -0.024 * | 0.000 | 0.53 |
| | RLD | 10 | 1.97 | -0.24 * | -0.10 * | 0.04 * | 0.010 * | 0.004 * | -0.011 * | 0.000 | 0.67 |
| | LLD | 0 | 5.73 | -0.10 * | 0.23 * | -0.23 * | 0.024 * | -0.015 * | -0.026 * | 0.000 | 0.35 |
| $V_A$,atel | LLD | 10 | 5.20 | -0.31 * | -0.25 * | -0.13 * | -0.022 * | -0.011 * | 0.006 | -0.003 * | 0.42 |
| | RLD | 0 | 4.98 | -0.05 | 0.04 | -0.08 * | 0.048 * | -0.005 | -0.006 | -0.002 | 0.06 |
| | RLD | 10 | 3.03 | -0.15 * | 0.05 * | -0.03 * | -0.012 * | 0.004 | 0.001 | 0.003 * | 0.09 |
| | LLD | 0 | 1.57 | -0.04 * | 0.13 * | -0.05 * | 0.011 * | -0.002 * | -0.019 * | 0.000 | 0.51 |
| | LLD | 10 | 2.20 | -0.02 | 0.01 | -0.03 * | -0.001 | 0.005 * | -0.016 * | 0.000 | 0.16 |
| $V_A/Q$ | RLD | 0 | 1.19 | 0.10 * | 0.05 * | -0.03 * | 0.018 * | -0.004 * | 0.005 * | 0.000 | 0.32 |
| | RLD | 10 | 1.79 | 0.18 * | 0.12 * | -0.05 * | 0.001 | -0.002 | 0.014 * | 0.002 * | 0.50 |
| | LLD | 0 | 671.60 | -0.31 * | 0.84 * | -0.35 * | 0.093 * | -0.009 | -0.150 * | 0.003 | 0.59 |
| $P_{RO2}$ | LLD | 10 | 675.50 | -0.17 * | 0.04 | -0.14 * | 0.001 | 0.034 * | -0.075 * | 0.002 | 0.18 |
| | RLD | 0 | 666.70 | 0.74 * | 0.44 * | -0.20 * | 0.100 * | -0.027 * | 0.056 * | -0.003 | 0.34 |
| | RLD | 10 | 673.40 | 0.95 * | 0.70 * | -0.27 * | -0.052 * | -0.001 | 0.075 * | 0.009 * | 0.55 |

* $P < 0.05$ compared with zero by 1-tailed unpaired t test.

† Equation: variable = I + ax + by +cz + dxy + eyz +fzx + gxyz .

All intercepts are significant. Post:posture; Int:intercept. Atel:atelectasis

Table A45. Coefficients and $R^2$ of multiple linear regression equation † fit to $\dot{Q}$ for whole, right and left lung of dog 17 during two-lung ventilation with hyperoxia

| | Post | PEEP | Int | a | | b | | c | | d | | e | | f | | g | | $R^2$ |
|---|---|---|---|---|---|---|---|---|---|---|---|---|---|---|---|---|---|---|
| | LLD | 0 | 5.03 | -1.04 | * | -0.11 | * | -0.19 | * | 0.005 | * | -0.0370 | * | 0.0290 | * | 0.0110 | * | 0.86 |
| Whole | LLD | 10 | 0.08 | -0.01 | * | 0.00 | * | 0.00 | * | 0.000 | * | -0.0004 | * | 0.0001 | * | 0.0001 | * | 0.86 |
| | RLD | 0 | 0.10 | -0.01 | * | -0.01 | * | 0.00 | | 0.001 | * | -0.0004 | * | 0.0000 | | 0.0000 | | 0.68 |
| | RLD | 10 | 2.52 | -0.07 | * | -0.10 | * | 0.01 | * | 0.002 | | -0.0050 | * | -0.0040 | * | -0.0003 | | 0.41 |
| | LLD | 0 | 2.50 | -0.60 | * | -0.049 | * | -0.116 | * | -0.004 | | -0.0110 | * | 0.0230 | * | 0.0050 | * | 0.77 |
| | LLD | 10 | 0.04 | -0.01 | * | -0.001 | * | -0.002 | * | -0.000 | | -0.0001 | * | 0.0002 | * | 0.0000 | | 0.78 |
| Right | RLD | 0 | 0.12 | -0.02 | * | -0.007 | * | 0.001 | * | 0.0020 | * | -0.0004 | * | -0.0005 | * | 0.0002 | * | 0.62 |
| | RLD | 10 | 2.67 | -0.12 | * | -0.120 | * | 0.022 | * | 0.0060 | * | -0.0020 | | -0.0110 | * | 0.0010 | * | 0.40 |
| | LLD | 0 | 8.78 | -2.24 | * | -0.250 | * | -0.12 | * | 0.065 | | -0.084 | * | -0.0160 | | 0.0360 | * | 0.81 |
| | LLD | 10 | 0.13 | -0.02 | * | -0.003 | * | -0.001 | * | 0.000 | | -0.001 | * | -0.0003 | * | 0.0002 | * | 0.81 |
| Left | RLD | 0 | 0.07 | 0.00 | * | -0.003 | * | 0.000 | | 0.000 | | 0.000 | * | 0.0000 | | 0.0001 | * | 0.45 |
| | RLD | 10 | 2.35 | -0.04 | * | -0.083 | * | 0.000 | | -0.010 | | -0.007 | * | 0.0010 | | 0.0020 | * | 0.42 |

* $P < 0.05$ compared with zero by 1-tailed unpaired t test.

† Equation: variable = I + ax + by +cz + dxy + eyz +fzx + gxyz .

All intercepts are significant. Post:posture; Int:intercept.

Table A46. Coefficients and $R^2$ of multiple linear regression equation † fit to $\dot{Q}$, $\dot{V}_A$, $\dot{V}_A/\dot{Q}$, and $P_{RO2}$ of right lung of dog 17 during one-lung ventilation with left lung atelectasis and hyperoxia

| | Post | PEEP | Int | x | y | z | xy | yz | zx | xyz | R2 |
|---|---|---|---|---|---|---|---|---|---|---|---|
| | LLD | 0 | 4.68 | -0.06 * | -0.14 * | -0.02 * | 0.005 | -0.013 * | 0.019 * | -0.001 | 0.43 |
| $\dot{Q}$,atel | LLD | 10 | 2.36 | -0.08 * | -0.06 * | -0.02 * | -0.001 | -0.009 * | 0.009 * | 0.000 | 0.51 |
| | RLD | 0 | 8.44 | -0.68 * | -0.61 * | 0.11 * | 0.050 * | -0.020 * | -0.046 * | 0.008 * | 0.64 |
| | RLD | 10 | 4.25 | -0.41 * | -0.23 * | 0.03 * | 0.013 * | -0.009 * | -0.022 * | 0.002 * | 0.71 |
| | LLD | 0 | 7.29 | -0.20 * | -0.02 | -0.26 * | -0.014 | -0.035 * | -0.001 | -0.004 * | 0.37 |
| $\dot{V}_A$,atel | LLD | 10 | 3.35 | -0.19 * | -0.24 * | -0.06 * | -0.032 * | -0.019 * | 0.010 * | -0.005 * | 0.43 |
| | RLD | 0 | 11.40 | 0.85 | -0.54 * | 0.25 * | 0.037 * | -0.046 * | 0.011 | 0.022 * | 0.28 |
| | RLD | 10 | 5.75 | -0.25 * | 0.02 | -0.01 | -0.057 * | -0.016 * | -0.009 | 0.003 * | 0.25 |
| | LLD | 0 | 1.60 | -0.02 | 0.05 * | -0.05 * | -0.020 * | -0.004 * | -0.008 | -0.001 * | 0.23 |
| | LLD | 10 | 1.42 | -0.04 * | -0.08 * | -0.02 * | -0.012 * | -0.004 * | -0.003 | -0.003 * | 0.24 |
| $\dot{V}_A/\dot{Q}$ | RLD | 0 | 1.35 | 0.23 * | 0.05 * | 0.00 | 0.029 * | -0.002 | 0.006 | 0.003 * | 0.43 |
| | RLD | 10 | 1.49 | 0.07 * | 0.10 * | -0.01 * | -0.017 * | 0.002 | 0.006 * | 0.001 | 0.31 |
| | LLD | 0 | 682.90 | -0.15 * | 0.29 * | -0.31 * | -0.037 * | -0.020 * | -0.050 * | -0.004 | 0.27 |
| $P_{RO2}$ | LLD | 10 | 678.70 | -0.37 * | -0.55 * | -0.14 * | -0.080 * | -0.025 * | -0.033 * | -0.021 * | 0.32 |
| | RLD | 0 | 681.20 | 1.38 * | 0.07 | 0.10 * | 0.088 * | -0.015 | 0.042 * | 0.018 * | 0.53 |
| | RLD | 10 | 680.16 | 0.51 * | 0.60 * | -0.08 * | -0.110 * | -0.001 | 0.043 * | 0.008 * | 0.37 |

* $P < 0.05$ compared with zero by 1-tailed unpaired t test.

† Equation: variable = I + ax + by +cz + dxy + eyz +fzx + gxyz .

All intercepts are significant. Post:posture; Int:intercept. Atel:atelectasis

Table A47. Coefficients and $R^2$ of multiple linear regression equation † fit to $\dot{Q}$ for whole, right and left lung of dog 18 during two-lung ventilation with hyperoxia

| | Post | PEEP | Int | a | | b | | c | | d | | e | | f | | g | | $R^2$ |
|---|---|---|---|---|---|---|---|---|---|---|---|---|---|---|---|---|---|---|
| | LLD | 0 | 4.19 | -0.41 | * | -0.05 | * | -0.19 | * | 0.013 | * | -0.013 | * | 0.082 | * | -0.004 | * | 0.74 |
| Whole | LLD | 10 | 2.44 | -0.25 | * | -0.10 | * | -0.06 | * | 0.007 | * | -0.013 | * | 0.007 | * | 0.000 | | 0.82 |
| | RLD | 0 | 6.89 | -0.90 | * | 0.05 | | -0.29 | * | 0.053 | * | -0.063 | * | -0.021 | * | 0.012 | * | 0.72 |
| | RLD | 10 | 2.44 | -0.29 | * | 0.05 | * | -0.07 | * | 0.005 | * | -0.007 | * | -0.007 | * | 0.000 | | 0.80 |
| | LLD | 0 | 3.29 | -0.39 | * | -0.07 | * | -0.013 | | -0.005 | | -0.027 | * | 0.008 | | 0.0090 | * | 0.54 |
| | LLD | 10 | 1.60 | -0.22 | * | -0.07 | * | -0.042 | * | -0.003 | | -0.014 | * | -0.001 | | 0.0020 | * | 0.69 |
| Right | RLD | 0 | 9.20 | -1.30 | * | 0.03 | | -0.146 | * | 0.152 | * | -0.099 | * | -0.011 | | 0.0020 | | 0.64 |
| | RLD | 10 | 3.33 | -0.35 | * | 0.05 | * | -0.044 | * | 0.014 | * | -0.005 | * | -0.010 | * | -0.0020 | | 0.62 |
| | LLD | 0 | 5.99 | -0.76 | * | -0.22 | * | -0.48 | * | 0.093 | * | -0.075 | * | 0.120 | * | 0.016 | * | 0.77 |
| | LLD | 10 | 3.55 | -0.25 | * | -0.17 | * | -0.08 | * | -0.015 | | -0.011 | * | 0.011 | * | -0.001 | | 0.63 |
| Left | RLD | 0 | 5.68 | -0.22 | * | 0.06 | | -0.47 | * | -0.014 | | 0.053 | | 0.022 | * | -0.007 | * | 0.63 |
| | RLD | 10 | 1.14 | -0.20 | * | 0.05 | * | -0.07 | * | 0.006 | * | -0.001 | | 0.002 | | 0.001 | * | 0.72 |

* $P < 0.05$ compared with zero by 1-tailed unpaired t test.

† Equation: variable = I + ax + by +cz + dxy + eyz +fzx + gxyz .

All intercepts are significant. Post:posture; Int:intercept.

Table A48. Coefficients and $R^2$ of multiple linear regression equation † fit to $\dot{Q}$, $\dot{V}_A$, $\dot{V}_A/\dot{Q}$, and $P_{RO2}$ of right lung of dog 18 during one-lung ventilation with left lung atelectasis and hyperoxia

| | Post | PEEP | Int | x | y | z | xy | yz | zx | xyz | R2 |
|---|---|---|---|---|---|---|---|---|---|---|---|
| | LLD | 0 | 3.58 | -0.17 * | -0.07 * | -0.05 * | -0.005 | -0.020 * | 0.005 | 0.006 * | 0.32 |
| $\dot{Q}$,atel | LLD | 10 | 1.66 | -0.14 * | -0.05 * | -0.03 * | -0.008 * | -0.012 * | 0.000 | 0.002 * | 0.56 |
| | RLD | 0 | 7.14 | -0.52 * | -0.14 * | -0.02 | 0.032 * | -0.015 * | -0.033 * | -0.007 * | 0.47 |
| | RLD | 10 | 3.37 | -0.27 * | -0.13 * | -0.03 * | 0.018 * | -0.005 * | -0.007 * | -0.001 | 0.59 |
| | LLD | 0 | 7.77 | -0.04 | -0.09 * | -0.16 * | 0.019 | -0.038 * | 0.018 | -0.003 | 0.20 |
| $\dot{V}_A$,atel | LLD | 10 | 3.40 | -0.26 * | -0.26 * | -0.07 * | 0.004 | 0.000 | 0.001 | 0.001 | 0.52 |
| | RLD | 0 | 10.35 | -1.05 * | 0.37 * | 0.07 * | 0.038 * | -0.057 * | -0.130 * | 0.000 | 0.49 |
| | RLD | 10 | 4.92 | -0.36 * | -0.27 * | 0.01 | -0.006 | -0.016 * | -0.013 * | 0.000 | 0.61 |
| | LLD | 0 | 2.22 | 0.10 * | 0.06 * | -0.02 * | 0.006 | 0.000 | 0.002 | -0.006 * | 0.18 |
| | LLD | 10 | 2.04 | 0.00 | -0.09 * | 0.00 | 0.007 * | 0.013 * | -0.001 | 0.000 | 0.33 |
| $\dot{V}_A/\dot{Q}$ | RLD | 0 | 1.48 | -0.05 * | 0.08 * | 0.01 * | -0.003 | -0.005 * | -0.012 * | 0.000 | 0.32 |
| | RLD | 10 | 1.45 | 0.00 | -0.03 * | 0.02 * | -0.017 * | 0.000 | 0.001 | 0.001 | 0.22 |
| | LLD | 0 | 684.40 | 0.52 * | 0.24 * | -0.10 * | 0.030 * | -0.002 | 0.012 | -0.023 * | 0.23 |
| $P_{RO2}$ | LLD | 10 | 681.10 | -0.02 | -0.55 * | 0.05 | 0.047 * | 0.063 * | -0.017 | 0.007 | 0.33 |
| | RLD | 0 | 681.70 | -0.30 * | 0.48 * | 0.09 * | -0.025 | -0.040 * | -0.073 * | 0.000 | 0.38 |
| | RLD | 10 | 680.10 | -0.07 | -0.24 * | 0.14 * | -0.130 * | -0.001 | 0.003 | 0.004 | 0.28 |

* $P < 0.05$ compared with zero by 1-tailed unpaired t test.

† Equation: variable = I + ax + by +cz + dxy + eyz +fzx + gxyz .

All intercepts are significant. Post:posture; Int:intercept. Atel:atelectasis

## Relationship among total variance, spatial variance and residual

Consider the ith measurement of flow ($\dot{Q}i$), the predicted value from regression analysis is $\dot{Q}ip$, and the mean value of $\dot{Q}$ is $\dot{Q}m$. From algebra, $\dot{Q}i - \dot{Q}m$ consists of two parts:

$$\dot{Q}i - \dot{Q}m = (\dot{Q}i - \dot{Q}ip) + (\dot{Q}ip - \dot{Q}m)$$

Square both sides:

$$(\dot{Q}i - \dot{Q}m)^2 = (\dot{Q}i - \dot{Q}ip)^2 + (\dot{Q}ip - \dot{Q}m)^2 + 2(\dot{Q}i - \dot{Q}ip)x(\dot{Q}ip - \dot{Q}m)$$

Sum each term for all values of Q:

$$\Sigma(\dot{Q}i - \dot{Q}m)^2 = \Sigma(\dot{Q}i - \dot{Q}ip)^2 + \Sigma(\dot{Q}ip - \dot{Q}m)^2 + \Sigma 2(\dot{Q}i - \dot{Q}ip)x(\dot{Q}ip - \dot{Q}m) \quad (1)$$

Divide each term by N-1, where N is number of $\dot{Q}$ values and normalize by dividing by $\dot{Q}m^2$:

The first term on the left becomes:

$(\Sigma(\dot{Q}i - \dot{Q}m)^2)/(N-1)/\dot{Q}m^2$, the total variance normalized by $\dot{Q}m^2$

The first term on the right hand side becomes:

$(\Sigma(\dot{Q}i - \dot{Q}ip)^2)/(N-1)/\dot{Q}m^2$, the residual.

The residual variance/ total variance is $1-R^2$

The second term on the right hand side becomes:

$(\Sigma(\dot{Q}ip - \dot{Q}m)^2)/(N-1)/\dot{Q}m^2$, the spatial variance.

The spatial variance/total variance is $R^2$

The third term on the right hand side is equal to zero. One can show this empirically.

In Statview, we used as the residual variance the mean squared residual, which is the sum of the squared residuals divided by (N-1-DF) instead of (N-1), so that

$(\Sigma(\dot{Q}i - \dot{Q}ip)^2)/(N\text{-}1\text{-}DF)/\dot{Q}m^2$ / total variance is 1-adjusted $R^2$.

DF is the degree of freedom, the number of terms in the regression equation In the event that the number of points (N = ~ 1000) is much greater than DF (~31 in the fourth order equation), $R^2$ is almost equal to adjusted $R^2$. The above results show that to a good approximation

Total variance = spatial variance +. residual variance

The use of 1-adjusted $R^2$ instead of 1- $R^2$ to represent the residual variance/total variance gives an error of 3% in the estimate of non-spatial variance. Similarly the use of adjusted $R^2$ instead of $R^2$ to represent spatial variance/total variance gives an error of 3% in the estimate of spatial variance. It is simple to use mean squared residual from Statview because it is listed. The adjusted $R^2$ tell us when the order of the regression equation reaches a maximum to produce the best fit to the data. Since $R^2$ always increases as more terms are included in the regression equation, we need to use adjusted $R^2$ to tell us when to stop adding more terms.

The relationship becomes less and less accurate as DF increases and breaks down altogether when DF approaches N. The best results are obtained when DF << N.

# CURRICULUM VITAE
## Hung Chang

**PERSONAL DATA**


| | |
|---|---|
| Birth: | March 1, 1963, Taipei, Taiwan |
| Marital Status: | Married, Mei-ling, Pao |
| Children: | Stanley Chang |
| | Audrey Chang |
| Address: | Division of Pulmonary and Critical Care Medicine, RM-12 |
| | Department of Medicine |
| | University of Washington |
| | Seattle, Washington 98195 |
| | Phone: (206) 543-3166 FAX: (206) 685-8673 |


**EDUCATION**

| | |
|---|---|
| 1996-present | University of Washington |
| | Ph.D., Physiology and Biophysics, August 2001 |
| 1995-1996 | Division of Chest surgery, Department of Surgery |
| | Tri-Service General Hospital, Taipei, Taiwan, R.O.C |
| | Attending surgeon |
| 1994-1995 | Chief resident |
| 1991-1994 | Surgical resident |
| 1981-1988 | National Defense Medical Center, Taiwan, R.O.C |
| | School of Medicine, MD., June, 1988 |

**AWARDS:**

| | |
|---|---|
| 1996-2001 | Scholarship (Ph.D. program in U.S.A) |
| | by the Government, Taiwan, R.O.C |

## BIBLIOGRAPHY

1. Hung C., Lai-Fook, S. T., Domino, K. B., Schimmel, C., Hildebrandt, J., Robertson, H. T., Glenny, R. W, Hlastala, M. P. Spatial distribution of ventilation and perfusion in the lateral posture in dogs. J. Appl. Physiol. (submitted)

2. Hung C., Lai-Fook, S. T., Domino, K. B., Schimmel, C., Hildebrandt, J., Robertson, H. T., Glenny, R. W, Hlastala, M. P. Redistribution of blood flow and lung volume between lungs in lateral decubitus postures during unilateral atelectasis and PEEP. (manuscript in preparation).

3. Hung C., Lai-Fook, S. T., Domino, K. B., Schimmel, C., Hildebrandt, J., Robertson, H. T., Glenny, R. W, Hlastala, M. P. Spatial distribution of ventilation and perfusion during differential ventilation with unilateral and bilateral PEEP in the lateral posture in dogs. (manuscript in preparation).

4. Hung C., Domino, K. B., Hildebrandt, J., Glenny, R. W, Hlastala, M. P. Spatial distribution of $\dot{V}_A$ and $\dot{Q}$ in the lateral decubitus posture with and without PEEP. American Journal of Respiratory and critical care medicine, Vol 161 (3), PA849, March 2000 (Abstract)

5. Hung C., Hildebrandt, J., Hlastala, M. P. Redistribution of blood flow and lung volume between lungs in lateral decubitus postures during unilateral atelectasis and PEEP. American Journal of Respiratory and critical care medicine, Vol 163 (5), PA920, April, 2001 (Abstract)

6. Hung C., Hildebrandt, J., Hlastala, M. P. Spatial distribution of ventilation and perfusion during differential ventilation with unilateral and bilateral PEEP in the lateral posture in dogs. . American Journal of Respiratory and critical care medicine, Vol 163 (5), PA920, April, 2001 (Abstract)